

Synthesis and Biological Activity of Anticoagulant Heparan Sulfate Glycopolymers

Thesis by
Young In Oh

In Partial Fulfillment of the Requirements for the
degree of
Doctor of Philosophy



California Institute of Technology

Pasadena, California

2013

(Defended 16 May 2013)

© 2013
Young In Oh
All Rights Reserved

for my parents...

ACKNOWLEDGEMENTS

This thesis would not have been possible without the help and support of many people. First and foremost, I would like to thank my advisor Linda Hsieh-Wilson, for her guidance and support throughout my years here at Caltech. I would also like to thank members of my committee, Peter Dervan, Harry Gray, and Bil Clemons, for their scientific advice and truly unwavering support. My committee has helped me develop as a scientist in all aspects of research, and I am indebted to them for their continued encouragement, guidance and mentorship, both scientifically and personally.

The members of the Hsieh-Wilson lab, both past and present, have been a wonderful group of people to work with. In addition to countless hours working in lab, we have laughed together, and cried together. I thank everyone for their help in lab and for their friendship, and I wish them the best in their future endeavors. In particular, I would like to thank Chithra Krishnamurthy, Abby Pulsipher, and Andrew Wang for their camaraderie and unconditional support.

Finally, I would like to thank those closest to my heart, for their encouragement, support, and friendship. My closest mentors (Harry Gray, Felicia Hunt, and Carol Carmichael) have supported me in areas both inside and outside of science, and have given me an extraordinary amount of encouragement and guidance. With their help, I have been able to embark on an exciting new career path, and they continue to inspire me in so many ways. I would also like to thank my wonderful friends at Caltech, for their companionship and unconditional support; our time together has made my experience at Caltech truly memorable.

Last but not least, I would like to thank my family for their unconditional love and support. My parents are two of the most thoughtful, compassionate, and passionate people in my life, and I am truly blessed to have them as my life-long mentors and ultimate support system. And finally, I would like to thank Matt Winston, for his unwavering support. Thank you for being my best friend, having so much faith in me, encouraging me to follow my dreams, and most importantly, giving me a reason to smile everyday.

ABSTRACT

Heparin has been used as an anticoagulant drug for more than 70 years. The global distribution of contaminated heparin in 2007, which resulted in adverse clinical effects and over 100 deaths, emphasizes the necessity for safer alternatives to animal-sourced heparin. The structural complexity and heterogeneity of animal-sourced heparin not only impedes safe access to these biologically active molecules, but also hinders investigations on the significance of structural constituents at a molecular level. Efficient methods for preparing new synthetic heparins with targeted biological activity are necessary not only to ensure clinical safety, but to optimize derivative design to minimize potential side effects. Low molecular weight heparins have become a reliable alternative to heparin, due to their predictable dosages, long half-lives, and reduced side effects. However, heparin oligosaccharide synthesis is a challenging endeavor due to the necessity for complex protecting group manipulation and stereoselective glycosidic linkage chemistry, which often result in lengthy synthetic routes and low yields. Recently, chemoenzymatic syntheses have produced targeted ultralow molecular weight heparins with high-efficiency, but continue to be restricted by the substrate specificities of enzymes.

To address the need for access to homogeneous, complex glycosaminoglycan structures, we have synthesized novel heparan sulfate glycopolymers with well-defined carbohydrate structures and tunable chain length through ring-opening metathesis polymerization chemistry. These polymers recapitulate the key features of anticoagulant heparan sulfate by displaying the sulfation pattern responsible for heparin's anticoagulant activity. The use of polymerization chemistry greatly simplifies the synthesis of complex

glycosaminoglycan structures, providing a facile method to generate homogeneous macromolecules with tunable biological and chemical properties. Through the use of *in vitro* chromogenic substrate assays and *ex vivo* clotting assays, we found that the HS glycopolymers exhibited anticoagulant activity in a sulfation pattern and length-dependent manner. Compared to heparin standards, our short polymers did not display any activity. However, our longer polymers were able to incorporate *in vitro* and *ex vivo* characteristics of both low-molecular-weight heparin derivatives and heparin, displaying hybrid anticoagulant properties. These studies emphasize the significance of sulfation pattern specificity in specific carbohydrate-protein interactions, and demonstrate the effectiveness of multivalent molecules in recapitulating the activity of natural polysaccharides.

TABLE OF CONTENTS

Acknowledgements	iv
Abstract.....	v
Table of Contents	vii
List of Figures.....	viii
List of Schemes	xii
List of Tables	xiv
List of Abbreviations.....	xvi
Chapter I: Heparan Sulfate Glycosaminoglycans	1
The glycosaminoglycan family.....	1
Heparin and heparan sulfate glycosaminoglycans	4
Use of heparin and heparan sulfate as an anticoagulant.....	10
Chapter II: Chemical Synthesis of Heparan Sulfate Glycopolymer Building Blocks	19
Background and motivation.....	19
Synthetic design of heparan sulfate glycopolymers	20
Synthesis of heparan sulfate monomer building blocks	26
Glycosylation, deprotection, and sulfation of heparan sulfate monomer.....	46
Experimental methods and spectral data	56
Chapter III: Polymerization of Glycosaminoglycan Polymers	104
Olefin metathesis and ring-opening metathesis polymerization chemistry	104
Multivalency effect of glycopolymers.....	108
Use of ring-opening metathesis chemistry for biomedical applications	113
Polymerization of glycosaminoglycan polymers	116
Experimental methods and spectral data	124
Chapter IV: Anticoagulant Activity of Heparan Sulfate Glycopolymers	131
Mechanism of anticoagulant activity	131
<i>In vitro</i> fXa and fIIa inhibition.....	138
<i>Ex vivo</i> activity of glycopolymers in human plasma.....	147
Experimental methods.....	156
Appendix: Progress Towards Cyclooctene-based Heparan Sulfate Polymers.....	161
Synthetic design of cyclooctene-based HS glycopolymers.....	161
Synthesis of cyclooctene linker.....	163
Coupling of glucosamine and cyclooctenol linker	164
Glycosylation and deprotection of orthogonally protected disaccharide	165
Experimental methods and spectral data	169
References.....	174

LIST OF FIGURES

Chapter 1		Page
Figure 1.1	Structures of glycosaminoglycans	2
Figure 1.2	Proteoglycans consist of a protein core and covalently linked GAG chains	3
Figure 1.3	The formation of a core protein linkage region tetrasaccharide	5
Figure 1.4	Scheme of HS chain biosynthesis	6
Figure 1.5	The three energetically stable conformers of sulfated L-iduronic acid.	8
Figure 1.6	Differences in charge between heparin and HS	9
Figure 1.7	Anticoagulant HS pentasaccharide, and its interactions with AT	11
Figure 1.8	Synthetic anticoagulants fondaparinux and idraparinux	12
Chapter 2		
Figure 2.1	Inhibition of factor Xa and thrombin by antithrombin and heparin	21
Figure 2.2	The structural features of native and pentasaccharide-activated AT	22
Figure 2.3	The antithrombin-pentasaccharide interactions	23
Figure 2.4	Natural HS polysaccharide vs synthetic HS glycopolymer	24
Figure 2.5	Structures of Arixtra and Org31550	25
Figure 2.6	Commonly used protecting groups in carbohydrate chemistry and organic synthesis	28

Figure 2.7	Schlenk flask used for glycosylation reactions	50
Figure 2.8	^1H NMR (300 MHz, CDCl_3) of compound 7	79
Figure 2.9	^1H NMR (300 MHz, CDCl_3) of compound 8	80
Figure 2.10	^1H NMR (500 MHz, CDCl_3) of compound 9	81
Figure 2.11	^1H NMR (300 MHz, CDCl_3) of compound 10	82
Figure 2.12	^1H NMR (300 MHz, CDCl_3) of compound 11'	83
Figure 2.13	^1H NMR (300 MHz, CDCl_3) of compound 12	84
Figure 2.14	^1H NMR (300 MHz, CDCl_3) of compound 13	85
Figure 2.15	^1H NMR (300 MHz, CDCl_3) of compound 14	86
Figure 2.16	^1H NMR (300 MHz, CDCl_3) of compound 15	87
Figure 2.17	^1H NMR (300 MHz, CDCl_3) of compound 17	88
Figure 2.18	^1H NMR (300 MHz, CDCl_3) of compound 18	89
Figure 2.19	^1H NMR (300 MHz, CDCl_3) of compound 22	90
Figure 2.20	^1H NMR (300 MHz, CDCl_3) of compound 24	91
Figure 2.21	^1H NMR (300 MHz, CDCl_3) of compound 25	92
Figure 2.22	^1H NMR (300 MHz, CDCl_3) of compound 28	93
Figure 2.23	^1H NMR (300 MHz, CDCl_3) of compound 30	94
Figure 2.24	^1H NMR (300 MHz, CDCl_3) of compound 32	95
Figure 2.25	^1H NMR (300 MHz, CDCl_3) of compound 33	96
Figure 2.26	^1H NMR (300 MHz, CDCl_3) of compound 34	97
Figure 2.27	^1H NMR (300 MHz, CDCl_3) of compound 38	98
Figure 2.28	^1H NMR (300 MHz, CDCl_3) of compound 44	99

Figure 2.29	^1H NMR (300 MHz, CDCl_3) of compound 45	100
Figure 2.30	^1H NMR (300 MHz, CDCl_3) of compound 46	101
Figure 2.31	^1H NMR (300 MHz, CDCl_3) of compound 47	102
Chapter 3		
Figure 3.1	Ruthenium-based metathesis catalysts	108
Figure 3.2	Modes of multivalent ligand binding	110
Figure 3.3	Different classes of multivalent ligands	111
Figure 3.4	Common architectural motifs in ROMP polymers designed to utilize multivalency	112
Figure 3.5	Different types of norbornene monomers for biologically relevant polymers	114
Figure 3.6	Representative GPC run for HS polymers	121
Figure 3.7	^1H NMR (400 MHz, D_2O) of compound 47_n	129
Chapter 4		
Figure 4.1	The coagulation cascade is divided into the intrinsic, extrinsic, and common pathways	133
Figure 4.2	Heparin-induced thrombocytopenia caused by heparin anticoagulant therapy	136
Figure 4.3	Mechanism of chromogenic substrates	138
Figure 4.4	Chemical structures of fXa and fIIa chromogenic substrates, and mechanisms of action	139
Figure 4.5	Anti-fXa and anti-thrombin activity of controls	140
Figure 4.6	Sulfation dependence of anti-fXa and anti-thrombin activity	141
Figure 4.7	Anti-fXa and anti-thrombin activity of short polymers	142

(57₄, 57₆, 57₈)

Figure 4.8	Anti-fXa and anti-thrombin activity of medium-length polymers (57 ₁₀ , 57 ₁₅)	143
Figure 4.9	Anti-fXa and anti-thrombin activity of long polymers (57 ₃₀ , 57 ₄₅)	144
Figure 4.10	PF4 neutralization of anti-thrombin activity of heparin, polymer 57 ₃₀ , and polymer 57 ₄₅	146
Figure 4.11	Activated partial thromboplastin time and prothrombin time tests	148

LIST OF SCHEMES

Chapter 1		Page
Scheme 1.1	Chemoenzymatic synthesis of ULMWHs	15
Chapter 2		
Scheme 2.1	The stereoselective formation of glycosidic bonds by neighboring group participation	29
Scheme 2.2	Retrosynthesis of HS glycopolymers	31
Scheme 2.3	Synthesis of orthogonally protected GlcA monomer	33
Scheme 2.4	Synthesis of orthogonally protected IdoA monomer	36
Scheme 2.5	Isomers produced by triol intermediate 15	37
Scheme 2.6	Saponification of TBS-protected cyclooctene-based HS disaccharide monomer	40
Scheme 2.7	Caged byproduct 22 formation	41
Scheme 2.8	Synthesis of norbornene-diethylene glycol linker	45
Scheme 2.9	Glycosylation using idoA-trichloroacetimidate donor	51
Scheme 2.10	Coupling of HS disaccharide trichloroacetimidate to norbornene-diethylene glycol linker	52
Scheme 2.11	Streamlined synthesis of HS disaccharide monomer 47	53
Chapter 3		
Scheme 3.1	General mechanism of olefin metathesis	105
Scheme 3.2	Types of olefin metathesis reactions	106
Scheme 3.3	Polymerization of cyclooctene-based CS polymers	117

Scheme 3.4	Polymerization reaction using bis-pyridine Grubbs 2 nd generation catalyst	118
Scheme 3.5	Hydrogenolysis of HS glycopolymer series	123
Appendix		
Scheme A.1	Retrosynthesis of cyclooctene-based HS glycopolymers	162
Scheme A.2	Synthesis of norbornene-based ROMP linker	163
Scheme A.3	Hydrolysis and saponification of TBS-protected cyclooctene-based HS disaccharide monomer 35	166
Scheme A.4	Proposed synthetic route to cyclooctene HS glycopolymers	168

LIST OF TABLES

Chapter 1		Page
Table 1.1	Major differences between heparin and HS	7
Table 1.2	Synthetic anticoagulant drugs	14
Chapter 2		
Table 2.1	Optimization of GlcA 3-O-benzyl oxidation reaction	34
Table 2.2	Optimization of C-4 TBS protection of 18	39
Table 2.3	Reaction conditions for TIPS protection of 18	40
Table 2.4	Reaction conditions for PMB protection of 18	41
Table 2.5	Optimization of benzylation of 18	42
Table 2.6	Optimization of glycosyl phosphate 25	44
Table 2.7	Optimization of GlcA donor and norbornene linker coupling reaction	46
Table 2.8	Optimization of donor 25 and acceptor 34 glycosylation reaction	49
Table 2.9	Optimization of methyl ester hydrolysis reaction	52
Chapter 3		
Table 3.1	Functional group tolerance of olefin metathesis catalysts	107
Table 3.2	Characterization of polymer series	120
Table 3.3	Hydrogenation catalysts used for compound 56_n	122

Chapter 4

Table 4.1 Factor Xa and thrombin inhibitory activity of glycopolymer series 144

Table 4.2 Activated partial thromboplastin time and prothrombin time tests 150

Appendix

Table A.1 Coupling of protected GlcA **10** and cyclooctene linker **62**. 164

Table A.2 Glycosylation reaction of IdoA donor **19** and GlcA acceptor **64** 165

LIST OF ABBREVIATIONS

Å	angstrom
A_{405}	absorbance at 405 nm
Ac	acetyl, acetate
ADMET	acyclic diene metathesis polymerization
Aq	aqueous
aPTT	activated partial thromboplastin time
AT	antithrombin
ATIII	antithrombin III
Bn	benzyl
Bu	butyl
Bz	benzoyl
° C	degrees Celsius
C ₅ -epi	C-5 epimerase
calcd	calculated
CAM	cerium ammonium molybdate
CM	cross metathesis
CS	chondroitin sulfate
CSA	(±)-DL-camphor-10-sulfonic acid
d	doublet
DBU	1,8-diazobicyclo[5.4.0]undec-7-ene
DCE	dichloroethane
DCM	dichloromethane
dd	doubly distilled or doublet of doublets
DIPEA	<i>N,N</i> -diisopropylethylamine
DMAP	4-dimethylaminopyridine
DMSO	dimethyl sulfoxide
DMF	<i>N,N</i> -dimethylformamide

DNA	deoxyribonucleic acid
DP	degree of polymerization
DS	dermatan sulfate
DTAB	dodecyltrimethylammonium bromide
DVT	deep vein thrombosis
Eq	equivalents
ESI	electrospray ionization
Et	ethyl
EtOAc	ethyl acetate
fIIa	factor IIa or thrombin
FGF	fibroblast growth factor
fXa	factor Xa
g	gram(s)
GAG	glycosaminoglycans
Gal	galactose
GalNAc	<i>N</i> -acetylgalactosamine
GlcNAc	<i>N</i> -acetylglucosamine
GlcA	glucuronic acid
Glu	glucose
GPC	gel permeation chromatography
h	hour(s)
HA	hyaluronan
HIT	heparin-induced thrombocytopenia
HMWK	high molecular weight kininogen
HPLC	high-performance liquid chromatography
HRMS	high resolution mass spectrometry
HS	heparan sulfate
HSQC	heteronuclear single-quantum correlation spectroscopy
Hz	hertz
IC ₅₀	half maximal inhibitory concentration

IdoA	iduronic acid
INR	international normalized ratio
<i>J</i>	coupling constant
KfiA	<i>N</i> -acetyl glucosaminyl transferase of <i>E. coli</i> K5
KS	keratan sulfate
l	liter
LMWH	low molecular weight heparin
m	multiplet or milli
mL	milliliter
<i>m/z</i>	mass to charge ratio
μ	micro
μL	microliter
MALLS	multi-angle laser light scattering
Me	methyl
MHz	megahertz
min	minute(s)
M_n	number-average molar mass
mol	mole(s)
Ms	methanesulfonyl
MS	mass spectrometry or molecular sieves
M_w	weight-average molar mass
MW	molecular weight
n	nano
NDST	<i>N</i> -deacetylase/ <i>N</i> -sulfotransferase
NHC	<i>N</i> -heterocyclic carbene
NMR	nuclear magnetic resonance
OH	alcohol
2-OST	2- <i>O</i> -sulfotransferase
6-OST	6- <i>O</i> -sulfotransferase
3-OST	3- <i>O</i> -sulfotransferase

<i>p</i>	para
Pd/C	palladium on carbon
Pd(OH) ₂ /C	palladium hydroxide on carbon (pearlman's catalyst)
PDGF	platelet-derived growth factor
PDI	polydispersity index
PF4	platelet factor 4
PG	proteoglycan or protecting group
Ph	phenyl
pH	hydrogen concentration in aqueous solution
PMB	<i>para</i> -methoxybenzyl
pmHS2	heparosan synthase-2 of <i>Pasteurella multocida</i>
ppm	parts per million
PPP	platelet poor plasma
PT	prothrombin time
PTS	polyoxyethanyl α -tocopheryl sebacate
PTT	partial thromboplastin time
pyr	pyridine
q	quartet
R	alkyl group
RCM	ring-closing metathesis
ROCM	ring-opening cross metathesis
ROMP	ring-opening metathesis polymerization
rt	room temperature
s	singlet
SDS	sodium dodecyl sulfate
t	triplet
TBAF	tetrabutylammonium fluoride
TBS	<i>tert</i> -butyldimethylsilyl
TBSOTf	<i>tert</i> -butyldimethylsilyl trifluoromethanesulfonate
<i>tert</i>	tertiary

TF	tissue factor
Tf	trifluoromethanesulfonate
TfOH	trifluoromethanesulfonic acid
THF	tetrahydrofuran
TIPS	triisopropylsilyl
TLC	thin-layer chromatography
TMA	trimethylamine
TMS	trimethylsilyl
TMSOTf	trimethylsilyl trifluoromethanesulfonate
UF	unfractionated
UHPLC	ultra high performance liquid chromatography
ULMWH	ultra low molecular weight Heparin
VLDL	very low density lipoprotein
vWF	von Willebrand factor

Chapter 1

HEPARAN SULFATE GLYCOSAMINOGLYCANS

The glycosaminoglycan family

Glycosaminoglycans (GAGs) are linear, sulfated polysaccharides, which consist of repeating disaccharide building blocks with an amino sugar (*N*-substituted glucosamine, or *N*-acetylgalactosamine), and a uronic acid (glucuronic or iduronic acid) or galactose.² These disaccharides can display differences in monosaccharide composition and more subtle variations in stereochemistry of glycosidic linkages and polysaccharide lengths. Adding to the complexity of these polysaccharide structures, each of the monosaccharide moieties can be sulfated at various positions. As a result, GAGs have high degrees of heterogeneity with regards to disaccharide composition, molecular weight, and sulfation due to the fact that GAG biosynthesis is dynamically modulated by enzymes, unlike proteins or nucleic acids, which are template driven.⁴

Carbohydrates are nature's most informationally rich macromolecules. When considering factors such as sequence, glycosidic linkages, ring-size permutations, and branching of glycans, the structural diversity of glycans far exceed that of nucleic acids and proteins. While only 4096 hexanucleotide combinations are possible with the four base pairs of DNA and 6.4×10^7 hexapeptide combinations from the 20 amino acids, a staggering 1.44×10^{15} hexasaccharide combinations can be formed from 20 unique monosaccharides.⁵ In addition to this large number of structural permutations based on

saccharide linkages, glycan epitopes are also subjected to posttranslational modifications (i.e., sulfation) to convey particular properties to specific sites,^{6,7} which adds an additional level of structural diversity to carbohydrates. As a result, carbohydrates are ideal for generating units with a vast array of informational properties.

GAGs can be classified into two broad categories based on their carbohydrate structures: Sugars with D-glucosamine (hyaluronan, keratan sulfate, heparin, and heparan sulfate) are classified as glucosaminoglycans, while sugars with D-galactosamine (chondroitin sulfate and dermatan sulfate) are classified as galactosaminoglycans. GAGs can be further categorized into four additional groups, depending on their uronic acid composition (Figure 1.1): heparin and heparan sulfate (HS), chondroitin sulfate (CS), keratan sulfate (KS), and hyaluronan (HA).⁸ While heparin, HS and DS contain both iduronic acid (IdoA) and glucuronic acid (GlcA) moieties, CS contains only GlcA units.

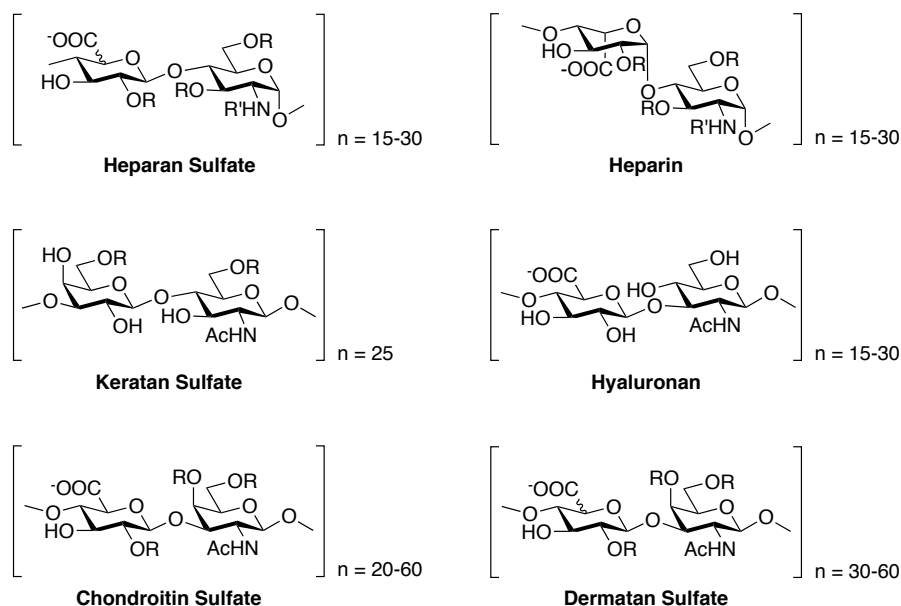


Figure 1.1: Structures of glycosaminoglycans. R = H or SO₃⁻; R' = Ac or SO₃⁻.

GAGs exist as free polysaccharide chains, or as proteoglycans (PGs), when the GAG chains are covalently linked to a protein core (Figure 1.2). PGs are major constituents of the extracellular matrix and cell membranes, and are important for biological processes such as axonal guidance,⁹ cancer metastasis,^{10,11} embryonic development,¹² as well as viral entry and attachment.^{13,14} For each PG, there can be a different number of GAG chains attached to the protein core, and the GAG chains can have different lengths, sugar compositions, and sulfation patterns.¹¹ The biological activities of GAGs are determined by

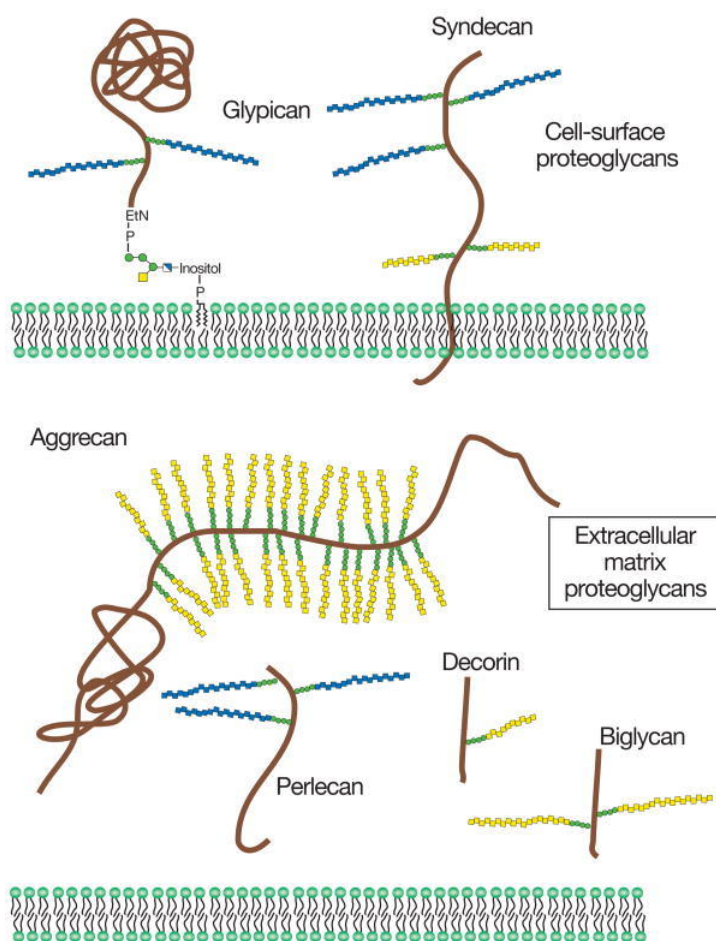


Figure 1.2: Proteoglycans consist of a protein core (brown) and covalently linked GAG chains (HS in blue; CS/DS in yellow). Membrane proteoglycans either span the plasma membrane or are linked by a GPI anchor. ECM proteoglycans are usually secreted, but some can be proteolytically cleaved and shed from the cell surface.²

the chemical composition and properties of these PGs, where the *N*- or *O*-linked glycans contribute towards distinct biological properties. The number and positions of sulfate groups on GAG chains are tightly controlled, and are thought to act as “patterns” for specific protein recognition.^{15,16} Unfortunately, the structural heterogeneity of PGs and individual GAG chains has made it difficult to isolate polysaccharide chains with defined sulfation sequences, hindering our understanding of the roles of GAG sulfation patterns at a molecular level.

Heparin and heparan sulfate glycosaminoglycans

Of the different classes of GAGs, HS GAGs have been the most-closely studied. The structural complexity and diversity of HS has resulted in a vast array of functions; hundreds of heparin-binding proteins have been identified, and many of these interactions have profound consequences in vertebrate and invertebrate physiology. HS is near-ubiquitous in animal tissues, and is expressed both on plasma membranes and in the extracellular matrix. The large polyanionic and hydrated domains of HS are thought to influence the general chemical and physical properties of pericellular regions. Thus, HS GAGs are strategically positioned to regulate interactions between cells and their microenvironments,^{17,18} and such interactions have been shown to be critical for normal cell growth and development, and for the maintenance of differentiated cellular functions.^{19,20} Additionally, they can inhibit the diffusion of macromolecules across basement membranes²¹ and control the access to the cell surfaces of important regulatory molecules.²²

The biosynthetic pathways for glycan assembly, processing, remodeling, and site-specific modification are elaborate and well-developed. Heparin/HS biosynthesis begins in the golgi apparatus,²³ beginning with the generation of a core protein linkage region tetrasaccharide, GlcA β (1,3)-Gal β (1,3)-Gal β (1,4)-xylose β -1-O-Ser (Figure 1.3). The biosynthetic pathway diverges from this tetrasaccharide linkage point to synthesize both CS

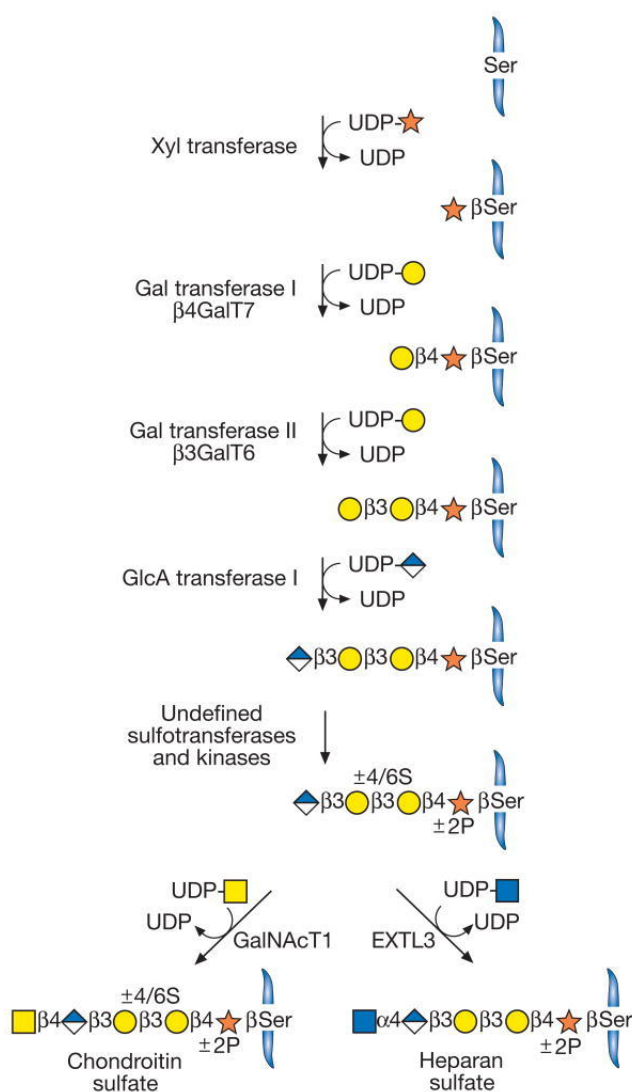


Figure 1.3: The biosynthesis of HS, heparin, and CS is initiated by the formation of a core protein linkage region tetrasaccharide.²

and HS GAGs; the addition of β (1,4) GalNAc initiates the biosynthesis of CS GAGs, and the addition of α (1,4) *N*-acetylglucosamine (GlcNAc) initiates the biosynthesis of heparin and HS GAGs. The addition of this first GlcNAc in heparin/HS biosynthesis is catalyzed by the enzyme EXTL3, and is followed by the alternating addition of GlcA and GlcNAc by the polymerase enzymes EXT1 and EXT2.⁹

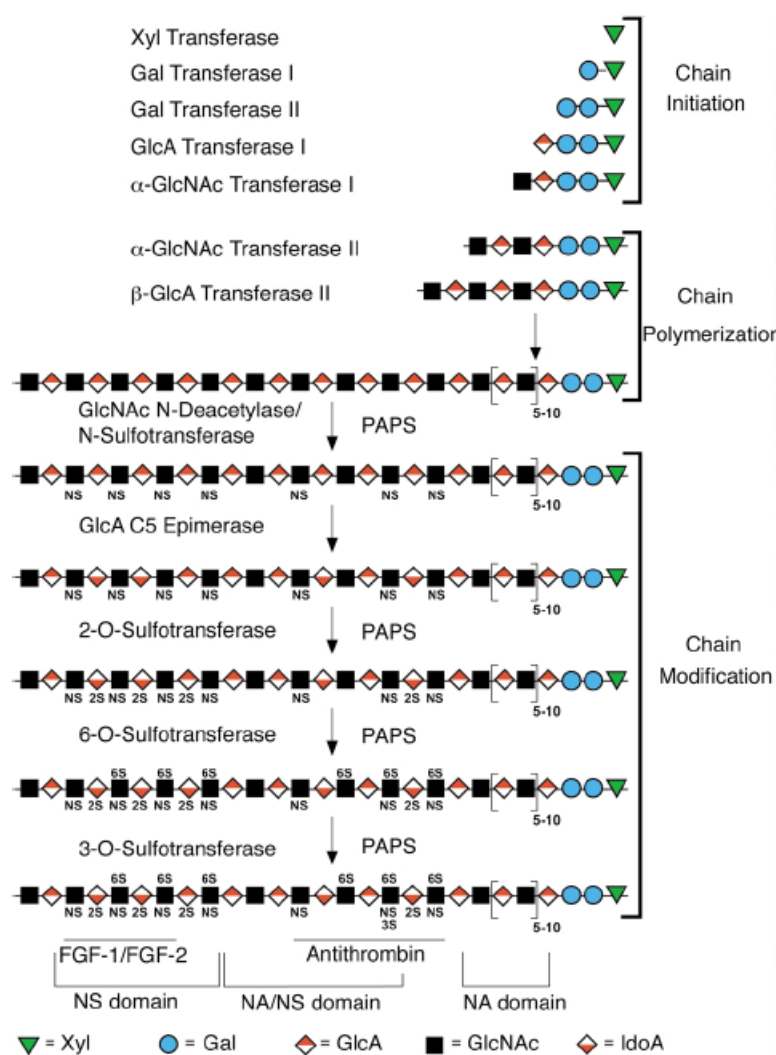


Figure 1.4: Scheme of HS chain biosynthesis. Structural domains (NA, NA/NS, NS) are defined with regards to the distribution of GlcNAc N-substituents as indicated. Regions that have been implicated in the binding of specific ligands, such as FGF-1/FGF-2 and antithrombin, are also shown.³

The resulting polysaccharide chains, consisting of repeating GlcNAc $\alpha(1,4)$ GlcA $\beta(1,4)$ units, undergo a series of modification reactions catalyzed by sulfotransferases and an epimerase (Figure 1.4).²⁴ GlcNAc *N*-deacetylase/*N*-sulfotransferase (NDST) deacetylates and sulfonates a subset of GlcNAc residues, some of which occur in clusters along the polysaccharide backbone. A C-5 epimerase (C₅-epi) then acts on GlcA residues immediately adjacent to and toward the reducing end of GlcNSO₃⁻ to convert some GlcA moieties to IdoA; the resulting heparin and HS chains consist of alternating uronic acid (GlcA or IdoA) and GlcN units.²⁵ Epimerization is then followed by *O*-sulfation of some of the C-2 positions of IdoA and GlcA by 2-*O*-sulfotransferase (2-OST),^{26,27} C-6 position of GlcN by 6-*O*-sulfotransferase (6-OST),^{28,29} and C-3 position of GlcN by 3-*O*-sulfotransferase (3-OST)³⁰⁻³² to afford variably sulfated HS GAG chains. Sulfation patterns of HS GAGs are not template derived and are dynamically adjusted by the availability of enzymes, substrates, and acceptors in space and time.³³ This ability of GAG backbones to be sulfated at various positions allows for a facile method of adding extraordinary structural complexity to a simple repetition of disaccharide units.

Understanding the biosynthesis of heparin and HS has clarified the rules governing

Characteristic	Heparan Sulfate	Heparin
Solubility in 2 M KCO ₂ Me	Yes	no
Size	10-70 kDa	10-12 kDa
Sulfate/hexosamine ratio	0.8-1.8	1.8-2.4
GlcN <i>N</i> -sulfates	40-60 %	>85 %
IdoA content	30-50 %	>70 %
Binding to antithrombin	0-0.3 %	~30 %
Site of synthesis	Virtually all cells	Mast cells

Table 1.1: Major differences between heparin and heparan sulfate¹.

their complex structures, leading to an understanding of the differences between heparin and HS (Table 1.1). Virtually all cells, from simple invertebrates to humans, have the capacity to produce HS.³ Whereas HS is found in virtually all cells, heparin expression is restricted to mast cells, where it mainly acts to store granular components such as histamine and mast cell proteases.³⁴ Heparin and HS are most easily differentiated by their disaccharide composition (i.e., the presence of variably sulfated or nonsulfated GlcA/IdoA and GlcN moieties), and the distribution of GlcN residue *N*-substituents. Generally, the same sets of disaccharides exist in most tissues, but their relative contents vary.

Selectivity for HS and heparin by protein binding-partners stems from a number of different structural variables that affect the overall charge and conformation these GAGs. In addition to the diversity in sulfation patterns, the three-dimensional layout of these sulfate groups is affected by rotation at the glycosidic linkages and through changes in ring conformations. In particular, the epimerization of D-GlcA to L-IdoA adds to the structural complexity of heparin and HS GAGs, due to the ability of IdoA to undergo structural rearrangements (Figure 1.5).³⁵ Theoretical and experimental studies indicate that IdoA residues exist in an equilibrium of different conformations (4C_1 , 2S_0 , 1C_4), where the relative proportion of conformers depends on the sulfation pattern and sequence of the GAG chain.^{36,37} This unique conformational flexibility adds an additional level of chemical

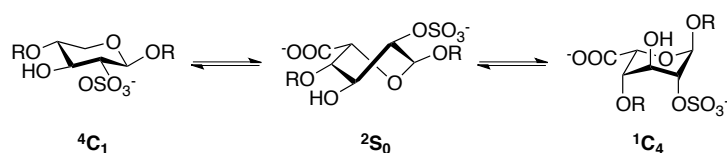


Figure 1.5: The three energetically stable conformers of sulfated L-iduronic acid. In the 4C_1 and 2S_0 conformers, substituents at C-2 and C-3 are in a diequatorial orientation, where as in the 1C_4 conformer, they are diaxially oriented.

diversity and binding capacity. This is reflected in the higher binding capacity of HS or DS compared to CS, which all have similar charge densities but differ in the rigidity of GluA moieties.³⁸

With regards to the distribution of variably substituted GlcN moieties along the GAG backbones, there can be areas of *N*-acetylated disaccharide units (NA domains), areas of *N*-sulfated sequences of variable lengths (NS domains), and areas of alternating *N*-acetylated and *N*-sulfated units (NA/NS domains). Simply put, heparin can be considered an unusually extended single NS domain. As subsequent *O*-glycosylation and epimerization modifications of GlcA depend on prior *N*-sulfation of GlcN, heparin has a more highly sulfated (Figure 1.6) and more homogeneous structure compared to HS. Additionally, variably sulfated HS disaccharides cluster in the NS or NA/NS domains,³⁹ resulting in HS chains with areas of high and low sulfation; the *N*-substitution patterns have been shown to be characteristic of the cells/tissues from which the heparin or HS is obtained.³

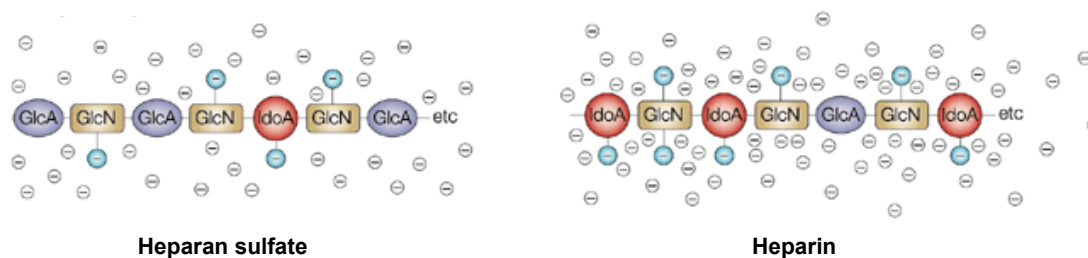


Figure 1.6: Differences in charge between heparin and heparan sulfate.

To a large extent, the biological functions of GAGs and PGs depend on the interactions between the GAG chains and relevant proteins. However, the disaccharide composition and the arrangement of NA and NS domains do not by themselves define

binding sites for specific ligands; binding occurs at specific sets of sulfated disaccharides within these domains.^{40,41} Examples of such interactions include the interactions of glycoprotein gD from Herpes simplex virus with an oligosaccharide containing IdoA2S-GlcN3S,⁴² and the interaction between FGF-1/FGF-2 with *N*-sulfated pentasaccharide sequences containing IdoA2S and GlcN6S.^{43,44} More recent studies have focused on HS sequences that mediate the binding and/or activation of PDGF,⁴⁵ hepatocyte growth factor,⁴⁶ dengue virus,⁴⁷ the angiogenesis inhibitor endostatin,⁴⁸ and chemokines.⁴⁹ To date, the best-studied example of the significant sulfation pattern specificity for biological activity is the interaction between HS/heparin and antithrombin,⁵⁰ and the role it plays as the most commonly used anticoagulant worldwide.

Use of heparin and heparan sulfate as an anticoagulant

Over 100 years after its discovery by Howell,⁵¹ heparin and heparin-derivatives remain one of the most important drugs in clinical practice and are used worldwide to prevent blood coagulation. The development of chemical degradation and enzymatic depolymerization methods has played a crucial role in the elucidation of the structure of heparin. These developments led to a detailed understanding of the structural basis of heparin's anticoagulant activity in the early 1980s. Today, approximately 33 metric tons of heparin, which represents 500 million doses, are used worldwide each year. Heparin-based products are the first choice when blood clotting needs to be prevented or controlled, and is commonly used for the prevention of postoperative thrombosis, the treatment of deep vein thrombosis (DVT),⁵² and extracorporeal therapies such as kidney dialysis.

When the first clinical trials evaluating the use of heparin began in the mid-1930s, very little was known about the chemistry and structure of heparin. Initially, it was discovered that thrombin was gradually inhibited when added to defibrinated plasma, due to the presence of a specific inhibitor of the enzyme, named antithrombin (AT; also known as antithrombin III, or ATIII).⁵³ It was not until 1939 that a specific compound was shown to be the active anticoagulant, and was identified as a plasma component initially called heparin-cofactor.⁵⁴ The link between heparin cofactor and AT was made in the 1950s, and it was suggested that the activity of AT was accelerated by heparin.^{55,56} This was confirmed through the isolation of pure AT by Abildgaard and coworkers in 1968,⁵⁷ and the mechanism of action was clarified in 1973 by Rosenberg and coworkers.^{58,59}

The identification of the precise structural components of heparin responsible for its anticoagulant activity began with efforts towards identifying its AT binding site.⁶⁰ Upon investigating the anticoagulant activity of samples obtained from the fractionation and enzymatic degradation of heparin, it was identified that short hexa- to deca-saccharide fragments of heparin could bind to AT.⁶¹⁻⁶⁴ Upon further partial degradation of these sequences, a critical pentasaccharide sequence (Figure 1.7) was identified as the required moiety for binding AT: GlcNS6S-GlcA-GlcNS3S6S-IdoA2S-GlcNS6S.

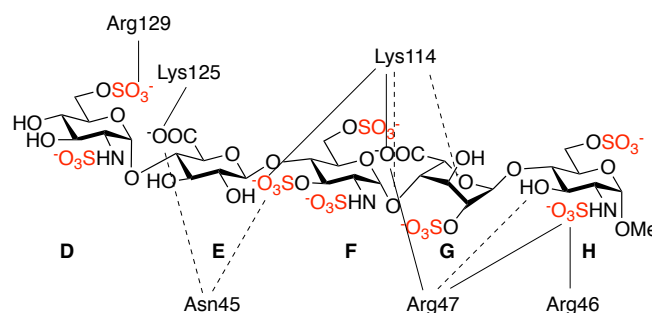


Figure 1.7: Anticoagulant HS pentasaccharide, and its interactions with AT.

The structural requirements for the HS pentasaccharide binding to AT were confirmed by chemically synthesizing a series of pentasaccharides with various combinations of sulfate and carboxyl groups.⁶⁵ The removal of certain sulfate or carboxylic groups has been shown to significantly compromise the binding affinity to AT, rendering particular functionalities more necessary than others. In particular, the 3-*O*-sulfate group from the third monosaccharide (Figure 1.7, monosaccharide F) decreases binding affinity to AT by nearly 20,000-fold.⁶⁶ Other sulfate, hydroxyl, and carboxylic groups have been shown to participate in AT binding, and have provided the basis for synthetic low molecular weight heparin (LMWH) derivatives.

With the discovery of the anticoagulant pentasaccharide and development of

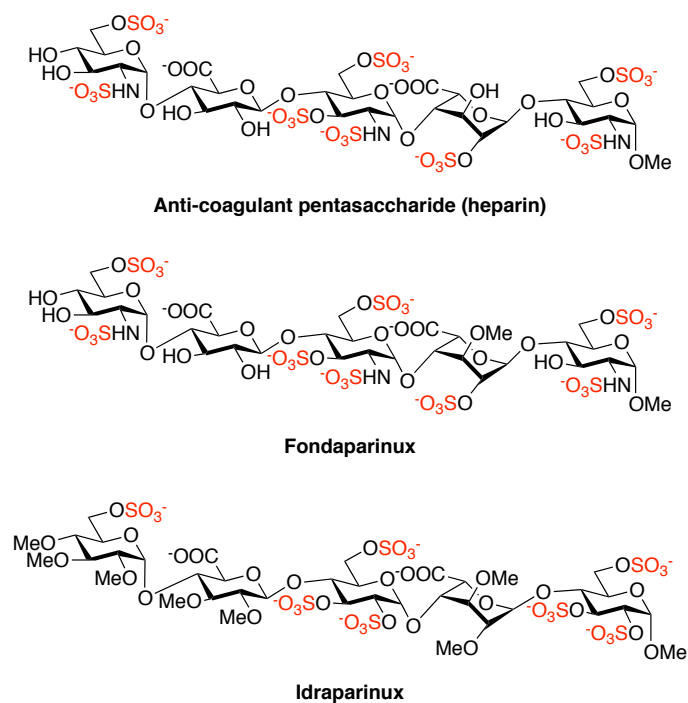


Figure 1.8: Synthetic anticoagulants fondaparinux and idraparinux.

structurally identical LMWHs, there are now three different forms of heparins used in clinical practice: unfractionated (UF) heparin, with an average molecular weight of ~14000; LMWH, with an average molecular weight of ~6000; and the synthetic ultralow molecular weight heparin (ULMWH) pentasaccharide Arixtra, with a molecular weight of 1728. UF heparin is most commonly used for surgery due to its relatively short half-life and its safety for renal-impaired patients.⁶⁷ However, standard heparin has some considerable shortcomings, such as poor bioavailability after subcutaneous administration, a poor pharmacokinetic profile, and the potential to induce antibody-associated thrombocytopenia due to its interaction with platelet factor 4 (PF4). In contrast, the newer synthetic LMWHs have improved the specificity of anticoagulant action and pharmacokinetics.⁶⁸

Fondaparinux sodium (Arixtra®) is a synthetic pentasaccharide (Figure 1.8) structurally analogous to the anticoagulant pentasaccharide (Figure 1.8), and was the first synthetic agent to be a selective antithrombin-mediated inhibitor of factor Xa (fXa).⁶⁹ It has complete bioavailability after subcutaneous injection and the peak plasma level is obtained after approximately 2 h. In contrast to other synthetic LMWHs such as enoxaparin (Lovenox®), fondaparinux is significantly more effective than the enoxaparin in preventing venous thromboembolism after major orthopedic surgery and has recently been approved for use in thromboprophylaxis post-surgery. While clinically effective, the chemical synthesis of Arixtra⁶⁵ entails over 50 steps with an overall yield of ~0.1%,⁷⁰ making it the most expensive drug among heparins. Efforts to improve the synthesis of Arixtra through optimization its synthetic steps have achieved only limited success.⁷¹

In addition to the purely synthetic method of obtaining fondaparinux, a series of LMWHs have been produced using enzymatic or chemical depolymerization methods to

Name	Target	Company
Dalteparin sodium (Fragmin®)	Thrombosis, anticoagulant	Pfeizer
Nadroparin calcium (Fraxiparin®)	Thrombosis, anticoagulant	GlaxoSmithKline
Enoxaparin sodium (Lovenox®)	Thrombosis, anticoagulant	Sanofi
Ardeparin (Normiflo®)	Thrombosis, anticoagulant	Wyeth
Danaparoid (Orgaran®)	Thrombosis, anticoagulant	Organon
Fondaparinux (Arixtra®)	Thrombosis, anticoagulant	GlaxoSmithKline

Table 1.2: Synthetic anticoagulant drugs

afford heparin with structures of defined chain lengths between 13 and 22 saccharides.^{72,73}

Table 1.2 portrays LMWH-based drugs that have been approved for the treatment of thrombosis. Different methods of production give rise to different preparations of LMWH with altered MW ranges and number of sulfation sites, but these heparins generally have average MWs of less than 8000 Da. Each commercially produced LMWH has a different recommended dose and reacts differently based on its structure and MW, and is commonly used worldwide.

As an alternative to obtaining the anticoagulant pentasaccharide and its analogues through purely synthetic methods, several labs have successfully prepared heparin oligosaccharides,⁷⁴⁻⁷⁶ as well as structurally well-defined HS oligosaccharides,^{77,78} using chemoenzymatic methods. By mimicking the biosynthetic pathway of heparin and HS, these methods are able to control the size of oligosaccharides, positions of the *N*-sulfate GluAs, 2-*O*-sulfate IdoAs, or 6-*O*- and *N*-disulfo GluA residues. Compared to lengthy chemical syntheses, chemoenzymatic syntheses are able to produce homogeneous ULMWH from 10- to 12- step chemoenzymatic syntheses.⁷⁹ These ULWMHs have displayed excellent *in vitro* anticoagulant activity and show comparable pharmacokinetic properties to Arixtra. However, these chemoenzymatic methods frequently face low

fermentation.⁸¹ Elongation of the disaccharides is accomplished using two bacterial glycosyl transferases, *N*-acetyl glucosaminyl transferase of *Escherichia coli* K5 (KfiA) and heparosan synthase-2 (pmHS2) from *Pasteurella multocida*. While this chemoenzymatic synthesis provides a general method for preparing heparins, target selection is still restricted by the substrate specificities of the enzymes; most importantly, smaller targets such as fondaparinux are still difficult to prepare using these methods.

Despite advances in the development of effective LMWHs, UF heparin remains the anticoagulant of choice because of its ease of use and low cost.⁸² Heparin is obtained by extraction from tissues of animals suitable for food (i.e., porcine intestine, bovine lung), and is processed to furnish pharmaceutical heparin as a purified heterogeneous mixture of chains⁸³ with different molecular weights and sulfation patterns. Only one-third of the chains comprising pharmaceutical grade heparin contain a binding site for AT. Current extraction methods that focus on recovery of anticoagulant heparin are required to meet US Pharmacopeal (USP) specifications, but are not able to eliminate other HS moieties from pharmaceutical heparin.

In 2007, multiple lots of animal-sourced heparin were associated with an acute, rapid onset of serious side effects indicative of an allergic-type reaction, which affected hundreds of individuals.^{84,85} This worldwide distribution of contaminated heparin resulted in an international public health crisis, raising concerns over the reliability and safety of animal-sourced heparins for clinical use.⁸⁶⁻⁸⁸ The main contaminant found in the problematic heparin samples was identified to be an oversulfated CS containing a tetrasulfated disaccharide unit. Interestingly, this oversulfated CS was structurally identical to the drug Arteparon®,⁸⁹ which is used for the treatment of degenerative joint disease in

Europe and has been demonstrated to produce an allergic-type response.⁹⁰ Given the nature of the contaminant and its structural similarity to heparin, traditional screening and separation methods cannot differentiate between affected and unaffected lots. As a result, cost-effective, reliable methods for preparing synthetic heparins are in high demand.

Chapter 2

CHEMICAL SYNTHESIS OF HEPARAN SULFATE GLYCOPOLYMER BUILDING BLOCKS

Background and motivation

Heparin has been the anticoagulant drug of choice for the treatment of arterial and venous thrombotic disorders for over a decade.⁶ This is largely due to heparin's rapid anticoagulant response, and because the excessive anticoagulant activity can be reversed by protamine.⁸ While heparin is the only drug that inhibits the activities of both factor Xa (fXa) and thrombin (fIIa), it is known to cause one of the most important and most frequently drug-induced, immune-mediated types of thrombocytopenia: heparin-induced thrombocytopenia (HIT). The condition is caused by the induction of antibodies against the complex of platelet factor 4 (PF4) and heparin.¹⁰ With such widespread use of heparin in clinics, the development of a new generation of improved heparin-based anticoagulant drugs with reduced side effects remains a high priority for the scientific community.

Low molecular weight heparins (LMWHs), such as Arixtra®, have been playing an increasingly important role in preventing venous thrombosis among high-risk patients^{11,12} due to more predictable anticoagulant doses, longer half-lives, and reduced risks of osteoporosis.¹³ The elucidation of the structure of the antithrombin-binding pentasaccharide sequence in heparin, and its mechanism of action, has accelerated the development of rationally designed synthetic heparins. Utilizing current knowledge of the anticoagulant activity of heparan sulfate (HS), its mechanism of action, and the effects of multivalency of biologically active polymers, we designed a HS glycopolymer through an efficient,

multistep converging synthesis. We envisioned the synthesis of a biologically active polymer by including the bioactive components of anticoagulant heparin, which would be easier to obtain than purely synthetic polysaccharides, while simultaneously eliminating the unwanted side effects of animal-sourced heparin caused by structural heterogeneity and contamination by other GAG-like compounds.

Synthetic design of HS glycopolymers

Mechanism of action

Blood coagulation is a tightly regulated process requiring rapid and localized activation of coagulation proteases at sites of vascular damage.¹⁴ If the hemostatic response is insufficient, the result is life-threatening bleeding; in contrast, if the response is not contained, the result is life-threatening thrombosis. Heparin, while most commonly used in clinics, is produced and secreted exclusively by mast cells and is not a physiological activator of AT; rather, the closely-related cousin HS, which lines the vascular wall, interacts with a fraction of the circulating AT to ensure the fluidity of the microvasculature.¹⁵ The chemical synthesis of biologically active heparin, HS oligosaccharides, and the anticoagulant pentasaccharide motif has led to a detailed understanding of heparin's mechanism of action within the coagulation cascade.

Antithrombin (AT) is the principal inhibitor of proteases in the coagulation cascade, and is the effector molecule for anticoagulant heparin. AT circulates in plasma at a high concentration of 2.3 μM ; thus, its activity must be strictly controlled to allow for proper and precise clot formation while preventing thrombosis. AT is activated by exploiting the inherent conformational plasticity of serine protease inhibitors (serpins). Serpins are best

described as having a ‘spring-loaded mousetrap’ mechanism,¹⁶ where disturbing the peptide loop activates the enzyme trap and catches the target protease in stoichiometric and irreversible inhibition. The active state of a serpin is metastable, and the energy released upon conversion to its most stable form is used to trap the protease. Based on rates of inhibition, AT’s primary protease targets are factors IXa, Xa, and thrombin. The anticoagulant effect of heparin and the new synthetic LMWHs is mediated through the activation of AT as an inhibitor of these coagulation proteases.^{17,18}

AT normally circulates in an inactive form, and only becomes an effective inhibitor upon interacting with anticoagulant HS, which is expressed on the blood vessel walls or in therapeutic heparin.¹⁹ It has been established through biochemical studies that heparin binding induces a large-scale conformational change in AT (Figure 2.1, A; Figure 2.2).²⁰⁻²³ AT first binds the pentasaccharide by an induced-fit mechanism involving an initial weak

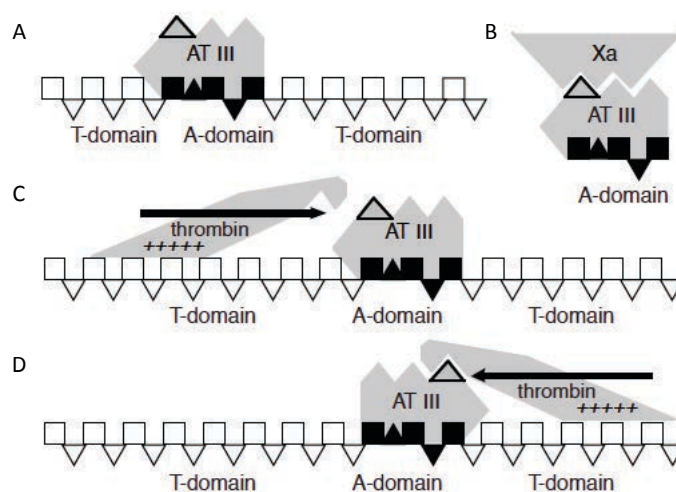


Figure 2.1: Inhibition of factor Xa and thrombin by antithrombin and heparin.⁴ Heparin is shown as a repetition of squares (glucosamine) and triangles (uronic acid). **A**, Antithrombin binds to the heparin pentasaccharide-binding site (A domain, black squares and triangles), and goes through a conformational change (hatched triangle). **B**, The conformational change alone is sufficient to inhibit fXa. **C**, Thrombin requires attraction by the negative charges of the thrombin-binding domain (T-domain). Thrombin ‘slides’ along the heparin chain until it hooks itself onto the exposed loop of activated antithrombin. **D**, The well-defined structure of the heparin-antithrombin complex requires thrombin to approach from the correct side to be irreversibly inhibited.

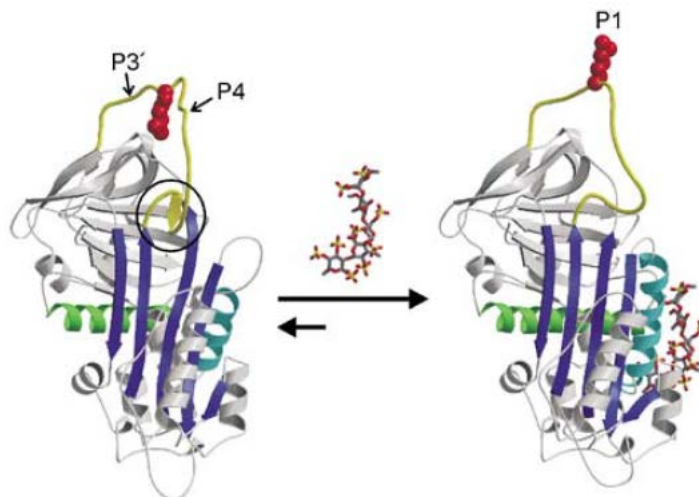


Figure 2.2: The structural features of native and pentasaccharide-activated AT.³ Binding of the heparin pentasaccharide (rods with gray C, red O, yellow S) induces local and global conformational changes, resulting in the expulsion of the hinge region (circle) and the reorientation of the RCL.

interaction; the resulting conformational change transforms AT to a high-affinity state, with an overall dissociation constant of ~ 50 nM.²¹ The structures of AT reveal conformational changes in the vicinity of the pentasaccharide and in the reactive center loop (RCL; Figure 2.2), indicating a global conformational change in response to heparin binding (allosteric mechanism).

Heparin accelerates the inhibitory activity of AT through two distinct mechanisms; this is reflected in the way certain heparin fragments are able to accelerate fXa inhibition by 500 fold, while not appreciably accelerating thrombin inhibition.²⁴ The allosteric activation of AT upon binding to the anticoagulant pentasaccharide results in the recognition and inhibition of fXa (Figure 2.1, B). In contrast, thrombin inhibition requires both AT and thrombin to bind to a single heparin chain, where heparin serves to bridge the two proteases. Upon AT activation, thrombin is electrostatically attracted by heparin's negatively charged template and collides with heparin-bound AT to form a ternary complex (Figure 2.1, C). Although the interaction between thrombin and a negatively charged

heparin chain is less specific than a pentasaccharide-AT interaction, thrombin inhibition requires a longer heparin chain,²⁵ which is more prone to react with other biological molecules such as platelet factor 4 (PF4).²⁶

The interaction between the anticoagulant pentasaccharide and AT is incredibly specific, where small alterations in either the sulfation pattern or carbohydrate sequence can significantly reduce binding affinity.²⁷ Of the eight-to-ten negatively charged groups on the pentasaccharide available for interaction with AT, six interact with AT (Figure 2.3). While these charged interactions of the HS pentasaccharide are sufficient for fXa inhibition, the necessary size of an oligosaccharide for thrombin inhibitory activity is much longer (14-20 saccharides).²⁸ Studies using a synthetic HS mimetic consisting of an AT-binding domain, a nonsulfated linker region, and a thrombin-binding domain suggest that the structural requirements for heparin binding to thrombin is less selective than for AT, and requires only sulfated saccharide units.²⁹

The roles of each of the charged groups of the biologically active pentasaccharide have been determined by chemically synthesizing a series of pentasaccharides with various combinations of sulfate groups and carboxyl groups.³⁰ Removal of specific sulfate and carboxyl groups (Figure 2.3, green boxes) significantly compromises the binding affinity to AT, suggesting these particular groups are critical for AT activation, and subsequent fXa

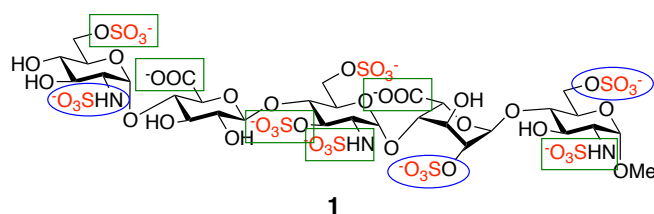


Figure 2.3: The antithrombin-pentasaccharide interactions.³ Charged groups required for AT binding are notated with green boxes; groups with blue circles are not required, but have been shown to contribute to AT binding.

inhibition.³¹ Of these sulfate groups, the most critical motif involved in HS binding to AT is the rare 3-O-sulfate group; a pentasaccharide lacking this 3-O-sulfate group has been shown to decrease binding affinity by nearly 20,000 fold. Interestingly, the introduction of an additional 3-O-sulfate group on a pentasaccharide analogue has been shown to increase AT binding affinities.³² In addition to the position and number of charges, the type of charge is also critical for biological activity; exchanging the sulfate groups for phosphate or carboxylate groups affect binding affinity to AT.³³

Although structure-function studies have revealed that a sulfated pentasaccharide represents the minimum active motif, we hypothesized that an HS disaccharide may be sufficient for biological activity, provided that its binding affinity could be enhanced through avidity. By repeatedly displaying a sulfated disaccharide along a polymer backbone in a pendant-like fashion (Figure 2.4), we hoped that a highly sulfated disaccharide would be sufficient due to enhanced local concentrations of a partially bioactive unit.³⁴ The effectiveness of this type of approach has been previously observed in our lab in studies of neuroactive disaccharide- and tetrasaccharide-based CS

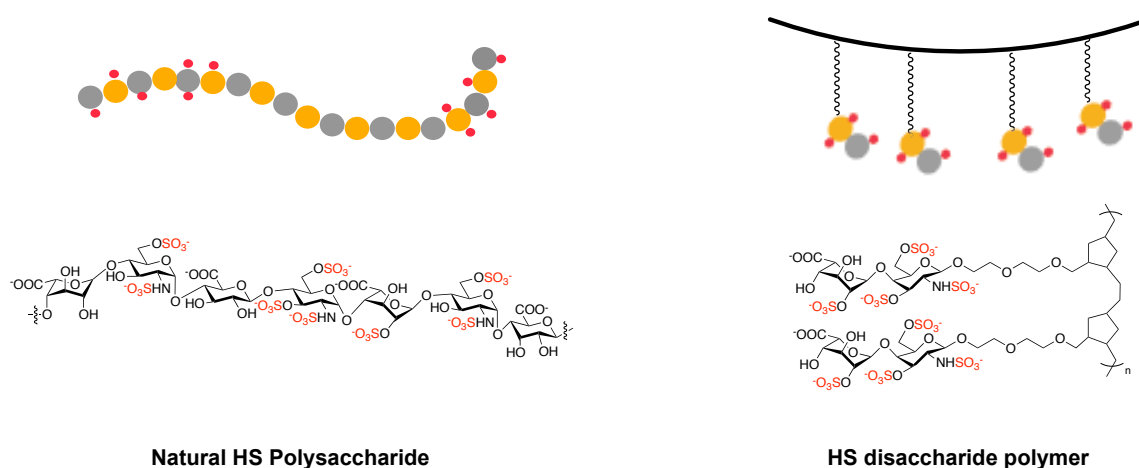


Figure 2.4: Synthetic HS glycopolymer vs natural HS polysaccharide.

glycopolymers.^{35,36}

In designing a disaccharide-based HS glycopolymer, it was critical to select a minimal unit that effectively encapsulated the key determinants of the AT-binding pentasaccharide. We selected a disaccharide motif from the reducing end of the pentasaccharide sequence (G and H, Figure 2.5). These two monosaccharides have well-characterized interactions with the A-helix (R46, R47) and P-helix (K114, D113) of AT,³⁷ and allowed us to exploit the conformational flexibility of the G unit L-IdoA, which has been shown to substantially improve the affinity of heparin for AT.³⁸ Importantly, the 3-O-sulfate group on unit H mimics the structure of Org31550, in the presence of the 3-O-sulfate group of unit F, was found to increase the anti-fXa activity by two-fold in pharmacological animal studies.³⁹ With all such considerations, the target disaccharide **GlcNS3S6S- α -(1 \rightarrow 4)-IdoA2S** would be presented along a polymeric backbone to display this bioactive anticoagulant sulfation pattern in a multivalent fashion to mimic the sulfation pattern and overall charge display of natural heparin and HS polysaccharides (Figure 2.4).

The mechanism of anticoagulant heparin activity suggests that a structure of an oligosaccharide that could mimic its full anti-fXa and anti-thrombin activity would require an AT-binding domain (Figure 2.1, A-domain) coupled to a thrombin-binding domain

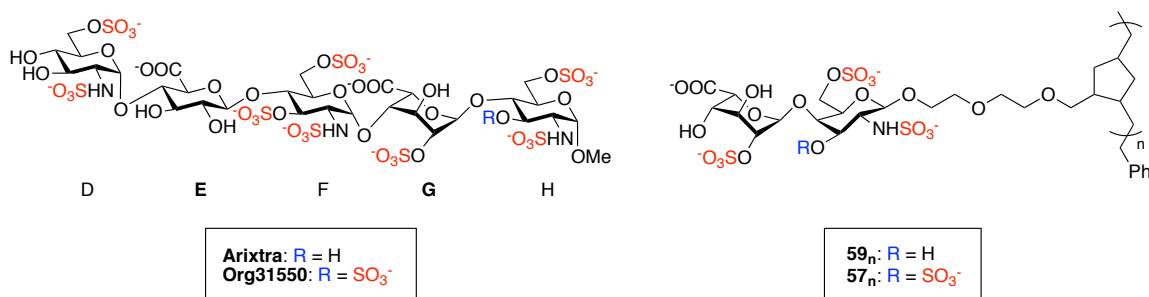


Figure 2.5: Structures of Arixtra and Org31550. The HS glycopolymers contain the monosaccharide units G and H of Arixtra and Org31550.

(Figure 2.1, T-domain).⁴⁰ Given that this type of heparin polysaccharide would comprise between 14 and 20 saccharide units,^{28,41-43} we envisioned that an extended A-domain displaying the pentasaccharide sulfation pattern could potentially serve as a T-domain, which would allow AT binding at either end of the molecule and attract thrombin. With this type of display, one could expect to observe thrombin inhibition as soon as the polysaccharide chain is long enough to simultaneously accommodate AT and thrombin.

Using chemical synthesis, we aimed to synthesize an anticoagulant HS mimetic with tunable length and charge, in order to understand the effects of sulfation pattern and macromolecular structure on the biological activity of GAG mimetic glycopolymers. We decided to utilize polymerization chemistry to achieve a multivalent display, to control the length of HS mimetics, and to mimic the macromolecular structure of natural GAG polysaccharides. By controlling polymer length strictly with the hydrocarbon backbone, we would retain the biologically active anticoagulant sulfation pattern and mimic the charge distribution of a heparin polysaccharide required for thrombin inhibition.

Synthesis of HS monomer building blocks

GAG-based oligosaccharides are generally perceived to be difficult to synthesize by purely chemical methods. Without the help of glycosyltransferases, it is synthetically challenging to establish the specific stereochemistry and regioselectivity of complex carbohydrate structures. Additionally, the polyfunctional nature of carbohydrates requires extensive protecting group (PG) chemistry for the synthesis of even the simplest derivatives.⁴⁴ While only hydroxyl groups need to be protected, a variety of PGs are necessary to precisely control the availability of each of the hydroxyl groups. Such PG manipulation is more pronounced in the preparation of complex oligosaccharides and GAG fragments.

PGs temporarily mask functional groups that interfere with intermediary reactions, and thus require a number of different properties for efficient syntheses: 1) reagents for their introduction and removal must be readily available; 2) their introduction should not be accompanied by the formation of a new asymmetric center or only one stereoisomer must be formed; 3) they should be stable throughout all intermediate reactions and work-up conditions. If possible, protecting groups can be manipulated to produce hydrophobic intermediates to simplify extractive work-ups, or can be used to afford crystalline compounds for convenient purification. Finally, separation of the protected or deprotected products should ideally be easily separated from the preceding compounds.

For the synthesis of complex carbohydrate structures, two types of PGs are generally used. 'Permanent' PGs are carried through to the very last synthetic steps, to unveil hydroxyl groups on target compounds. Benzyl or benzyl-derivative groups are often applied as permanent PGs if the target compound is sensitive to basic conditions; ester-PGs

are used when compounds carry unsaturated groups that can be reduced by hydrogenolysis reactions. ‘Temporary’ PGs are selectively removed during the synthetic route to expose hydroxyl groups for specific transformations (i.e., glycosylation reactions or other chemical modifications). In the case of a branched oligosaccharides or when substituents (e.g., sulfate, phosphate) are present, numerous *orthogonal* temporary groups are necessary so they can be selectively removable in the presence of each other.

The PGs employed in carbohydrate chemistry are essentially identical to those commonly used in organic chemistry (Figure 2.6). To differentiate the hydroxyl groups on carbohydrates, multiple PG manipulations are usually necessary. Of the possible PG functionalities, acetyl, benzoyl, and benzyl groups are most commonly used because of their ease of orthogonal introduction and removal. Many other groups, such as silyl, chloroacetyl, *p*-methoxybenzyl, and various acetal groups are also used as temporary PGs for their efficient introduction at multiple positions and their selective cleavage. Benzoate esters can be used as permanent groups with selectively removable acetate or chloroacetate esters. Pivaloyl, levulinoyl, or chloroacetyl groups can also be selectively removed in the

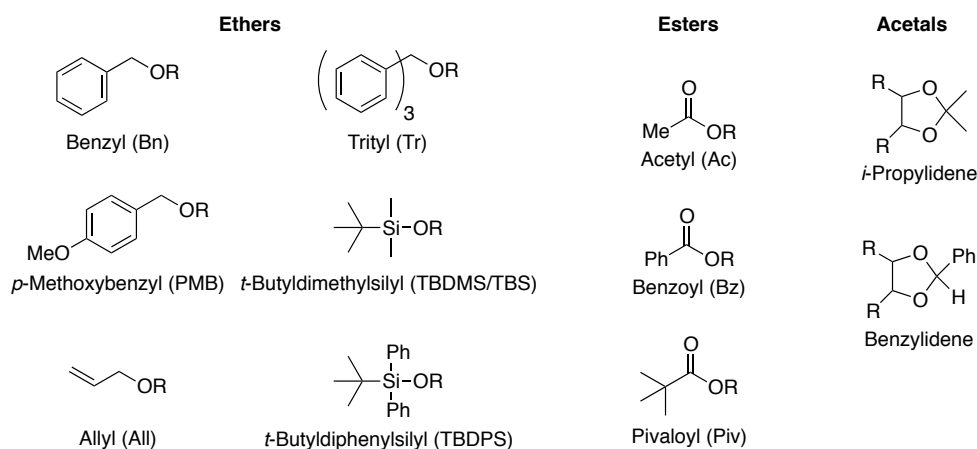
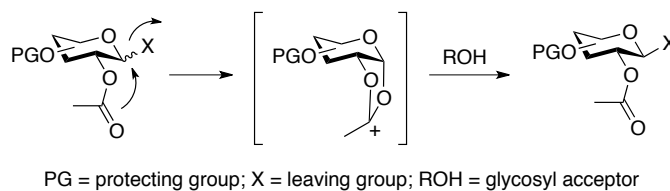


Figure 2.6: Commonly used protecting groups in carbohydrate chemistry and organic synthesis.

presence of permanent acetate esters. Acetals are usually employed for the simultaneous temporary protection of multiple hydroxyl groups, and can be cleaved in a selective manner.

Although PGs are traditionally used to simply mask specific functional groups, in the context of carbohydrate chemistry, they can also indirectly participate in reactions. While carbohydrate PGs still serve to inhibit the participation of hydroxyl or other functional groups, incorporation of particular PGs into the donor and acceptor molecules can strongly influence the stereochemical outcome of activation and coupling reactions through electronic and/or steric influences. This influence of PGs on the stereochemistry of reactions is known as ‘neighboring-group participation’ or ‘anchimeric assistance’.

The most common form of neighboring-group participation is the participation of acyl groups at the C-2 position of monosaccharides. During glycosylation reactions (Scheme 2.1), the neighboring acyl group of the donor assists the departure of the activated anomeric leaving group, subsequently leading to the formation of a stable dioxolenium ion. Because the glycosyl acceptor can only attack from the backside, forming a 1,2-*trans* glycoside. With this effect, glucosyl-type donors afford β -glycosides, and manno-type donors produce α -glycosides. Many ester-type PGs such as acetate, chloroacetate, benzoate, and pivaloate are used to construct 1,2-*trans* glycosidic linkages. Recently, new participating groups have been developed to expand their scope beyond 1,2-*trans*



Scheme 2.1: The stereoselective formation of glycosidic bonds by neighboring-group participation.

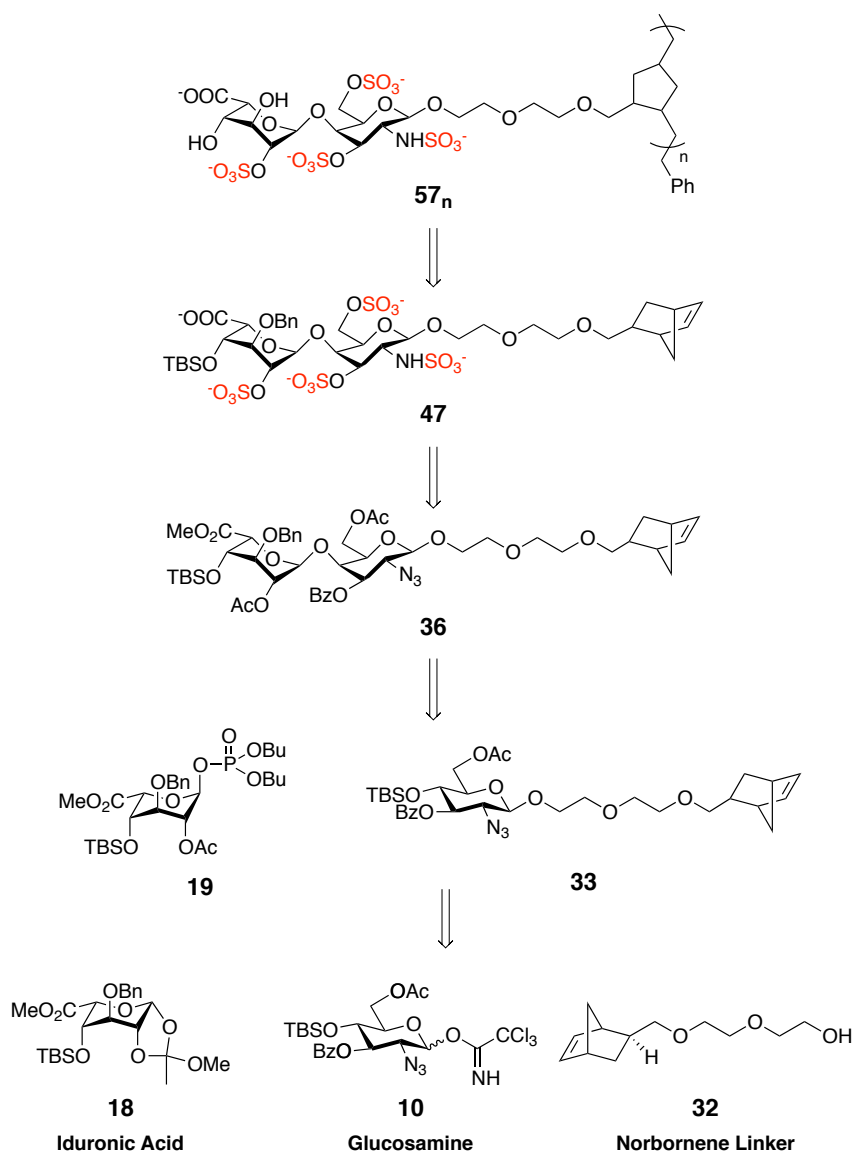
glycosidic linkages to construct 1,2-*cis* glycosides, by allowing the intermediate oxocarbenium-ions to be attacked from one particular side.

With the importance of orthogonal PGs and the role of neighboring-group participation in mind, we designed a retrosynthetic strategy for the proposed HS glycopolymers based on a tetrasulfated HS disaccharide and norbornene-based linker (Scheme 2.2). The HS disaccharide monomer can be divided into three main building blocks: a protected IdoA, a protected GlcN, and a norbornene-diethylene glycol linker. Protecting groups on the disaccharide were selected to be orthogonal to allow access to a variety of different sulfation patterns, as well as two distinct glycosidic bonds. These HS building blocks have been used to synthesize anticoagulant HS glycopolymers, as well as tunable HS glycopolymers that can modulate chemokine activity.⁴⁵

A combination of permanent and temporary protecting groups were selected to allow for orthogonal protection of the disaccharide hydroxyl groups. Permanent benzyl (Bn) and *tert*-butyldimethylsilyl (TBS) groups were selected to protect the C-3 and C-4 positions of IdoA, respectively. While the Bn group would not be removed until the final hydrogenolysis reaction, the TBS group would be available for selective removal from the IdoA monosaccharide to allow for the GlcN $\alpha(1\rightarrow4)$ IdoA glycosylation reaction. The C-2 hydroxyl of IdoA was protected with an acetyl group that could be simultaneously installed with an anomeric glycosyl phosphate from an idoA 1,2-orthoester precursor. This C-2 acetyl group would also act as a participating group to guide the stereoselectivity of the IdoA-GlcN glycosidic bond.

Similarly, the GlcN monosaccharide was also designed to entail a variety of permanent and temporary protecting groups. The amine was protected as an azide

throughout the majority of synthesis, until it would be reductively aminated and subsequently sulfated. The C-3 hydroxyl was protected with benzoate (Bz) for simultaneous deprotection with the C-6 GlcN acetate (Ac) and C-3 acetate of IdoA under basic conditions. A TBS group was used to protect the C-4 hydroxyl group of GlcN; by being orthogonal to the C-3 benzoate group, the TBS group could be selectively removed



Scheme 2.2: Retrosynthesis of HS glycopolymers. Bn = benzyl, Me = methyl, Ac = acetyl, Bz = benzoyl, TBS = *tert*-butyldimethylsilyl.

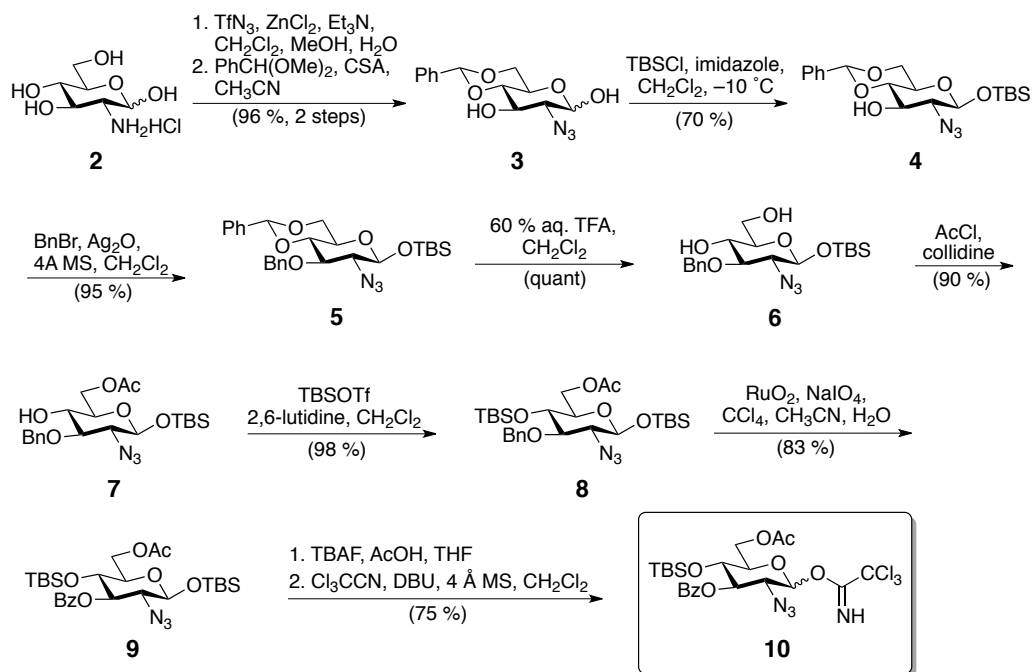
for glycosidic bond formation. For an alternative polymer derivative (GlcN-IdoA-linker monomer), the TBS group would act as a permanent protecting group and be desilylated towards the end of the synthesis. Finally, the anomeric position of the GlcN was activated with a trichloroacetimidate for efficient coupling with the norbornene linker or idoA acceptor.

Overall, the ester-based protecting groups installed on the C-2 of IdoA and C-3/C-6 of GlcN were selected to reduce the number of synthetic steps by allowing for simultaneous deprotection under basic conditions and subsequent *O*-sulfation at three unique positions. Additionally, both *O*- and *N*-sulfation reactions would be carried out before polymerization; while this was expected to affect solubility of the monomers, it would ensure complete, homogeneous sulfation of the HS disaccharides.

A norbornene-based linker was utilized to take advantage of its ring-strain during ring-opening metathesis polymerization (ROMP) chemistry; ROMP chemistry has been previously shown to have high functional group tolerance and has been used for other biologically relevant polymer species (see chapter 3). ROMP's mild reaction conditions were essential for HS monomer polymerization due to their labile sulfate groups. A diethylene glycol linker was added to the norbornene ring to increase hydrophilicity and flexibility, which could potentially aid in protein recognition. This type of norbornene-based linker has been previously used in our lab for the synthesis of various CS glycopolymers.^{35,36}

Synthesis of protected glucosamine

The orthogonally protected glcN trichloroacetimidate building block can be synthesized from commercially available glucosamine hydrochloride in 10 steps with an overall 35% yield (Scheme 2.3). D-Glucosamine hydrochloride **1** was subjected to a diazo transfer reaction to convert the 2-amino group into the corresponding azide,⁴⁶ which was necessary for α -selective glycosylations and masked the free amine until it was sulfated at a later stage. This type of direct installation of an azide from commercially available amino sugars was first reported for the preparation of 2-azido-2-deoxy-D-*gluco*, D-*manno*, D-*galacto*, and D-*allo* derivatives.⁴⁷ The resulting azide intermediate was directly subjected to benzylation using benzaldehyde dimethyl acetal and catalytic camphorsulfonic acid (CSA) in acetonitrile to install the 4,6-benzylidene on **3**.^{46,48-51} Both reactions proceed in

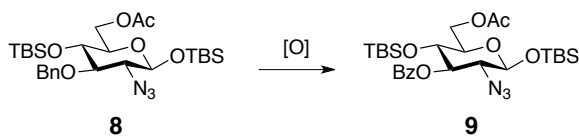


Scheme 2.3: Synthesis of orthogonally protected GlcA monomer. Ac = acetyl, CSA = (\pm)-DL-camphor-10-sulfonic acid, Ph = phenyl, TBSCl = *tert*-butyldimethylsilyl chloride, TBS = *tert*-butyldimethylsilyl, Bn = benzyl, TFA = trifluoroacetic acid, TBSOTf = *tert*-butyldimethylsilyl trifluoromethanesulfonate, Bz = benzoyl, TBAF = tetrabutylammonium fluoride, DBU = 1,8-diazabicyclo[5.4.0]undec-7-ene.

near-quantitative yield and are highly scalable (~150g).

Stereoselective silylation installed an anomeric TBS group using TBSCl and imidazole to reach compound **4** in 70% yield.⁵² Subsequent benzylation of the 3-hydroxyl group using freshly prepared Ag₂O and benzyl bromide afforded **5** in 95% yield.⁵³ This protected glucosamine derivative was then subjected to 60% aqueous TFA, which removed the 4,6-benzylidene and exposed the two corresponding hydroxyl groups of compound **6**. This compound was then subjected to acetylation, which resulted in the selective primary acetylation to afford **7** in 90% yield.⁵⁴ A TBS group was then installed on the remaining C-4 hydroxyl group using *tert*-butyldimethylsilyl trifluoromethanesulfonate (TBSOTf), to afford the fully protected glucosamine intermediate **8**.

Compound **8** could be directly used towards syntheses with final C-3 hydroxyl groups; for use towards our anticoagulant HS glycopolymers, **8** was subjected to further reactions to oxidize the Bn group to a Bz functionality to allow for removal under basic conditions. Towards this end, several oxidation conditions were examined. Ozonolysis⁵⁵ of



NaIO₄	RuO₂	Yield	Sm recovery
4.1	5 mol %	No conversion	100 %
4.1	20 mol %	25 %	70 %
4.1	50 mol %	52 %	39 %
10	20 mol %	31 %	60 %
10	50 mol %	78 %	12 %
10	1 eq ^a	61 %	n/a
10	1 eq^b	83 %	13 %

^aReaction stirred for 36 h at rt;

^bReaction stirred for 18 h at rt.

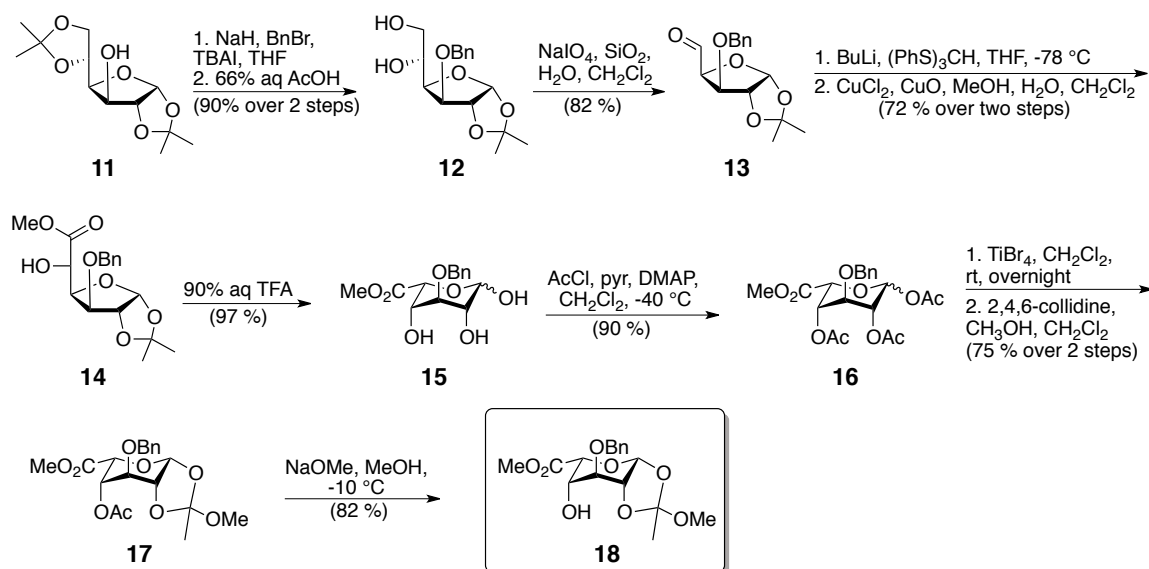
Table 2.1: Optimization of 3-O benzyl oxidation reaction.

8 afforded benzoate protected compound **9** in 62% yield. In an effort to increase reaction yields, ruthenium-mediated oxidation conditions were explored.⁵⁶⁻⁵⁸ Unlike the conditions reported in literature, excess amounts of NaIO₄ (10 eq) and RuO₂ (1 eq) were necessary to drive the reactions closer to completion (83 %). Upon exploring the effects of reaction times, it was found that extending the reaction times from 18 h to 36 h was detrimental to the reactions due to decomposition of the product under acidic conditions.

Following the oxidation of the 3-*O*-benzyl group to a benzoate group, the final GlcN building block was synthesized by anomeric desilylation of the TBS group and subsequent installation of the trichloroacetimidate. Compound **9** was first subjected to desilylation using TBAF and AcOH;⁵⁹ this crude material was subjected to a trichloroacetimidate reaction using trichloroacetonitrile and catalytic K₂CO₃ or DBU to reach desired compound **10** in 75% yield over the two synthetic steps. Both α and β isomers were observed, but subjecting both isomers to coupling reactions had little or no effect on the stereochemical outcome of the reactions.

Synthesis of protected iduronic acid

The synthesis of the partially protected idoA intermediate **18** was synthesized in 30% yield over 10 steps (Scheme 2.4). Commercially available diacetone-D-glucose **11** was first transformed to diol **12** through benzylation with NaH and benzyl bromide and selective acetal cleavage with aqueous acetic acid.⁵⁴ This afforded the monobenzylated diol **12** in 90% yield over two steps. Subsequent oxidative cleavage of **12** with aqueous NaIO₄ adsorbed onto silica yielded aldehyde **13**.⁶⁰⁻⁶³ Unlike reaction conditions that have



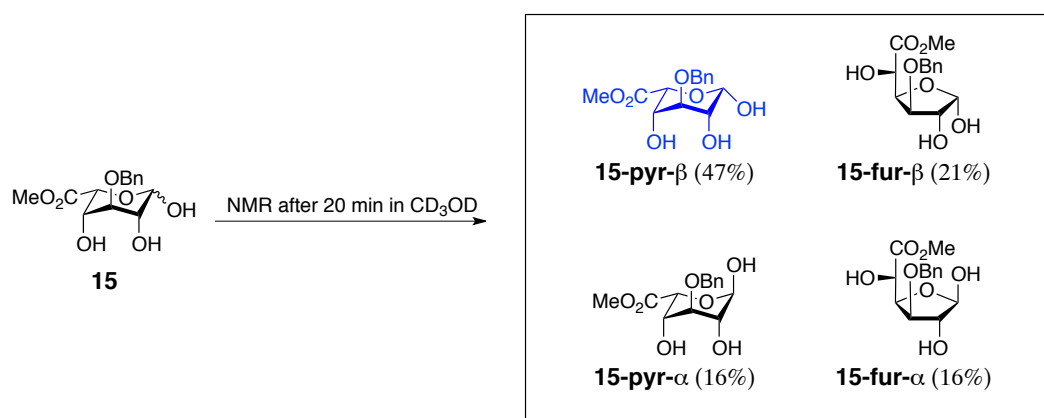
Scheme 2.4: Synthesis of orthogonally protected IdoA monomer. TBAI = tetrabutylammonium iodide, Ac = acetyl, Bn = benzyl, Bu = butyl, TFA = trifluoroacetic acid, pyr = pyridine, Me = methyl, DMAP = 4-dimethylaminopyridine.

previously been reported,⁶⁴ a second portion of SiO_2 was necessary after the reaction was complete. The crude aldehyde intermediate **13** was directly subjected to the next reaction.

Due to the conformational flexibility of furanose rings and various chelate possibilities, it is difficult to control the stereochemical outcome of organometallic reagent additions on dialdose derivatives such as **13**. Previous studies have demonstrated that the addition of bulky groups such as *tris*-(phenylthio)methyl lithium⁶⁵ led to high conversion to *L-ido* diastereomers.^{63,66} Reaction of aldehyde **13** with freshly prepared *tris*-(phenylthio)orthoformate and *n*-butyl lithium produced *tris*-(phenylthio)methyl lithium *in situ*, forming the *L*-idose configured thioortho ester intermediate in high yield.⁶³ The resulting *tris*-phenylthioorthoester was treated with CuCl_2/CuO in a $\text{MeOH}/\text{H}_2\text{O}/\text{CH}_2\text{Cl}_2$ solvent mixture^{67,68} to cleave the thioortho ester to furanose methyl ester **14** in 72 % yield over two steps.⁶⁹ Though previous studies have reported the need for K_2CO_3 in methanol to convert small amounts of a phenylthioester byproduct,⁵⁴ this byproduct was not observed.

The 1,2-isopropylidene was removed from furanose **14** in quantitative yield using 90 % aqueous trifluoroacetic acid. This yielded the crystalline 3-*O*-benzyl iduronic methyl ester monosaccharide **15** in its pyranose form in near-quantitative yield.⁶² Recrystallization was required to obtain the desired pyranose **15-pyr-β**; purification with silica gel chromatography resulted in the formation of undesired pyranose and furanose isomers (Scheme 2.5). AcCl was used as an acetylating agent with pyridine as base and DMAP as catalyst; conditions using Ac₂O were avoided because it has previously been shown to give low yields of the desired furanose compounds.⁷⁰

Nearly quantitative conversion of **16α/β** into anomeric bromide intermediate was then performed with TiBr₄, as previously described.⁶⁹ The crude brominated intermediate was immediately subjected to a reaction to install a 1,2-methylorthoester using methanol and 2,4,6-collidine.⁷¹ The methylorthoester was intentionally installed to simultaneously protect the C-2 position with an acetyl group during the installation of an activating group to the anomeric position. Additionally, the orthoester served to lock the monosaccharide in a stable ¹C₄ pyranose form. Compound **18** was designed to serve as a glycosyl acceptor in the synthesis of different HS disaccharide molecules by adjusting the C-4 PG. For the



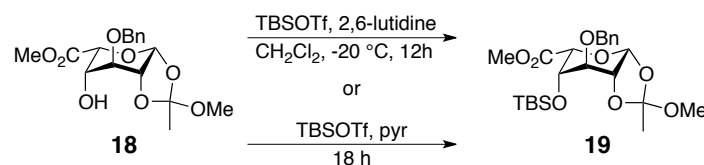
Scheme 2.5: Isomers produced by triol intermediate **15** *in situ*. Me = methyl, Bn = benzyl.

purpose of synthesizing the proposed anticoagulant HS glycopolymers, the C-4 hydroxyl group of **18** was first protected, and then subsequently converted to a glycosyl donor by activating the anomeric position as a glycosyl phosphate.

The introduction of different protecting groups, including silyl ethers, esters, and alkyl ethers on the open C-4 hydroxyl can be readily achieved, as seen in various idoA derivatives.⁵⁴ Silylation can be accomplished through the use of silyl triflates, and esters can be introduced with acid anhydrides and DMAP. In contrast, alkylation poses more of a challenge; the C-5 stereocenter can epimerize in the presence of a strong base, but alkylation has been successfully accomplished with silver oxide and corresponding alkyl bromides.⁶⁴ Several attempts were made to install a variety of silyl and alkyl ethers to the C-4 hydroxyl group of methylorthoester IdoA **18**.

Following the original retrosynthesis, reaction conditions were first examined to install a TBS group to **18** (Table 2.2); this would allow for the selective deprotection of the C-4 hydroxyl group, allowing access to a GlcN- α (1,4)-IdoA glycosidic bond in addition to the IdoA- α (1,4)-GlcN glycosidic linkage. At low temperatures (-20 °C), the desired TBS protected compound **19** was generated using *tert*-butyldimethylsilyl trifluoromethanesulfonate (TBSOTf) and 2,6-lutidine, but only in low to moderate yields.^{72,73} Upon optimizing the equivalents of TBSOTf and reaction temperatures, **19** was furnished in up to 94 % yield using an excess amount of TBSOTf in pyridine at 0 °C for 18 h. Compound **19** was then used to prepare glycosyl phosphate **20** for use in the glycosylation reaction with GlcN acceptor **34**.

Although 1,2-glycosyl orthoesters are valuable synthetic intermediates use to prepare carbohydrate building blocks, direct coupling generally results in poor yields, and

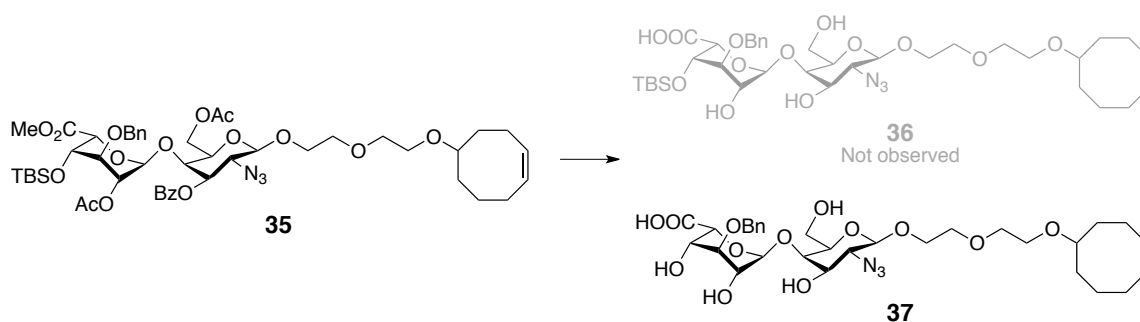


Entry	TBSOTf	Base	Temperature	Yield
1	2.5 eq	2,6-lutidine; 3 eq	-20 °C	25 %
2	10 eq	2,6-lutidine; 10 eq	-20 °C	49 %
3	3 eq	pyridine (0.1 M)	0 °C to rt	43 %
4	10 eq	pyridine (0.1 M)	0 °C to rt	50 %
5	3 eq	pyridine (0.1 M)	0 °C	75 %
6	10 eq	pyridine (0.1 M)	0 °C	94 %

Table 2.2: Optimization of C-4 TBS protection of **18**. Me = methyl, Bn = benzyl, TBSOTf = *tert*-butyldimethylsilyl trifluoromethanesulfonate, pyr = pyridine, TBS = *tert*-butyldimethylsilyl.

excess orthoester is required.⁷⁴ Recently, the Seeberger group reported the stereoselective conversion of 1,2-orthoesters to glycosyl 1-phosphate triesters by employing phosphate diesters as both a nucleophile and an acidic activator.⁷⁵ Although there are a variety of traditionally used anomeric leaving groups,⁷⁶ such as glycosyl chlorides, bromides, iodides, trichloroacetimidates, fluorides, *n*-pentenyl glycosides, anhydro sugars, anomeric aryl sulfoxides, and thioglycosides for the construction of glycosidic linkages,⁷⁷ we decided to employ glycosyl phosphates as glycosylating agents⁷⁸ to utilize the methylorthoester's functionality to simultaneously install the C-2 acetyl PG during anomeric activation.

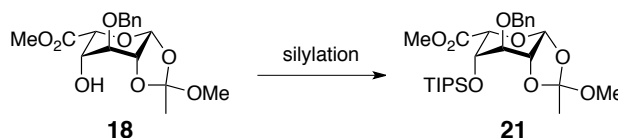
Conversion of the TBS-protected **19** to the glycosyl phosphate **20** was achieved by following the simplified reaction conditions reported by the Seeberger group,⁷⁵ without further optimization. However, in the process of synthesizing cyclooctene-based glycopolymers using glycosyl phosphate **20**, it was discovered that while the glycosylation reaction proceeded smoothly, the C-4 IdoA silyl group was removed during the saponification stage of the synthesis (Scheme 2.6; also see Appendix). This required us to reexamine the PG strategy for the C-4 hydroxyl of **18**. Attempts were made to synthesize



Scheme 2.6. Saponification of TBS-protected cyclooctene-based HS disaccharide monomer. Me = methyl, TBS = *tert*-butyldimethylsilyl, Bn = benzyl, Bz = benzoyl, Ac = acetyl.

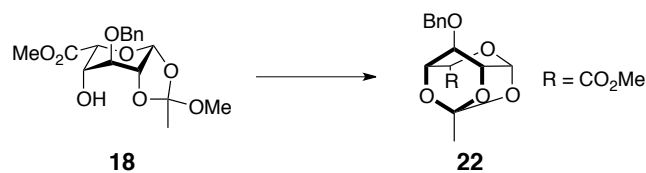
glycosyl phosphates with triisopropylsilyl (TIPS), *p*-methoxybenzyl (PMB), and benzyl (Bn) groups.

Following the installation of the C-4 TBS group, a TIPS protected derivative of **18** was synthesized. Attempts to install a TIPS group at the open hydroxyl group using triisopropyl trifluoromethanesulfonate (TIPSOTf) were largely unsuccessful (Table 2.3). The reaction conditions most frequently resulted in the formation of a ‘caged’ iduronic acid byproduct (Table 2.3, entries 2-4; Scheme 2.7); this particular byproduct formation was irreversible, and was frequently observed during the installation of various other PGs.



Entry	Reaction conditions	Temp/time	yield
1	TIPSOTf (2 eq), NaH (1.5 eq), THF ^{1,2}	-10 °C to 0 °C, 20 min	decomposition
2	TIPSOTf (5 eq), pyr	rt to -10 °C, 1.5 h	Byproduct 22
3	TIPSOTf (5 eq), 2,6-lutidine ¹	rt to -10 °C, 1.5 h	Sm and byproduct 22
4	TIPSOTf (1.3 eq), pyr (2 eq), CH ₂ Cl ₂	0 °C, o/n	Incomplete conversion to 22

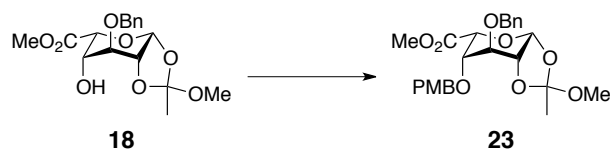
Table 2.3: Reaction conditions for TIPS protection of **ido8**. Me = methyl, Bn = benzyl, TIPS = triisopropylsilyl.



Scheme 2.7: Caged byproduct formation

Following the silylation of **18**, attempts were also made to install a PMB PG. PMB trichloroacetimidate (PMBTCA) was selected to introduce the functional group with $\text{BF}_3 \cdot \text{OEt}_2$ as the promoter.⁷⁹ Previously reported reaction conditions using 1.2 eq of PMBTCA and 2.5 mol% of the promoter afforded the desired product in only moderate yields, even at elevated temperatures. By increasing the eqs of PMBTCA to 10 eqs and $\text{BF}_3 \cdot \text{OEt}_2$ to 0.1 eq, the desired product could be obtained in 70 % yield. Milder reaction conditions using PMBTCA and lanthanum triflate were also used in an attempt to increase the reaction yield further.⁸⁰ Although high yields (~95 %) were reported for the protection of protected monosaccharides in under 5 min, the reported reaction conditions only yielded 30 % of the desired PMB protected idoA derivative **23**.

A protecting group of particular interest to the HS disaccharide synthesis was the installation of a C-4 benzyl group; since the C-4 IdoA position on the target compound is

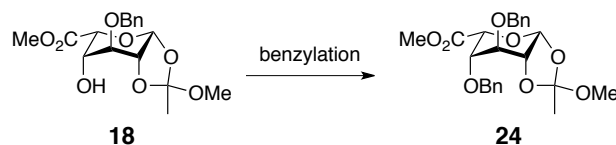


Entry	Reaction Conditions	Temp/time	yield
1	PMBTCA (1.2 eq), $\text{BF}_3 \cdot \text{OEt}_2$ (2.5 mol%), CH_2Cl_2	-40 °C, 30 min	32 %
2	PMBTCA (1.1 eq), $\text{BF}_3 \cdot \text{OEt}_2$ (2.5 mol%), CH_2Cl_2	-20 °C, 3 h	62 %
3	PMBTCA (10 eq), $\text{BF}_3 \cdot \text{OEt}_2$ (0.1 eq), CH_2Cl_2	-40 °C, 30 min	70 %
4	PMBTCA (1.5 eq), $\text{La}(\text{OTf})_3$ (5 mol%), toluene	rt	30 %

Table 2.4: Reaction conditions for PMB protection of **ido8**. Me = methyl, Bn = benzyl, PMB = *p*-methoxybenzyl, PMBTCA = *p*-methoxybenzyl trichloroacetimidate.

not sulfated, this permanent benzyl group could be simultaneously removed with the C-3 benzyl group, reducing the number of synthetic steps. Initial attempts utilized traditional benzylation conditions, using benzyl bromide with sodium hydride or silver oxide. Conditions using NaH with benzyl bromide in DMF or THF resulted in low conversion or decomposition of the starting material (Table 2.5, entries 1-3). For conditions utilizing BnBr and Ag₂O, higher equivalents of benzyl bromide and Ag₂O were required to achieve moderate yields of the desired product (Table 2.5, entries 4-7).

Many attempts were made to synthesize benzyl-protected compound **24**, using a



Entry	Reaction conditions	Temp/time	Yield
1	BnBr (2.5 eq), NaH (2.5 eq), DMF ⁵	0 °C-rt, o/n	Low conversion
2	BnBr (1.5 eq), NaH (1.5 eq), THF	4 °C, 3 h	Decomposition
3	BnBr (1.5 eq), NaH (1.2 eq), THF	-25 °C-0 °C, o/n	Decomposition
4	BnBr (2.5 eq), Ag ₂ O (3 eq), 4 Å MS, CH ₂ Cl ₂	rt, o/n	Low conversion
5	BnBr (1.5 eq), Ag ₂ O (2 eq), 4 Å MS, CH ₂ Cl ₂	rt, o/n	Byproduct 22
6	BnBr (10 eq), Ag ₂ O (4 eq), 4 Å MS, CH ₂ Cl ₂	rt, 3d	35 %
7	BnBr (10 eq), Ag ₂ O (5 eq), 4 Å MS, DMF ⁷	rt, 2d	~ 50 %
8	Bn-OPT (3 eq), Et ₃ N (2 eq), toluene	90 °C, o/n	Decomposition
9	Bn-OPT (2 eq), MgO (2 eq), toluene	90 °C, o/n	Byproduct 22
10	BnONHCCl ₃ (20 eq), BF ₃ ·OEt ₂ (0.05 eq), CH ₂ Cl ₂	-40 °C-rt, 1.5 h	Low conversion to 22
11	BnONHCCl ₃ (10 eq), BF ₃ ·OEt ₂ (0.1 eq), CH ₂ Cl ₂	-40 °C, 1.5 h	Low conversion
12	BnONHCCl ₃ (20 eq), BF ₃ ·OEt ₂ (2 eq), CH ₂ Cl ₂	-20 °C, 2 h	Low conversion
13	BnONHCCl ₃ (20 eq), TBSOTf (0.2 eq), CH ₂ Cl ₂	-20 °C, 2 h	Low conversion
14	BnONHCCl ₃ (20 eq), TBSOTf (2 eq), CH ₂ Cl ₂	-20 °C, 2 h	Low conversion
15	Ag ₂ O (4 eq), 4 Å MS, TBAI (0.1 eq), BnBr ⁹	rt, 12 h	50 %
16	Ag ₂ O (5 eq), 4 Å MS, TBAI (0.5 eq), BnBr	rt, 12 h	63 %
17	Ag₂O (4 eq), 4 Å MS, TBAI (0.8 eq), BnBr	rt, 12h	80 %

Table 2.5: Optimization of benzylation reaction using Ag₂O and BnBr. Me = methyl, Bn = benzyl, Bn-OPT = 2-benzyloxy-1-methylpyridinium triflate, TBSOTf = *tert*-butyldimethylsilyl trifluoromethanesulfonate, TBAI = tertbutylammonium iodide.

variety of reagents and reaction conditions. 2-Benzyloxy-1-methylpyridinium triflate (Bn-*OPT*) releases an electrophilic benzyl species upon warming, and has been used for the mild etherification of alcohols.⁸¹ The triflate salt can be pre-activated, precluding the need for strong acid or base in the reaction mixture. Initially, benzylation was attempted using Et₃N as a base (Table 2.5, entry 8), but the reaction did not proceed and resulted in the decomposition of the starting material. As an alternative, the benzylation reaction was run with magnesium oxide (MgO), which has been successfully used for the benzylation of alcohols,⁸² but the reaction resulted in the formation of caged byproduct **22** (Table 2.5, entry 9). Unfortunately, alternative acid-catalyzed benzylation reaction conditions using benzyl trichloroacetimidate^{83,84} also resulted in low conversion to the desired product, or conversion to the caged byproduct (Table 2.5, entries 10-14).

The successful benzylation of **18** was accomplished by subjecting the compound to harsher conditions than reported in literature. **18** was subjected to a reaction where benzyl bromide was used as a solvent (in large excess), in the presence of freshly prepared Ag₂O and catalytic tetrabutylammonium iodide (TBAI).⁹ While the reaction proceeded relatively smoothly, reaction yields resulting from catalytic (0.1 eq) amounts of TBAI only afforded the desired compound **19** in moderate yields (~50%). Upon further optimization, increasing the amount of TBAI to near-stoichiometric amounts (0.8 eq) resulted in the successful benzylation of **19** in 80 % yield (Table 2.5, entries 15-17).

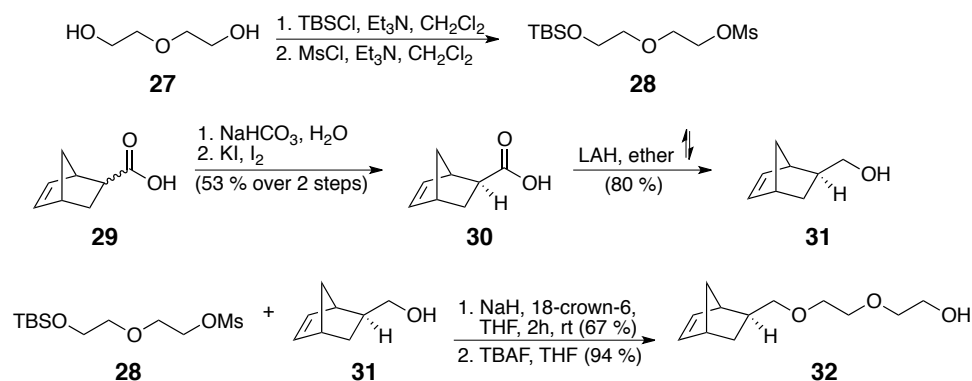
Upon obtaining the TIPS- (**21**), PMB- (**23**), and Bn-protected (**24**) idoA derivatives, glycosyl phosphate reactions were performed. Phosphorylation reactions of TIPS-protected (**21**) and PMB-protected (**23**) using the same reaction conditions used for the phosphorylation of TBS-protected (**19**) were unsuccessful. This procedure utilized the

is believed that the chances of the 4Å MS introducing small amounts of moisture into the reaction are higher than their ability to remove water from the HOPO(OBu)₂ reagent. Unfortunately, due to the hygroscopic nature of the HOPO(OBu)₂ reagent, the amount of hydrolyzed byproduct varied depending on the batch of the reagent.

Synthesis of norbornene-diethylene glycol linker

The synthesis of the norbornene-diethylene glycol linker was adapted from the synthesis of a cyclooctene-diethylene glycol linker previously used in the lab.⁸⁵ The synthesis comprises two main building blocks: the diethylene glycol linker, and a norbornene-methanol moiety (Scheme 2.8). The diethylene glycol linker was first mono-functionalized using *tert*-butyldimethylsilyl chloride (TBSCl) and triethylamine. Subsequent mesyl (Ms) protection of the remaining hydroxyl group afforded the TBS and Ms di-functionalized product in 83 % yield over two steps.

Generally, *exo*-isomers have been shown to be more reactive in olefin metathesis reactions.⁸⁶ To take advantage of this reactivity, the norbornene *exo*-isomer was first

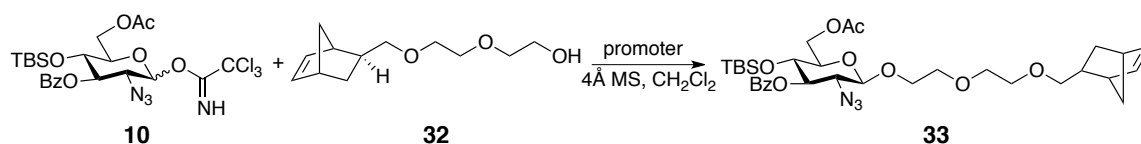


Scheme 2.8: Synthesis of norbornene-diethylene glycol linker. TBSCl = *tert*-butyldimethylsilyl chloride, MsCl = methanesulfonyl chloride, TBS = *tert*-butyldimethylsilyl, MS = methanesulfonyl, LAH = lithium aluminum hydride.

isolated from a commercially available *exo/endo*-isomer mixture of norbornene carboxylic acid **29** utilizing kinetic resolution by iodolactonization.⁸⁷ This *exo*-norbornene carboxylic acid **30** was then reduced to the corresponding alcohol **31** using LAH.

Previously, coupling of the *exo*-norbornene methanol to the diethylene glycol linker was accomplished using sodium hydride in DMF at 60 °C overnight.³⁵ Unfortunately, the yields for this coupling were low (< 40 %), regardless of the quality of reagents or reaction time. By introducing a catalytic amount of 18-crown-6 and using 95 % NaH, the reaction proceeded to significantly higher yields (67 %). In addition to the increased reaction yield, the reaction conditions were much easier to work with; THF was used as a solvent instead of DMF, and the reaction proceeded to completion at rt within 2 h, compared to the previous 12 h reaction times. The TBS-functionalized intermediate was then deprotected under standard desilylation conditions using TBAF to afford the desired norbornene diethylene linker.

Upon obtaining the *exo*-norbornene linker, the protected glcN imidate **10** was coupled to linker **32** to afford the protected acceptor **33**. Original reaction conditions using 1 eq of BF₃·OEt₂ at -30 °C produced the desired product in only 43.5% yield (Table 2.7,



Entry	Eq 10	Eq 32	Promoter	Rxn conditions	yield
1	1.0	1.2	0. 25 M BF ₃ ·OEt ₂ (1 eq)	-30 °C, 2 h	43.5 %
2	1.0	1.2	0. 25 M BF ₃ ·OEt ₂ (1.2 eq)	-30 °C, 2 h	56 %
3	1.0	1.2	0. 25 M BF ₃ ·OEt ₂ (0.9 eq)	-30 °C, 1 h	57 %
4	1.0	1.2	0. 25 M BF ₃ ·OEt ₂ (0.5 eq)	-30 °C, 1 h	94 %

Table 2.7: Optimization of glucosamine donor and norbornene linker. TBS = *tert*-butyldimethylsilyl, Bz = benzoyl, Ac = acetyl.

entry 1). Upon optimizing the reaction based on eqs of the promoter, the yield could be increased to 94% (Table 2.7, entry 4). Although original optimizations took place in the presence of 4Å MS, the optimized reaction proceeds quickly enough that omission of MS did not affect the outcome of this reaction.

With the coupled TBS-protected acceptor **33** in hand, conditions were sought to efficiently desilylate the C-4 hydroxyl functionality; the glycosylation with the C-1 position of glycosyl phosphate **25** to the C-4 position of acceptor **34** yields the desired $\alpha(1\rightarrow4)$ glycosidic bond of heparan sulfate. Many of the standard desilylation conditions for TBS protecting groups failed to yield the desired compound **34** even in moderate yields (Table 2.8, entries 1,4,5). Reactions using TBAF, even under neutral reaction conditions with the help of AcOH (Table 2.8, entries 1, 3),⁸⁸ also resulted in low conversion to **34** or decomposition of the starting material **33**. Seeking out even milder reaction conditions, we turned to the use of hydrogen fluoride stabilized in pyridine (HF/pyridine), which had been previously used for the desilylation of CS derivatives.⁸⁹ When the compound **33** was subjected to excess HF/pyr in a THF/pyridine co-solvent system overnight, the desired product **34** was obtained in 87 % yield (Table 2.8, entry 6); 5-10 % of the starting material could be recovered upon purification using silica gel chromatography.

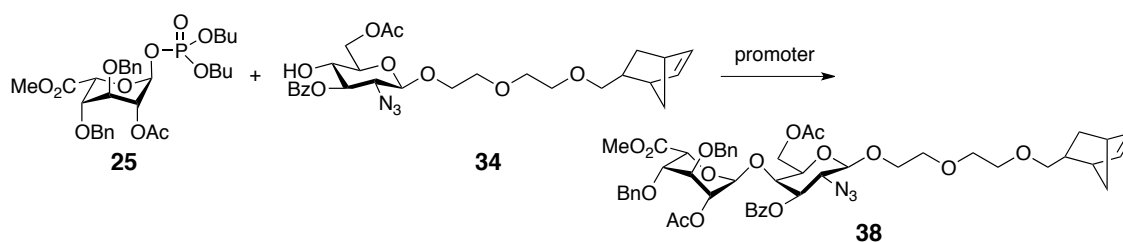
Glycosylation, deprotection, and sulfation of HS disaccharide monomer

Fundamentally, methods to chemically install glycosidic bonds are closely related to those observed in nature. The biosynthetic method of glycosylation involves a glycosyl donor, a nucleotide sugar such as UDP-Glc with a good leaving group (pyrophosphate) in the anomeric position. In the presence of a glycosyltransferases, this activated nucleotide

sugar reacts to exchange the leaving group with the free hydroxyl group of an acceptor to form the product glycosidic linkage. Chemists mimic this strategy by using glycosyl donors containing anomeric leaving groups and acceptors with free hydroxyl groups. In place of glycosyltransferases, chemical activators are used to couple the glycosyl donors and acceptors, and to obtain correct glycosidic regio- and stereoselectivity. Although there is no universal glycosyl donor, a variety of donors such as halides, trichloroacetimidates and thioglycosides are commonly utilized for glycosylation reactions according to their different properties, stabilities, and reactivities.

Two different mechanisms are possible during glycosylation reactions: the direct displacement of the leaving group by the acceptor, which leads to inversion at the anomeric center, or a two-step mechanism where leaving group dissociation is aided by a promoter to create a positively charged oxocarbenium intermediate, which is then attacked by the acceptor. The latter mechanism is by far the most common in chemical glycosylations. However, since the acceptor can attack the intermediate from the α or the β face, an anomeric mixture of products is formed, making stereoselective glycosylations challenging. Methods that allow the control of stereoselectivity in the attack of the acceptor on the activated glycosyl donor intermediate are required to form stereoselective glycosidic linkages.

Silyl triflate reagents (TMSOTf and TBSOTf)⁷⁸ have been shown to ensure high-yielding glycosylations while the use of $\text{BF}_3\cdot\text{OEt}_2$ generally yields modest results.⁹⁰ Initial attempts to install the glycosidic linkage of our HS disaccharides revolved around screening different activators, and optimizing reaction conditions based on eqs of the activator and reaction temperatures. As presented in Table 2.8 (entries 1-12), glycosylation



Entry	Eq 25	Eq 34	Promoter	Rxn conditions	yield
1	1.3 eq	1.0 eq	1.5 eq $\text{BF}_3 \cdot \text{OEt}_2$	$-40\text{ }^\circ\text{C}$, 30 min	< 10 %
2	1.5 eq	1.0 eq	1.5 eq $\text{BF}_3 \cdot \text{OEt}_2$	$-30\text{ }^\circ\text{C}$, 30 min	< 10 %
3	1.3 eq	1.0 eq	1.5 eq TfOH	$-10\text{ }^\circ\text{C} \rightarrow 0\text{ }^\circ\text{C}$, 30 min	< 20 %
4	1.3 eq	1.0 eq	0.2 eq TMSOTf	$-10\text{ }^\circ\text{C} \rightarrow 0\text{ }^\circ\text{C}$, 1 h	no rxn
5	2.0 eq	1.0 eq	1.2 eq TMSOTf	$-50\text{ }^\circ\text{C} \rightarrow -30\text{ }^\circ\text{C}$, 1 h	no rxn
6	1.3 eq	1.0 eq	1.3 eq TMSOTf	$-30\text{ }^\circ\text{C} \rightarrow -20\text{ }^\circ\text{C}$, 1 h	< 10 %
7	1.3 eq	1.0 eq	1.3 eq TMSOTf	$-10\text{ }^\circ\text{C}$, 30 min	20 %
8	1.3 eq	1.0 eq	1.5 eq TMSOTf	rt, 4 h	41 %
9	1.3 eq	1.0 eq	1.3 eq TBSOTf	$-30\text{ }^\circ\text{C} \rightarrow -20\text{ }^\circ\text{C}$, 1h	< 10 %
10	1.3 eq	1.0 eq	1.5 eq TBSOTf	$-40\text{ }^\circ\text{C}$, 30 min	< 10 %
11	1.5 eq	1.0 eq	1.5 eq TBSOTf	$-30\text{ }^\circ\text{C}$, 40 min	< 10 %
12	1.3 eq	1.0 eq	1.3 eq TBSOTf	$-10\text{ }^\circ\text{C}$, 40 min	25 %
13	2.0 eq	1.0 eq	1.5 eq TBSOTf	$-40\text{ }^\circ\text{C}$, 1 h	45 %*
14	1.3 eq	1.0 eq	1.5 eq TBSOTf	$-20\text{ }^\circ\text{C}$, 1h	75 %*

* Reactions were run in Schlenk flask

Table 2.8: Optimization of reaction conditions using TBSOTf and TMSOTf for glycosylation reactions. Me = methyl, Bn = benzyl, Ac = acetyl, Bu = butyl, Bz = benzoyl, TMSOTf = trimethylsilyl trifluoromethanesulfonate, TBSOTf = tert-butyl dimethylsilyl trifluoromethanesulfonate.

reactions were run at a range of different temperatures with the TMSOTf, TBSOTf, and $\text{BF}_3 \cdot \text{OEt}_2$; unfortunately, these initial reaction conditions yielded very little of the desired disaccharide **38**. During this process, it was discovered that the GlcN acceptor **34** was stable under these reaction conditions, even in the presence of high eqs of the activators. In contrast, the glycosyl phosphate donor **25** hydrolyzed or decomposed under most of these reaction conditions, which led us to focus on different aspects of the reaction set up.

Following the two most promising glycosylation conditions using TBSOTf and TMSOTf (Table 2.8, entries 8, 13), we explored the use of alternative experimental

procedures for the optimization of the reaction. Initial attempts used various activator stock solutions of different concentrations, and stock solutions that were cooled prior to addition to the reaction mixture. The reaction was run several times using an inverse procedure, where a glycosyl phosphate donor **25** was added to a solution of the acceptor **34** and activator. Additionally, reactions were run in the presence and absence of 4Å MS. Unfortunately, none of these experimental procedures had an effect on the outcome of the reactions.

Fortuitously, we discovered that the acceptor's sensitivity to water/moisture could be diminished by using a Schlenk flask for the reaction and adjusting cooling times. Connecting an argon line to the 14/20 ground glass joint and a placing septum on the valve outlet created the an air-free environment protected from perturbations, because the reaction flask is sufficiently removed from both valves (Figure 2.7). In addition to the air-free setup, the solution of acceptor and donor was cooled for no longer than 1 min prior to the addition of the activator; this minimized any condensation of moisture from the environment. A combination of specialized glassware and moisture-sensitive techniques proved to be essential for the glycosylation reaction to proceed in up to 75% yield (Table 2.9, entries 13, 14).

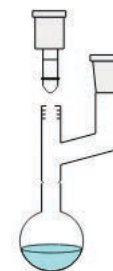
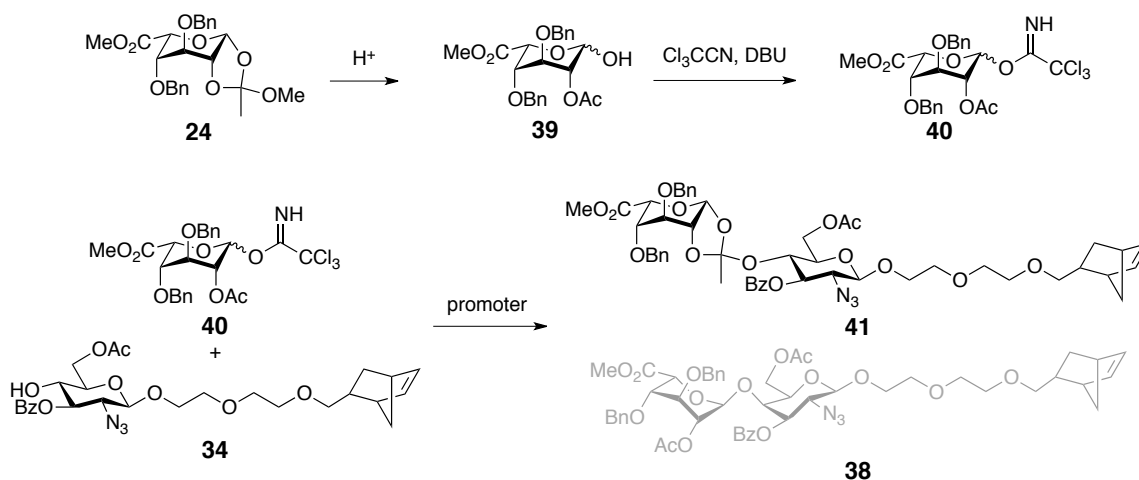


Figure 2.7: Schlenk flask used for glycosylation reactions.

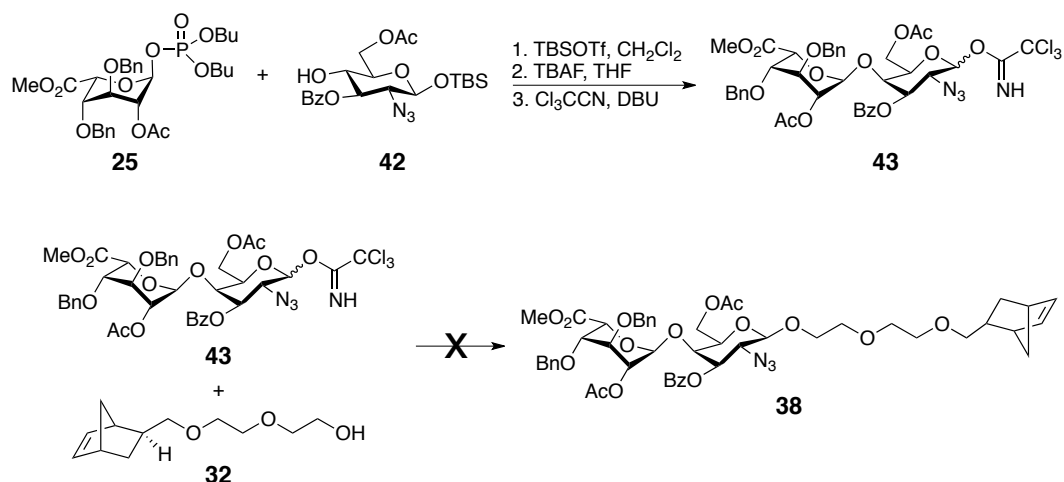
During the optimization process of the glycosylation reaction, two other methods to generate the HS monomers were developed in an attempt to increase reaction yields; as the prior glycosylation was sensitive to moisture, reactions did not always proceed in consistently high yields. To avoid the decomposition and hydrolysis of the donor **25**, we first sought out to synthesize a trichloroacetimidate IdoA donor **40**. Starting from the di-



Scheme 2.9: Glycosylation using idoA-trichloroacetimidate donor. Me = methyl, Bn = benzyl, Ac = acetyl, Bz = benzoyl.

benzylated IdoA intermediate **24**, the monosaccharide was subjected to hydrolysis and opening of the orthoester using DOWEX H^+ resin. Subsequent treatment of the anomeric hydroxyl compound **39** with trichloroacetonitrile and DBU, as used in the synthesis of GlcN trichloroacetimidate, afforded the desired idoA **40**. The glycosylation of trichloroacetimidate donor **40** and acceptor **34** was attempted using the same promoters as presented in Table 2.9. Unfortunately, a screen of the different activators at temperatures between $-40\text{ }^\circ\text{C}$ and rt all yielded the orthoester byproduct **41**.

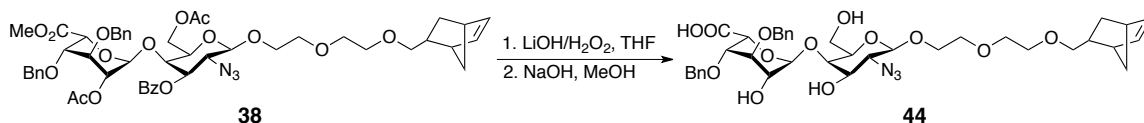
As a second alternative, the HS disaccharide monomer was built in a different order, where the disaccharide building block was assembled first, followed by the coupling to the norbornene linker. This order of HS glycopolymer assembly has been used to synthesize trisulfated HS glycopolymers.⁴⁵ Unlike the coupling between glycosyl donor **25** and acceptor **34**, the coupling between the two monosaccharides **25** and **42** proceeded smoothly in over 80% yield, albeit in slightly lower yields than usual trichloroacetimidate activation reactions ($>90\%$). Unfortunately, preliminary attempts to couple the disaccharide



Scheme 2.10: Coupling of HS disaccharide trichloroacetimidate to linker. Me = methyl, Bn = benzyl, Ac = acetyl, Bu = butyl, TBSOTf = tert-butyldimethylsilyl trifluoromethanesulfonate, TBAF = tetrabutylammonium fluoride, DBU = 1,8-diazabicycloundec-7-ene, Bz = benzoyl.

to the norbornene linker **32** using conventional lewis acid promoters (TBSOTf, TMSOTf, $\text{BF}_3 \cdot \text{OEt}_2$) failed (Scheme 2.10).

Following efforts to optimize the glycosylation to reach the fully protected HS disaccharide monomer, selective PG removal, and sulfation reactions were carried out in the final stages of the HS monomer synthesis. The removal of protecting groups began with methyl ester hydrolysis using LiOH, which was formed *in situ* by the simultaneous addition of LiOH and H_2O_2 .⁹¹ While the number of eqs of LiOH and H_2O_2 in previously published literature on heparin fragment syntheses⁹² led to product formation (Table 2.9,



Entry	LiOH	H ₂ O ₂	result
1	20 eq	100 eq	incomplete rxn
2	20 eq	3.7 eq	incomplete rxn
3	20 eq	50 eq	incomplete rxn
4	20 eq	10 eq	82 %

Table 2.9: Optimization of methyl ester hydrolysis reaction. Me = methyl, Bn = benzyl, Ac = acetyl, Bz = benzoyl.

desired product was isolated by purification via silica gel column chromatography using a triphasic eluent system of EtOAc, methanol, and water.

Following the *O*-sulfation with SO_3TMA , azide reduction using Staudinger reaction conditions with PMe_3 and NaOH furnished the amine intermediate **46** in quantitative yield. A size exclusion LH-20 column was used with a 1:1 methanol/ CH_2Cl_2 eluent system to separate out any excess reagents, and the crude material was subjected to *N*-sulfation using 15 eq SO_3pyr in a pyridine and triethylamine cosolvent system. The final tetrasulfated HS disaccharide monomer **47** was purified using silica column chromatography and was subjected to ring-opening metathesis polymerization chemistry to afford tetrasulfated HS glycopolymers. The streamlined synthesis of the HS monomer is presented in Scheme 2.11.

We have successfully synthesized a HS disaccharide monomer targeted to have anticoagulant activity from three main building blocks: orthogonally protected IdoA and GluA monosaccharides, and a diethylene glycol-linked norbornene. This HS monomer was synthesized to take advantage of multivalency effects, and is comprised of a minimal HS anticoagulant disaccharide motif for targeted biological activity. This disaccharide contains the G and H monosaccharide units seen in Org31550, a derivative of the anticoagulant pentasaccharide with an additional 3-*O*-sulfate group, which has been shown to enhance *in vitro* anticoagulant activity. In addition to allowing access to an anticoagulant sulfation pattern, the orthogonally protected IdoA and GluA monosaccharide building blocks also allow for easy access to a variety of different sulfation patterns, through manipulation of the various PGs. This protected anticoagulant HS monomer **47** was subjected to

polymerization and deprotection chemistry to afford the desired tetrasulfated glycopolymer and was tested for *in vitro* and *ex vivo* anticoagulant activity.

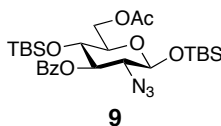
Experimental methods and spectral data

Unless otherwise stated, reactions were performed in flame-dried glassware under an argon atmosphere using dry solvents. Solvents were dried by passage through an activated alumina column under argon. All other reagents were purchased from Sigma-Aldrich, Acros Organics, Strem, or Alfa Aesar and used as received unless otherwise stated. Reaction temperatures were controlled by an IKAmag temperature modulator. Analytical LC/MS was performed on an Agilent 6140 single quadropole LC/MS with an Agilent 1290 Infinity UHPLC system. Thin layer chromatography (TLC) was performed using E. Merck silica gel 60 F254 precoated plates (0.25 mm). Visualization of the developed chromatograms was performed by UV, cerium ammonium molybdate, or ninhydrin stain as necessary. ICN silica gel (particle size 0.032-0.063 mm) was used for flash chromatography.

^1H NMR and proton decoupling experiments were recorded on a Varian Mercury 300 (300 MHz), Varian MR-400 (400 MHz), or Varian Inova 500 (500 MHz) spectrometer and are reported in parts per million (δ) relative to residual CDCl_3 (7.26 ppm), CD_3OD (4.87 ppm), and D_2O (4.80 ppm). Data for the ^1H NMR spectra are reported as follows: chemical shift (δ ppm), multiplicity (s = singlet, bs = broad singlet, d = doublet, dd = doublet of doublet, t = triplet, q = quartet, m = multiplet), coupling constants in Hz, and integration. ^{13}C NMR spectra were obtained on a Varian MR-400 (101 MHz) or Varian Inova 500 (125 MHz) spectrometer and are reported relative to CDCl_3 (77.2 ppm), CD_3OD (49.0 ppm), and $(\text{CD}_3)_2\text{SO}$ (39.5 ppm). Mass spectra were obtained from the Protein/Peptide MicroAnalytical Laboratory, the Caltech Mass Spectrometry Facility (EI+ or FAB+), or on an Agilent 6200 Series TOF with an Agilent G1978A Multimode source

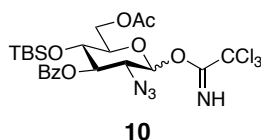
in electrospray ionization (ESI), atmospheric pressure chemical ionization (APCI), or mixed (MM) ionization mode.

Trifluoromethanesulfonyl azide:^{50,51} NaN₃ (15.6 g, 0.24 mmol) was dissolved at room temperature in H₂O (40 mL) in a 1 L three-neck round bottom flask. The flask was fitted with an addition funnel, a septum, and an argon balloon. CH₂Cl₂ (50 mL) was added to the vigorously stirred solution at 0 °C. Tf₂O (8 mL, 0.05 mmol) was added dropwise over 1 h. The mixture was stirred further for 2 h at 0 °C, and the organic layer was separated. The aqueous layer was extracted with CH₂Cl₂ (2 x 19.5 mL). The combined organic layers were washed with saturated aq NaHCO₃ (39 mL) and H₂O (39 mL), dried with MgSO₄ and filtered to yield a 0.4 M solution of TfN₃. **Warning: TfN₃ has been reported to be explosive when not in solution.**



tert-Butyldimethylsilyl 6-O-acetyl-2-azido-3-O-benzoyl-4-tert-butyldimethylsilyl-2-deoxy-β-D-glucopyranoside (9). Compound **8** (200 mg, 0.35 mmol) was added to a mixture of 1 mL of carbon tetrachloride, 1 mL of acetonitrile, and 1.5 mL of H₂O. To this, sodium metaperiodate (755 mg, 10 eq) and ruthenium dioxide (47 mg, 1 eq) were added sequentially, and the reaction was left to stir for 18 h at room temp in the dark. The resulting slurry was diluted with CH₂Cl₂, and the aqueous layer was extracted with CH₂Cl₂ (3x). The organic layers were then combined, filtered through a pad of Celite, and concentrated *in vacuo*. The residue was purified by chromatography on silica gel (20:1

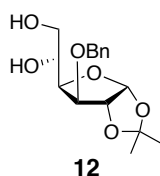
hexanes: ethyl acetate) to deliver 164 mg (80%) of **9** as a colorless oil. ¹H NMR (300 MHz, CDCl₃) δ 8.07 (d, *J* = 7.2 Hz, 2H), 7.59 (t, *J* = 7.5 Hz, 1H), 7.47 (t, *J* = 7.5 Hz, 2H), 5.16 (dd, *J* = 10.2, 9.0 Hz, 1H), 4.72 (d, *J* = 7.5 Hz, 1H), 4.43 (dd, *J* = 11.7, 1.8 Hz, 1H), 4.12 (dd, *J* = 12.0, 6.3 Hz, 1H), 3.85 (t, *J* = 9.0 Hz, 1H), 3.61 – 3.56 (m, 1H), 3.44 (dd, *J* = 10.5, 7.8 Hz, 1H), 2.10 (s, 3H), 0.93 (s, 9H), 0.75 (s, 9H), 0.16 (s, 6H), 0.02 (s, 3H), -0.20 (s, 3H); ¹³C NMR (75 MHz, CDCl₃) δ 170.6, 165.4, 133.3, 129.9, 128.5, 97.1, 74.9, 74.4, 69.6, 66.8, 63.0, 25.5, 22.2, 20.8, 17.9, 17.8, -4.1, -4.5, -4.9, -5.3; HRMS ES *m/z* calcd for C₂₇H₄₄N₃O₇Si₂ [M-H]⁻ 578.2718, obsd 578.2718.



6-O-Acetyl-2-azido-3-O-benzoyl-4-*tert*-butyldimethylsilyl-2-deoxy-β-D-glucopyranoside trichloroacetimidate (10). To a solution of *tert*-butyldimethylsilyl 6-*O*-acetyl-2-azido-3-*O*-benzoyl-4-*tert*-butyldimethylsilyl-2-deoxy-β-D-glucopyranoside **9** (5.01 g, 8.63 mmol) in 60 mL THF at 0 °C was added glacial acetic acid (0.67 mL) and TBAF (1 M in THF, 10.4 mL) simultaneously. The reaction mixture was stirred at 0 °C for 2 h, and was then diluted with 200 mL diethyl ether, and washed with brine three times. The organic layer was dried over anhydrous MgSO₄, filtered, and concentrated *in vacuo*.

The crude residue was dissolved in CH₂Cl₂ (215 mL) and cooled to 0 °C. Trichloroacetonitrile (13 mL, 130 mmol) and 1,8-diazabicyclo[5.4.0]undec-7-ene (130 μL, 0.87 mmol) were added and the reaction mixture was stirred for 2 h at 0 °C. After 2 h, the reaction mixture was concentrated *in vacuo*, and purified by silica gel chromatography (hexanes:ethyl acetate 10:1) to afford a mixture of **10** α and β (10/1, 3.8 g, 92%) as a light

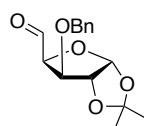
yellow foam. ^1H NMR (500 MHz; CDCl_3): δ 8.34 (s, 1H), 8.08 (d, $J = 7.0$ Hz, 2H), 7.61 (t, $J = 7.5$ Hz, 1H), 7.48 (t, $J = 7.5$ Hz, 2H), 6.52 (d, $J = 3.6$ Hz, 1H), 5.73 (dd, $J = 10.5, 8.4$ Hz, 1H), 4.42 (d, $J = 10.5$ Hz, 1H), 4.18-4.10 (m, 2H), 4.05 (t, $J = 9.0$ Hz, 1H), 3.64 (dd, $J = 10.5, 3.5$ Hz, 1H), 2.09 (s, 3H), 0.77 (s, 9H), 0.03 (s, 3H), -0.14 (s, 3H); ^{13}C NMR (126 MHz, CDCl_3) δ 170.58, 165.50, 160.96, 133.61, 130.04, 129.67, 128.65, 94.91, 90.78, 73.20, 72.85, 69.26, 62.51, 61.63, 29.83, 25.71, 25.71, 25.69, 25.67, 20.92, 18.04, -3.90, -4.79; HRMS ESI MS: m/z calcd for $\text{C}_{23}\text{H}_{31}\text{Cl}_3\text{N}_4\text{O}_7\text{SiNa}$ $[\text{M}+\text{Na}]^+$ 631.0925, obsd 631.0925.



3-O-benzyl-1,2-isopropylidene- α -D-glucopyranoside (12). Commercially available diacetone glucose **11** (4.15 g, 15.95 mmol) was dissolved in THF (40 mL) and NaH (60% in mineral oil; 0.78 g, 19.25 mmol) was added in portions. After evolution of hydrogen ceased, tetrabutylammonium iodide (40 mg, 0.1 mmol) and benzyl bromide (2 mL, 16.8 mmol) were added and the mixture was stirred for 12 h at room temperature. Water was added slowly to the reaction mixture and the organic layer evaporated under reduced pressure. The aqueous phase was extracted with ethyl acetate (3 x 100 mL), and the organic phases combined and dried over MgSO_4 , filtered through a plug of silica, and the solvent removed under pressure.

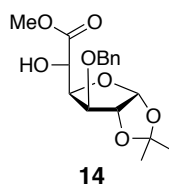
Aqueous acetic acid (66%, 25 mL) was added to the resulting oil and stirred 16 h at room temperature. The reaction mixture was evaporated under reduced pressure and the residue dissolved in CH_2Cl_2 and washed with saturated aq. NaHCO_3 . The aqueous phase

was extracted with CH_2Cl_2 (2 x 100 mL) and the combined organic phases dried over MgSO_4 and the solvent removed under reduced pressure. Flash silica column chromatography gel (hexanes/ethyl acetate 9:1 \rightarrow 1:1) yielded **12** in 90%. ^1H NMR (300 MHz, CDCl_3): δ 7.27 (m, 5H), 5.87 (d, $J = 3.6$, 1H), 4.55 (dd, $J = 3.6$, 2H), 4.54 (d, $J = 3.6$, 2H), 4.05 (m, 1H), 3.94 (m, 1H), 3.74 (d, $J = 3.3$, 1H), 3.71 (d, $J = 3.3$, 1H), 3.62 (m, 1H), 1.40 (s, 3H), 1.23 (s, 3H).

**13**

Methyl 3-O-benzyl-1,2-isopropylidene- α -D-glucofuranosyluronate (13). To a suspension of silica gel (9.5 g) in CH_2Cl_2 (80 mL) was added a solution of NaIO_4 (1.31 g, 6.13 mmol) in water (9.5 mL). The suspension was stirred vigorously for 30 min, followed by addition of a solution of **12** (1.47 g, 4.73 mmol) in CH_2Cl_2 (7.5 mL). The reaction was stirred for 2 h, followed by filtration through Celite and concentration under reduced pressure. The residue was dried under vacuum and used without further purification.

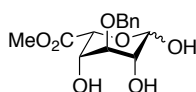
Tris(phenylthio)orthoformate. In a roundbottom flask, thiophenol (100 mL, 0.97 mol) and trimethyl orthoformate (35.5 mL, 0.32 mol) were added. To this, $\text{BF}_3 \cdot \text{OEt}_2$ (5 mL, 0.04 mol) was added dropwise, and was stirred for 8 days at room temperature. The resulting reaction mixture was diluted with CHCl_3 and 1 M KOH, and washed with 1 M KOH (3 x 1500 mL). The solution was dried with MgSO_4 , and dried under vacuum. ^1H NMR (400 MHz, CDCl_3): δ 7.48 (m, 6H), 7.29 (m, 9H), 5.41 (s, 1H); ^{13}C NMR (22.53 MHz, CDCl_3): δ 134.20, 132.97, 128.94, 128.33, 65.18.



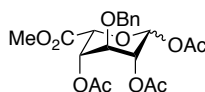
Methyl 3-O-benzyl-1,2-isopropylidene- α -L-idofuranosiduronate (14). To a flame-dried flask was added freshly made tris(phenylthio)orthoformate (1.94 g, 5.68 mmol), followed by THF (7.5 mL). The reaction vessel was cooled to -78 °C and n-butyllithium (1.6M in hexanes, 3.25 mL, 5.2 mmol) was added dropwise. The bright yellow solution was allowed to warm slowly to -50 °C over 1 h, then cooled to -78 °C and stirred for 30 min. Crude **13** (1.32 g, 4.73 mmol) was dissolved in THF (5 mL) and added dropwise via cannula to the reaction flask over 15 min. The reaction was stirred at -78 °C for 1 h, allowed to warm to room temperature over 30 min, and then quenched with saturated aqueous NH_4Cl (25 mL). The aqueous phase was extracted with EtOAc (3 x 25 mL), and the combined organic phases were dried over MgSO_4 , filtered, concentrated under reduced pressure, and dried under vacuum. The crude product was used without further purification.

To CuCl_2 (0.345 g, 2.02 mmol) and CuO (66 mg, 0.825 mmol) suspended in methanol/water (12:1, 6.5 mL) was added crude material from the previous step (0.27 g, 0.4075 mmol) in CH_2Cl_2 (2.5 mL). The reaction was stirred at ambient temperature for 5 min and then the solvent was evaporated under reduced pressure with gentle heat. The resulting green-white solid was dissolved in EtOAc (70 mL) and washed with 1N HCl (2 x 10 mL), brine (2 x 10 mL), and saturated aqueous NaHCO_3 (10 mL). The combined organic layers were dried over MgSO_4 , filtered, concentrated under reduced pressure, and dried under vacuum for 1 h. The resulting oil was dissolved in CH_2Cl_2 (6 mL), and methanol (1 mL) and K_2CO_3 (15 mg, 0.11 mmol) were added. The reaction was stirred at

ambient temperature for 1.5 h, then the solution was filtered through Celite and concentrated under reduced pressure. Purification via flash silica gel column chromatography (10%→15%→20%→25%→30% ethyl acetate/hexanes) afforded **14** in 85% yield as a light yellow oil. ^1H NMR (300 MHz, CDCl_3): δ 7.40-7.27 (m, 5H), 6.04 (d, $J = 3.9$, 1H), 4.70-4.52 (m, 4H), 4.41 (dd, $J = 6.2, 2.8$, 1H), 4.16 (d, $J = 3.8$, 1H), 3.76 (s, 3H), 3.34 (d, $J = 9.1$, 1H), 1.50 (s, 3H), 1.34 (s, 3H). The spectral data was in agreement with the reported data.⁶⁹

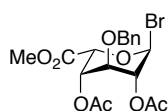
**15**

Methyl 3-O-benzyl-L-idopyranuronate (15). Compound **14** (mg, mmol) was dissolved in 90% aqueous trifluoroacetic acid (mL) and stirred at ambient temperature for 35 min. The reaction solvent was removed and the crude product coevaporated with toluene (5 x mL), and dried under vacuum for 18 h. The resulting brown solid was recrystallized in ethyl acetate as necessary to obtain the triol product **15**. ^1H NMR (300 MHz, CD_3OD): δ 7.26 (s, 5H), 4.92 (broad s, 1H_α), 4.48 (d, $J = 1.5$, 1H), 3.94 (m, 1H), 3.80 (t, 1H), 3.70 and 3.60 (2s, 3H).⁹⁸

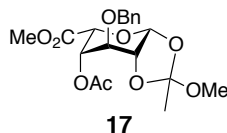
**16**

Methyl 1,2,4-tri-O-acetyl-3-O-benzyl- α/β -L-idopyranuronate (16). CH_2Cl_2 (100 mL) was cooled to 0 °C. To this was added compound **15** (5 g, 16.75 mmol), and this was cooled further to -40 °C. 4-dimethylaminopyridine (0.2 g, 1.675 mmol) was added to the

mixture, followed by the addition of pyridine (13.5 mL, 167.5 mmol). Acetyl chloride (7.14 mL, 100.5 mmol) was added dropwise to the reaction mixture, and stirred for 10 hr at -40 °C. This was quenched with aqueous NaHCO₃, extracted with CH₂Cl₂ (2 x 250 mL), then washed with H₂O, 1M H₂SO₄, and H₂O. The combined organic fractions were dried over MgSO₄ and concentrated under reduced pressure. Purification via silica column chromatography (3:1 hexanes/ethyl acetate) afforded compound **16** in quantitative yield. ¹H NMR (300 MHz, CDCl₃): δ 7.32 (s, 5H), 6.23 (broad s, 1H), 5.24 (m, 1H), 4.95 (m, 2H), 4.72 (s, 2H), 3.88 (m, J_{2,3} and J_{3,4} = 3, 1H), 3.75 (s, 3H), 2.06 and 2.04 (2s, 9H).

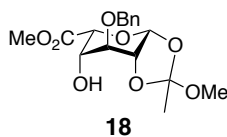


Methyl (2,4-di-O-acetyl-3-O-benzyl- α -L-idopyranosyl bromide) uronate. This compound is the intermediate compound in the formation of the 1,2-(methyl-orthoacetate). To a solution of compound **16** (2.6 g, 6.13 mmol) in anhydrous CH₂Cl₂ (50 mL) at room temperature, TiBr₄ (3.04 g, 8.27 mmol) was added. This reaction mixture was stirred overnight with exclusion of light. This mixture was then quenched with ice cold H₂O (2 x 250 mL), filtered through a pad of celite, and concentrated under reduced pressure. This resulted in a brown oil, that was used in the next reaction without further purification. ¹H NMR (300 MHz, CDCl₃): δ 7.30 (m, 5H), 6.41 (broad s, 1H), 3.75 (s, 3H), 2.04 (s, 6H).



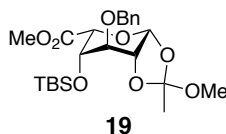
Methyl 4-O-acetyl-3-O-benzyl-1,2-methylorthoaceto- α -L-idopyranosiduronate (17).

The crude bromide intermediate (6.13 mmol) was dissolved in CH_2Cl_2 (75 mL) at room temperature. To this was added 2,4,6-collidine (4 mL, 30.04 mmol) and methanol (2.7 mL, 66.82 mmol). After stirring overnight, the reaction mixture was diluted with CH_2Cl_2 , and washed with aqueous NaHCO_3 and H_2O . The combined organics were dried over MgSO_4 , concentrated under reduced pressure, and purified via silica column chromatography (6:1 hexanes/ethyl acetate + 0.5 % triethylamine) to yield the desired product **17** in 66 % yield over two steps. ^1H NMR (300 MHz, CDCl_3): δ 7.31 (s, 5H), 5.52 (d, $J = 3$, 1H), 5.18 (dd, $J_{3,4} = 3$, $J_{4,5} = 1.5$, 1H), 4.71 (s, 2H), 4.51 (d, $J = 1.5$, 1H), 4.10 (m, 2H), 3.74 (s, 3H), 3.22 (s, 3H), 2.00 (s, 3H), 1.71 (s, 3H).

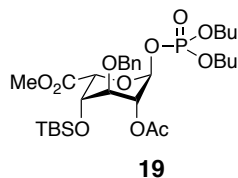


Methyl 3-O-benzyl- β -L-idopyranuronate 1,2-(methylorthoacetate) (18). Methyl 4-O-acetyl-3-O-benzyl- β -L-idopyranuronate 1,2-(methyl-orthoacetate) **17** (1.6 g, 3.99 mmol), was dissolved in methanol (10 mL) and cooled to -10 °C. A 0.5 M solution of NaOMe was added (3 x 0.4 mL) and stirred at -10 °C for 4 hr. Then the reaction mixture was stirred further at 4 °C overnight. This solution was then cooled to 0 °C, diluted with CH_2Cl_2 , and quenched with aqueous NaHCO_3 and H_2O . Purification via silica column chromatography (4:1 hexanes/ethyl acetate + 0.5% triethylamine) afforded compound **18** in 72 % yield. ^1H

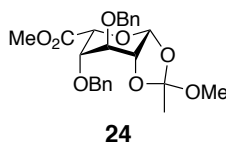
NMR (300 MHz, CDCl₃): δ 7.35 (s, 5H), 5.50 (d, *J* = 2, 1H), 4.68 (s, 2H), 4.49 (d, *J* = 1, 1H), 3.81 (s, 3H), 3.30 (s, 3H), 2.80 (d, *J* = 12, 1H), 1.76 (s, 3H).



Methyl 3-O-benzyl-1,2-methylorthoaceto-4-O-tert-butyltrimethylsilyl- α -L-idopyranosiduronate (19). A solution of compound **18** (4.2 g, 11.85 mmol) in pyridine (60 mL) was cooled to -10 °C. TBSOTf (24.5 mL, 106.7 mmol) was added dropwise, and the reaction mixture was stirred at -10 °C for 1.5 h. The reaction was warmed to 4 °C and left to stir overnight. After confirming the completion of the reaction via TLC, the reaction was diluted with CH₂Cl₂, quenched with aqueous NaHCO₃, and extracted with ethyl acetate (3 x 150 mL). Purification via silica column chromatography (7:1 hexanes/ethyl acetate + 0.5 % triethylamine) afforded compound **19** in 72% yield. ¹H NMR (300 MHz, CDCl₃): δ 7.45 – 7.30 (m, 5H), 5.51 (d, *J* = 2.7 Hz, 1H), 4.65 (d, *J* = 5.4 Hz, 2H), 4.39 (d, *J* = 1.2 Hz, 1H), 4.40 – 4.15 (m, 2H), 3.85 (t, *J* = 2.0 Hz, 1H), 3.77 (s, 3H), 3.29 (s, 3H), 1.72 (s, 3H), 0.82 (s, 9H), -0.04 (s, 3H), -0.06 (s, 3H); ¹³C NMR (75 MHz, CDCl₃): δ 169.6, 137.0, 128.9, 128.6, 128.2, 124.6, 97.1, 76.3, 74.6, 72.8, 72.5, 67.9, 52.4, 49.5, 29.9, 25.7, 25.6, -4.4, -5.2; HRMS ES *m/z* calcd for C₂₃H₃₆O₈SiNa [M + Na]⁺ 491.2077, obsd 491.2070.

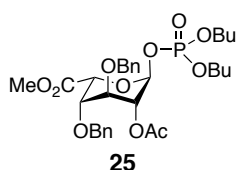


Methyl dibutylphosphate-2-O-acetyl-3-O-benzyl-4-O-tert-butyldimethylsilyl- α -L-idopyranosiduronate (19). Compound **18** (40 mg, 0.085 mmol) was dissolved in CH₂Cl₂ (1.5 mL) at rt. To this was added freshly activated 4Å molecular sieves (100 mg, 1g/mmol) and the solution was stirred for 30 min. Dibutylphosphate (48 μ L, 0.257 mmol) was added slowly, and the reaction mixture was left to stir overnight. After confirming the completion of phosphorylation by TLC, the reaction was quenched with triethylamine and concentrated under reduced pressure. Silica column chromatography (4:1 hexanes/ethyl acetate + 0.5% triethylamine) afforded the desired product **19** quantitatively. ¹H NMR (300 MHz, CDCl₃): δ 7.36 (m, 5H), 5.828 (d, J = 6.3, 1H), 4.97 (s, 1H), 4.81 (m, 2H), 4.63 (m, 1H), 4.067 (5H), 3.77 (s, 3H), 3.61 (s, 1H), 2.04 (s, 3H), 1.62 (m, 4H), 1.35 (m, 4H), 0.90 (s, 6H), 0.81 (s, 9H), -0.07 (s, 3H), -0.17 (s, 3H); ¹³C NMR (75 MHz, CDCl₃): δ 169.85, 169.19, 146.59, 137.33, 128.45, 127.98, 95.38, 77.42, 77.00, 76.58, 73.77, 71.97, 69.98, 68.06, 67.82, 67.01, 66.89, 52.09, 32.12, 25.44, 20.93, 18.56, 17.75, 13.54, -4.70, -5.72; ESI HRMS: *m/z* calcd for C₃₀H₅₂O₁₁PSi [M + H]⁺ 647.3017, obsd 647.3001.



Methyl 3,4-di-O-benzyl-1,2-methylorthoaceto- α -L-idopyranosiduronate (24). Methyl 3-O-benzyl- β -L-idopyranuronate 1,2-(methyl-orthoacetate) **18** (1.60 g, 4.52 mmol) was dissolved in neat benzyl bromide (20 mL, 5 mL/mmol) along with activated 4 Å molecular

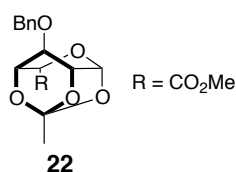
sieves (500 mg/mmol). Benzyl bromide was filtered through a pad of activated basic alumina immediately before use. To this was added tetrabutylammonium iodide (1.34 g, 3.62 mmol) and the resulting mixture was stirred at room temperature for 15 min. Freshly prepared silver oxide (4.19 g, 18.1 mmol) was added to the mixture and stirred at room temperature for 8 h in the absence of light. The resulting reaction mixture was diluted with diethyl ether, filtered through a pad of Celite®, and concentrated *in vacuo*. Flash silica gel chromatography (hexanes:ethyl acetate 6:1 → 2:1, 0.5% Et₃N) afforded the desired product **24** (1.51 g) in 75% yield. ¹H NMR (500 MHz, CDCl₃) δ 7.38 – 7.19 (m, 10H), 5.50 (d, *J* = 2.9 Hz, 1H), 4.58 – 4.52 (m, 3H), 4.44 – 4.37 (m, 2H), 4.13 – 4.08 (m, 1H), 4.08 – 4.04 (m, 1H), 3.85 – 3.80 (m, 1H), 3.71 (s, 3H), 3.25 (s, 3H), 1.67 (s, 3H); ¹³C NMR (125 MHz; CDCl₃) δ 169.31, 137.72, 137.07, 128.74, 128.39, 128.36, 127.99, 127.83, 127.81, 124.50, 96.85, 77.41, 77.16, 76.91, 76.31, 72.82, 72.77, 72.00, 71.40, 71.19, 52.43, 49.25, 25.08; HRMS ESI MS: *m/z* calcd for C₂₄H₂₈O₈ [M + Na]⁺ 467.1687, obsd 467.1675.



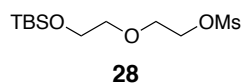
Methyl dibutylphosphate-2-O-acetyl-3,4-di-O-benzyl- α -L-idopyranosiduronate (25).

The 1,2-orthoester **24** (688 mg, 1.55 mmol) was azeotropically dried with toluene (3 x 10 mL) followed by 1 h under vacuum. Activated 4Å molecular sieves (500 mg/mmol 1,2-orthoester) under flux of argon were added and the sugar was dissolved in CH₂Cl₂ (1 mL/0.10 mmol 1,2-orthoester). After stirring for 10 min at room temperature, this mixture was added dropwise via cannula (within 30 min) to a 3 M solution of dibutyl phosphate in CH₂Cl₂ (977 μ L, 4.65 mmol) in the presence of 4Å molecular sieves (500 mg/mmol

dibutyl phosphate). After 5 h at room temperature, the reaction was cooled to 0°C and triethylamine (865 μ L, 6.20 mmol) was added. The solution was warmed to room temperature and filtered through a pad of deactivated silica gel. The resulting mixture was concentrated in vacuo, and purified using flash silica gel chromatography (Hexanes:EtOAc 4:1 \rightarrow 2:1, 0.5% Et₃N) to afford the desired product **25** (888 mg) in 92% yield. ¹H NMR (500 MHz, CDCl₃) δ 7.45 – 7.16 (m, 10H), 5.86 (d, J = 6.9, 1.3 Hz, 1H), 5.03 (dt, J = 2.8, 1.2 Hz, 1H), 4.95 (d, J = 2.5 Hz, 1H), 4.83 – 4.57 (dd, 2H), 4.55 – 4.40 (dd, 2H), 4.15 – 3.98 (m, 4H), 3.95 – 3.82 (m, 2H), 3.74 (s, 3H), 2.04 (s, 3H), 1.69 – 1.59 (m, 4H), 1.46 – 1.32 (m, 4H), 0.99 – 0.87 (m, 6H); ¹³C NMR (126 MHz, CDCl₃) δ 169.65, 168.74, 137.21, 137.05, 128.30, 128.22, 127.86, 127.82, 127.80, 127.66, 95.33, 95.29, 77.42, 77.16, 76.90, 73.49, 72.32, 72.08, 70.62, 68.89, 67.82, 67.77, 67.75, 67.71, 66.83, 66.76, 52.04, 32.06, 32.00, 31.95, 20.71, 18.44, 13.42, 13.41; HRMS ESI MS: m/z calcd for C₃₁H₄₄O₁₁P [M + H]⁺ 623.2616, obsd 623.2624.

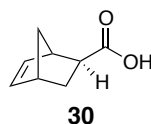


3-O-Benzyl-1,2,4-O-ethylidene- β -L-idopyranuronate (22). ¹H NMR (300 MHz, CDCl₃) δ 7.30 (s, 5H, Ph), 5.83 (d, 1H, J = 4.5 Hz, H-1), 4.37 (dd, 1H, J = 4.5, 2.5 Hz, H-2), 3.99 (dd, 1H, J = 2.5, 4.5 Hz, H-3), 3.75 (s, 3H, CO₂Me), 1.55 (s, 3H, Me)



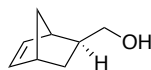
2-[2-[[[(1,1-dimethylethyl)dimethylsilyl]oxy]ethoxy]ethyl-1-methanesulfonate (28). To a solution of diethylene glycol **27** (150 mL, 1.58 mol) in CH₂Cl₂, *tert*-butyldimethylsilyl chloride (24 g, 158 mmol) and triethylamine (26 mL, 0.19 mol) was added, and the resulting mixture was stirred at rt for 2 h. The solution was extracted with hexanes:ethyl acetate (1:1) and washed with water to remove the excess diethylene glycol. The organic layer was dried with MgSO₄, concentrated *in vacuo*, and used without further purification.

To a solution of the TBS protected diethylene glycol intermediate (2.0 g, 9.08 mmol) in CH₂Cl₂ at 0 °C, Et₃N (1.05 mL, 13.6 mmol) and methanesulfonyl chloride (2.15 mL, 15.4 mmol) were added dropwise. The reaction mixture was warmed to rt and stirred overnight. The resulting reaction mixture was concentrated in vacuo, and purified using silica column chromatography (hexanes:ethyl acetate 2:1) to afford the desired product **28** in near-quantitative yield.

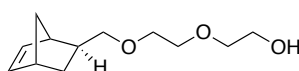


Exo-5-norbornene-2-carboxylic acid (30). Commercially available endo/exo-5-norbornene-2-carboxylic acid **29** (25 mL, 202 mmol) was dissolved in 0.75 M NaHCO₃ (500 mL). To this, a solution of KI (101 g, 608 mmol) and I₂ (51 g, 202 mmol) in H₂O (260 mL) was added dropwise. The resulting brown mixture was stirred at room temp for 4 h. The aqueous layer was extracted with Et₂O (5 x 100 mL) to remove the lactone. The aqueous layer was decolorized using 10 % NaHSO₃ and adjusted to pH 2 with 1 N H₂SO₄. This aqueous layer was extracted again with Et₂O (4 x 100 mL), with the pH adjusted to

pH 2 each time. The ether layers were combined, dried, and concentrated *in vacuo* to afford the desired product **30** (4.74 g) in 53 % yield. ^1H NMR (300 MHz, CDCl_3) δ 6.14 (p, $J = 5.4$ Hz, 2H), 3.19 – 3.04 (m, 1H), 2.95 (s, 1H), 2.34 – 2.18 (m, 1H), 1.96 (dt, $J = 12.8, 4.1$ Hz, 1H), 1.53 (s, 1H), 1.48 – 1.31 (m, 2H).

**31**

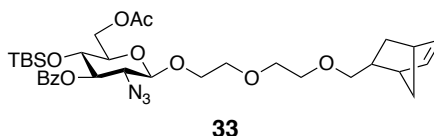
Exo-5-norbornene-2-methanol (31). *Exo*-5-norbornene-2-carboxylic acid **30** (1 g, 7.24 mmol) was dissolved in THF (13 mL) and cooled to 0 °C. LAH (0.83 g, 22 mmol) was added in small portions. The resulting mixture was warmed to rt and refluxed at 80 °C for 2 h. After cooling back to room temp, the reaction was quenched with H_2O (0.83 mL), 10 % NaOH (1.66 mL) and H_2O (2.49 mL) in sequence. The resulting slurry was filtered through Celite, and concentrated under vacuum to obtain compound **31**. **Note: This compound is volatile and should not be dried completely or left on the high-vac line.**

**32**

2-(2-((2S)-Bicyclo[2.2.1]hept-5-en-2-ylmethoxy)ethoxy)ethanol (32). *Exo*-5-norbornene-2-methanol **31** (4.09 g, 33.0 mmol) was dissolved in THF (60 mL) with 4Å molecular sieves and was stirred at room temperature for 30 min. The solution was cooled to 0 °C, and 95% NaH in mineral oil (1.06 g, 41.2 mmol) was added in portions and left to stir at 0 °C for 30 min. To this, a solution of 2-[2-[(1,1-dimethylethyl)dimethylsilyl]oxy]ethoxy]ethyl-1-methanesulfonate **28** (8.20 g, 27.5 mmol)

and 18-crown-6 (1.45 g, 5.49 mmol) in THF (15 mL) was added dropwise. The reaction mixture was stirred for 2 h at room temperature, and water was added dropwise to quench the reaction until there was no further gas formation. The resulting solution was diluted with CH₂Cl₂, washed with saturated NaHCO₃, and dried and concentrated under reduced pressure. Flash silica gel column chromatography (hexanes:ethyl acetate 20:1 → 5:1) afforded the desired *tert*-butyldimethylsilyl-protected intermediate (7.21 g) in 67% yield. ¹H NMR (500 MHz; CDCl₃): δ 6.00 (d, J = 25 Hz, 2H), 3.71 (t, J = 5.5 Hz, 2H), 3.60 – 3.28 (m, 8H), 2.72 (s, 1H), 2.69 (s, 1H), 1.65-1.62 (m, 1H), 1.26 – 1.21 (m, 2H), 1.19 – 1.14 (m, 1H), 1.05-1.01 (m, 1H), 0.83 (s, 9H), 0.00 (s, 6H); ¹³C NMR (125 MHz; CDCl₃): δ 147.1, 86.4, 83.0, 81.1, 80.7, 73.1, 55.3, 54.0, 51.9, 49.1, 40.0, 36.3, 28.7, 5.1. ESI MS: *m/z* calcd for C₁₈H₃₅O₃Si [M + H]⁺ 327.2356, obsd 327.2356.

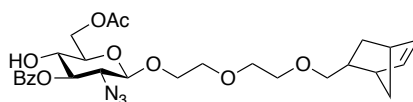
The product from the previous step (7.21 g, 22.1 mmol) was dissolved in THF (100 mL) and the temperature was lowered to 0 °C. A solution of 1 M TBAF in THF (44.2 mL, 44.2 mmol) was added to the reaction mixture dropwise, and the reaction was stirred for 2 h at 0 °C. The reaction was quenched with H₂O and extracted with ethyl acetate (3 x 15 mL). The organic layers were combined, dried over MgSO₄, and concentrated under reduced pressure. Flash silica gel chromatography (hexanes:ethyl acetate 5:1 → 1:1) afforded the final linker **32** (4.55 g) in 97% yield. ¹H NMR (500 MHz; CDCl₃): δ 6.11 – 6.04 (m, 2H), 3.72 – 3.37 (m, 10H), 2.80 (s, 1H), 2.74 (s, 1H), 2.48 (m, 1H), 1.71 (m, 1H), 1.34 – 1.23 (m, 3H), 1.13 – 1.09 (m, 1H); ¹³C NMR (125 MHz; CDCl₃): δ 136.9, 136.8, 76.4, 72.2, 70.7, 70.6, 62.1, 45.2, 43.9, 41.8, 39, 30. ESI MS: *m/z* calcd for C₁₂H₂₁O₃ [M + H]⁺ 213.1491, obsd 213.1483.



6-O-Acetyl-2-azido-3-O-benzoyl-4-O-tert-butyltrimethylsilyl-1-O-(2-(2-((2S)-bicyclo[2.2.1]hept-5-en-2-ylmethoxy)ethoxy)ethyl)-2-deoxy- β -D-glucopyranoside (33).

6-O-Acetyl-2-azido-3-O-benzoyl-4-tert-butyltrimethylsilyl-2-deoxy- β -D-glucopyranoside trichloroacetimidate **10** (444 mg, 0.72 mmol) and 2-(2-((2S)-Bicyclo[2.2.1]hept-5-en-2-ylmethoxy)ethoxy)ethanol **32** (230 mg, 1.08 mmol) were combined and azeotroped three times with toluene (5 mL) followed by 1 h under high vacuum. A solution of azeotroped starting materials in CH_2Cl_2 (5 mL) was mixed with activated 4 Å molecular sieves for 20 min at room temperature. The reaction mixture was cooled to $-20\text{ }^\circ\text{C}$, and $\text{BF}_3\cdot\text{OEt}_2$ (0.72 mL of 0.5 M solution in CH_2Cl_2 , 0.36 mmol) was added dropwise. After stirring at $-20\text{ }^\circ\text{C}$ for 30 min, the reaction mixture was gradually warmed to $0\text{ }^\circ\text{C}$, quenched with triethylamine, and filtered through a pad of Celite® with an ethyl acetate rinse. After removal of organic solvents *in vacuo*, the residue was purified by flash silica gel chromatography (hexanes:ethyl acetate 3:1) to afford **33** (370 mg) in 84% yield as a white solid. ^1H NMR (500 MHz; CDCl_3): δ 8.04 (dt, $J = 7.1, 1.4$ Hz, 2H), 7.56 (t, 1H), 7.44 (t, 2H), 6.04 (ddd, $J = 26.4, 5.7, 2.9$ Hz, 2H), 5.15 (dd, $J = 10.4, 8.9$ Hz, 1H), 4.58 (dd, $J = 8.1, 1.2$ Hz, 1H), 4.43 (dd, $J = 12.0, 2.2$ Hz, 1H), 4.12 – 4.10 (m, 1H), 4.00 (dt, $J = 11.2, 4.4$ Hz, 1H), 3.92 – 3.76 (m, 2H), 3.75 – 3.65 (m, 2H), 3.65 – 3.44 (m, 7H), 3.34 (td, $J = 9.3, 4.3$ Hz, 1H), 2.79 – 2.69 (m, 2H), 2.01 (s, 3H), 1.29 – 1.26 (m, 1H), 1.07 (dt, $J = 11.6, 3.9$ Hz, 1H), 0.72 (s, 7H), -0.02 (s, 3H), -0.22 (s, 3H); ^{13}C NMR (126 MHz, CDCl_3) δ 170.76, 165.51, 136.68, 136.61, 133.41, 129.93, 128.53, 102.22, 77.41, 77.16, 76.90, 76.11, 75.21, 74.37, 70.71, 70.45, 70.30, 69.36, 69.29, 64.51, 62.81, 60.46, 45.05, 43.68, 41.57, 38.77,

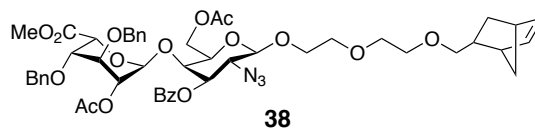
29.77, 25.61, 21.09, 20.96, 17.87, 14.24, -4.02, -4.88; HRMS ESI MS: m/z calcd for $C_{33}H_{50}N_3O_9Si$ $[M+H]^+$ 660.3311, obsd 660.3297.



34

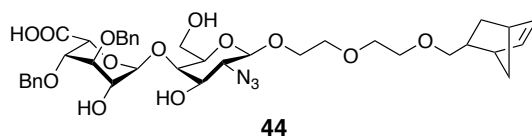
6-O-Acetyl-2-azido-3-O-benzoyl-1-O-(2-(2-((2S)-bicyclo[2.2.1]hept-5-en-2-ylmethoxy)ethoxy)ethyl)-2-deoxy- β -D-glucopyranoside (34). To a solution of **33** (370 mg, 0.60 mmol) in THF (6 mL) and pyridine (6 mL) at 0 °C was added HF·pyridine (3.5 mL) dropwise. The reaction mixture was allowed to warm up to room temperature and was stirred overnight. The reaction was quenched with saturated $NaHCO_3$ solution and diluted with ethyl acetate. The separated aqueous layer was extracted with ethyl acetate three times, the combined organic layers were washed with saturated $NaHCO_3$ solution, brine, and 10% $CuSO_4$. The organic layer was dried over $MgSO_4$ and concentrated *in vacuo*. The residue was purified by flash silica gel chromatography (CH_2Cl_2 :hexanes:ethyl acetate 1:1:2) to furnish compound **34** (250 mg) in 83 % yield as a white solid. 1H NMR (500 MHz; $CDCl_3$): δ 8.06 (dt, $J = 6.8, 1.4$ Hz, 2H), 7.64 – 7.54 (m, 1H), 7.49 – 7.42 (m, 2H), 6.06 (ddd, $J = 24.1, 5.6, 2.9$ Hz, 2H), 5.06 (dd, $J = 10.3, 9.1$ Hz, 1H), 4.57 (d, $J = 8.0$ Hz, 1H), 4.44 – 4.33 (m, 2H), 4.08 – 4.00 (m, 1H), 3.84 (ddd, $J = 10.9, 6.1, 4.2$ Hz, 1H), 3.75 – 3.71 (m, 2H), 3.68 – 3.65 (m, 2H), 3.62 – 3.55 (m, 3H), 3.51 (ddd, $J = 9.5, 6.2, 3.2$ Hz, 1H), 3.36 (td, $J = 9.2, 4.8$ Hz, 1H), 2.81 – 2.69 (m, 2H), 2.09 (s, 3H), 1.69 (tt, $J = 9.4, 5.6$ Hz, 1H), 1.34 – 1.26 (m, 2H), 1.08 (ddd, $J = 11.7, 4.3, 3.3$ Hz, 1H); ^{13}C NMR (125 MHz; $CDCl_3$): δ 171.61, 167.00, 149.51, 136.76, 136.64, 133.76, 130.09, 129.17, 128.62, 102.36, 76.16, 76.06, 74.17, 70.77, 70.46, 70.33, 69.53, 69.29, 63.90, 63.11, 45.09, 43.73, 41.62,

38.82, 29.82, 20.98; HRMS ESI MS: m/z calcd for $C_{27}H_{36}N_3O_9$ $[M+H]^+$ 546.2446, obsd 546.2453.



Methyl 2-O-acetyl-3,4-di-O-benzyl- α -L-idopyranosiduronate-(1 \rightarrow 4)-6-O-acetyl-2-azido-3-O-benzoyl-1-O-(2-(2-((2S)bicyclo[2.2.1]hept-5-en-2-ylmethoxy)ethoxy)ethyl)-2-deoxy- β -D-gluco-pyranoside (38). Glycosyl phosphate donor **25** (51.6 mg, 0.083 mmol) and acceptor **34** (29.7 mg, 0.064 mmol) were combined and azeotropically dried with toluene (3 x 5 mL) followed by 2 h under vacuum. The mixture was dissolved in CH_2Cl_2 (2 mL/0.10 mmol acceptor) and cooled to -30 °C for 2 min. *tert*-Butyldimethylsilyl trifluoromethanesulfonate (22 μ L, 0.096 mmol) was added dropwise. After stirring at -30 °C for 1 h, the reaction mixture was quenched with triethylamine (2 eq) and filtered through a pad of Celite® with an ethyl acetate rinse. After removal of organic solvents *in vacuo*, the residue was purified by flash silica gel chromatography (hexanes:ethyl acetate 3:1) to afford compound **38** (47.5 mg) in 85 % as a colorless oil. 1H NMR (500 MHz; $CDCl_3$): δ 8.07 – 8.02 (m, 2H), 7.59 – 7.52 (m, 1H), 7.42 (dd, J = 8.3, 7.2 Hz, 2H), 7.36 – 7.19 (m, 8H), 7.12 – 7.07 (m, 2H), 6.07 (ddd, J = 25.9, 5.7, 3.0 Hz, 2H), 5.25 (dd, J = 10.3, 9.2 Hz, 1H), 5.09 (d, J = 4.7 Hz, 1H), 4.77 – 4.72 (m, 1H), 4.63 (d, J = 12.1 Hz, 1H), 4.57 – 4.52 (m, 2H), 4.41 (dd, J = 12.2, 2.0 Hz, 1H), 4.32 (dd, 2H), 4.22 – 4.15 (m, 2H), 4.08 – 3.98 (m, 2H), 3.88 – 3.77 (m, 1H), 3.72 (dd, J = 5.7, 3.6 Hz, 2H), 3.68 – 3.50 (m, 6H), 3.41 (s, 3H), 3.39 – 3.32 (m, 1H), 2.82 – 2.72 (m, 2H), 2.04 (s, 3H), 1.96 (s, 3H), 1.78 – 1.61 (m, 1H), 1.33 – 1.19 (m, 2H), 1.13 – 1.06 (m, 1H); ^{13}C NMR (125 MHz; $CDCl_3$): δ 170.73,

170.01, 169.66, 165.46, 137.91, 137.31, 136.75, 136.72, 133.09, 130.12, 129.90, 128.50, 128.43, 128.32, 128.04, 127.91, 127.81, 127.65, 102.39, 99.00, 77.41, 77.16, 76.91, 76.20, 76.09, 75.09, 74.16, 73.03, 73.01, 72.77, 72.60, 70.87, 70.74, 70.55, 70.43, 70.41, 70.25, 69.55, 64.45, 62.28, 60.52, 51.79, 45.12, 43.75, 41.66, 38.86, 29.84, 21.19, 20.97, 20.90, 14.33; HRMS ESI MS: m/z calcd for $C_{50}H_{59}N_3O_{16}Na$ $[M+Na]^+$ 980.3788, obsd 980.3783.

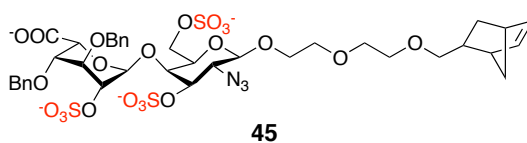


3,4-Di-O-benzyl- α -L-idopyranosiduronate-(1 \rightarrow 4)-2-azido-1-O-(2-(2-

((2S)bicyclo[2.2.1]hept-5-en-2-ylmethoxy)ethoxy)ethyl)-2-deoxy- β -D-glucopyranoside

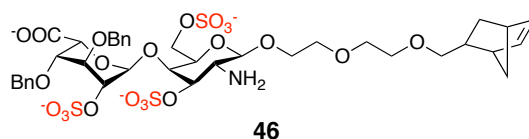
(44). To a solution of **38** (60mg, 0.063 mmol) in THF (5 mL) at -10 °C was added LiOH (1 M solution, 0.63 mL) and H_2O_2 (30% solution, 0.36 mL) simultaneously. After stirring for 12 h at room temperature, the mixture was cooled to -10 °C followed by the addition of methanol (5 mL) and NaOH (4 M solution, 0.79 mL). This reaction mixture was stirred at ambient temperature for 12 h, and neutralized with Amberlite® IR120 Hydrogen form resin, filtered, and concentrated *in vacuo*. The residue was first purified by Sephadex® LH-20 chromatography with 1:1 methylene chloride:methanol, followed by silica gel chromatography (40:2:1 ethyl acetate: methanol: water) to furnish compound **44** (40.2 mg) in 82% as a colorless oil. 1H NMR (500 MHz, CD_3OD) δ 7.39 – 7.20 (m, 10H), 6.06 (ddd, $J = 20.5, 5.7, 3.0$ Hz, 2H), 4.99 (d, $J = 3.6$ Hz, 1H), 4.69 (d, $J = 11.3$ Hz, 1H), 3.71 – 3.67 (m, 3H), 4.65 (d, $J = 2.6$ Hz, 1H), 4.62 – 4.54 (m, 3H), 4.40 (d, $J = 8.1$ Hz, 1H), 4.09 (ddd, $J = 3.6, 2.7, 0.8$ Hz, 1H), 3.99 (dt, $J = 11.2, 4.3$ Hz, 1H), 3.83 (dd, $J = 12.1, 2.3$ Hz, 1H), 3.81 – 3.69 (m, 2H), 3.68 – 3.56 (m, 6H), 3.52 (dd, $J = 9.5, 6.3$ Hz, 1H), 3.46 – 3.36 (m,

2H), 3.17 (dd, $J = 9.8, 8.2$ Hz, 1H), 2.74 (d, $J = 27.8$ Hz, 2H), 1.65 (dddd, $J = 14.7, 8.4, 4.4, 1.4$ Hz, 1H), 1.36 – 1.26 (m, 3H), 1.21 (dddd, $J = 11.5, 8.4, 2.4, 0.8$ Hz, 1H), 1.16 – 1.09 (m, 1H); ^{13}C NMR (126 MHz, CD_3OD) δ 176.22, 139.73, 139.44, 137.69, 137.55, 129.45, 129.29, 128.85, 128.77, 128.60, 103.76, 103.04, 79.61, 78.74, 78.61, 77.02, 76.78, 75.10, 74.39, 73.31, 72.06, 71.62, 71.56, 71.40, 70.79, 69.99, 68.38, 61.87, 45.85, 44.89, 42.76, 40.08, 30.63; HRMS ESI MS: m/z calcd for $\text{C}_{38}\text{H}_{49}\text{N}_3\text{O}_{13}\text{Na}$ $[\text{M} + \text{Na}]^+$ 778.3158, obsd 778.3160.

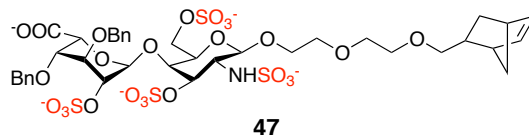


3,4-Di-O-benzyl-2-O-sulfonato- α -L-idopyranosiduronate-(1 \rightarrow 4)-2-azido-3,6-di-O-sulfonato-1-O-(2-(2-((2S)bicyclo[2.2.1]hept-5-en-2-ylmethoxy)ethoxy)ethyl)-2-deoxy- β -D-glucopyranoside (45): To a solution of **44** (42.8 mg, 0.055mmol) in anhydrous DMF (3.5 mL) at ambient temperature was added $\text{SO}_3\cdot\text{NMe}_3$ complex (237 mg, 1.70 mmol) as a solid in one portion. The reaction mixture was stirred at 55 °C for 2 days and then quenched with triethylamine (1 mL) and MeOH (3 mL). Upon evaporation of organic solvent, the residue was purified by Sephadex® LH-20 chromatography with 1:1 methylene chloride: methanol to obtain compound **45** (39.7 mg) in 71% yield as a white solid. ^1H NMR (500 MHz, CD_3OD) δ 7.53 – 7.45 (m, 2H), 7.42 – 7.20 (m, 8H), 6.08 (ddd, $J = 23.8, 5.7, 3.0$ Hz, 2H), 4.67 (d, $J = 12.1$ Hz, 2H), 4.48 (t, $J = 9.4$ Hz, 2H), 4.36 (t, $J = 9.0$ Hz, 1H), 4.31 – 4.18 (m, 4H), 4.00 (dt, $J = 11.3, 4.4$ Hz, 1H), 3.92 (s, 1H), 3.81 (dt, $J = 10.7, 4.9$ Hz, 2H), 3.75 – 3.57 (m, 9H), 3.53 (dt, $J = 9.5, 6.3$ Hz, 1H), 3.41 (td, $J = 9.2, 5.8$ Hz, 2H), 2.75 (d, $J = 30.2$ Hz, 2H), 1.67 (dddd, $J = 9.4, 7.5, 5.3, 3.7$ Hz, 1H), 1.40 – 1.32

(m, 3H), 1.23 (ddd, $J = 11.0, 8.3, 2.3$ Hz, 1H), 1.14 (dt, $J = 11.7, 3.9$ Hz, 1H); ^{13}C NMR (126 MHz, CD_3OD) δ 179.50, 157.52, 153.60, 144.04, 137.60, 129.40, 128.68, 127.75, 112.94, 110.71, 106.19, 101.94, 79.98, 77.03, 71.56, 70.36, 67.22, 63.39, 56.82, 45.87, 44.90, 42.77, 40.04, 38.10, 35.00, 30.66, 30.65, 21.09, 20.04, 10.98; ESI MS: m/z calcd for $\text{C}_{38}\text{H}_{48}\text{N}_3\text{O}_{22}\text{S}_3\text{Na}$ $[\text{M} + \text{Na}]^+$ 1017.1795, obsd 1017.9629.



3,4-Di-O-benzyl-2-O-sulfonato- α -L-idopyranosiduronate-(1 \rightarrow 4)-2-amido-3,6-di-O-sulfonato-1-O-(2-(2-((2S)bicyclo[2.2.1]hept-5-en-2-ylmethoxy)ethoxy)ethyl)-2-deoxy- β -D-glucopyranoside (46). To a solution of **45** (78 mg, 0.079 mol) in THF (10 mL), and NaOH (0.1 M solution, 4.7 mL) at ambient temperature was added PMe_3 (1 M in THF, 0.63 mL). The reaction mixture was stirred at room temperature overnight and was neutralized with a 0.1 M solution of HCl. After concentration *in vacuo*, the residue was purified using Sephadex® LH-20 chromatography with methanol, and this crude product **46** was used for the next reaction. ^1H NMR (500 MHz, CD_3OD) δ 7.47 (d, $J = 7.8$ Hz, 2H), 7.43 – 7.20 (m, 6H), 6.09 (ddd, $J = 22.5, 5.7, 2.9$ Hz, 2H), 4.65 (d, $J = 11.8$ Hz, 2H), 4.56 (d, $J = 10.3$ Hz, 2H), 4.33 (q, $J = 8.2$ Hz, 3H), 4.25 (s, 1H), 4.08 – 3.98 (m, 1H), 3.94 (s, 2H), 3.87 – 3.77 (m, 1H), 3.77 – 3.58 (m, 13H), 3.59 – 3.49 (m, 1H), 3.48 – 3.39 (m, 1H), 2.76 (d, $J = 37.3$ Hz, 2H), 1.73 – 1.65 (m, 1H), 1.36 (dd, $J = 20.9, 12.3$ Hz, 3H), 1.29 – 1.20 (m, 1H), 1.21 – 1.11 (m, 1H); ESI MS: m/z calcd for $\text{C}_{38}\text{H}_{49}\text{NO}_{22}\text{S}_3\text{Na}$ $[\text{M} + 2\text{H} + \text{Na}]^+$ 990.1806, obsd 990.2563.



3,4-Di-O-benzyl-2-O-sulfonato- α -L-idopyranosiduronate-(1 \rightarrow 4)-2-sulfonatamido-3,6-di-O-sulfonato-1-O-(2-(2-((2S)bicyclo[2.2.1]hept-5-en-2-ylmethoxy)ethoxy)ethyl)-2-deoxy- β -D-glucopyranoside (47). To a solution of crude **46** (78.2 mg, 0.079 mmol) in anhydrous pyridine (15 mL) and triethylamine (3 mL) at ambient temperature was added SO₃·pyr complex (mg, mmol) as a solid in one portion. The reaction mixture was stirred at rt for 24 h and then quenched with triethylamine (5 mL) and methanol (10 mL). After evaporation of the organic solvent, the residue was purified by Sephadex® LH-20 with methanol to obtain **47** (45.5 mg) in 54% yield over two steps as a white solid. ¹H NMR (500 MHz, CD₃OD) δ 7.58 – 7.51 (m, 2H), 7.41 – 7.20 (m, 8H), 6.10 (ddd, J = 26.5, 5.8, 3.0 Hz, 2H), 4.97 (d, J = 12.4 Hz, 1H), 4.72 (d, J = 12.4 Hz, 1H), 4.66 (d, J = 6.3 Hz, 1H), 4.49 (d, J = 12.3 Hz, 2H), 4.43 (d, J = 10.8 Hz, 1H), 4.33 – 4.18 (m, 4H), 4.18 – 4.09 (m, 2H), 4.03 (ddd, J = 9.9, 5.8, 3.8 Hz, 3H), 3.90 – 3.61 (m, 7H), 3.57 (td, J = 9.9, 6.4 Hz, 1H), 3.52 – 3.39 (m, 1H), 3.37 (s, 1H), 2.77 (d, J = 20.4 Hz, 2H), 1.72 (dt, J = 13.6, 6.8 Hz, 1H), 1.39 – 1.29 (m, 3H), 1.25 (d, J = 7.1 Hz, 1H), 1.19 – 1.14 (m, 1H); ¹³C NMR (126 MHz, (CD₃)₂SO) δ 172.59, 138.60, 138.46, 136.53, 136.35, 128.33, 128.01, 127.82, 127.65, 127.32, 126.96, 101.02, 76.54, 74.88, 73.70, 71.30, 70.88, 70.36, 70.05, 69.81, 69.63, 69.50, 68.97, 67.32, 64.83, 55.73, 55.31, 44.67, 43.20, 41.00, 38.46, 31.28, 29.26, 22.09, 21.01, 18.65, 13.96; ESI MS: m/z calcd for C₃₈H₄₆NO₂₅S₄Na [M + Na]⁻ 1067.1134, obsd 1067.7520.

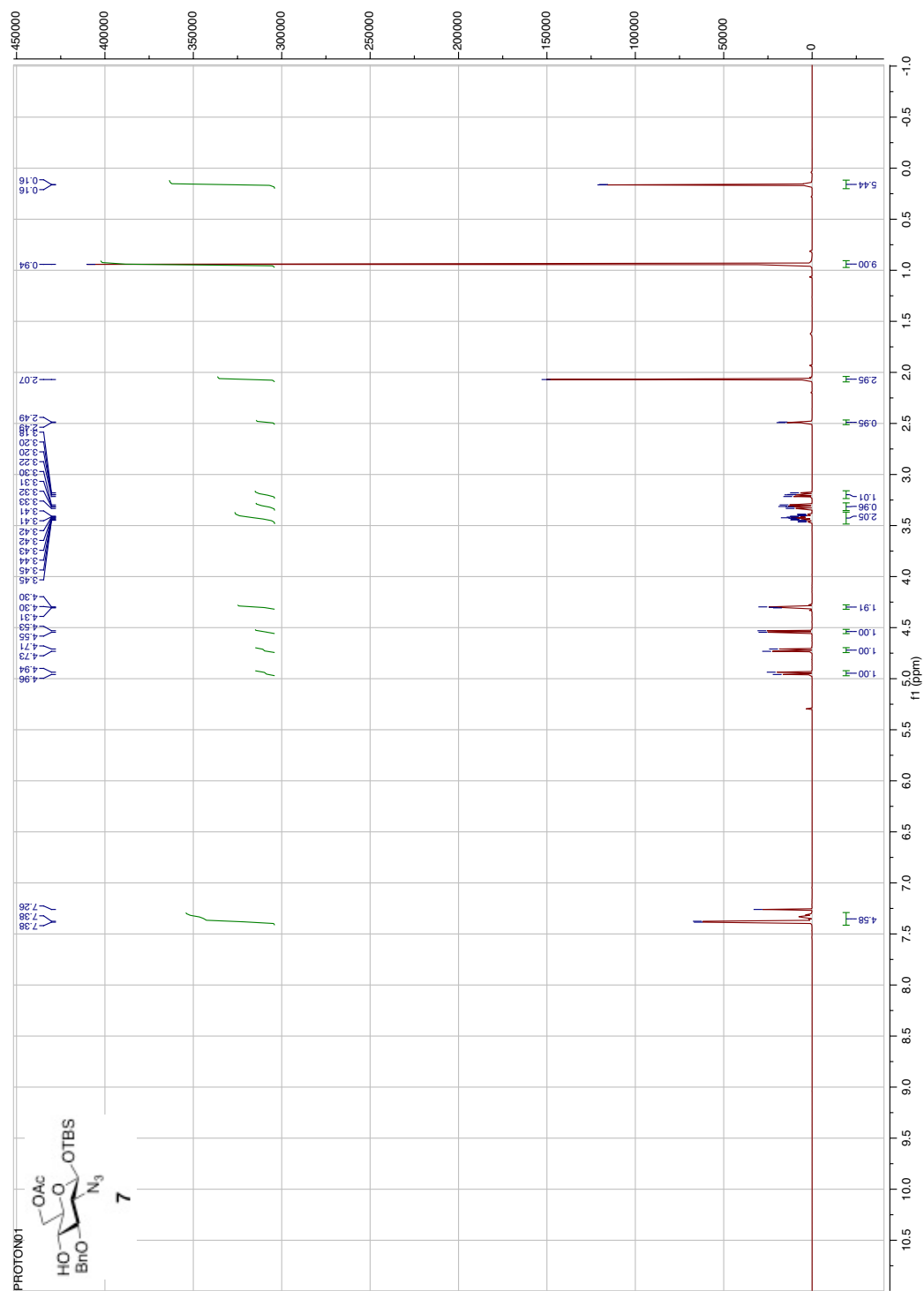


Figure 2.8: ^1H NMR (300 MHz, CDCl_3) of compound 7.

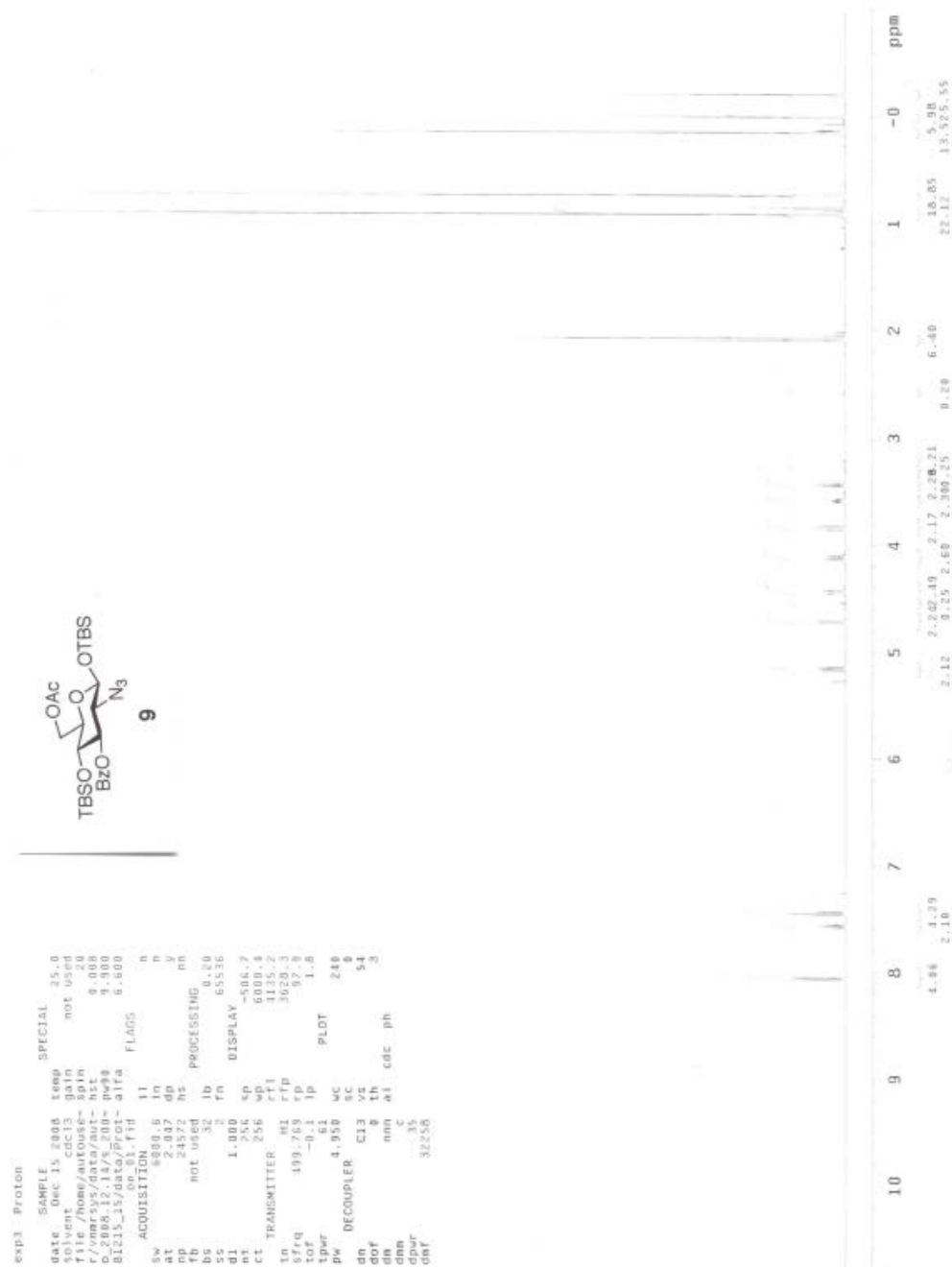
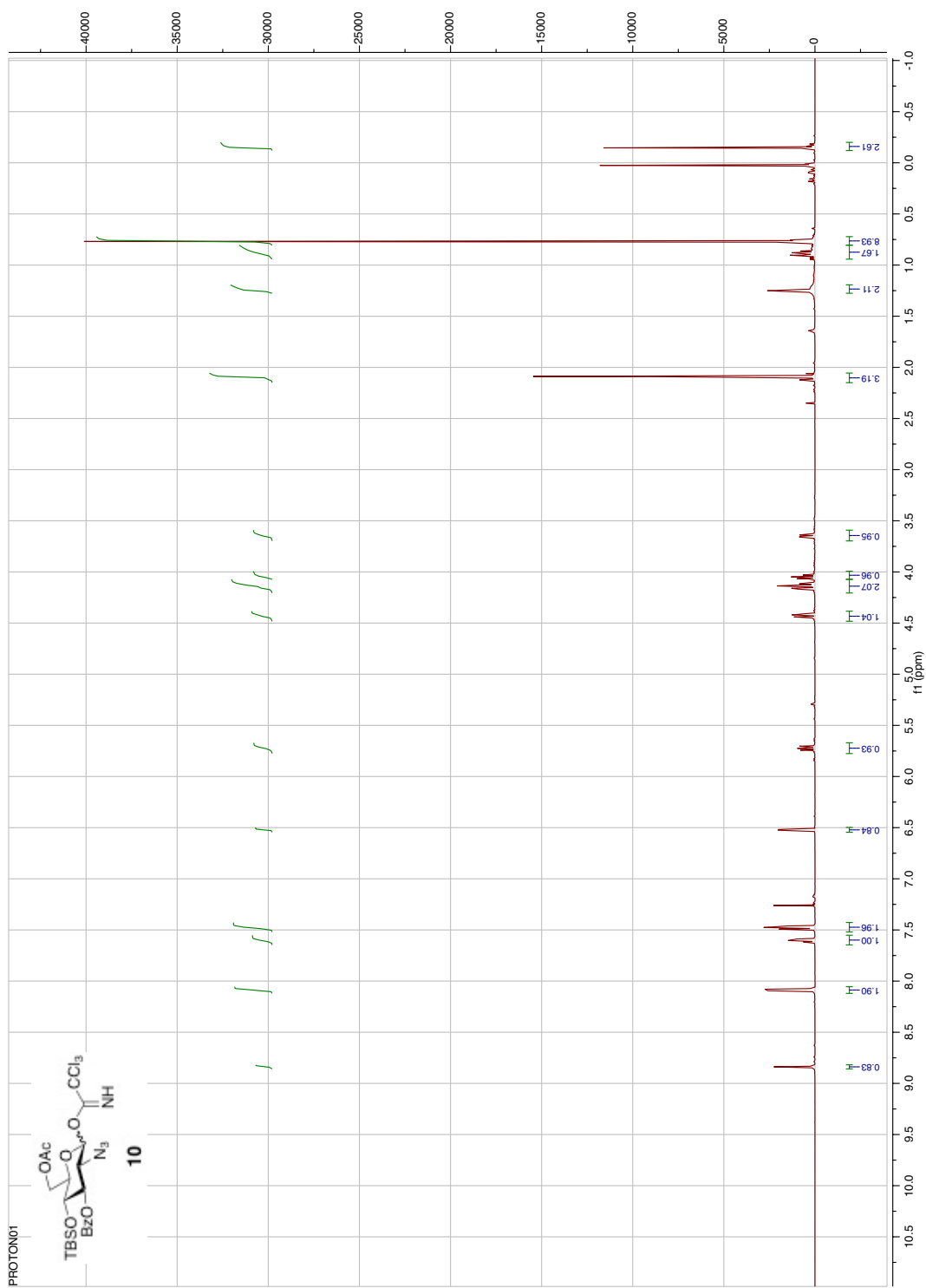


Figure 2.10: ^1H NMR (500 MHz, CDCl_3) of compound 9.

Figure 2.11: ^1H NMR (300 MHz, CDCl_3) of compound **10**.

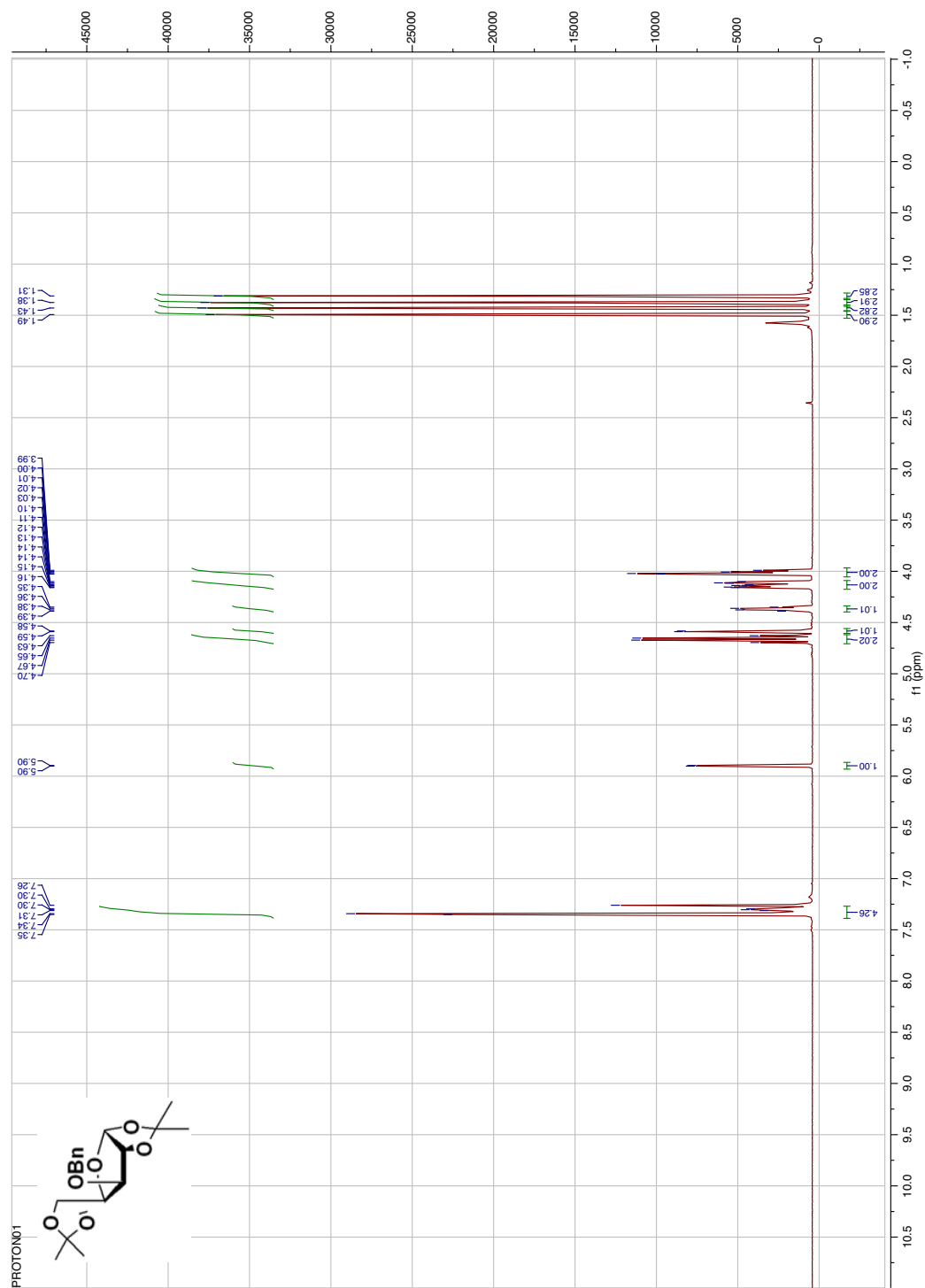


Figure 2.12: ^1H NMR (300 MHz, CDCl_3) of intermediate compound 11'.

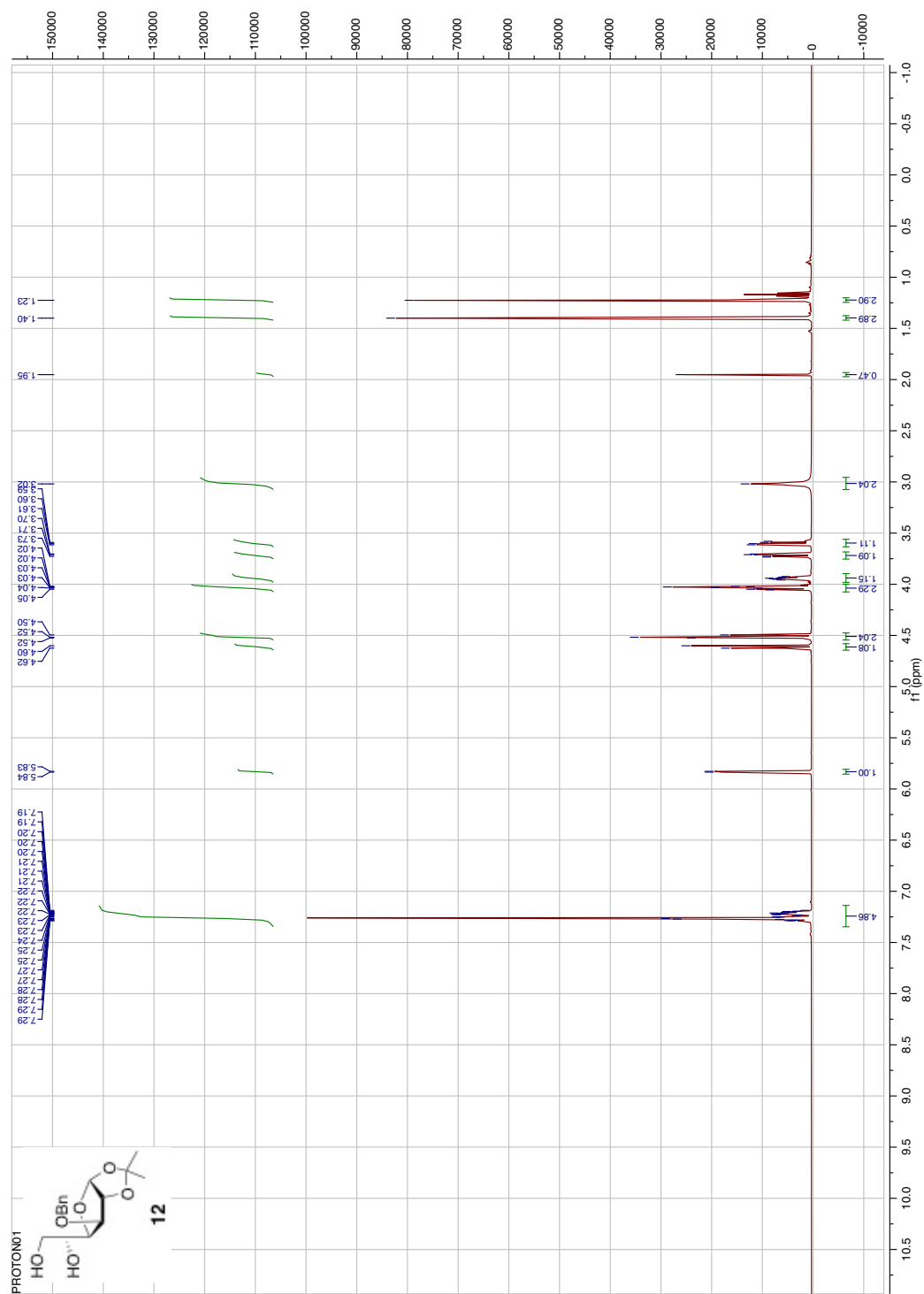


Figure 2.13: ¹H NMR (300 MHz, CDCl₃) of intermediate compound 12.

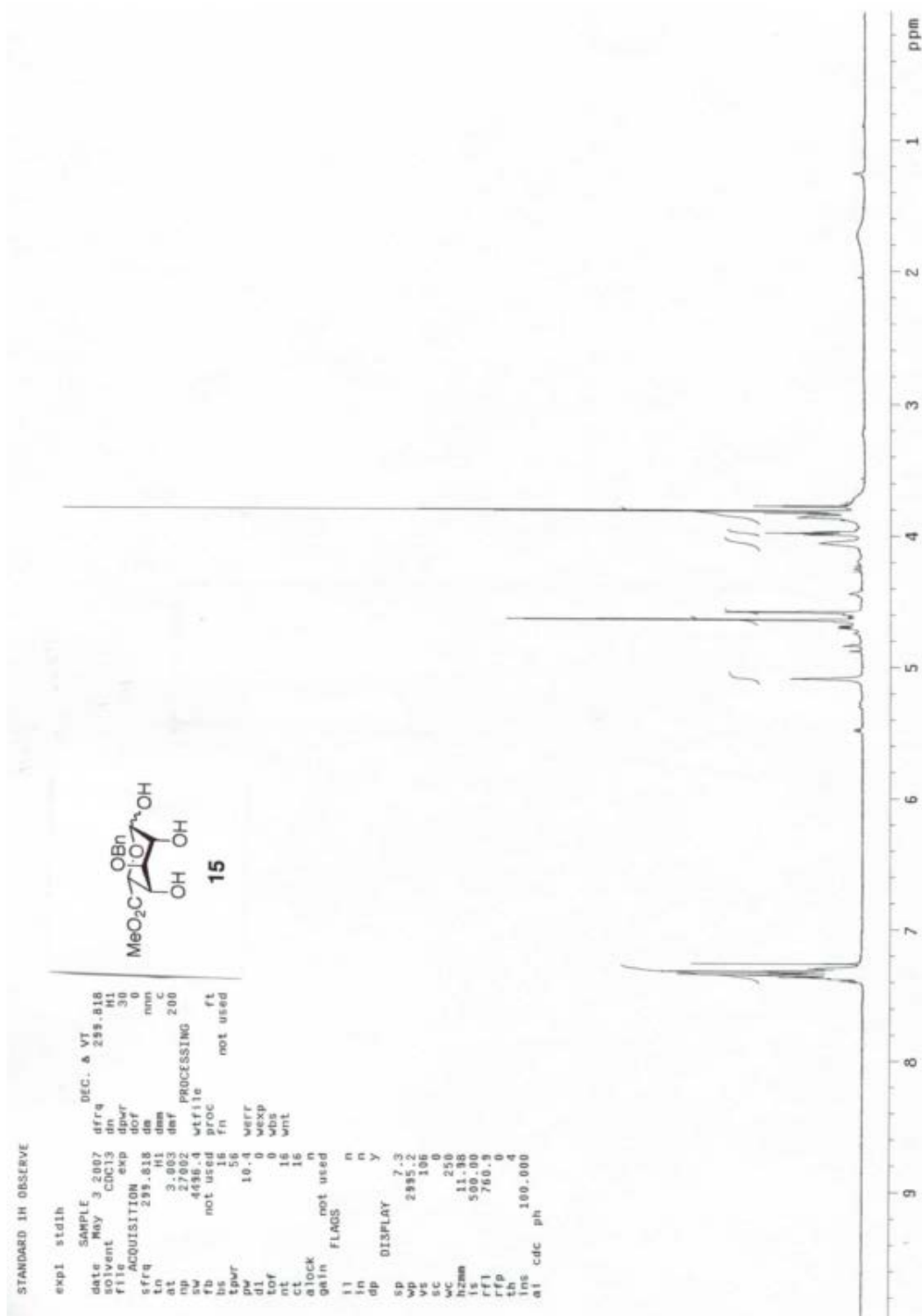


Figure 2.16: ^1H NMR (300 MHz, CDCl_3) of intermediate compound **15**.



Figure 2.17: ¹H NMR (300 MHz, CDCl₃) of intermediate compound 17.

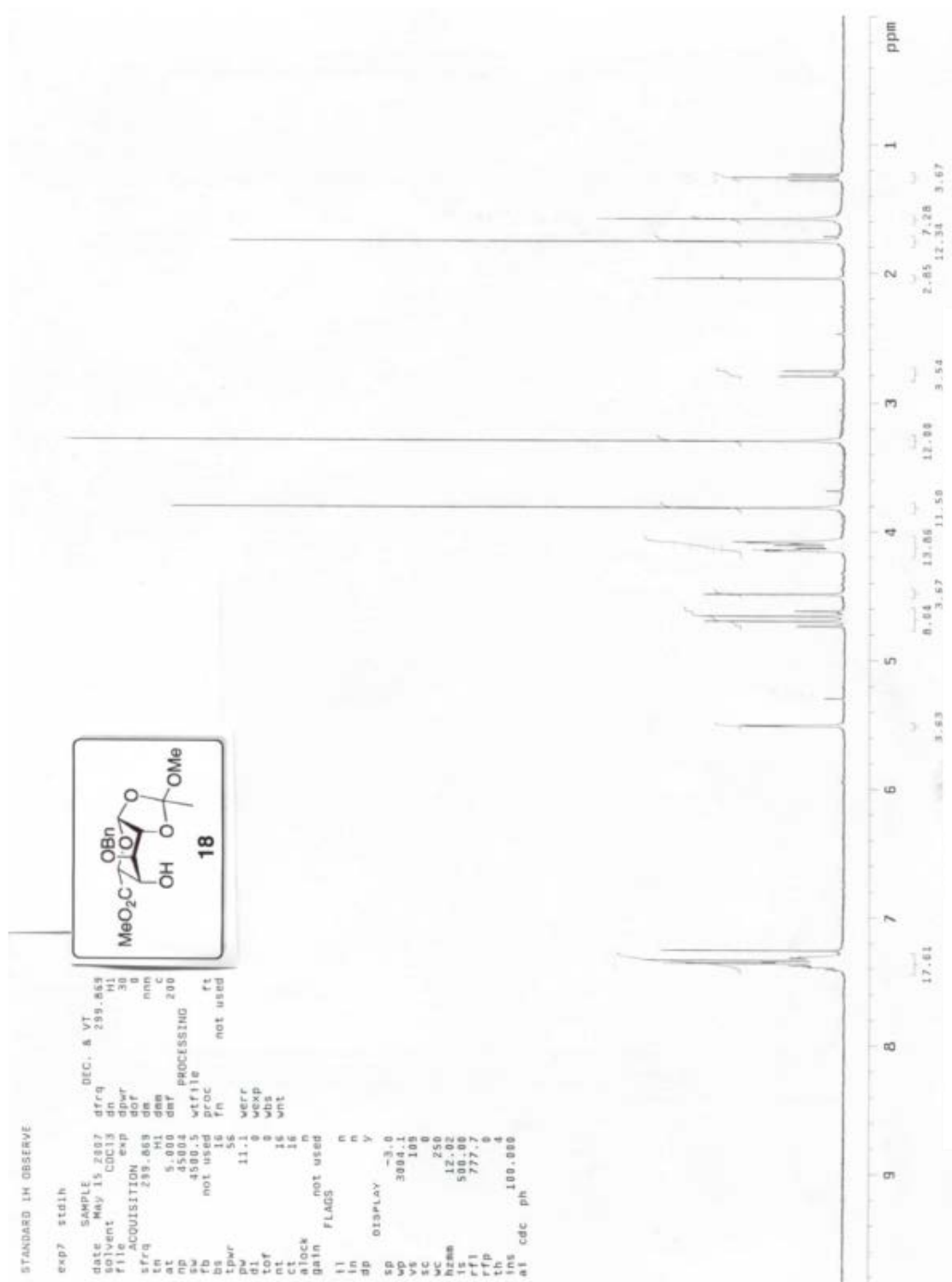
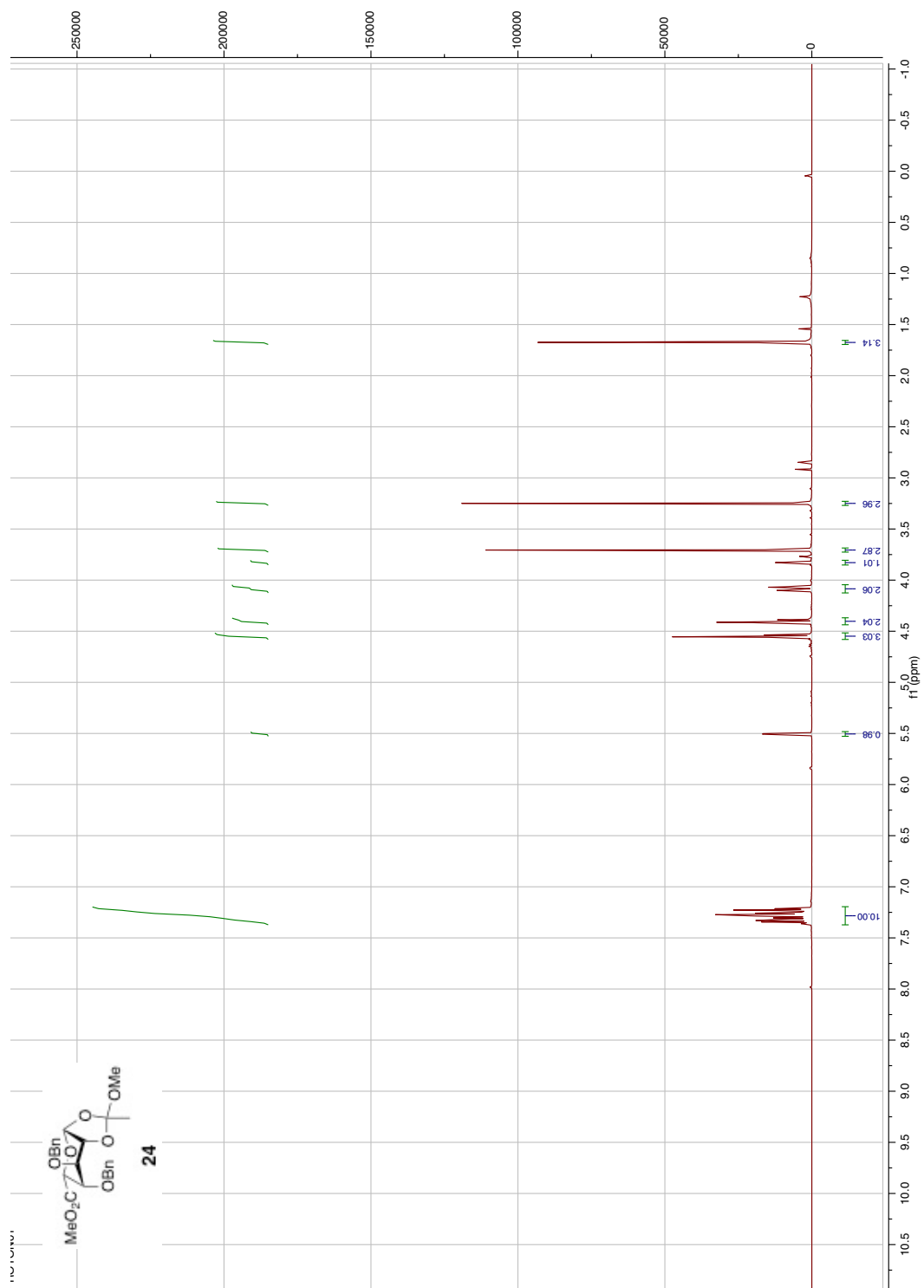


Figure 2.18: ^1H NMR (300 MHz, CDCl_3) of intermediate compound **18**.



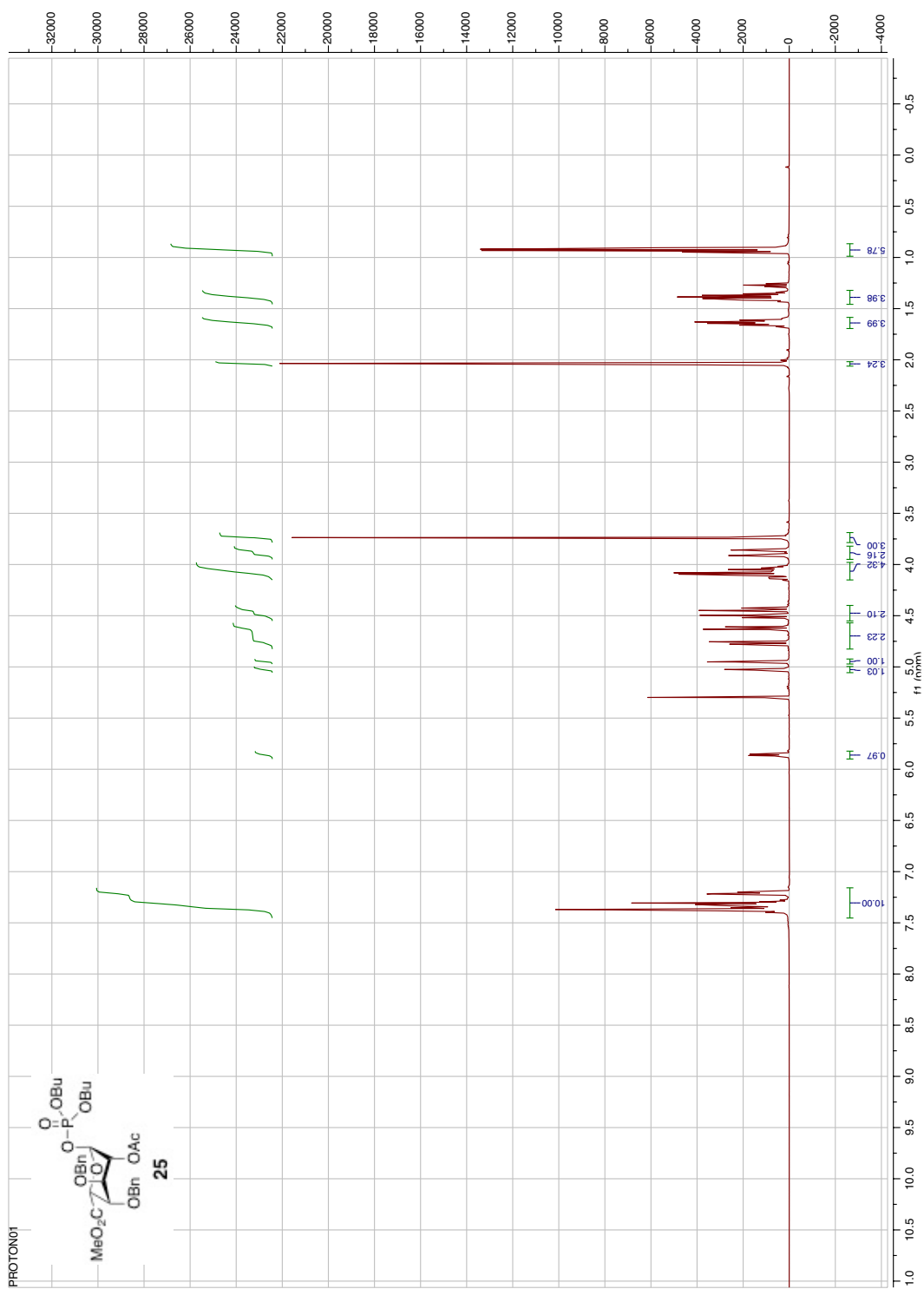
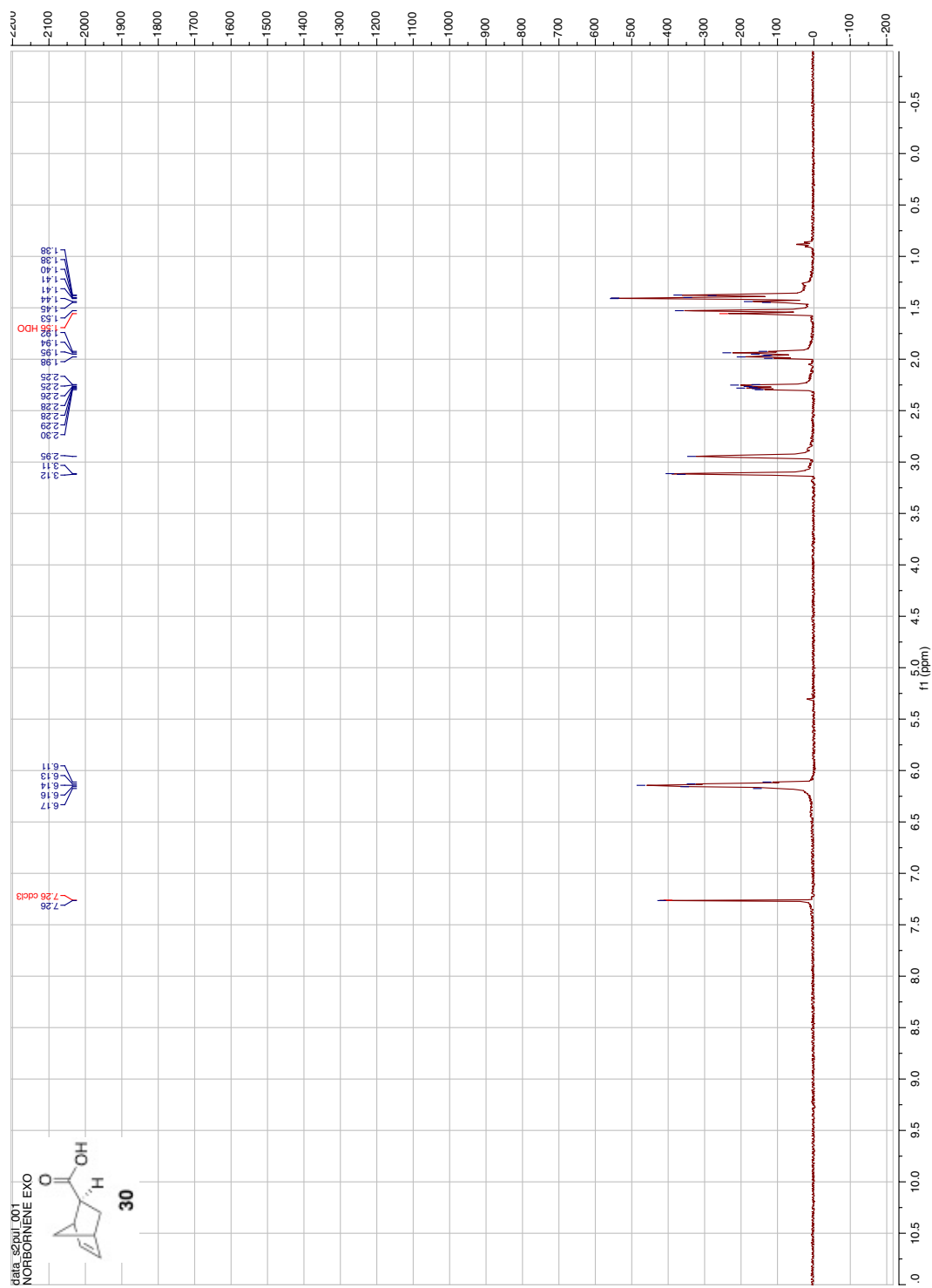


Figure 2.21: ¹H NMR (300 MHz, CDCl₃) of compound **25**.



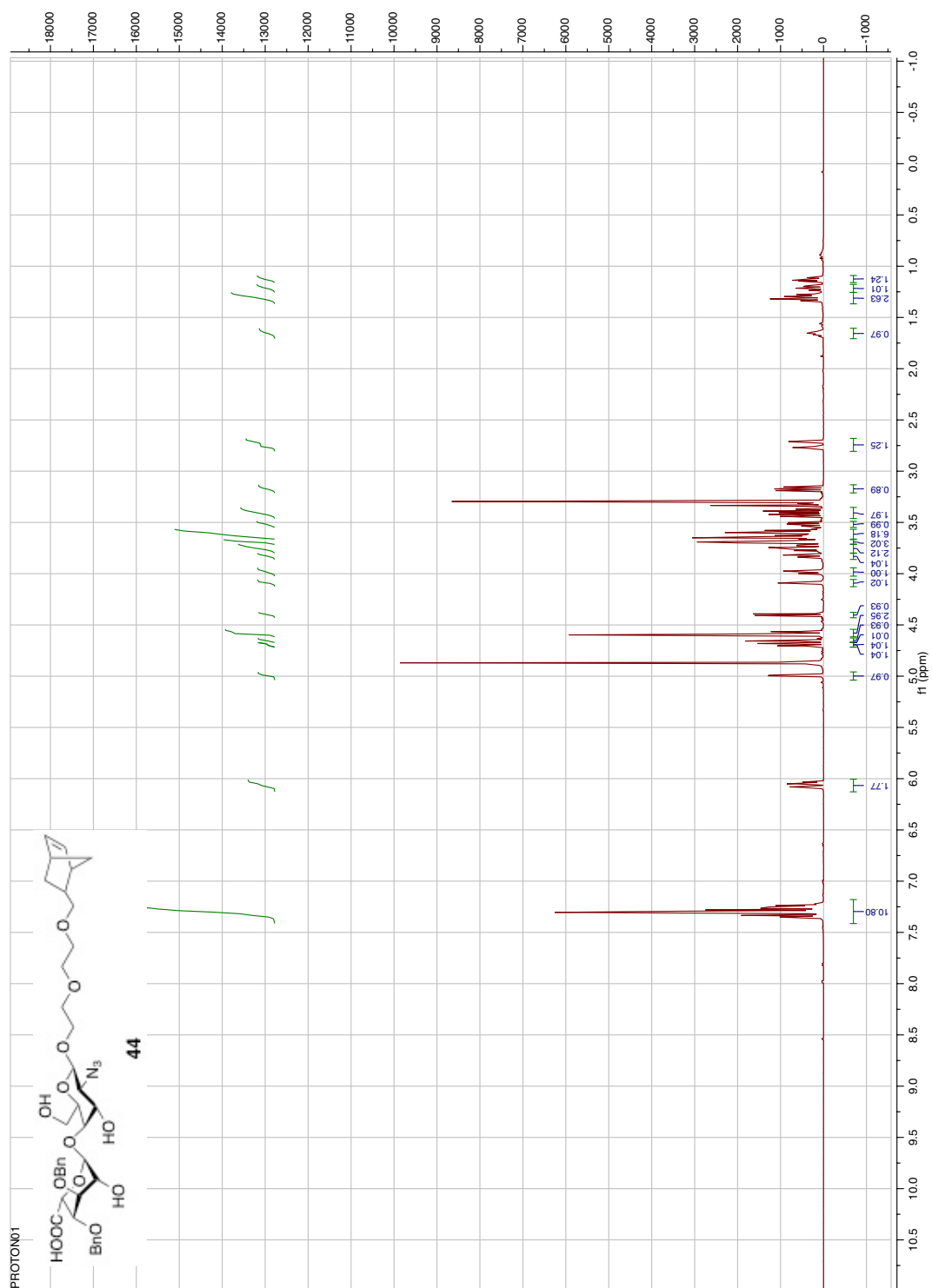
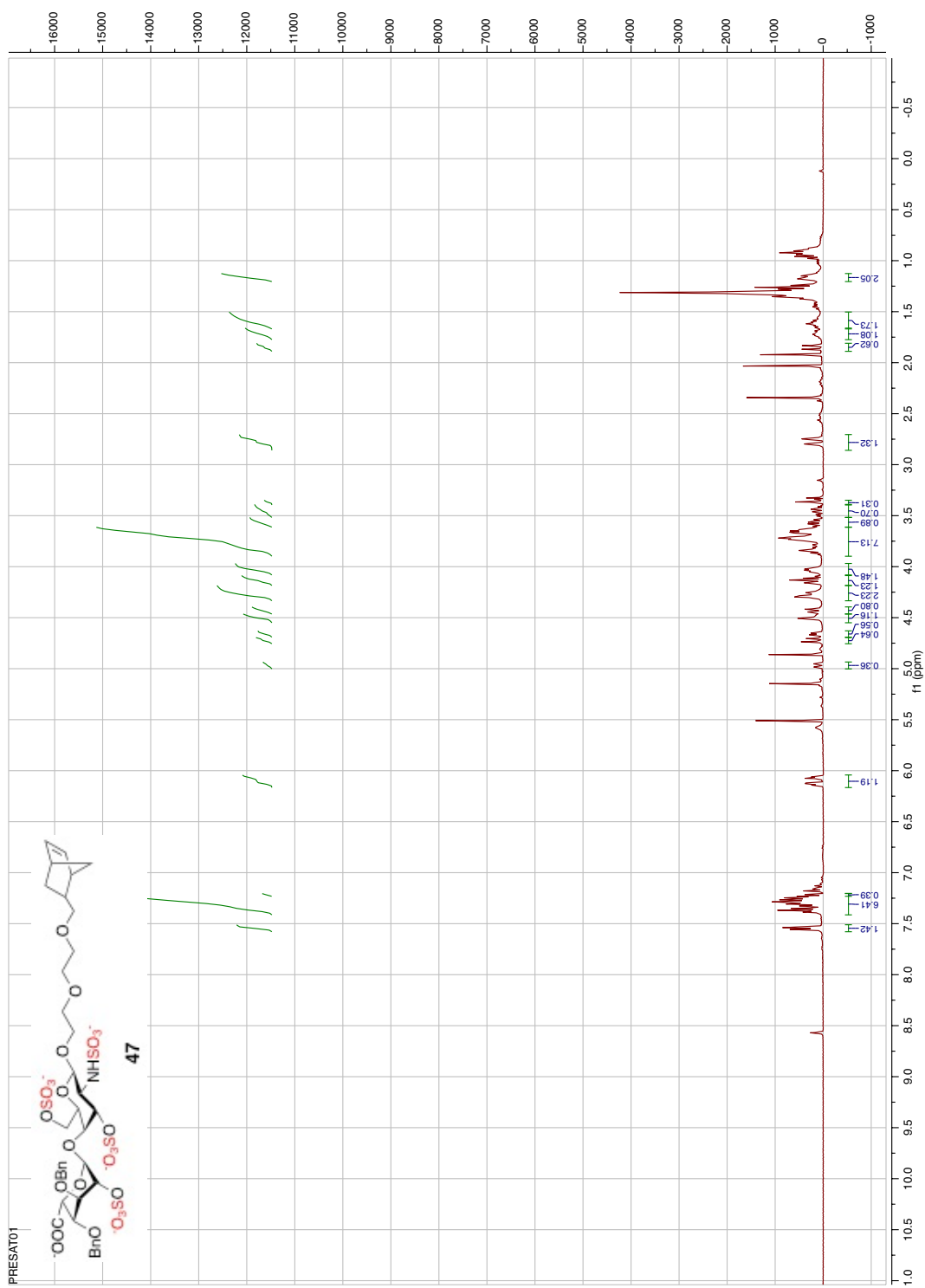


Figure 2.28: ¹H NMR (500 MHz, CD₃OD) of compound 44.

Figure 2.31: ¹H NMR (500 MHz, CD₃OD) of compound 47.

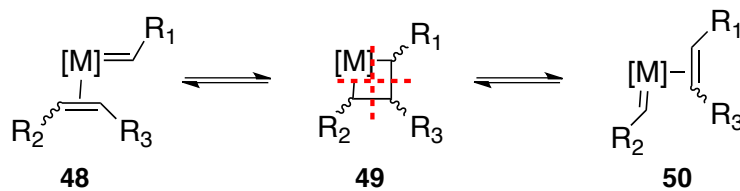
Chapter 3

POLYMERIZATION OF HEPARAN SULFATE GLYCOPOLYMERS

Synthetic polymers continue to be utilized in biomedical applications for use in prostheses, dental materials, medical devices,⁴ as supports for the fabrication of engineered tissues,⁷ and as therapeutics or drug delivery agents.⁸ Successful polymerization chemistry of such biopolymers largely depends on finding appropriate reaction conditions that can accommodate the generally hydrophilic monomer units. It is necessary to control the polymerization chemistry to afford well-defined materials with specific polymer chain lengths, molecular weight distributions, block architectures, and composition of pendant and end-group functionalities to ensure biocompatibility of the materials that are designed for service in biological contexts. Although the target polymer properties can be altered by any or all of these parameters, the capacity to specify and vary structure is essential in controlling and developing structure-function relationships. Using modern ruthenium-based metathesis catalysts in both organic and aqueous solutions, it is possible to construct biologically active polymers to study the effects of macromolecular architecture on biological functions.

Olefin metathesis and ring-opening metathesis polymerization chemistry

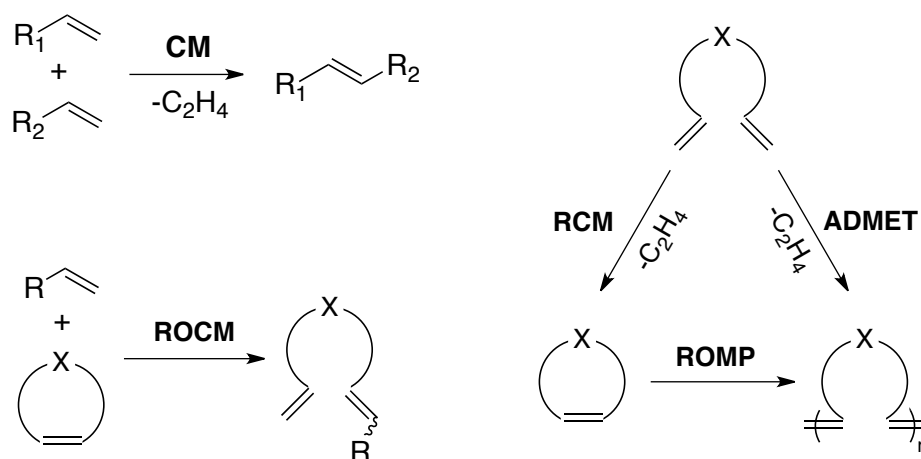
Olefin metathesis is a powerful chemical transformation that is widely used for the formation of carbon-carbon double bonds. This metal-catalyzed transformation acts on carbon-carbon double bonds and rearranges them via cleavage and reassembly.^{5,9-11} The



Scheme 3.1: General mechanism of olefin metathesis.³

widely accepted mechanism of transition metal metathesis proposed by Chauvin³ involves the coordination of an olefin to a metal carbene catalytic species, a direct [2+2] cycloaddition of the two alkenes, which then results in the reversible formation of a metallocyclobutane (Scheme 3.1). This intermediate can then undergo cycloreversion through two possible paths: the first is the non-productive path, which results in the re-formation of the two starting materials; the second path is product-forming, which yields an olefin that has exchanged a carbon with the catalysts' alkylidene species. As both processes are fully reversible in the absence of a thermodynamic driving force, only statistical mixtures of starting materials and other rearrangement products are produced.

The thermodynamic equilibrium of olefin metathesis reactions can be easily influenced with two main approaches to drive the reaction towards the desired metathesis product. The first approach utilizes Le Chatelier's principle by continuously removing one of the undesired products from the reaction to shift the equilibrium in favor of the desired product. This method is especially effective for cross metathesis (CM)¹² reactions, ring-closing metathesis (RCM),^{13,14} and acyclic diene metathesis polymerization (ADMET)¹⁵⁻¹⁷ by removing the volatile ethylene gas by-product. The second approach takes advantage of the ring strain of cyclic olefins such as cyclooctenes and norbornenes. The energy released during the ring-opening step is sufficient to drive the reaction forward, and is the driving force behind ring-opening cross metathesis (ROCM)^{18,19} and ring-opening metathesis



Scheme 3.2: Types of olefin metathesis reactions.

polymerization (ROMP) (Scheme 3.2).²⁰⁻²² In addition to these two main approaches, substrate concentrations or catalyst sensitivity to olefin substitution can also be exploited to influence product selectivity.²³⁻²⁶

Upon confirming the proposed mechanism with experimental evidence, rational catalyst design has resulted in the development of several well-defined, single-species metal catalysts. These transition metal catalysts have been developed with metals such as titanium,²⁷ tungsten,²⁸⁻³⁰ molybdenum,³¹ rhenium,^{32,33} osmium,^{34,35} and ruthenium.^{36,37} While such early transition metal catalysts are extremely active, some are sensitive to a variety of functional groups commonly used in organic synthesis. Air and moisture sensitivity limits their synthetic utility substantially; thus, appropriate catalysts must be selected for metathesis chemistry according to their functional group tolerance.

As demonstrated in Table 3.1, transition metal metathesis catalysts exhibit variations in functional group tolerance. For example, tungsten metathesis catalysts preferentially react with olefins in the presence of esters or amides, but favor ketones, aldehydes, alcohols, acids, and water over existing olefins.⁵ In contrast, ruthenium-based

Titanium (Ti)	Tungsten (W)	Molybdenum (Mo)	Ruthenium (Ru)
Acids	Acids	Acids	<i>Olefins</i>
Alcohols, Water	Alcohols, Water	Alcohols, Water	Acids
Aldehydes	Aldehydes	Aldehydes	Alcohols, Water
Ketones	Ketones	<i>Olefins</i>	Aldehydes
Esters, Amides	<i>Olefins</i>	Ketones	Ketones
<i>Olefins</i>	Esters, Amides	Esters, Amides	Esters, Amides

Functional group tolerance →

↑
Increasing order of reactivity

Table 3.1: Functional group tolerance of olefin metathesis catalysts.⁵

catalysts are tolerant towards most polar functional groups and water, though overall reactivity of the catalyst is diminished compared to earlier transition metals.³⁸ Molybdenum and ruthenium catalysts are most prominently used due to their versatility, high functional group tolerance, and reliable activity. For polymers with biomedical and/or biological applications, such as our HS glycopolymers, ruthenium catalysts are most frequently used due to their high functional group tolerance and ability to accommodate extremely polar functionalities (i.e., multiple sulfate groups of GAG-based polymers).

Despite the moderate activity of early ruthenium catalysts, their exceptional selectivity of olefins has led to the development of a number of modified catalysts. Initial ruthenium bis-triphenylphosphine (PPh₃) catalysts were limited to ROMP of strained monomers, but performed well in polar media.³⁸ Replacement of the PPh₃ ligands with tricyclohexyl phosphines (PCy₃) resulted in a much more active catalyst, commonly known as the “first generation Grubbs catalyst” **51** (Figure 3.1); this catalyst is capable of CM of acyclic olefins with high functional group tolerance.³⁹ Further substitution of one of the phosphine ligands for an electron donating N-heterocyclic carbene (NHC) ligand resulted

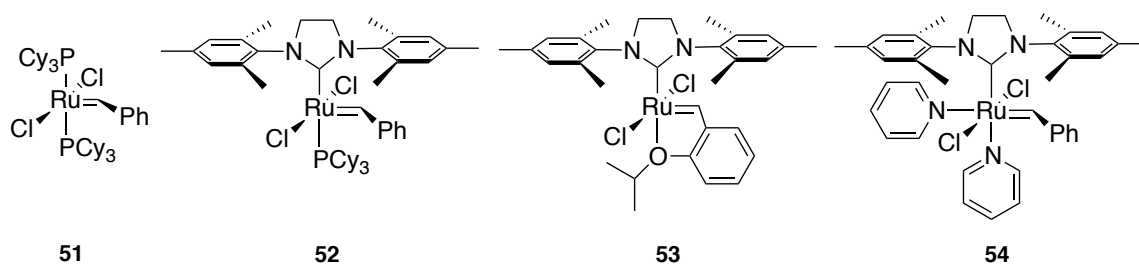


Figure 3.1: Ruthenium-based metathesis catalysts.

in the “second generation Grubbs catalyst” **52**⁴⁰ and the phosphine-free catalyst **53**.⁴¹ Although both **52** and **53** maintain excellent selectivity for olefins and exhibit high functional group tolerance, their slow initiation rates have limited their applicability. More recently, the bispyridine catalyst **54**⁴² has been utilized to promote ROMP of norbornenes with both high selectivity and functional group tolerance, and has been used towards the synthesis of GAG-based glycopolymers.⁴³ The continuing development of metathesis catalysts has widened the scope of metathesis chemistry into asymmetric reactions,⁴⁴ sterically demanding monomers,⁴⁵ and aqueous reaction conditions,⁴⁶ which all have potential to be beneficial in the synthesis of polymers with biomedical applications.

Multivalency effect of glycopolymers

Carbohydrates have the capability to present diverse chemical motifs in high density through structural elements such as branching and multivalency. The valency of molecular structures with carbohydrate ligands is defined as the number of identical units that contribute to receptor binding.⁴⁷ Multivalent interactions are defined as associations of the multiple carbohydrate ligands present on a structure that bind multiple receptors expressed on proteins or cell-surfaces. Such interactions are critical to carbohydrate–protein interactions in several biological phenomena. Multivalent ligand-

receptor interactions can produce potent biological activity by simply enhancing affinity,^{47,48} or through other methods such as clustering the relevant receptors.⁶ Thus, the mechanisms through which multivalent ligands act are important factors in determining methods to control the biological activity of synthetic multivalent scaffolds.

Many carbohydrate-protein interactions appear to take advantage of multivalent interactions to compensate for weak single ligand-receptor interactions. Association constants for monovalent carbohydrate-protein interactions are often low ($K_a = 10^{3-4} \text{ M}^{-1}$), even though the strength and specificity required for recognition in physiological settings is high.^{47,48} To compensate for these weak interactions, carbohydrate ligands are often displayed in multivalent arrays, where multiple copies of ligands are presented at the cell membrane or distributed along a glycoprotein. Similarly, a receptor can possess multiple binding sites or be present in multiple copies at the cell surface. The interaction between multivalent biomolecules and receptors with multiple ligand binding sites can result in the formation of numerous simultaneous binding events, resulting in the overall enhancement of affinity.

Monovalent and multivalent ligands can interact with receptors via several different mechanisms. Monovalent ligands have access to a limited number of binding mechanisms, and typically bind a single receptor or dimerize receptors using two receptor-binding faces. In contrast, multivalent ligands can interact with receptors through many different mechanisms (Figure 3.2), such as enhancing ligand affinity by decreasing the off-rate (chelate effect), allowing for secondary interactions in addition to binding the primary receptor (subsite binding), preventing competing interactions (steric stabilization), and by receptor clustering or by increasing the local concentration of the ligand.² Although the

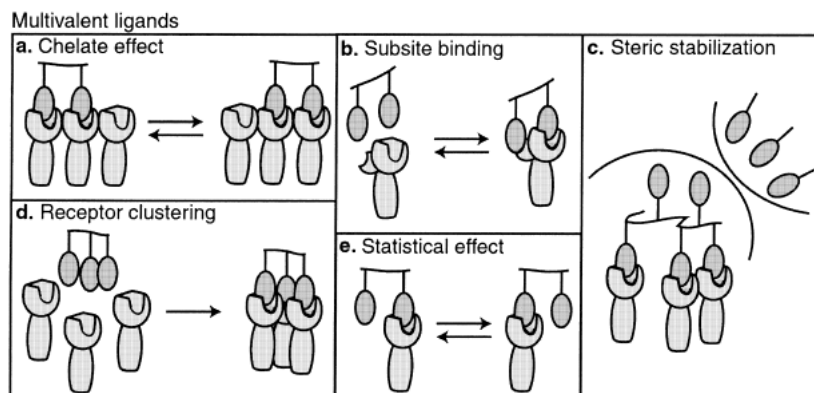


Figure 3.2: Modes of multivalent ligand binding.² (a) The *chelate effect* functions by enhancing ligand affinity by decreasing the off-rate. (b) *Subsite binding* enhances ligand affinity through secondary interactions. (c) *Steric stabilization* prevents competing interactions. (d) *Receptor clustering* increases the proximity between bound receptors maximizing binding events. (e) *Statistical effects* enhance ligand affinity through an increase in local concentration of ligand.

structural complexity of multivalent macromolecules is greater than that of monovalent ligands, their modes of ligand binding can still be influenced by adjusting their macromolecular architecture.⁴⁹

To mimic the multivalent architectures observed in biological systems, and to manipulate the resulting carbohydrate-protein interactions, synthetic chemists have assembled a variety of multivalent arrays with carbohydrate epitopes (Figure 3.3). The synthetic homogeneous glycan structures generally serve as better tools for carbohydrate-protein interaction studies, compared to naturally heterogeneous macromolecules. Recent progress in synthetic and chemoenzymatic methods allows for the preparation of well-defined multivalent carbohydrate structures with precise control over the size, shape, valency, and functional group incorporation of glycopolymers. By virtue of their carbohydrate moieties, these structures constitute potent carbohydrate scaffolds that insure multivalency, and have been receiving increasing interest due to their numerous applications.⁵⁰⁻⁵³ Additionally, they can have several practical and financial advantages

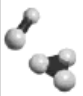
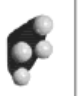
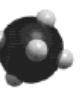
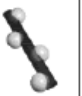
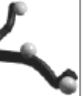
					
	Low molecular weight compounds	Dendrimers (PAMAM)	Globular proteins (BSA)	Linear polymers (from ROMP)	Polydisperse polymers (PEMA)
Size: (Da)	small (600-700)	small (1,500-7,500)	large (~250,000)	medium (3,000-34,000)	large (~100,000)
Maximum Valency:	low (2-3)	variable (4-16)	intermediate (15-20)	variable (5-100)	high (700)

Figure 3.3: Different classes of multivalent ligands.⁶

over other forms of neoglycoconjugates (i.e., neoglycoproteins, neoglycolipids, and liposomes) depending on their method of assembly.

Glycopolymer synthetic strategies include homo/heteropolymerization of carbohydrate monomers or polymer post-glycosylation, which can all result in tailored chemical functionalities. Homopolymers are the result of self-condensation of monomeric carbohydrate derivatives in the absence of any other added molecules. The polymerizable functionality can be placed at any position on the carbohydrate ring, and can be prepared as fully protected or deprotected carbohydrate monomers. Polymerization processes are initiated by suitable catalysts or by heating, and the resulting polymers are often isolated by precipitation or dialysis. This strategy has allowed the successful synthesis of a variety of glycopolymers with polyvinyl, polystyrene or poly(iminomethylene) backbones with potential biological applications such as biocompatible glycopolymers, drug delivery carriers, and immunodiagnostics.⁵⁴

While homopolymers contain a single polymerizable species, heteropolymers are built with added noncarbohydrate comonomers, which confer special physical and biophysical properties. These copolymers can be synthesized by direct copolymerization of two different monomers⁵⁵ or by a post-polymerization modification⁵⁶ approach.

Heteropolymers have the advantage of having the ability to control the incorporation of desired ratios of two monomers and thus determine saccharide density; custom-designed hybrid glycopolymers have also been synthesized using three distinct components to fine-tune desired properties.⁵⁷ Our lab has utilized this approach to alter the saccharide density of CS polymers, and have observed differences in biological activity by using a blank norbornene-diethylene glycol linker as a comonomer.⁵⁸

Organic chemistry allows access to novel architectures that provide a better understanding of biological processes involving carbohydrates. Polymerization chemistry allows for the effective presentation of multiple recognition elements on a single macromolecule, increasing their binding affinities relative to monovalent species. ROMP chemistry is commonly used to prepare multivalent polymers for biological applications⁵⁹⁻⁶¹ because of its ability to tolerate biologically relevant functional groups and its ease of controlling valency, ligand density, and chain length. Some common architectural motifs of multivalent ROMP polymers include polynorbornene or cyclooctadiene bearing pendant functional groups (Figure 3.4, A), amphiphilic block copolymer micelles (Figure 3.4, B), and end-functionalized polymer structures (Figure 3.4, C). For the synthesis of our HS

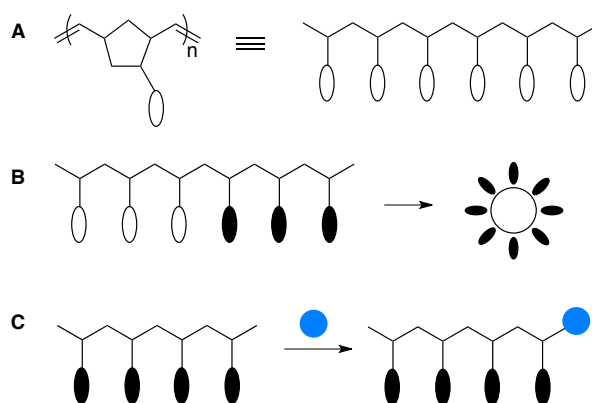


Figure 3.4: Common architectural motifs in ROMP polymers designed to utilize multivalency.¹

glycopolymers, we utilized the most common multivalent ROMP array: a polynorbornene homopolymers bearing the HS disaccharide pendant groups.

Use of ring-opening metathesis polymerization chemistry for biomedical applications

Ruthenium catalyzed ROMP is an attractive method to obtain multivalent polymer scaffolds because of its exceptional versatility and synthetic convenience.^{62,63} Polymerization reactions which proceed in the absence of termination steps and chain transfer reactions, such as ROMP, are considered 'living polymerizations'.⁶⁴ Because the rate of polymer chain initiation is faster than chain propagation in these living systems, ROMP affords polymers with controllable molecular weights, narrow polydispersities, and block copolymer scaffolds,⁶⁵ expanding opportunities to allow for the molecular level design of macromolecular structures for an enormous range of applications.

Norbornene-based monomer derivatives are commonly used for ROMP chemistry, taking advantage of the ring strain of the bicyclic structure and the resulting high reactivity towards irreversible ring-opening. An increase in steric bulk limits backbiting and interchain metathesis, and allows for the controlled synthesis of single chain multivalent polymers. With appropriate initiators and reaction conditions, living ROMP can be achieved with a variety of norbornene monomers to enable precise control over chain lengths and block copolymer architectures. However, due to the steric bulk associated with most biologically relevant functionalities, such as functionalized carbohydrates, norbornene-based monomers impose a considerable demand on the reactivity of ROMP initiators.

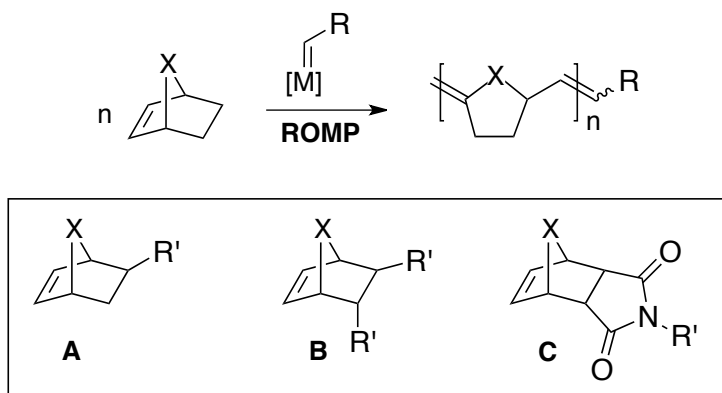


Figure 3.5: Different types of norbornene monomers for biologically relevant polymers.¹

Several different types of norbornene monomers are used to obtain biologically relevant polymers, based on the solubility and biocompatibility of the resulting polymer backbones. Oxanorbornenes (Figure 3.5, A; X=O) are readily accessible by Diels–Alder reactions with furan. The furan ring of the resulting polymer backbone increases solubility in water, and its structural resemblance to furanose sugars has shown to improve biocompatibility.⁶⁶ 5,6-Disubstituted norbornene monomers containing two distinct pendant groups (Figure 3.5, B) are not commonly used due to the high density of functional groups of the resulting polymer chain. Although the steric bulk may hinder efficient chain elongation, a large number of polar groups could be valuable in improving solubility while masking potentially bioincompatible polymer backbones. Succinimide norbornenes are most commonly used, which are accessible from norbornene-5, 6-dicarboxylic anhydride (Figure 3.5, C). For all these norbornene derivatives, both *endo* and *exo* isomers are possible, but the *exo* monomers have been shown to have higher ROMP reactivity.⁶⁷

Solubility is a major issue in ROMP of polymers with biomedical applications, because they often bear hydrophilic functionalities. Like many other organometallic reactions, olefin metathesis is usually carried out in dry, degassed aprotic organic solvents

to avoid catalyst deactivation by oxygen and moisture. However, completely deprotected biologically relevant monomers are rarely soluble in the aprotic organic solvents required for efficient ROMP. Thus, precipitation of growing polymer chains is a common obstacle when organic solvents are used for ROMP of monomers with polar substituents, especially as chain lengths increase. To accommodate the highly polar functionalities, it is critical for metathesis reactions of functionalized biopolymers to be carried out in polar solvents such as methanol or water.

Fortunately, the robustness of Ru initiators opens the possibility of metathesis in polar solvents such as methanol and water. Degassed water is an attractively inexpensive, nontoxic solvent that offers the potential for ROMP of hydrophilic monomers without need for protecting groups. While a number of water-soluble catalysts have been developed,^{46,68,69} these methodologies are not able to precisely control the polymerization of biological substrates. For reactions that require aqueous conditions, contact between the monomer and catalyst can be promoted using methanol as a co-solvent by use of an emulsifying agent such as dodecyltrimethylammonium bromide (DTAB).^{70,71} Emulsion polymerization has been shown to improve yields, and enable preparation of longer polymer chains.⁷² In most cases, the catalyst is usually predissolved in a chlorocarbon solvent such as CH₂Cl₂, because of its low solubility in aqueous media.

ROMP of carbohydrate-functionalized monomers have traditionally exhibited limited control over polymer chain lengths in the presence of methanol, often resulting in incomplete conversion. Previous examples of glycopolymer synthesis includes ROMP of a glucose-functionalized norbornene by RuCl₂(PCy₃)₂(=CHCHCPh₂) in 2:3 CH₂Cl₂:MeOH, which afforded only trace polymer even after 2 days at 50 °C.⁷³ Similarly, Kiessling and

coworkers reported that ROMP of a monosulfated galactose monomer via $\text{RuCl}_2(\text{PCy}_3)(\text{H}_2\text{IMes})(=\text{CHPh})$ in 1.5:1 $\text{CH}_2\text{Cl}_2:\text{MeOH}$, which proceeded to only 25% yield after 2 days at 65 °C.⁷⁴ Catalyst decomposition in the presence of methanol and insolubility of growing polymer chains is likely the cause of premature termination of these polymerization reactions.

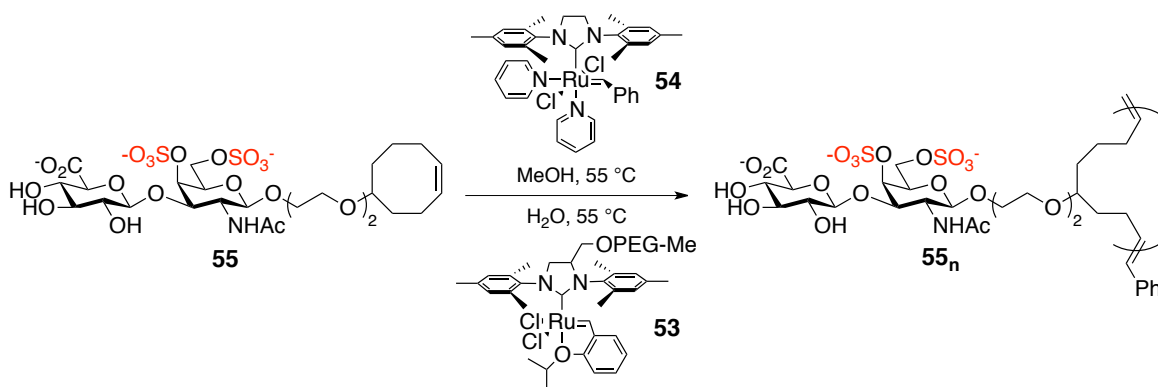
ROMP has emerged as a versatile and powerful tool for the preparation of complex polymeric materials with high control over polymer chain lengths and architecture. Although polymerization conditions where the monomer and initiator are present in a homogeneous organic solution are ideal, the biologically active functionalities on many polymers for use in biomedical applications require the use of polar solvents. In an effort to accommodate the high polarity of our tetrasulfated HS disaccharide monomers, we investigated the effects of different Ru ROMP catalysts, reaction conditions, and solvent systems based on previously synthesized carbohydrate-based glycopolymers.

Polymerization of glycosaminoglycan polymers

Investigations of efficient ROMP conditions for GAG-based glycopolymers were first investigated in our lab during the synthesis of CS-E cyclooctene-based glycopolymers.⁷⁵ When CS-E monomers were reacted with 2.5 mol% of fast initiating bipyridine catalyst in MeOH, the reaction resulted in incomplete conversion (36%) with a low degree of polymerization (DP = 21). Similarly, ROMP in aqueous media using the same catalyst loading of water soluble catalyst $(\text{H}_2\text{IMes-poly(ethyleneglycol))}(\text{Cl})_2\text{Ru}=\text{CH}(o\text{-}i\text{PrOC}_6\text{H}_4)_{14}$ resulted in incomplete conversion (7%) and even lower molecular weight polymers (DP = 8). It is likely that these reactions did not

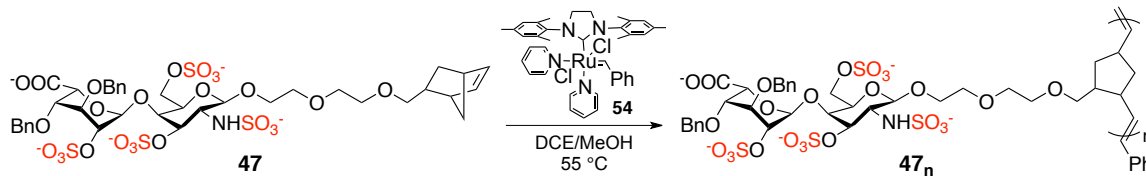
go to completion due to slow initiation of the water soluble catalyst⁷⁶ and coordination of MeOH to the catalyst reactive intermediates, which reduced propagation rates and resulted in premature chain termination.⁴²

To address the problem of low polymer conversion in MeOH and aqueous conditions, the CS glycopolymers utilized polymerization in a cosolvent system comprised of MeOH and dichloroethane ((CH₂Cl)₂). Elevated temperatures were still necessary to completely solubilize the CS-E cyclooctene monomers. Reaction of the CS monomers with 2.5 mol% catalyst with 1:5 MeOH/((CH₂Cl)₂) at 55 °C resulted in complete conversion to the desired polymer with 40 repeating units. These reaction conditions were applied to successfully synthesized norbornene-based CS-E polymers as well.⁴³



Scheme 3.3. Polymerization of cyclooctene-based chondroitin sulfate polymers

With the reaction conditions used to obtain CS glycopolymers, HS monomer **47** was first subjected to polymerization with 2 mol% catalyst using the MeOH/((CH₂Cl)₂) cosolvent system (Scheme 3.4). In contrast to the disulfated CS monomers, we expected that tetrasulfated HS monomers would have compromised solubility as a result of the higher number of sulfate groups and fewer of organic PGs. Therefore, we tried the first polymerization reaction with an increased amount of methanol using 1:4 MeOH/((CH₂Cl)₂).



Scheme 3.4. Polymerization reaction using bis-pyridine Grubbs 2nd generation catalyst.

Unfortunately, solubility of the monomers remained low even with increased amounts of MeOH and at elevated temperatures, which resulted in only moderate yields. Product conversion stalled around 50% conversion, and the monomer could be recovered from the reaction mixture. Upon addition of the catalyst to the monomer solution, compound precipitated out immediately, suggesting that the tetrasulfated HS monomer was too polar and crashed out of the solution at an oligomeric stage.

A few varying approaches were initially taken to increase monomer and polymer solubility while retaining catalyst activity. A series of different solvent systems were used to attempt successful polymerization. Dry, degassed nitromethane (CH₃NO₂) was used as a solvent, but led to minimal polymer conversion. Additionally, a cosolvent system using CH₂Cl₂, a more commonly used solvent for ROMP reactions, at both 2:1 DCE/MeOH and 1:1 DCE/MeOH was unsuccessful. No significant product formation was observed, and the unreacted monomer was recovered.

Upon attempting to control monomer and polymer solubility using different solvent systems, we looked into emulsion polymerization systems, which are commonly used for polar monomers in aqueous media. For emulsion polymerization reactions, the monomers were dispersed in deoxygenated water using an emulsifying agent, and the polymerizations were initiated by the injection of the catalyst dissolved in a small amount of DCE or DCM. We employed emulsification polymerization chemistry to our tetrasulfated monomers

using the cationic emulsifying agent, dodecyltrimethylammonium bromide (DTAB), as it has been shown to afford higher yields of polar polynorbornenes than an anionic surfactant such as sodium dodecyl sulfate (SDS).⁷⁷

To a 4-dram vial equipped with a Teflon-coated stir bar, monomer **47** and DTAB (3 eq) were added under argon. Degassed water was first added to dissolve the monomer, and the reaction was stirred vigorously at room temperature for 30 min. Bispiperidine catalyst **54** was dissolved in DCE, was briefly sonicated to ensure complete dissolution of the catalyst, and then injected (2 mol%) to the monomer solution via a gas-tight syringe. The ROMP reaction was terminated by adding an excess of ethyl vinyl ether to the reaction mixture. Unfortunately, this initial polymerization reaction was unsuccessful, and the unreacted monomer was recovered.

The Kiessling group had previously reported successful synthesis of high molecular weight neoglycopolymers from a norbornene-succinimide monomer with a fully deprotected monosaccharide.⁷¹ At lower catalyst loadings, the polymerization stalled at approximately 50% conversion, suggesting that termination processes were competing with elongation of the polymer chains. Emulsion conditions were successfully employed to synthesize longer neoglycopolymers (DP = 143) with 1 mol % catalyst loading. Following the experimental procedure reported in the synthesis of these long neoglycopolymers, monomer **47** was subjected to the reported reaction conditions: the monomer was subjected to a reaction with 3 eq DTAB with 2 mol% of catalyst **54** in 2:1 DCE/H₂O. After stirring at rt for 30 min, the mixture was stirred vigorously at 55 °C overnight. The reaction was terminated by adding an excess of ethyl vinyl ether to inactivate the catalyst, but there was minimal polymer product formation.

In addition to ROMP under emulsifying conditions, we also investigated ROMP conditions that utilize nanometer micelles. ROMP has been reported to proceed with high efficiency at room temperature by including a small percentage of noniononic, vitamin E-based amphiphile, polyoxyethanyl α -tocopheryl sebacate (PTS) in aqueous media.⁷⁸ The presence of this amphiphilic “dissolves” the otherwise water-insoluble reaction components (organic catalyst) within its nanometer micelles that self-assemble in aqueous media. Monomer **47** was subjected to ROMP with 2.5% PTS by weight and 2 mol % catalyst loading in water at rt for 3 h; unfortunately, there was minimal conversion of the monomer to the desired glycopolymer.

After exploring different polymerization reactions using emulsifiers in aqueous media, the previous DCE/MeOH cosolvent system was modified to accommodate the insoluble monomer. With these homogeneous conditions, a linear relationship between the catalyst loading and average degree of polymerization were observed, which is characteristic of living polymerizations; DCE/MeOH ratios were adjusted according to the various target polymer lengths (Table 3.1). Reactions targeting short polymers were run in 4:1 DCE/MeOH with high catalyst loadings, to afford polymers with lengths varying from DP = 4 – 8. Medium length polymers were run in a higher 3:1 DCE/MeOH cosolvent ratio and appropriately low catalyst loadings. Polymerization reactions with the longest target

Entry	DCE/MeOH	Mol % 54	Polymer	n	Mn (g/mol)	PDI
1	4:1	30	47 ₄	4	4 373	2.03
2	4:1	17	47 ₆	6	6 167	1.25
3	4:1	12.5	47 ₈	8	8 535	1.54
4	3:1	10.7	47 ₁₀	10	11 207	1.29
5	3:1	6.5	47 ₁₅	15	15 452	1.32
6	2.5:1	5.2	47 ₃₀	30	32 721	1.41
7	2.5:1	2	47 ₄₅	45	42 970	1.25

Table 3.2: Characterization of polymer series.

lengths had the lowest catalyst loadings, and were run in 2.5:1 DCE/MeOH to accommodate the decrease in solubility of the long polymer chains. Even at a cosolvent ratio of 2.5:1 DCE/MeOH, longer polymers crashed out within minutes of initiation, and afforded polymers with lengths of ~45 repeating units; HS and CS polymers with fewer sulfate groups have been shown to furnish polymers with up to 200 repeating units. Further increases in the amount of MeOH (i.e., 1:1 DCE/MeOH) resulted in incomplete conversion of the monomer, likely due to coordination of MeOH to the active catalyst species.

Upon purification of the various polymer species with an aqueous G-50 column, the glycopolymers were characterized by ^1H NMR spectroscopy and gel permeation chromatography (GPC). A representative GPC run is shown in Figure 3.6. GPC for polymers 47_n were carried out in an organic system in 0.2 M LiBr in DMF on two I-series Mixed Bed Low Molecular Weight ViscoGel columns (Viscotek), connected in series with a DAWN EOS multi-angle laser light scattering (MALLS) detector and an Optilab DSP differential refractometer (both from Wyatt Technology).

Once the synthesized polymers were characterized, they were subjected to

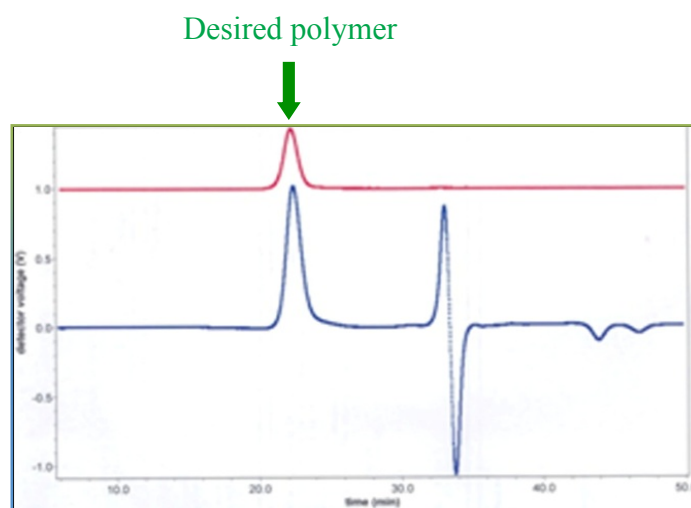
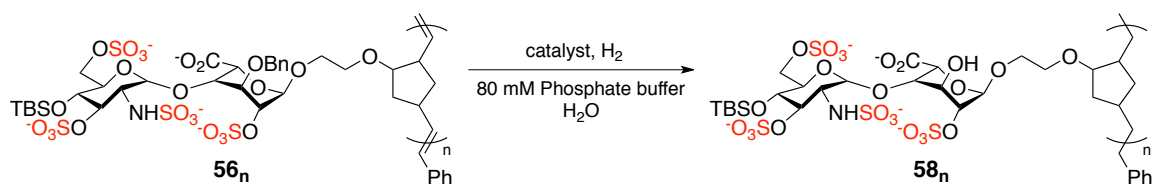


Figure 3.6: Representative GPC run for HS glycopolymers.

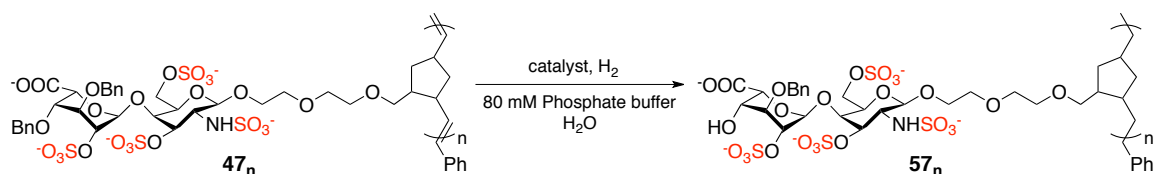
hydrogenation/hydrogenolysis to remove the permanent benzyl PGs to afford the final, fully deprotected tetrasulfated HS glycopolymers. Several different hydrogenation catalysts were tested for their effectiveness of removing benzyl groups and reducing the olefins along the hydrocarbon backbone of the polymers. These catalysts were tested on previously synthesized HS glycopolymers with a GlcN-IdoA acid linkage (Table 3.3). We began with the classically used Pd/C and pearlman's catalyst, Pd(OH)₂/C. Pd/C resulted in incomplete conversion, even after 3 days at 800 psi of H₂. Pearlmans's catalyst resulted in complete hydrogenation and debenzylation of the protected polymers. Simultaneously, Pt/C, Rh(OAc)₆, and Rh/C were used for hydrogenation chemistry, but all resulted in either incomplete hydrogenation or debenzylation of the polymers. The polymers were subjected to hydrogenations in a cosolvent for 80 mM phosphate buffer (pH = 7.2) and MeOH; the phosphate buffer ensured solubility of the polymer and maintained the pH of the reaction to protect against the loss of sulfate groups. Interestingly, at these high H₂ atms, we still observed removal of the C-4 TBS group in conjunction with debenzylation and reduction of the hydrocarbon backbone.



Entry	Catalyst	Amount	Result
1	Pd/C	6x by weight	incomplete
2	Pd(OH)₂/C	6x by weight	complete
3	Pt/C	6x by weight	incomplete
4	Rh(OAc) ₆	6x by weight	incomplete
5	Rh/C	10x by weight	incomplete

Table 3.3: Hydrogenation catalysts used for the compound **56_n**. Reactions were run in 1:1 80 mM phosphate buffer:MeOH, 800 psi H₂ for 3 days at room temperature.

Pearlman's catalyst was successfully employed to fully hydrogenate and debenzylate the series of polymers **47_n** (Scheme 3.5). However, we found that it was unnecessary to apply the polymers to such harsh reaction conditions (800 psi H₂). Hydrogenation using balloons with H₂ gas over 3 days resulted in full hydrogenation and deprotection of all HS glycopolymers. After hydrogenation, the reaction mixtures were filtered, lyophilized, then further purified using G-50 columns in ddH₂O to remove trace amounts of remaining catalyst. These polymers were then desalted for subsequent use in biological testing for anticoagulant activity.



Scheme 3.5: Hydrogenation of HS glycopolymer series.

Polymerization reactions of highly functionalized biological monomers are often challenging, due to the presence of charged functional groups and solubility issues related to the hydrophilic monomer species. By employing a DCE/MeOH cosolvent system at elevated temperatures, we have been able to successfully utilize ROMP chemistry to afford desired tetrasulfated HS glycopolymers **57_n**. A series of glycopolymers were synthesized, with polymer lengths ranging between 4 – 45 repeating units. The final polymer series was obtained by subjecting each of the polymers to a single-step hydrogenation reaction, which simultaneously reduced double bonds and cleaved the remaining Bn groups. With the glycopolymer series in hand, we then investigated the effects of length and sulfation pattern specificity on anticoagulant activity *in vitro* and *ex vivo*.

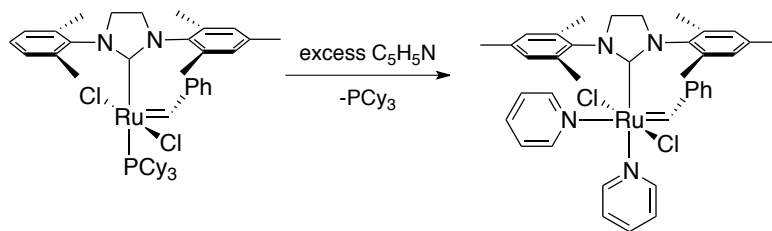
Experimental methods and spectral data

Unless otherwise stated, reactions were performed in flame-dried glassware under an argon atmosphere using dry, degassed solvents. Solvents were dried by passage through an activated alumina column under argon. All other reagents were purchased from Sigma-Aldrich, Acros Organics, Strem, or Alfa Aesar and used as received unless otherwise stated. Reaction temperatures were controlled by an IKAmag temperature modulator. Thin layer chromatography (TLC) was performed using E. Merck silica gel 60 F254 precoated plates (0.25 mm). Visualization of the developed chromatograms was performed by UV, cerium ammonium molybdate, or ninhydrin stain as necessary. Sephadex G-25 and G-50 columns were used for size exclusion chromatography.

^1H NMR and proton decoupling experiments were recorded on a Varian Mercury 300 (300 MHz), Varian MR-400 (400 MHz), or Varian Inova 500 (500 MHz) spectrometer and are reported in parts per million (δ) relative to residual D_2O (4.80 ppm). Data for the ^1H NMR spectra are reported as follows: chemical shift (δ ppm), multiplicity (s = singlet, bs = broad singlet, d = doublet, dd = doublet of doublet, t = triplet, q = quartet, m = multiplet), coupling constants in Hz, and integration. ^{13}C NMR spectra were obtained on a Varian MR-400 (101 MHz) or Varian Inova 500 (125 MHz) spectrometer.

The glycopolymers were characterized by ^1H NMR spectroscopy and gel permeation chromatography (GPC). GPC for polymers **47** were carried out in an organic system, and GPC for polymer **10** was carried out in an aqueous systems. The organic GPC was carried out in 0.2 M LiBr in DMF on two I-series Mixed Bed Low Molecular Weight ViscoGel columns (Viscotek), connected in series with a DAWN EOS multi-angle laser light scattering (MALLS) detector and an Optilab DSP differential refractometer (both

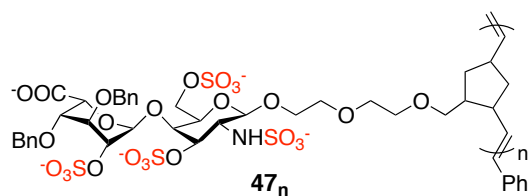
from Wyatt Technology). The aqueous system was carried out in 100 mM NaNO₃ and 200 ppm NaN₃ in H₂O on a single OHPak SB-804 HQ column (Shodex), connected in series with a miniDAWN TREOSTM multi-angle laser light scattering (MALLS) detector and an Optilab® rEXTM refractive index detector (both from Wyatt Technology).



Grubbs 2nd-generation bis-pyridine catalyst (IMesH₂)(C₅H₅N)₂(Cl)₂Ru=CHPh (54**)**^{36,42}

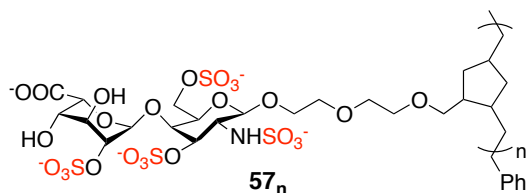
Grubbs 2nd generation catalyst (1.0 g, 1.18 mmol) was dissolved in pyridine (7.5 mL, 92.5 mmol). The reaction was stirred for 5 min at room temperature, during which time a color change from red to bright green was observed. To this reaction mixture, cold pentane (-10 °C, 25 mL) was added, and a green solid precipitated. The precipitate was filtered, washed with 4 x 15 mL of pentane, and dried under vacuum¹ to afford catalyst **54** as a green powder (0.73 g, 85% yield). Alternatively, pentane was added to the solution of complex A and pyridine, and was left in the cold room overnight to facilitate crystallization of the desired catalyst **54**.

¹ Do not leave prepared catalyst under vacuum for more than 15 minutes. The catalyst will decompose as a result of pyridine being pulled off from the complex.



Polymerization Procedure for Protected HS Monomers (47_n). In a typical polymerization experiment, a small vial was charged with HS monomer **47** (22.0 mg, 0.021 mmol) and a small stirbar under the flow of argon. To this was added dry, degassed methanol (150 μ L) and dry, degassed DCE (750 μ L). The ratio of MeOH:(CH₂Cl)₂ varied from 1:5 to 1:2.5 depending on the target polymer length. The monomer solution was heated and stirred at 55 °C for 10 min. The desired amount of bis-pyridine catalyst (0.013M stock solution in (CH₂Cl)₂) was then quickly added via syringe at 55 °C. The reaction mixture was stirred and heated at 55 °C for 2 h. At this point, the reaction mixture turned cloudy and the TLC of the crude reaction mixture showed complete consumption of starting material. The polymerization reaction was quenched by the addition of ethyl vinyl ether (300 μ L). The solvent was removed *in vacuo* to obtain a solid precipitate, which was dissolved in a minimal amount of CH₂Cl₂:MeOH (10:1). The polymer was then precipitated by slowly adding this solution to 25 mL of hexanes in a 50 mL beaker. This solution was centrifuged, and the hexanes was decanted to obtain the HS polymer 47_n as a white precipitate (n = number of repeating units determined by GPC). The ¹H NMR of the crude product showed the disappearance of the norbornene olefinic protons ~6 ppm, indicating completion of the polymerization reaction. The resulting pellet was dried, and purified using a Sephadex G-50 column eluted with water. ¹H NMR (400 MHz, D₂O) δ 7.39 – 7.11 (m, 10H), 4.94 – 4.87 (m, 1H), 4.81 – 4.68 (m, 1H), 4.69 – 4.60 (m, 1H), 4.61 – 4.53 (m, 1H), 4.53 – 4.44 (m, 2H), 4.38 (bs, 3H), 4.28 (bs, 2H), 4.23 – 4.09 (m, 3H), 4.10 –

4.00 (m, 1H), 4.00 – 3.74 (m, 4H), 3.73 – 3.37 (m, 6H), 4.23 – 4.09 (m, 2H), 2.22 – 1.99 (m, 2H), 1.99 – 1.70 (m, 3H), 1.69 – 1.37 (m, 3H).



Polymer Hydrogenation/hydrogenolysis. A mixture of the protected polymer **47_n** (21 mg) and 20% Pd(OH)₂/C (126 mg, 6x by weight) was dissolved in a mixed solvent of phosphate buffer (80 mM, pH = 7.2) and methanol (1/3 ratio, 2 mL). The reaction vessel was equipped with a hydrogen balloon, and the mixture was stirred at room temperature for 2 days. The reaction mixture was filtered through a Millipore Nylon Membrane (pore size 0.45 μM, Filter diameter 47 mm, Product #HNWP04700), and the membrane filter was washed with warm water (37 °C), and the filtrate was lyophilized. The dry residue was dissolved in H₂O (500 μL), and purified through a Sephadex G-50 column eluted with water, and desalted using a Sephadex G-25 column in water. The product fractions were lyophilized to obtain the target polymers **57_n**. ¹H NMR (500 MHz, D₂O) δ 5.16 (bs, 1H), 4.85 – 4.73 (m, 1H), 4.63 – 4.52 (m, 1H), 4.40 – 4.32 (m, 1H), 4.31 – 4.20 (m, 3H), 4.05 (bs, 1H), 4.03 – 3.92 (bs, 3H), 3.82 – 3.53 (m, 16H), 3.51 – 3.44 (m, 1H), 3.37 – 3.22 (bs, 2H), 1.89 – 1.70 (m, 2H), 1.68 – 1.55 (bs, 1H), 1.51 – 1.08 (m, 8H).

Recovery of Polymers After GPC Runs

Samples were prepared from fresh 0.2 M LiBr in DMF at 1 mg/mL concentrations. Both organic and aqueous GPCs have an injection loop of 100 μL. The injection loops were

flushed with fresh eluent (DMF or ddH₂O) to clean the loop prior to sample injection. 1 mL of the sample solution was injected into the injection loops, and the excess sample (0.9 mL) was collected into a conical tube at the end of the injection loop and lyophilized for recovery. This samples was run through G-25 columns with ddH₂O, and were salted (0.2 M NaCl) then desalted (ddH₂O) for further use in biological assays.

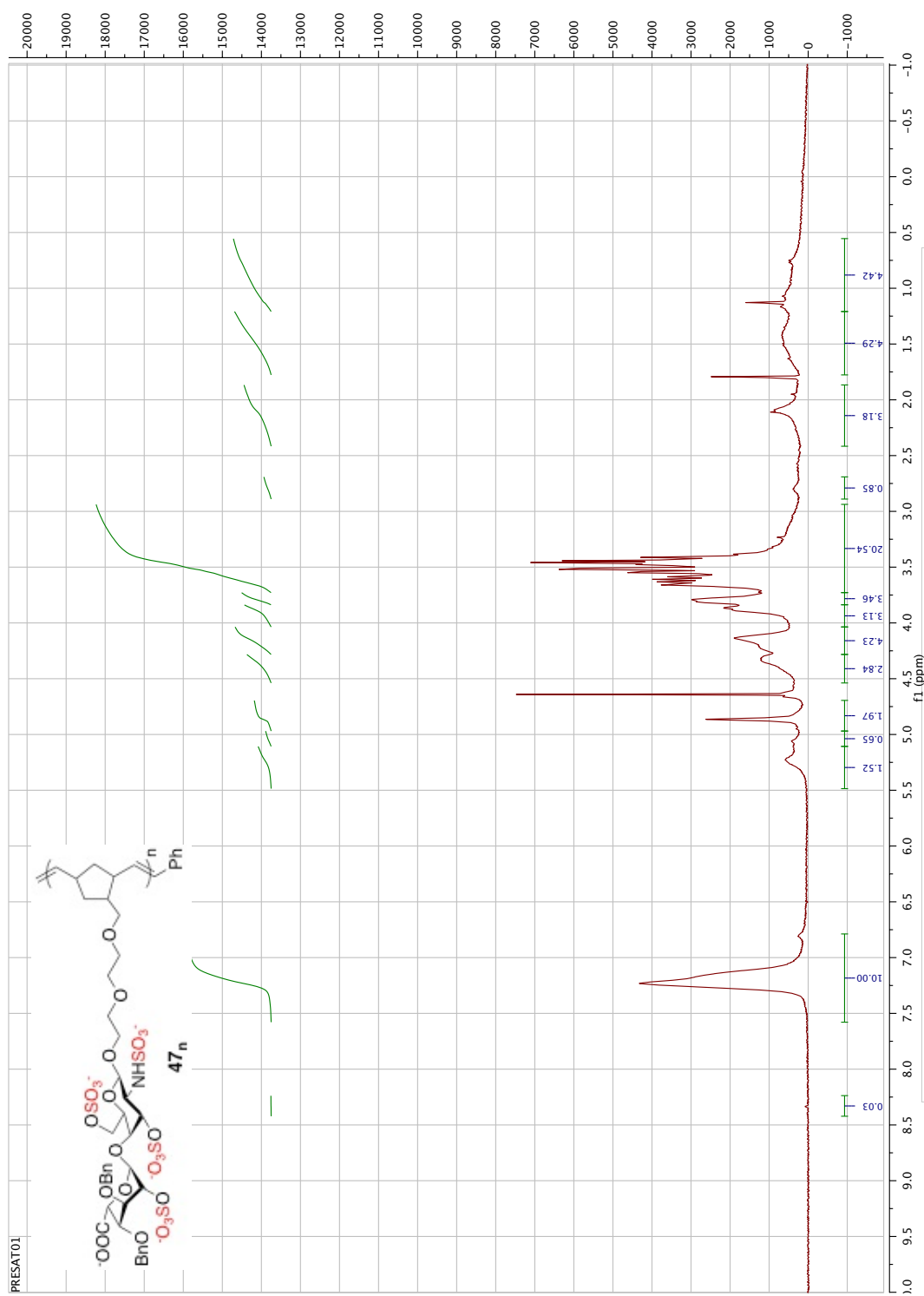


Figure 3.7: ¹H NMR (400 MHz, D₂O) of compound **47_n**.

Chapter 4

EVALUATING THE ANTICOAGULANT ACTIVITY OF HEPARAN SULFATE GLYCOPOLYMERS

Mechanism of anticoagulant activity

Heparin is widely used as an anticoagulant drug, based on its ability to accelerate the rate at which AT inhibits serine proteases in the blood coagulation cascade. In the simplest terms, blood coagulation is the process that converts the circulating soluble blood protein, fibrinogen, into an insoluble fibrin gel; this gel plugs blood vessel leaks and stops the loss of blood.⁴ Despite the widespread clinical use of heparin and related LMWHs as anticoagulants, heparin based drugs have major disadvantages, such as their inherent structural diversity,⁵ their potential for contamination due to their origin from animal tissues, and the clinical occurrence of heparin-induced thrombocytopenia (HIT).

Hemostasis is a process that stops bleeding by keeping blood within a damaged blood vessel, and is the first stage of wound healing. This process occurs when blood is present outside of the blood vessels, and is the body's instinctive response to stop bleeding. During hemostasis, three steps occur in a rapid sequence: 1) the vascular spasm constricts blood vessels to reduce blood loss, 2) platelet plug formation forms a temporary seal of platelets to cover the break in the vessel wall, and 3) blood coagulation reinforces the platelet plug with fibrin threads and acts as a "molecular glue."⁶

The coagulation process begins almost instantly after injury to the blood vessel has damaged the endothelium lining. During 'primary hemostasis,' platelets immediately aggregate to form a plug at the site of injury to temporarily reduce the loss of blood. This

sets the stage for initiation of the coagulation cascade by presenting negatively charged phospholipids such as phosphatidylserine on the surface of the activated platelets or damaged cell membranes. 'Secondary hemostasis' occurs simultaneously, where coagulation factors in the blood plasma respond in a complex cascade to form fibrin strands to strengthen the platelet plug and begin the process of tissue repair.⁷ Within seconds of a blood vessel's epithelial wall being disrupted, platelets begin to adhere to the sub-endothelium surface; it takes approximately sixty seconds until the first fibrin strands begin to interdisperse around the wound, and platelet plugs are completely formed within several minutes.⁸

Although damage to blood vessels is the primary trigger for hemostasis, the coagulation cascade of secondary hemostasis can be initiated by two pathways (Figure 4.1):⁹ the extrinsic pathway is triggered by release of tissue factor (TF) from the site of injury of a damaged blood vessel, and the intrinsic pathway is stimulated by contact with a negatively charged surface. The explosive activation of the hemostatic system is possible because of the cascade system of coagulation, in which inactive zymogens and cofactors are sequentially activated by proteolytic cleavage. Following the initial triggers, a series of serine proteases is sequentially activated, culminating in the formation of thrombin, which is responsible for the conversion of soluble fibrinogen to the insoluble fibrin clot. Almost immediately, the fibrinolytic system is stimulated, limiting fibrin deposition to the site of injury, and feedback in the system of naturally occurring anticoagulants blocks further activation of the coagulation cascade.

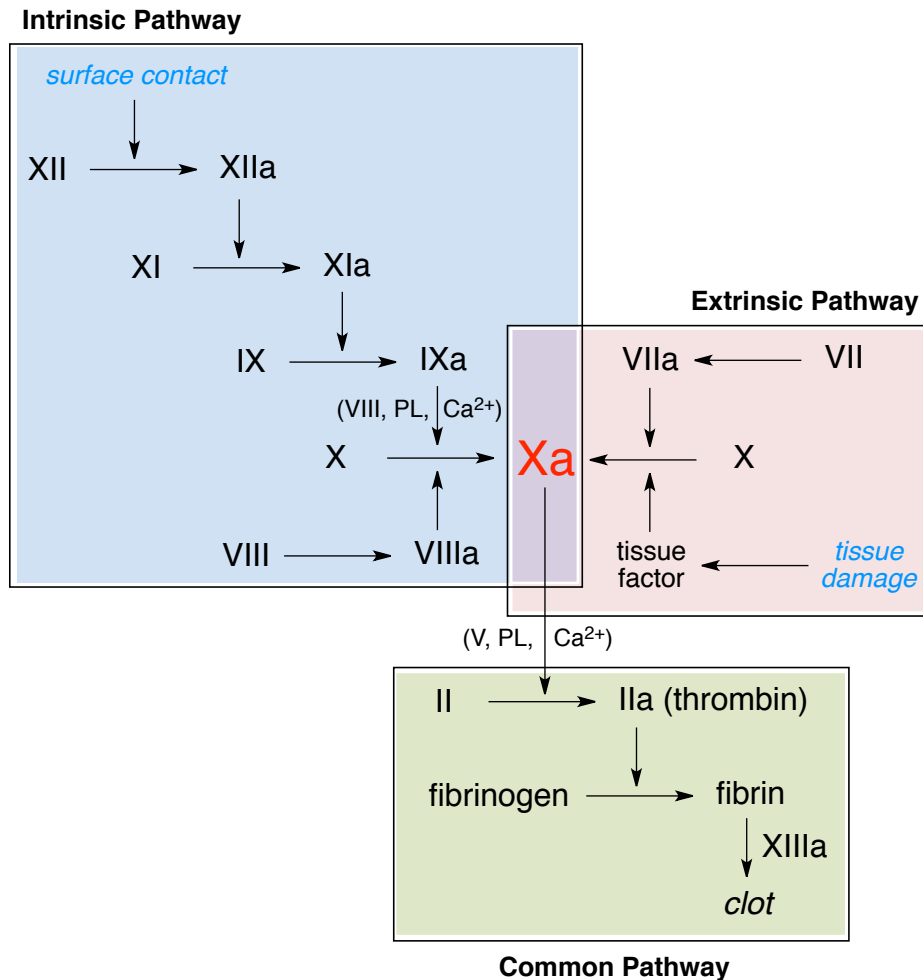


Figure 4.1: The coagulation cascade is divided into the intrinsic, extrinsic, and common pathways.^{1,2} (a) The intrinsic pathway is initiated by non-endothelial cells, followed by the activation of circulating coagulation factors, leading to the formation of fXa. (b) The extrinsic pathway is activated by tissue damage, releasing thromboplastin, calcium and phospholipids from the cell membrane. These factors activate factor VII, transforming factor X to its active form, factor Xa. Both the intrinsic and extrinsic pathways merge into a final common pathway. (c) The common pathway includes the conversion of prothrombin (factor II) to thrombin (factor IIa) under fXa catalysis, then thrombin cleavage of fibrinogen to form a fibrin clot.

The intrinsic pathway

The intrinsic pathway, also called the contact pathway, is activated by the binding of factor XII to a negatively charged surface. This surface contact results in the formation of the primary complex on collagen by high-molecular-weight kininogen (HMWK), prekallikrein, and fXII (Hageman factor). Here, prekallikrein is converted to kallikrein, which activates fXII to fXIIa. The intrinsic pathway continues when fXIIa activates fXI

into fXIa, fXIa activates fIX to fIXa, and the resulting fIXa forms a tenase complex with its co-factor fVIIIa, which finally converts fX to fXa. Proteins of the intrinsic pathway have diverse biological roles throughout the vascular system. Prekallikrein and HMWK are involved in the regulation of blood pressure and participate in fibrinolysis. Additionally, fXII can activate neutrophils and upregulate the release of cytokines from monocytes and macrophages.¹⁰

Despite the diverse roles of the coagulation factors in the intrinsic pathway, the intrinsic pathway has low significance under normal physiological conditions. Although *in vitro* defects in the intrinsic pathway manifest as a prolongation of partial thromboplastin time (PTT), deficiencies in these factors do not cause bleeding. The most clinically significant activation of the intrinsic pathway is by contact of the vessel wall with lipoprotein particles, very-low-density-lipoproteins (VLDLs) and chylomicrons, which demonstrates the role of hyperlipidemia in the generation of atherosclerosis. The intrinsic pathway can also be activated by vessel wall contact with bacteria.

The extrinsic pathway

The main role of the extrinsic pathway is to generate a “thrombin burst,” where thrombin is very rapidly released; thrombin is the most important constituent of the coagulation cascade in terms of its feedback activation roles. When a blood vessel is damaged, TFs are released from the vessel, which triggers the extrinsic pathway (also called the tissue factor pathway). Unlike other members of the coagulation cascade, TF is always present as an active cofactor. Although TF is not normally expressed in cells that come into contact with plasma, upon vascular injury cells expressing membrane-bound TF

are exposed to plasma and can bind factor VII. The binding of factor VII to TF leads to the formation of TF-VIIa which, when attached to the cell membrane, becomes the most potent activator known of the coagulation cascade. Upon formation of TF-VIIa, fX is activated to fXa and platelets begin to stick to the damaged vessel wall and form a mesh of fibrin, trapping more platelets in a process called thrombosis.²

The common pathway

Following activation of fX to fXa by the intrinsic or extrinsic pathways, coagulation is maintained in a prothrombotic state until it is down-regulated by the feedback anticoagulant pathways. In this prothrombotic state, prothrombin is converted to thrombin; although thrombin has a large array of functions, its primary role is the conversion of fibrinogen to fibrin, the building block of a hemostatic plug. While fXa alone can catalyze the conversion of prothrombin to thrombin, this reaction is greatly accelerated by the addition of fVa and the binding of the resulting complex to the phospholipid surface of either activated platelets or monocytes. Upon activation of prothrombin to thrombin, soluble fibrinogen is converted into an insoluble fibrin polymer, which seals the site of injury and protects damaged tissue during wound healing. Here, dimeric fibrinogen molecules are cleaved by thrombin to produce soluble fibrin monomers, and subsequent non-covalent interactions result in the formation of fibers or strands that aggregate to form a mesh. The newly formed fibrin clot is then stabilized by cross-linking, which is catalyzed by thrombin-activated coagulation factor XIIIa.

The coagulant activity of these cascades is balanced by several natural anticoagulant mechanisms; binding of HS to AT represents the most important of these mechanisms. For both fXa and thrombin, heparin-bound AT acts by forming stable 1:1 enzyme-inhibitor complexes, thus blocking the active sites and preventing blood from clotting. Despite its invaluable benefits in anticoagulant therapy, heparin has substantial limitations due to the negatively charged polysaccharide chains interacting with a number of biological components outside the coagulation cascade.¹¹

The main disadvantage of therapeutic heparin is its potential to cause HIT type 2,¹² an immunological response that involves the generation of antibodies against heparin-platelet factor 4 (PF4) complexes (Figure 4.2).¹³ The origin of the heparin appears to have little bearing on this response, although bovine material is reported to be more immunogenic.¹⁴ The route of heparin administration also appears to have no effects on the prevalence of HIT. The sulfation grade of heparin, and the length of the oligosaccharide chains are expected to correlate with its ability to generate antibodies and subsequently

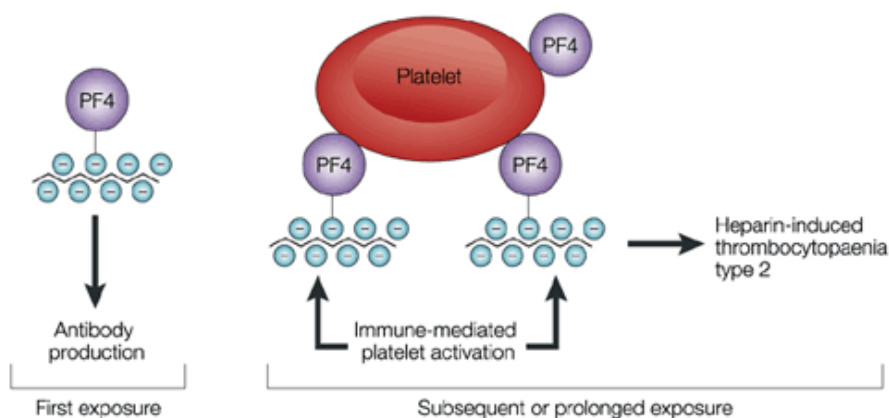


Figure 4.2: Heparin-induced thrombocytopenia caused by heparin anticoagulant therapy.³ Heparin-induced thrombocytopenia type 2 arises when antibodies are raised against a complex of heparin and PF4. Subsequent binding of platelet-surface PF4 by heparin results in immune-mediated platelet activation and possible thrombosis.

produce HIT. When HIT and thrombosis occur as sudden and acute life-threatening complications,¹⁵ it then becomes necessary to withdraw heparin and replace it with an alternative anticoagulant according to the patient's immediate clinical risk.¹⁶ HIT occurs in 0.5-2 % of patients treated with UF heparin and in less than 0.2 % of those treated with LMWH, although the generation of heparin-dependent antibodies is far more frequent.^{15,17} HIT is now better recognized and managed; however, this disease remains difficult to diagnose in many clinical contexts, depending on the presence of other causes of thrombocytopenia.¹⁸

Heparin polysaccharides with at least 12-14 sulfated oligosaccharide chain lengths are required to wrap around PF4 tetramers and render it antigenic; thus, LMWHs based on the anticoagulant pentasaccharide motif do not form immunoreactive complexes with PF4.¹⁹ Compared to UF heparin, LMWH compounds have risen in popularity over the past decade, due to their more attractive pharmacokinetic profile and reduction of side effects. Today, LMWH heparins have expanding applications and are the drug of choice for the acute-phase treatment of thrombosis and for its prevention in high-risk surgical or clinical contexts, even with the risk of HIT.²⁰

With our tetrasulfated HS glycopolymers in hand, we sought to understand their anticoagulant activity *in vitro* and *ex vivo*. Given that our glycopolymers were designed to incorporate key components of the anticoagulant pentasaccharide sulfation motif, we investigated their anticoagulant activity intersection of the intrinsic and extrinsic pathways, where the pentasaccharide selectively inhibits fXa. Additionally, as our glycopolymers were potentially long enough to interact with thrombin, we examined their ability to inhibit thrombin activity following fXa inhibition. To test the specific binding and inhibition of

fXa and thrombin, we turned to assays that allowed us to quantify the inhibition of fXa and thrombin *in vitro*, as well as methods to determine compound anticoagulant activities *ex vivo* in the presence of other coagulation factors.

***In vitro* fXa and fIIa inhibition**

Several techniques, including clot-based tests, chromogenic or color assays, direct chemical measurements, and ELISAs, are used for coagulation testing. Of these techniques, chromogenic and clot-based assays are most commonly used; whereas chromogenic tests are designed to measure the level or function of specific factors, clotting assays provide a global assessment of coagulation function. We first evaluated the inhibitory activity of our glycopolymers on fXa and thrombin using enzyme specific chromogenic substrate assays.

A chromogenic substrate is a compound that, after reaction with a specific enzyme, generates a colored product (Figure 4.3). Taking advantage of the specificity that serine proteases have for specific peptide bonds, a variety of synthetic substrates have been developed to match enzyme specificity. Many chromogenic substrates have been developed on the basis of short peptide fragments terminating with *p*-nitroaniline, which fluoresce upon cleavage. Fluorescence measurements, along with the specificity of chromogenic substrates, allow for the efficient determination of the

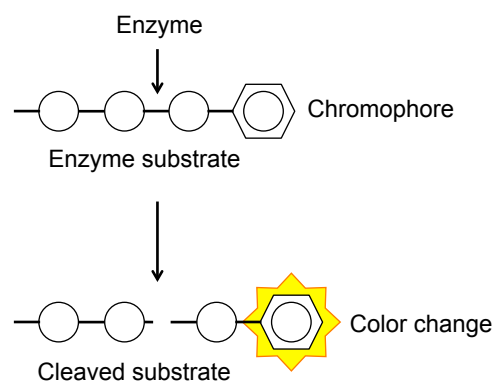


Figure 4.3: Mechanism of chromogenic substrates.

activity of a single coagulation factor in the presence of other coagulation factors.

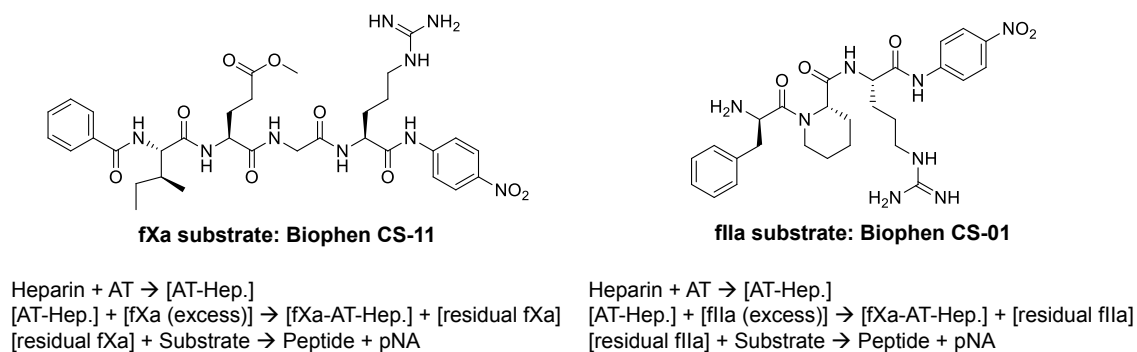


Figure 4.4: Chemical structures of fXa and fIIa chromogenic substrates, and mechanisms of action. fXa chromogenic assays use substrate CS-11, and fIIa chromogenic assays use CS-01.

The anti-fXa chromogenic assay used the chromogenic substrate CS-11, which has a *p*-nitroaniline chromophore attached to a fXa-specific peptide fragment (Figure 4.3). When fXa cleaves the chromogenic substrate, it releases *p*-nitroaniline as a yellow color that can be detected with a spectrophotometer; the resulting fluorescence is directly proportional to the amount of fXa present. When a known amount of fXa is added to an *in vitro* sample containing heparin, the heparin inhibits fXa by binding to AT and fXa, leaving residual fXa to cleave the substrate. By determining fXa inhibitory activity at various concentrations of heparin compounds, we established half maximal inhibitory concentrations (IC₅₀) values of heparin standards and the glycopolymer series. To determine the thrombin inhibitory activity, chromogenic substrate CS-01 was used (Figure 4.3), following the same mechanism as described for the fXa substrate.

Both the anti-fXa and anti-fIIa chromogenic substrate assays were used to determine the *in vitro* anticoagulant activity of each of the standards and HS glycopolymer samples. The anti-fXa and anti-fIIa activities were first determined using three controls: heparin (MW 20k), LMWH (MW 3.5k), and the pentasaccharide drug Arixtra (MW 1727) (Figure 4.5). The anti-fXa and fIIa activity of heparin were determined to be 16.5 nM and 11.0 nM, respectively. In contrast, the anti-fXa activities of LMWH and Arixtra were

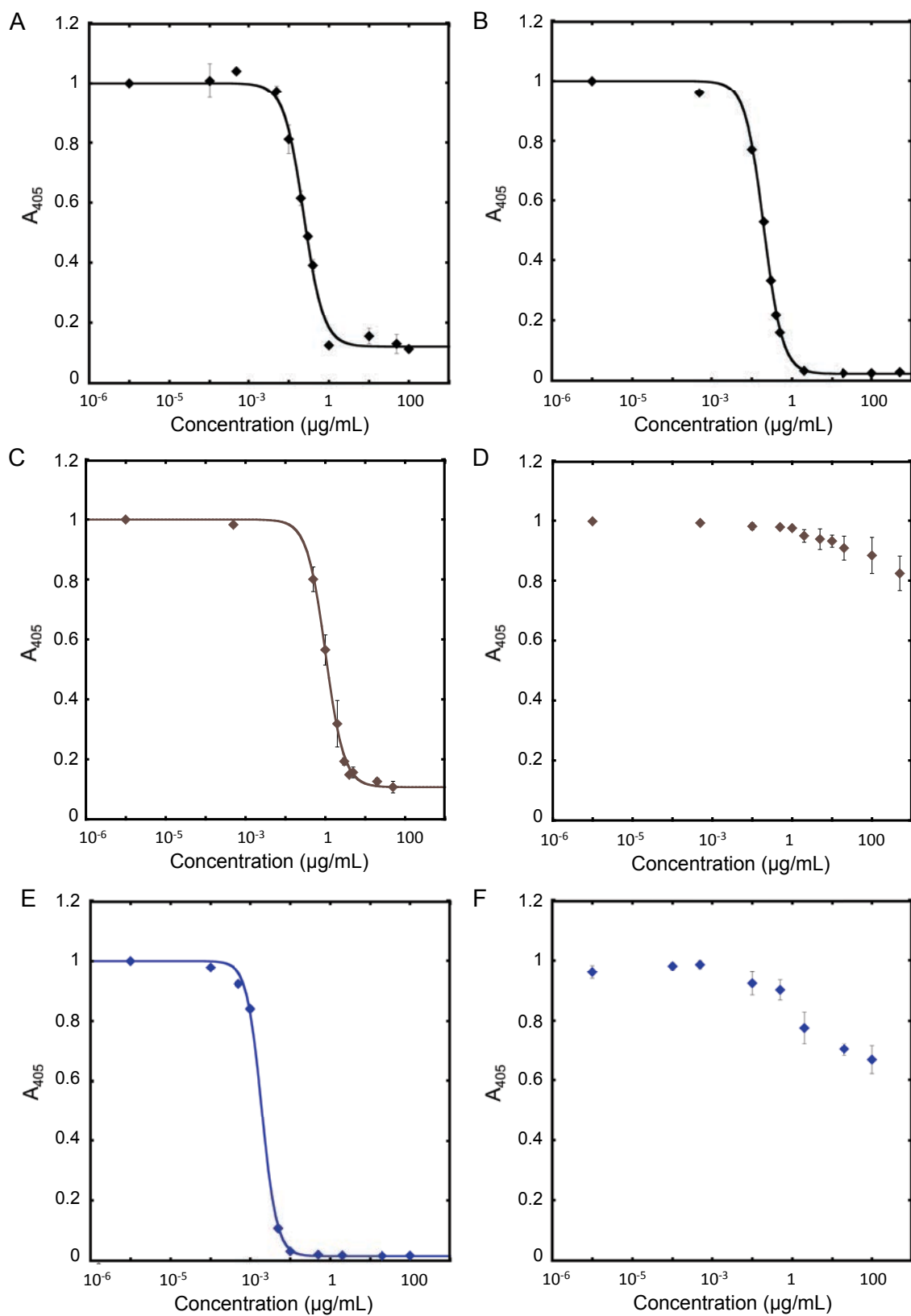


Figure 4.5: Anti-fXa and anti-thrombin activity of controls. Heparin has an anti-fXa activity of 16.5 nM (A) and anti-fIIa activity 11.0 nM (B); LMWH has an anti-fXa activity of 526 nM (C), and has no anti-fIIa activity (D); Arixtra has anti-fXa activity of 11.0 nM (E), but has no anti-fIIa activity (F).

determined to be 526 nM and 11.0 nM (Table 4.1, entries 1-3). As expected, heparin had the highest IC₅₀ values of the three controls. While LMWH displayed significantly lower anti-fXa activity than heparin, Arixtra exhibited similar potency to heparin, which can be attributed to its specificity in targeting fXa. Neither LMWH nor Arixtra displayed anti-fIIa activity, which reflects previously published observations that shorter heparin chains do not have long enough charged polysaccharides to bind thrombin after AT binding and activation.

We first sought to understand the effects of sulfation pattern specificity of our glycopolymers. The anti-fXa and anti-fIIa activity of polymer 57₄₅, the longest of the tetrasulfated HS polymer series (n = 45), was compared to the activity of a trisulfated HS polymer²¹ 59 (Figure 4.7). Compared to the tetrasulfated glycopolymers, the trisulfated HS

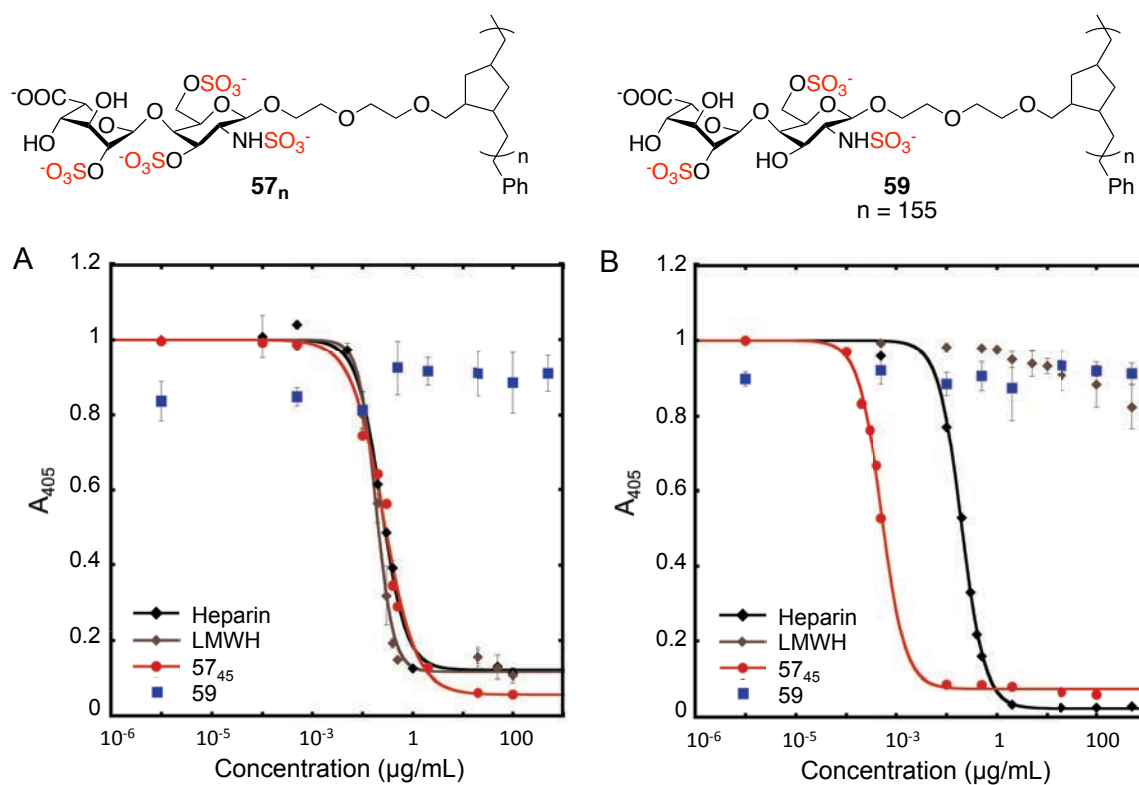


Figure 4.6: Sulfation dependence of Anti-fXa (A) and anti-thrombin (B) activity of polymer 57₄₅, and 59.

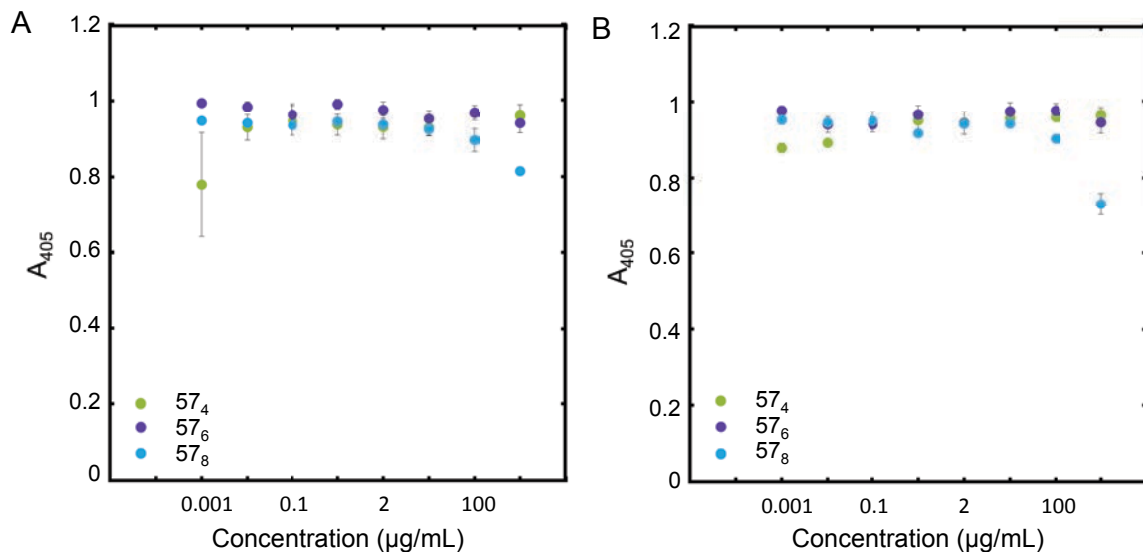


Figure 4.7: Anti-fXa (A) and anti-thrombin (B) activity of short polymers (57₄, 57₆, 57₈).

polymer lacks the 3-*O*-sulfate group on the glucosamine residue, which is known to be critical for the anticoagulant activity of the biologically active HS pentasaccharide. To our delight, the anti-fXa (Figure 4.7, A) and anti-fIIa (Figure 4.7, B) activities were completely abolished with the elimination of the critical 3-*O*-sulfate group (Table 4.1, entry 12). It is important to note that the trisulfated polymer is significantly longer than the tetrasulfated polymer ($n = 155$ vs $n = 45$). The contrast in activity, despite the differences in polymer lengths and overall charge, emphasizes the significance of sulfation pattern specificity for biological activity in the context of blood coagulation.

It is well understood that the allosteric activation of AT after heparin pentasaccharide-binding results in the recognition and inhibition of fXa.^{22,23} In contrast, thrombin inhibition requires both AT and thrombin to bind to the same heparin chain; thrombin is electrostatically attracted to the negative charges along the heparin polysaccharide chain of the heparin-bound AT complex. Previous studies have shown that a heparin polysaccharide of 14 and 20 saccharide units is required for thrombin binding,²⁴⁻

²⁷ and we envisioned mimicking these extended domains by tuning polymer lengths. An extended display of repeating HS disaccharides could, in theory, accommodate AT-binding by the active sulfation motif, and still be able to attract thrombin with the remaining disaccharide units.

The polymers synthesized in Chapter 3 were tested for their anti-fXa and anti-fIIa activity using the previously mentioned chromogenic substrate assays. Based on their inhibitory activities, we could split the polymer series into three groups: short polymers $57_{4,6,8}$, medium-length polymers $57_{10,15}$, and long polymers $57_{30,45}$. The shortest polymers (57_4 and 57_6) did not exhibit either anti-fXa or fIIa activity, but polymer 57_8 began to display some measurable inhibition for both assays at high concentrations (Figure 4.8). Similarly, the medium length polymers 57_{10} and 57_{15} (Figure 4.8) displayed measurable inhibition for both assays, but their inhibitory effects were not high enough to determine IC_{50} values.

In stark contrast to the short and medium length polymers, the longer polymers 57_{30}

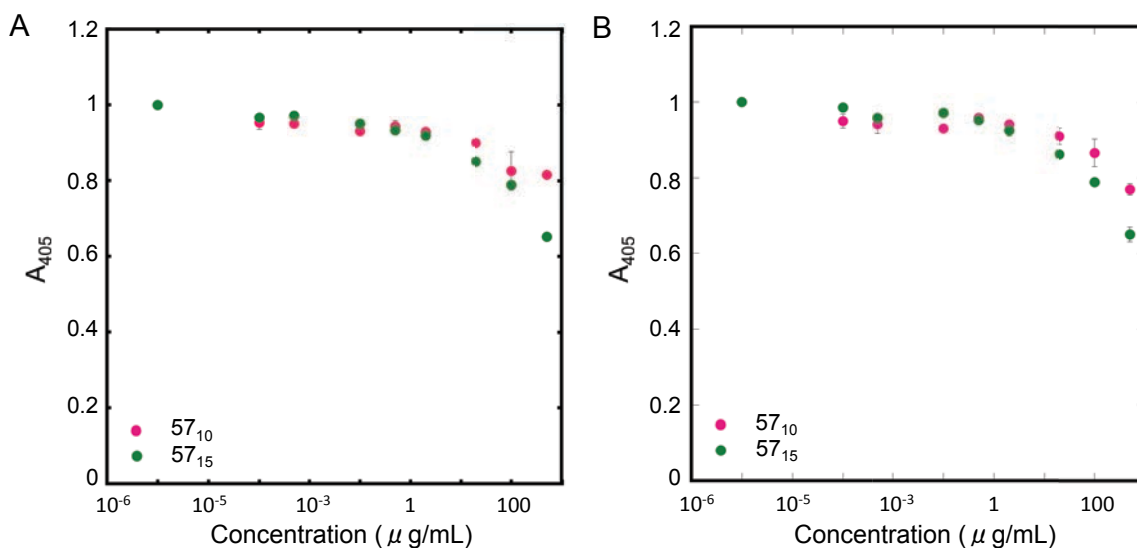


Figure 4.8: Anti-fXa (A) and anti-thrombin (B) activity of medium-length polymers (57_{10} , 57_{15}).

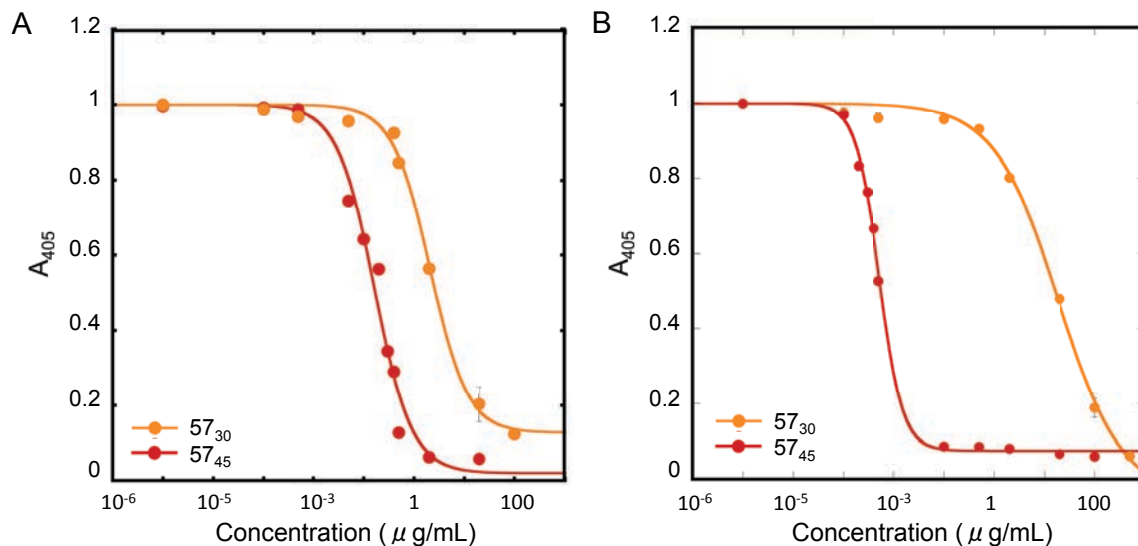


Figure 4.9: Anti-fXa (A) and anti-thrombin (B) activity of long polymers (57₃₀, 57₄₅).

Entry	Polymer	# saccharides	Anti-fXa IC_{50} (nM)	Anti-fIIa IC_{50} (nM)
1	Heparin	45-50	16.5	11.0
2	LMWH	4-5	526	>1000
3	Arixtra	5	11.0	>1000
4	57 ₄	8	>1000	>1000
5	57 ₆	12	>1000	>1000
6	57 ₈	16	>1000	>1000
7	57 ₁₀	20	>1000	>1000
8	57 ₁₅	30	1 473	>1000
9	57 ₃₀	60	684	577
10	57 ₄₅	90	5.76	0.114
11	59	310	>1000	>1000

Table 4.1 Factor Xa and thrombin inhibition activity of glycopolymer series.

and 57₄₅ displayed potent fXa and fIIa inhibitory activity (Figure 4.9). Polymer 57₃₀ had an anti-fXa activity of 684 nM and anti-fIIa activity of 577 nM (Table 4.1, entry 9). The longest polymer 57₄₅, comprised of 45 repeating disaccharide units, displayed even higher potency, with an anti-fXa activity of 5.76 nM and anti-fIIa activity of 0.114 nM (Table 4.1, entry 10). Compared to the controls, 57₃₀ exhibited anti-fXa activity comparable to

LMWH, but had strong anti-fIIa activity unlike LMWH. Most importantly, the longest polymer 57₄₅ proved itself to have 3 fold higher anti-fXa activity and 100 fold higher anti-fIIa activity compared to fXa and thrombin inhibition of the heparin control (Table 4.1). The dramatic increase in thrombin inhibition is thought to be a result of the extremely high charge density of the 45-mer polymer. Most heparin chains found in nature are di- or tri-sulfated disaccharides, so it was somewhat expected that the high charge of our HS disaccharide polymers would interact with coagulation factors such as thrombin in this fashion, especially since thrombin is known to form complexes by interacting with the negative charges of heparin chains.

An important goal for this project was to synthesize anticoagulant HS mimetics that had reduced side effects. Following the evaluation of our polymers' anti-fXa and anti-fIIa activity, we examined the potential for our HS glycomimetics to cause HIT. Similar to the electrostatic interactions required for thrombin inhibition, the negatively charged sulfate groups attract the positively charged lysine and arginine groups of PF4, resulting in complexes against which an immune response is formed. Based on previously published literature reporting 12-14 oligosaccharide chain lengths causing PF4 neutralization, we hypothesized that our polymers may have the same antigenic results.

PF4 neutralization was tested by subjecting the heparin standards and polymers to the anti-fIIa chromogenic substrate assay in the presence of PF4. Aside from the addition of PF4, all other reaction conditions were kept constant. Heparin was first used as a control to determine an appropriate concentration of PF4; the addition of 20 µg/mL PF4 completely neutralized fIIa inhibition by heparin (Figure 4.10, A). Unfortunately, subjecting glycopolymers 57₃₀ and 57₄₅ also resulted in neutralization of thrombin inhibition; polymer

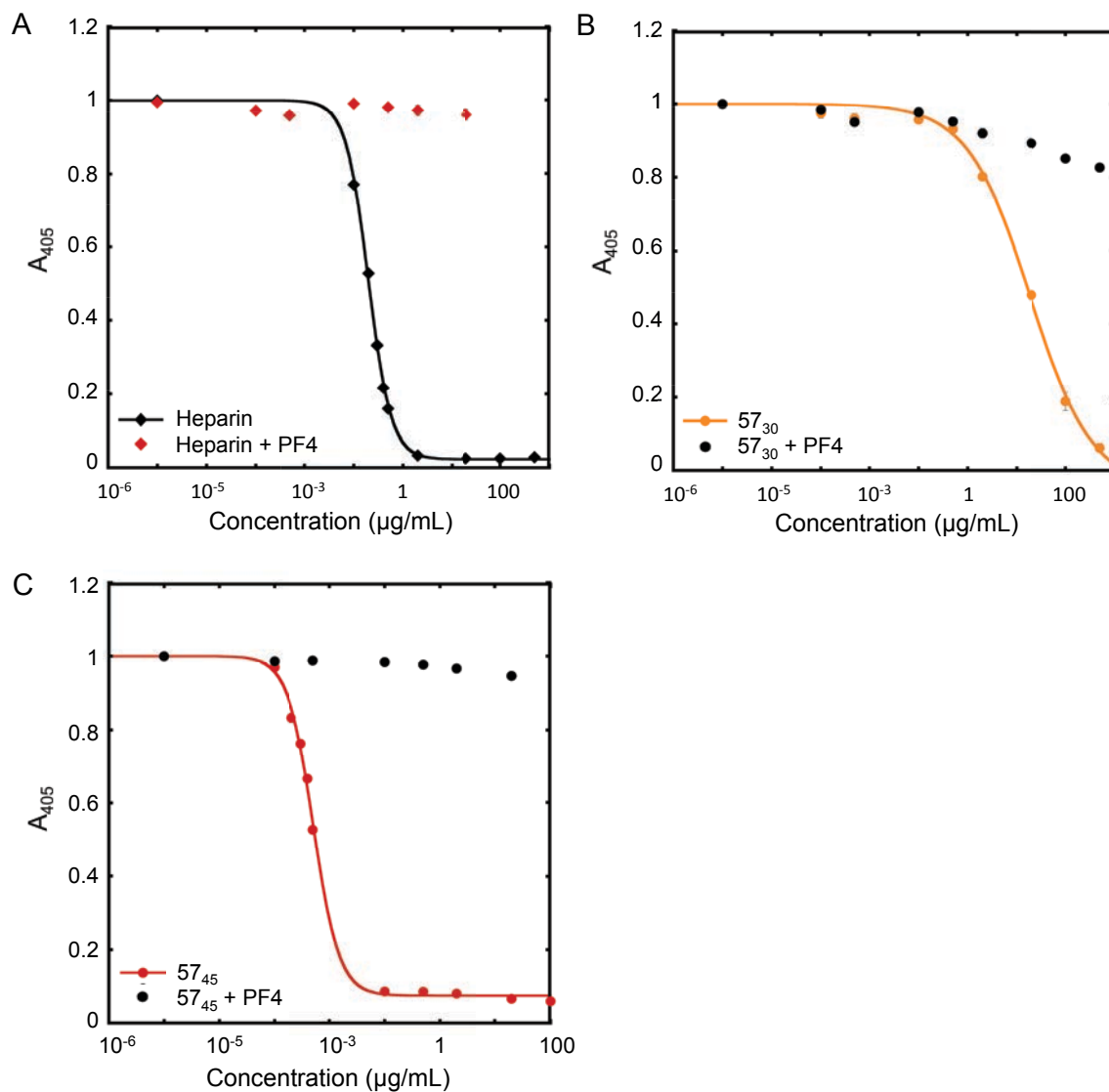


Figure 4.10: PF4 neutralization of anti-thrombin activity of heparin (A), polymer 57₃₀ (B), and polymer 57₄₅ (C).

57₃₀ was only partially neutralized (~20%), while polymer 57₄₅ was completely neutralized as observed with the heparin standard.

Based on these *in vitro* studies, we were able to understand how our polymers interacted with the key coagulation factors fXa and fIIa in the context of polymer lengths. Short polymers, even with the key sulfation moieties from the anticoagulant pentasaccharide, did not display any anticoagulant activity. With increasing chain length,

we were able to observe increased *in vitro* anticoagulant activity. Importantly, medium length glycopolymers behaved similarly to LMWH, with moderate fXa activity and no thrombin inhibition. In contrast, the longer polymers behaved very much like heparin, where the polymers exhibited potent fXa and thrombin inhibitory activity. Our findings support the notion that an extended pentasaccharide domain can act to mimic the electronegative template of natural heparin polysaccharides, with which thrombin can interact with to form a heparin-AT-fIIa complex to inhibit blood coagulation.

The first set of chromogenic substrate assays was used to determine the activity of our glycopolymers with purified fXa and thrombin, which are the two main coagulation factors at the junction of the intrinsic and extrinsic pathways. While fXa and thrombin are the critical components that interact with heparin-based anticoagulants, it was important to evaluate their activity in a more native environment, and in the presence of various other plasma factors. To this end, we subjected the glycopolymers to the two most commonly used *ex vivo* clot-time assays.

***Ex vivo* activity of HS glycopolymers in human plasma**

Clot-based assays are commonly used to evaluate patients with suspected bleeding abnormalities and to monitor anticoagulant therapy.²⁸ Prothrombin time (PT) and activated partial thromboplastin time (aPTT) tests help differentiate intrinsic, extrinsic, and common, and multiple pathway deficiencies. When used in conjunction, these tests allow clinicians to specifically detect the location of coagulation disorders to one or more of the three pathways, and are the testing protocols of choice when testing for coagulation disorders or monitoring progress after heparin therapy.

PT and its derived measures of prothrombin ratio (PR) and international normalized ratio (INR) are measures of the extrinsic and common coagulation pathways. PT specifically measures the classic factors of the extrinsic and common pathways: factors I (fibrinogen), II (prothrombin), V, VII, and X, and is clinically used to determine the clotting tendency of blood in the measure of warfarin dosage, liver damage, and vitamin K status. PT times are performed by measuring the clotting time upon addition of a thromboplastin reagent, which contains tissue factor and calcium, to plasma, which then initiates the extrinsic pathway (Figure 4.11). Typically, PT reagents contain excess phospholipid such that nonspecific inhibitors, which react with anionic phospholipids, do not prolong clot times.²⁹ PT times are prolonged with deficiencies of factors VII, X, V, prothrombin, or fibrinogen and by antibodies directed against these factors. Additionally,

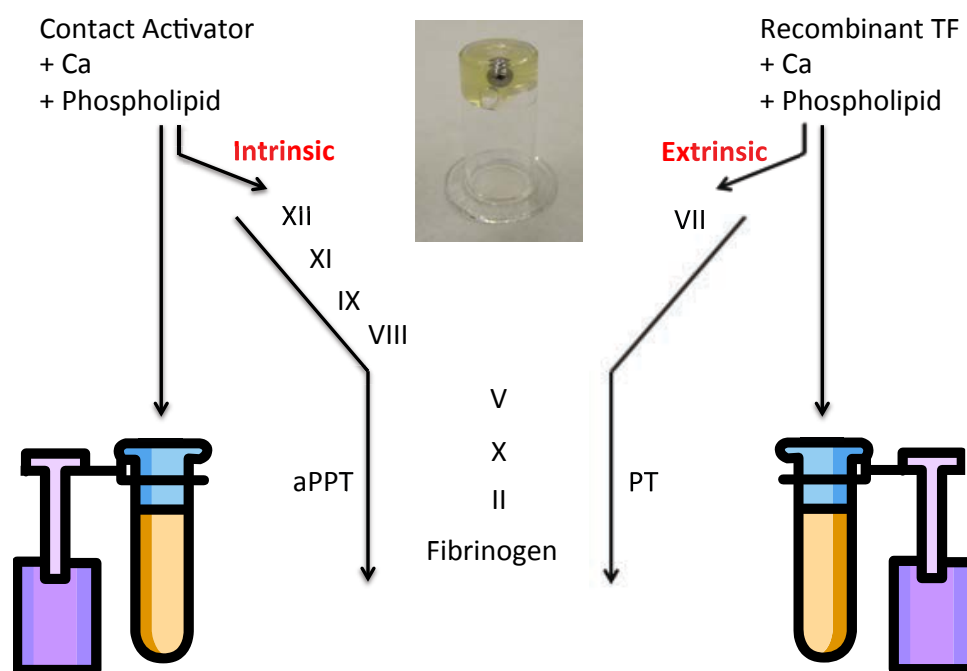


Figure 4.11: Activated partial thromboplastin time (aPTT) and prothrombin (PT) time tests. The intrinsic pathway is activated by addition of a contact activator, calcium, and phospholipids to plasma samples; the efficacy of the intrinsic and common pathways is measured by aPTT tests. The extrinsic pathway is activated by tissue factor (TF), calcium, and phospholipids; the efficacy of the extrinsic and common pathways is measured by PT tests.

patients with inhibitors of fibrinogen-to-fibrin conversion, including high doses of heparin or warfarin, and the presence of fibrin degradation products result in abnormal PT times. While PT times vary with reagents and coagulometers, normal times typically range between 10-14 seconds.³⁰

While PT tests measure abnormalities in the extrinsic and common pathways, aPTT tests are a performance indicator measuring the efficacy of the intrinsic and common coagulation pathways. Normal aPTT times require the presence of the coagulation factors I, II, V, VIII, IX, X, XI, and XII; prolonged clot times are commonly observed with deficiencies of contact factors such as IX, VIII, X, V, prothrombin, or fibrinogen. Antiphospholipid antibodies, deficiencies in coagulation factors (hemophilia), and sepsis (coagulation factor consumption) may also prolong aPTT. Specific factor inhibitors, fibrin degradation products, and anticoagulants also prolong the aPTT, although aPTT is less sensitive to warfarin than is the PT.³¹ aPTT is performed by first adding a surface activator (e.g., kaolin, Celite, ellagic acid, or silica) and diluted phospholipid (e.g., cephalin) to citrated plasma (Figure 4.11);³⁰ the phospholipid in this assay is called partial thromboplastin because TF is absent, and normal clot times typically range between 22-45 seconds.³²

Our HS glycopolymers were each subjected to aPTT and PT tests in human plasma to test their anticoagulant activity *ex vivo*. Initially, varying concentrations of standards were subjected to the clot tests to evaluate appropriate sample concentrations. High sample concentrations (150 µg/mL) were used for all standard and polymer samples to increase the range of clot times; this allowed us to observe more easily the differences between aPTT and PT values. 3.2% Citrate concentration in flash frozen human platelet-poor plasma (PPP)

was necessary for these assays, as higher citrate concentrations (3.8%) did not give clot times within the instrument detection range. Samples without added anticoagulants produced clot times within the expected normal ranges (Table 4.2, entry 1).

The aPTT and PT values of the standards reflected the trends obtained from the *in vitro* chromogenic substrate assays (Table 4.2, entries 2-4). At sample concentrations of 150 $\mu\text{g/mL}$, heparin displayed an aPTT time of greater than 180 seconds (maximum instrument limit), and a PT time of 84 seconds. LMWH had a slightly lower aPTT time of 117 seconds, and Arixtra had an even lower aPTT time of 78 seconds; neither LMWH nor Arixtra had noticeably prolonged PT times. As expected, the higher MW of LMWH (MW 3500) compared to Arixtra resulted in prolonged aPTT times, likely because Arixtra reacts selectively with fXa, while LMWH is known to interact with other coagulation factors in the intrinsic pathway.³³

With the normal and control aPTT and PT times in hand, we tested our polymer series to examine the effects of polymer length and sulfation pattern on their anticoagulant

Entry	Polymer	# saccharides	APTT (s)	PT (s)
1	None	n/a	31.2 ± 0.25	13.3 ± 0.06
2	Heparin	45-50	>180	84.2 ± 17.8
3	LMWH	4-5	116.9 ± 3.00	14.8 ± 0.15
4	Arixtra	5	78.3 ± 0.40	15.1 ± 0.31
5	57 ₄	8	32.5 ± 0.31	13.2 ± 0.1
6	57 ₆	12	32.2 ± 0.17	13.2 ± 0.26
7	57 ₈	16	not determined	not determined
8	57 ₁₀	20	59.6 ± 0.32	15.8 ± 0.4
9	57 ₁₅	30	82.9 ± 0.55	23.4 ± 1.85
10	57 ₃₀	60	100.8 ± 0.52	50.8 ± 6.3
11	57 ₄₅	90	119.4 ± 0.50	52.2 ± 7.83
12	59	310	46.1 ± 0.38	12.7 ± 0.06

Table 4.2. Activated partial thromboplastin time (APTT) and prothrombin time (PT) experiments. Assays were determined using citrated human plasma. The number of monosaccharide units are noted for comparison of standards and polymers.

activities *ex vivo*. Glycopolymer **59**, which lacks the critical 3-*O*-sulfate group, exhibited a slight prolongation in aPTT clot time, but produced PT times within the normal range. When studying the effects of length dependence on *ex vivo* anticoagulant activity, our glycopolymers **57_n** exhibited activity in a length-dependent manner, similar to our observations *in vitro*. In agreement with the chromogenic substrate assays, the shortest polymers **54₄₋₈** did not display noticeable prolongation of aPTT or PT times, producing normal clot times (Table 4.2, entries 5-7).

The glycopolymers **57_{10,15,30,45}** prolonged both aPTT and PT clot times, with the most interesting activity observed with the longest polymers. Polymer **57₁₀** exhibited activity very similar to that of Arixtra, where aPTT times were prolonged moderately while producing normal PT times (Table 4.2, entry 8). In contrast, **57₁₅** prolonged aPTT times with clot times close to Arixtra, but moderately increased PT times to 23 seconds; this increase in PT times is characteristic of the anticoagulant activity of heparin, albeit to a lesser degree (Table 4.2, entry 9). We began to observe significantly increased clot times for both aPTT and PT for polymers **57₃₀** and **57₄₅**. Both polymers had significantly prolonged aPTT times with values similar to LMWH (100-120 sec). Although these aPTT times mirrored values produced by LMWH, the PT times of polymers **57₃₀** and **57₄₅** approached values observed with heparin. Interestingly, based on the extents to which our glycopolymers prolong aPTT and PT clot times, they exhibit hybrid properties by recapitulating the anticoagulant activity of both heparin and LMWH/Arixtra.

Based on observations of polymers' *in vitro* and *ex vivo* activity in the aPTT and PT assays, we have demonstrated how we are able to simultaneously recapitulate anticoagulant properties of both heparin and LMWH/Arixtra by chemically controlling the HS

glycopolymer structures. We found that at least 10 repeating units are required for effective anticoagulant activity *in vivo* and *ex vivo*. In contrast, the longer polymers exhibit interesting hybrid characteristics, by simultaneously recapitulating anticoagulant properties of both LMWH/Arixtra and heparin. With increasing polymer lengths, we observed that our HS glycopolymers could prolong aPTT clot times close to those of Arixtra and LMWH, and also moderately prolong PT clot times, which is characteristic of the anticoagulant activity of heparin.

Discussion and conclusions

Heparin-based therapeutics are essential to modern medicine and will likely remain an important class of drugs. Modern biotechnological methods have advanced manufacturing processes for heparins through improvements in the extractive methods developed in the early 20th century and more modern chemoenzymatic and synthetic methods. By assessing the effects of structural variations on the anticoagulant pentasaccharide, structure-activity relationships have been established and utilized towards the synthesis of a new generation of heparin therapeutics.

We have described, starting from a detailed analysis of the interactions between heparin and the coagulation factors AT and thrombin, how we were able to design and synthesize a novel anticoagulant HS mimetic glycopolymer. By displaying the key sulfation moieties of the anticoagulant heparan sulfate pentasaccharide derivative on a disaccharide pendant homopolymer, we have been able to mimic the multivalent nature of the natural polysaccharides. Our goal was to recapitulate the three-dimensional display of

recognition epitopes by installing stereoselective glycosidic bonds of HS, and sulfate groups onto a disaccharide for the selective recognition by key coagulation factors.

A series of glycopolymers were synthesized, which comprise of repeating tetrasulfated HS disaccharides. These polymers exhibited *in vitro* and *ex vivo* anticoagulant activity in a sulfation dependent manner; polymers lacking the critical 3-*O*-sulfate group had negligible activity in all assays. Two of the longest polymers, with 30 and 45 repeating disaccharide units, displayed potent fXa and thrombin inhibition *in vitro*. In particular, the glycopolymer with 45 repeating units exhibited anti-fXa activity 10-fold higher than heparin and Arixtra, and 2-fold higher inhibitory activity than LMWH. Most notably, this same polymer displayed substantially higher fIIa inhibitory activity in comparison to heparin, with a 100-fold increase in activity. Although this observed thrombin inhibition was neutralized by the addition of PF4, we believe that we may be able to tune this effect by altering the chemical properties of our polymers during polymerization.

These *in vitro* chromogenic substrate assays emphasize the significance of both sulfation pattern and the length of polymers required for anticoagulant activity. The abolishment of *in vitro* fXa and thrombin inhibition by trisulfated polymer **59** emphasizes and supports previous studies that have determined the necessity of the 3-*O*-sulfate group of glucosamine for anticoagulant activity. The increase in anti-thrombin activity in a length-dependent manner supports the accepted mechanism for thrombin inhibition, where the formation of a ternary complex involving heparin, thrombin and AT requires negatively charged polysaccharide chains of at least 14-20 monosaccharide units. We have observed that our polymers require at least 30 repeating units (60 monosaccharide units) to be long enough to bind both AT and thrombin. We believe that the high charge density of our

polymers is responsible for the efficient binding of AT and thrombin, which occurs mainly through electrostatic interactions.

Following the *in vitro* assays, *ex vivo* clotting assays were conducted in human plasma, which revealed interesting length-dependent anticoagulant activity of our glycopolymers. aPPT and PT tests resulted in the prolonged clot times of the polymers with 10, 15, 30 and 45 repeating disaccharide units. Specifically, polymer 57₁₀ only moderately prolonged aPTT clot times, exhibiting anticoagulant activity comparable to Arixtra. In contrast, polymer 57₁₅ affected both aPTT and PT times, and exhibited aPTT times characteristic of Arixtra, and prolonged PT times characteristic to heparin. The longer polymers 57₃₀ and 57₄₅ prolonged both aPTT and PT clot times substantially, though the observed values were lower than those produced by heparin. aPTT times were characteristic to clot times resulting from LMWH, while prolongation of PT clot times were, again, characteristic to heparin. Together, these observations reflect the tunable anticoagulant activity of our HS glycopolymers, where we can modulate the LMWH-like or heparin-like anticoagulant activity by altering polymer lengths.

Our polymers have a number of advantages over the heterogeneous, animal-sourced heparin, which remains the anticoagulant drug of choice. The homogeneity of our glycopolymers should presumably yield more predictable biological activity, and minimize side effects that result from undesired interactions with competing GAG-based structures (i.e., over-sulfated CS). Based on the partial neutralization of 57₃₀ by PF4 in fIIa inhibition *in vitro*, we believe that our polymers can successfully incorporate hybrid anticoagulant properties of heparin and its low molecular weight variants, while diminishing potential side effects, such as PF4-mediated immune responses. We have the ability to utilize

chemistry to tune such chemical properties of these HS glycopolymers from late-stage monomer intermediates; we can alter the sulfation pattern, length of the PEG linker, and polymer architecture to modulate biological activity. Additionally, the predictability of ROMP chemistry gives us the ability to control the display and distribution of the bioactive disaccharide moieties using spacer groups, as well as polymer architectures. We believe that the versatility and synthetic accessibility of these HS glycopolymers are an attractive alternative to commercially available anticoagulants, and are a powerful tool in understanding the effects of sulfation pattern specificity and multivalency in the interaction between GAG mimetic structures and their biological receptors.

In summary, we have synthesized a series of novel HS mimetic glycopolymers through ROMP of tetrasulfated HS disaccharide monomers. These polymers recapitulate the key features of anticoagulant HS GAGs by displaying the critical sulfate groups found on a biologically active HS pentasaccharide motif. The use of polymerization chemistry greatly simplifies the synthesis of such complex GAG structures, providing a facile method of generating homogeneous GAG-based macromolecules with tunable biological and chemical properties. These studies emphasize the significance of multivalent interactions of GAG mimetics, and highlights the extent to which sulfation pattern specificity affects biological activity. The presented method of preparing carbohydrate-mimetics is a useful method of efficiently generating GAG-like molecules. By taking advantage of the multivalency effects of carbohydrate-protein interactions, such polymer scaffolds could potentially recapitulate many different biological functions and be useful as synthetically accessible carbohydrate-based therapeutics.

Experimental methods

Heparin was purchased from Sigma-Aldrich and Neoparin (Alameda, CA), low molecular weight heparin was purchased from Neoparin (Alameda, CA). Arixtra® was generously provided by Professor Jian Liu at the University of North Carolina at Chapel Hill. BIOPHEN Heparin Anti-Xa (2 stages) USP/EP (Product # A221010-USP) kits from Aniara (West Chester, OH) were used for the factor Xa activity assays. BIOPHEN Heparin Anti-IIa (2 stages) USP/EP (Product # A221025-USP) chromogenic assay kits from Aniara were used for the factor IIa activity assays. Human platelet factor 4 was purchased from Haematologic Technologies, Inc. (Product # HPF4-0180). The chromogenic anti-fXa and anti-fIIa methods for measuring homogeneous heparin in plasma or in purified systems using a two stage method are in compliance with Pharmacopoeias (USP, EP) and FDA guidelines. The clot time assays were performed by the Clinical & Translational Research Laboratory, Department of Pathology & Laboratory Medicine at the University of California, Los Angeles using the Sysmex® CA-1500 Coagulation Analyzer (Siemens AG, Erlangen, Germany).

Chromogenic Assays for the Measurement of Anti-fXa and Anti-thrombin Activity

Factor Xa Activity. All reagents were prepared according to manufacturer instructions and incubated at 37 °C for 15 min. Varying concentrations of heparin, low molecular weight heparin, Arixtra® or synthetic glycopolymers (40 µL) and antithrombin (40 µL) were added to a microcentrifuge tube, mixed, and incubated at 37 °C for 2 min. To this, Factor Xa (40 µL) was added and was incubated at 37 °C for exactly 2 min (stage 1), then factor Xa chromogenic substrate (40 µL) was added. After exactly 2 min (stage 2), the reaction

was stopped by introducing (240 μL) citric acid (20 g/L). Absorbance at 405 nm was measured. The sample blank was obtained by mixing the reagents in reverse order from that of the test i.e.: Citric acid (20 g/L), factor Xa substrate, factor Xa, antithrombin, and heparinized sample. The sample blank value was deducted from the absorbance measured for the corresponding assay.

Factor IIa Activity. All reagents were prepared according to manufacturer instructions and incubated at 37 °C for 15 min. Varying concentrations of heparin, low molecular weight heparin, or synthetic glycopolymers (40 μL), and antithrombin (40 μL) were added to a microcentrifuge tube, mixed, and incubated at 37 °C for 2 min. To this, thrombin (40 μL) was added and was incubated at 37 °C for exactly 2 min (stage 1), then Thrombin chromogenic substrate (40 μL) was added. After exactly 2 min (stage 2), the reaction was stopped by introducing (240 μL) citric acid (20 g/L). Absorbance at 405 nm was measured. The sample blank was obtained by mixing the reagents in reverse order from that of the test i.e., Citric acid (20 g/L), factor Xa substrate, factor Xa, Antithrombin and heparinized sample. The sample blank value was deducted from the absorbance measured for the corresponding assay.

Platelet Factor 4 Neutralization. All reagents were prepared according to manufacturer instructions and incubated at 37 °C for 15 min. Varying concentrations of heparin, low molecular weight heparin, or synthetic glycopolymers (40 μL) and antithrombin (40 μL) were added to a microcentrifuge tube, mixed, and incubated at 37 °C for 2 min. To this, thrombin (40 μL) was added and was incubated at 37 °C for exactly 2 min (stage 1) in the

presence or absence of PF4 ($20 \mu\text{g mL}^{-1}$). Thrombin chromogenic substrate ($40 \mu\text{L}$) was then added and incubated for exactly 2 min (stage 2). The reaction was stopped by introducing ($240 \mu\text{L}$) citric acid (20 g/L), and absorbance at 405 nm was measured. The sample blank was obtained by mixing the reagents in reverse order from that of the test i.e., Citric acid (20 g/L), factor Xa substrate, factor Xa, Antithrombin and heparinized sample. The sample blank value was deducted from the absorbance measured for the corresponding assay.

Activated Partial Thromboplastin Time and Prothrombin Time Analysis

Citrated Plasma. Flash frozen, platelet-poor human plasma with 3.2% citrate was purchased from Valley Biomedical (Winchester, VA) for coagulation assays. Samples were thawed at room temperature over 30 min and used immediately for aPPT and PT assays.

Activated Partial Thromboplastin Time (aPTT) Analysis.³⁴ Samples were prepared by mixing $300 \mu\text{L}$ of the heparin standard or glycopolymer in 0.9% saline with 2.7 mL citrated human plasma. The tube was inverted 3 times to mix the sample thoroughly. Dade® Actin® activated cephaloplastin reagent was used as a plasma activator. To $100 \mu\text{L}$ of the plasma/anticoagulant sample, $100 \mu\text{L}$ of prewarmed aPTT reagent (0.2% ellagic acid) was added. After incubation for 4 min, clotting was initiated by adding $100 \mu\text{L}$ of 25 mM CaCl_2 at $37 \text{ }^\circ\text{C}$ and the time to clot formation was measured. Clotting time in the absence of an anticoagulant was determined using $300 \mu\text{L}$ saline solution water. Each clotting assay was performed in triplicate.

Prothrombin Time (PT) Determination Analysis.³⁵ Samples were prepared by mixing 300 μL of the heparin standard or glycopolymer in 0.9% saline with 2.7 mL citrated human plasma. The tube was inverted 3 times to mix the sample thoroughly. Dade® Innovin® reagent was reconstituted according to manufacturer's directions and warmed to 37 °C. 100 μL of the submitted plasma/anticoagulant sample was incubated for 3 min at 37 °C followed by the addition of 200 μL prewarmed thromboplastin, and the time to clot formation was measured. Clotting time in the absence of an anticoagulant was determined using 300 μL saline solution. Each clotting assay was performed in triplicate.

A p p e n d i x

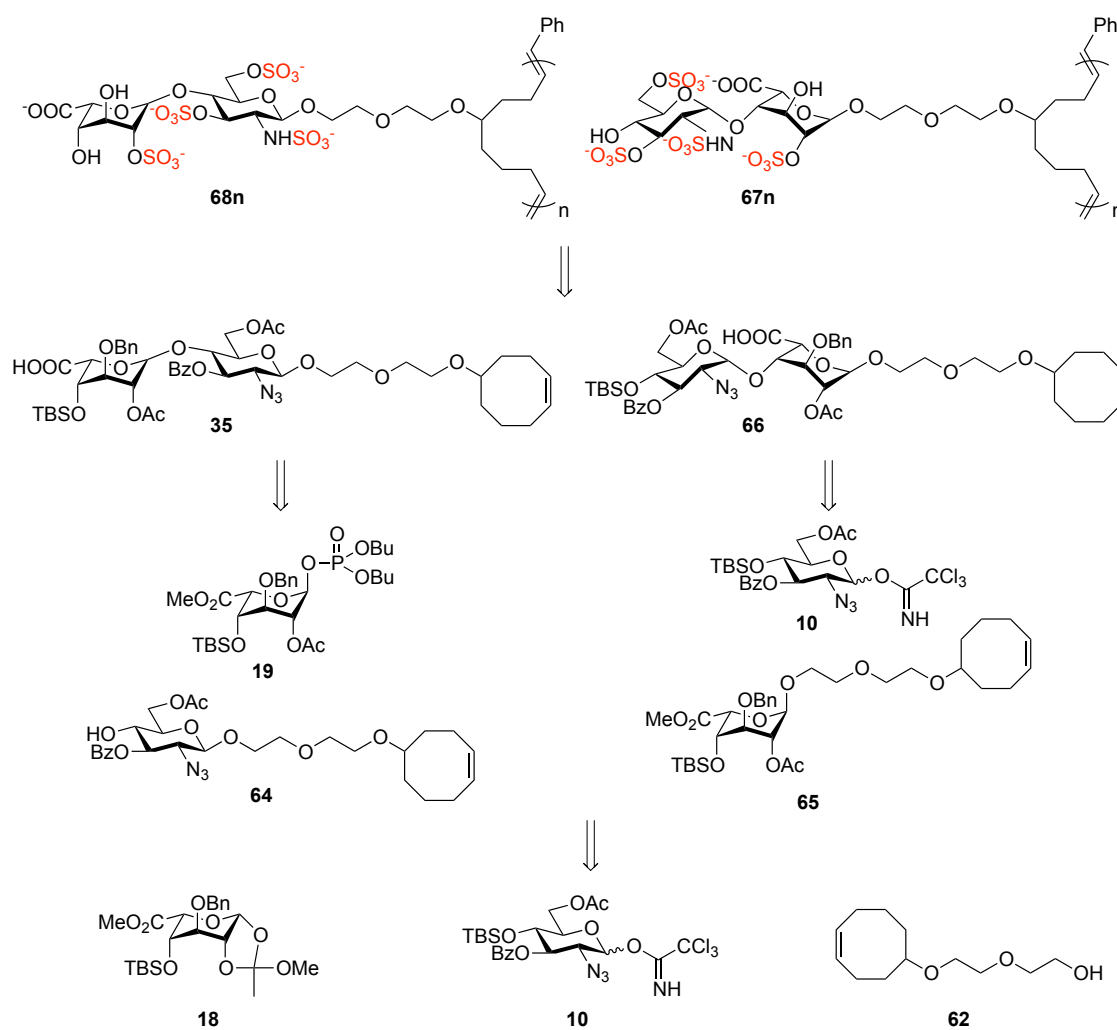
PROGRESS TOWARDS CYCLOOCTENE-BASED HEPARAN SULFATE GLYCOPOLYMERS

Our lab has been working on the development of synthetically accessible CS and HS mimetics that retain key properties of natural polysaccharides. These synthetic polysaccharides have defined sulfation sequences and tunable chemical and biological properties. Our initial approach towards synthesizing HS mimetic glycopolymers utilized a cyclooctene-based polymer backbone to furnish polymers with good control over chain length and polydispersity. Additionally, reduction of the unsaturated backbone was expected to allow for maximum conformational flexibility to facilitate efficient protein interactions. This chemistry was successfully employed in the synthesis of neuroactive CS glycomimetics.³⁶ The goal of this portion of the HS project was to synthesize two polymers with opposing carbohydrate sequences, and to evaluate their anticoagulant activity as seen in Chapter 4.

Synthetic design of cyclooctene-based HS glycopolymers

The rationale behind the design of the cyclooctene HS glycopolymers is identical to that presented for the synthesis of norbornene-based HS glycopolymers. The retrosynthetic schemes (Scheme A.1) of the two polymers are very similar, and revolve around three main building blocks: orthogonally protected IdoA, GlcA monosaccharides, and a cyclooctene-diethylene glycol linker. The target disaccharide **GlcNS3S6S- α -(1 \rightarrow 4)-IdoA2S** is based on the critical sulfate groups found on the anticoagulant HS pentasaccharide, and the

orthogonal protecting group strategy allows access to a variety of different sulfation patterns. Global deprotection of esters allows for simultaneous *O*-sulfation, minimizing the number of synthetic steps to functionalize the disaccharide monomer. Similar to the norbornene-based HS glycopolymers, sulfated monomers were used in the polymerization reactions to ensure a high degree of control over the sulfation pattern. Further details regarding the rationale behind the carbohydrate structures and protecting group strategy can be found in Chapter 2.

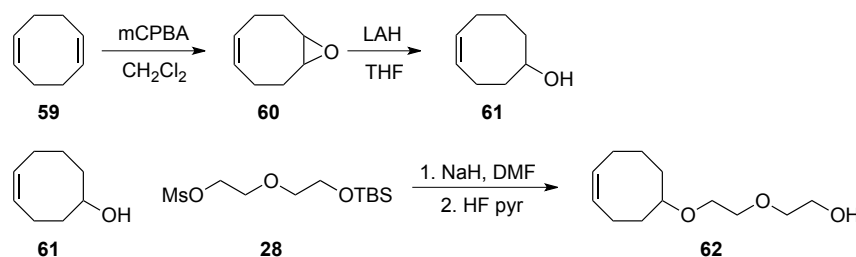


Scheme A.1: Retrosynthesis of cyclooctene-based HS glycopolymers. Bn = benzyl, Me = methyl, Ac = acetyl, Bz = benzoyl, TBS = *tert*-butyldimethylsilyl.

A cyclooctene polymer backbone was selected before norbornene because we expected its hydrocarbon backbone to offer a more flexible scaffold, allowing it to adapt better to relevant receptors. While the ring-strain is not as high as that of norbornene, it is sufficient to thermodynamically drive the ROMP reaction towards the desired product. As described in Chapter 3, ROMP chemistry was utilized to accommodate the functional complexity of the sulfated HS monomers to afford glycopolymers of controllable length and narrow polydispersities.

Synthesis of cyclooctene linker

The cyclooctene-based linker is comprised of a cyclooctene unit and a diethylene glycol chain (Scheme A.2), much like the norbornene-diethylene glycol linker. 4-cyclooctenol was obtained by epoxidation of commercially available cyclooctadiene **59** with *meta*-chloroperoxybenzoic acid (mCPBA). The resulting epoxide **60** was opened with lithium aluminum hydride (LAH) to afford the cyclooctene alcohol **61**. The methanesulfonyl (Ms) and *t*-butyldimethylsilyl (TBS) protected diethylene glycol **28** is identical to the one used for the norbornene linker synthesis. 4-Cyclooctenol was coupled to the protected diethylene glycol chain using NaH in DMF, and the resulting TBS protected linker intermediate was desilylated using HF•pyridine. All reactions are highly

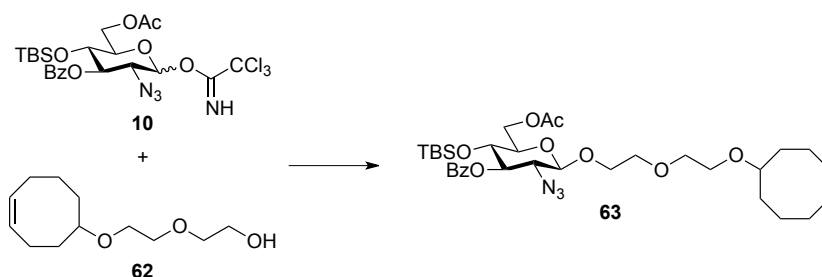


Scheme A.2: Synthesis of norbornene-based ROMP linker. mCPBA = *m*-Chloroperoxybenzoic acid, LAH = lithium aluminum hydride, MS = methanesulfonyl, TBS = *tert*-butyldimethylsilyl.

scalable and have been optimized to proceed at up to a 30 gram reaction scale.

Coupling of Glucosamine and Cyclooctenol Linker

In order to efficiently couple the glucosamine monomer and the cyclooctenol linker, activation of the monomer's anomeric carbon was necessary for the reaction to proceed cleanly with the free hydroxyl group of the linker. Imidate formation is commonly used in carbohydrate chemistry because of its high reactivity and stability to silica gel chromatography, and was therefore the chosen method of activation. The orthogonally protected GlcA trichloroacetimidate **10** was reacted with cyclooctene linker **62** using a



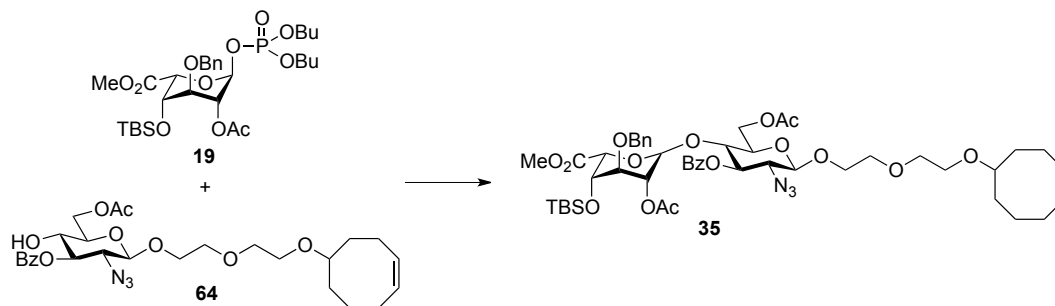
Reagent	Solvent	Conditions	Time	Results
TMSOTf (0.2 eq)	CH ₂ Cl ₂	-78 °C → rt	2 hr	70% β-product
TMSOTf (0.2 eq)	CH ₂ Cl ₂	-78 °C → -60 °C	12 hr	Reaction incomplete
TMSOTf (0.2 eq)	CH₂Cl₂	-78 °C → -40 °C	2 hr	85% β-product
TMSOTf (0.2 eq)	Et ₂ O	-78 °C → -20 °C	2 hr	β-product + 3 others
CSA (0.1 eq)	CH ₂ Cl ₂	Room temp	2 hr	β-product + 4 others
CSA (0.1 eq)	Et ₂ O	-20 °C	2 hr	β-prod. + 4 others
TfOH (0.1 eq)	Et ₂ O:CH ₂ Cl ₂	Room temp	2 hr	β-prod. > α-prod.
TsOH (0.1 eq)	Et ₂ O	-20 °C	2 hr	α -prod. > β -prod.
TsOH (0.5 eq)	Et ₂ O	-20 °C	2 hr	β-prod. > α-prod. + major byproduct
TsOH (1 eq)	Et ₂ O	-20 °C	2 hr	β-prod. > α-prod. + major byproduct + decomposition

Table A.1: Coupling of protected glcA and cyclooctene linker. TBS = *tert*-butyldimethylsilyl, Bz = benzoyl, Ac = acetyl.

variety of lewis acid activators (Table A.1). All reactions were carried out with three equivalents of the cyclooctene linker, with freshly activated 4Å molecular sieves. Upon testing reaction conditions by varying solvents and reaction temperatures, the reaction was optimized to use 0.2 eq of TMSOTf in CH₂Cl₂ at -40 °C, which yielded the β-product in 85% yield. The resulting TBS-protected compound **63** was desilylated using HF•pyridine deprotection conditions to afford the free acceptor **64**.

Glycosylation and deprotection of orthogonally protected disaccharide

Upon obtaining the cyclooctene acceptor **64**, the α-1→4 glycosidic linkage was installed by coupling the TBS-protected glycosyl phosphate **19** to the cyclooctene acceptor **64**. All reactions were carried out with 1.5 eq glycosylphosphate monomer in CH₂Cl₂ and

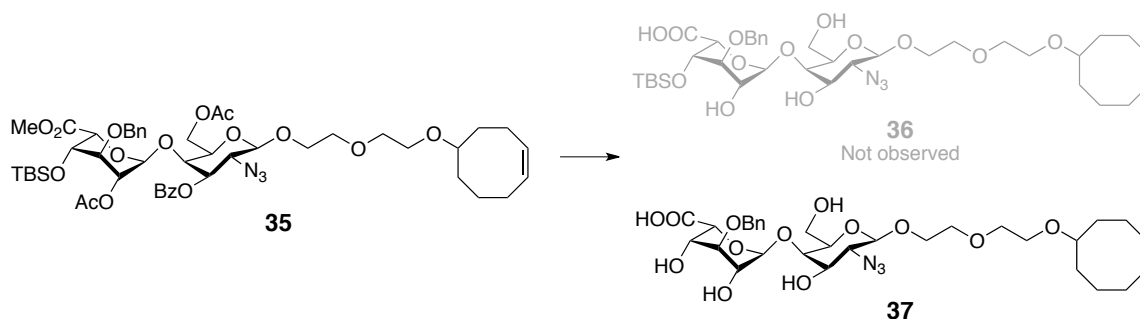


Entry	Reagent	Eq 19	Temp	Time	Result
1	BF ₃ •OEt ₂	2.0	-30 °C	1 hr	40%, 4 byproducts
2	BF ₃ •OEt ₂	1.5	-78 °C	1 hr	40%, 2 byproduct
3	BF ₃ •OEt ₂	1.2	-30 °C → 0 °C	Overnight	45%, 2 byproducts
4	TMSOTf	1.5	-78 °C	1 hr	Decomposition
5	TMSOTf	1.5	-78 °C → 0 °C	Overnight	23%
6	TMSOTf	1.5	-30 °C → 0 °C	2 hr	46%
7	TBSOTf	1.5	-78 °C → 0 °C	1 hr	35%, byproduct Decomposition
8	TBSOTf	1.5	-30 °C → 0 °C	2 hr	86%

Table A.2: Glycosylation reaction of idoA donor **19** and glcA acceptor **64**. Me = methyl, TBS = *tert*-butyldimethylsilyl, Bn = benzyl, Bz = benzoyl, Ac = acetyl.

freshly activated 4Å molecular sieves. Although trimethylsilyl triflate (TMSOTf) had been reported to effectively activate glycosyl phosphates, a thorough analysis of other activating reagents under a variety of reaction conditions revealed that glycosylation using 1.5 eq TBSOTf at controlled temperatures furnished the desired protected disaccharide **65** at a high yield of 86% (Table A.2, entry 8).

With the orthogonally protected HS disaccharide in hand, methyl ester hydrolysis and saponification of the disaccharide was planned according to previously reported procedures.³⁷ Unfortunately, the C-4 TBS group of GlcA proved itself to be unstable during methyl ester hydrolysis using LiOOH, under mildly basic conditions. Various concentrations of LiOH and H₂O₂ were used, but all protecting groups except the benzyl-group were consistently removed (Scheme A.3). The TBS group was only labile in the case of disaccharide **35**; the ester hydrolysis and saponification of protected disaccharide **66** proceeded without complications. We believe that the TBS group of disaccharide **35** is particularly labile due to its neighboring functional groups. The neighboring C-2 acetate and C-5 methyl ester are most likely withdrawing electron density from C-4, allowing the TBS group to leave, even under extremely mild conditions.



Scheme A.3: Saponification of TBS-protected cyclooctene-based HS disaccharide monomer. Me = methyl, TBS = *tert*-butyldimethylsilyl, Bn = benzyl, Bz = benzoyl, Ac = acetyl.

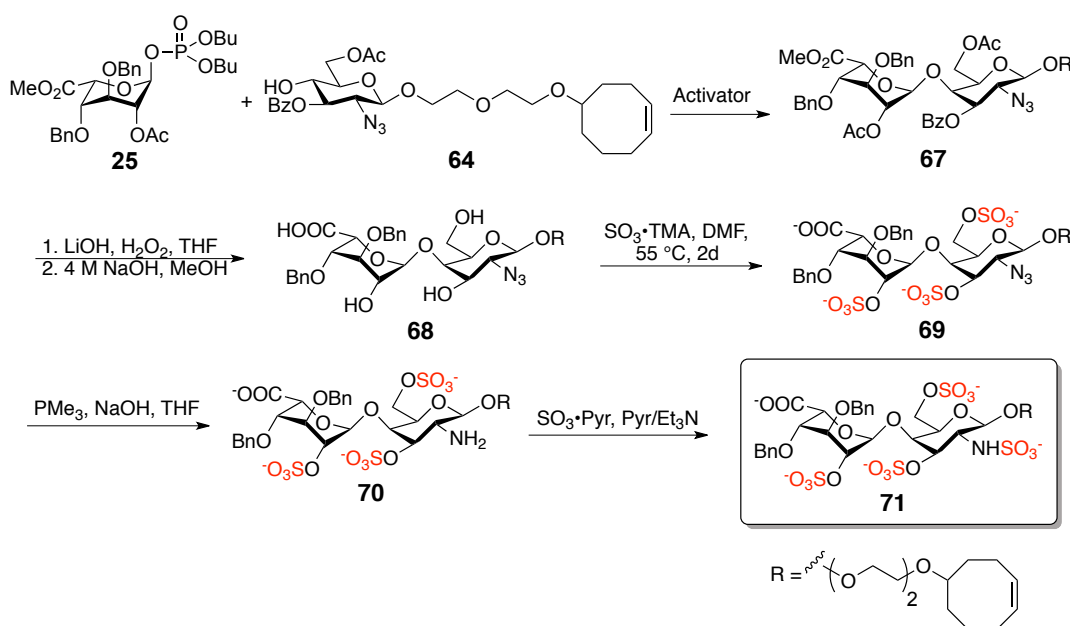
Upon discovering the instability of the C-4 TBS group, attempts were made to switch the TBS group to more stable functional groups. TBS protected disaccharide **35** was first desilylated in order to add another functional group; standard HF•pyr procedures, as used previously for CS glycopolymer synthesis, afforded the desired product in 80% yield. The main concerns of installing a new protecting group at this stage was stability of the other functional groups during the introduction of the new functional group, steric hindrance, electron withdrawal from the neighboring methyl ester and acetate groups, and most importantly, base stability of the new functional group, to avoid deprotection during the hydrolysis and saponification reactions.

Several attempts were made to protect the free C-4 hydroxyl group with other ester-type protecting groups, such as p-methylbenzyl (PMB), benzyl (Bn), or triisopropylsilyl (TIPS) ethers, using standard methods commonly used in organic synthesis. However, protection strategies using benzyl imidate, PMB imidate, and TIPS imidate did not result in the successful introduction of any of these functional groups. At this stage, different C-4 protected idoA derivatives were synthesized to incorporate benzyl, TIPS, and PMB functionalities (see Chapter 2).

Simultaneous to our discovery of the instability of the C-4 TBS group, our lab decided to switch to norbornene-based monomers from the cyclooctene-based monomers. The cyclooctene-based CS polymers had proven difficult to purify and had given moderate PDI values. The increased ring-strain of the norbornene bicyclic species generally result in easier purification and narrow PDIs, and allow for easy access to block copolymer species. With all such advantages in mind, the new IdoA derivatives and norbornene-diethylene

glycol linker were used towards the synthesis of the norbornene-based HS glycopolymer series.

Although the cyclooctene-based HS glycopolymer series were not pursued further, the synthesis should proceed smoothly as originally planned. Based on the optimization process for both monomer species, the cyclooctene-based monomers have proven to be more stable than the norbornene variants and display more predictable reactivity. Using the benzyl-protected IdoA glycosyl phosphate **25** and reaction conditions used for the synthesis of the norbornene HS glycopolymers, the following scheme (Scheme A.4) is proposed for the synthesis of cyclooctene HS glycopolymers:

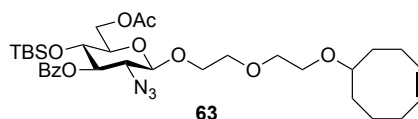


Scheme A.4: Proposed synthetic route to cyclooctene HS glycopolymers. Me = methyl, Bn = benzyl, TBAI = tetrabutylammonium iodide, Ac = acetyl, Bu = butyl, Bz = benzoyl, THF = tetrahydrofuran, TBSOTf = tert-butyltrimethylsilyl trifluoromethanesulfonate, TMA = trimethylamine, DMF = dimethylformamide, Pyr = pyridine.

Experimental methods and spectral data

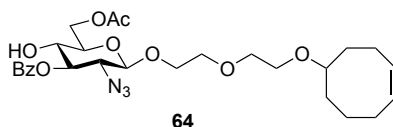
Unless otherwise stated, reactions were performed in flame-dried glassware under an argon atmosphere, using dry solvents. Solvents were dried by passage through an activated alumina column under argon. All other commercially obtained reagents were used as received unless otherwise noted. Thin layer chromatography (TLC) was performed using E. Merck silica gel 60 F254 precoated plates (0.25 mm). Visualization of the developed chromatogram was performed by UV, cerium ammonium molybdate and ninhydrin stain as necessary. ICN silica gel (particle size 0.032 - 0.063 mm) was used for flash chromatography. Gel filtration chromatography (Sephadex LH-20) was used in order to achieve purification of the final products.

^1H NMR and proton decoupling experiments were recorded on Varian Mercury 300 (300 MHz) and Varian Mercury 500 (500 MHz) spectrometers and are reported in parts per million (δ) relative to CDCl_3 (7.26 ppm). Data for ^1H are reported as follows: chemical shift (δ ppm), multiplicity (s = singlet, d = doublet, t = triplet, q = quartet, m = multiplet), coupling constant in Hz, and integration. ^{13}C NMR spectra were obtained on a Varian Mercury 300 (75 MHz) spectrometer and are reported in terms of chemical shift. Mass spectra were obtained from the Protein/Peptide Microanalytical Laboratory and the Mass Spectrometry facility at the California Institute of Technology.



2-(2-(Cyclooct-4-enyloxy)ethoxy)ethyl 6-O-acetyl-2-azido-3-benzoyl-4- β -D-glucopyranoside (63). A mixture of compound **10** (50 mg, 0.082 mmol) and cyclooctenol linker **62** (88 mg, 0.41 mmol) was azeotroped with toluene (3 x 10 mL). To this was added freshly activated 4Å molecular sieves (82 mg, 1g/mmol) and CH₂Cl₂ (1 mL). The mixture was stirred for 30 min at room temperature, and then cooled to -78 °C. TMSOTf (70 μ L, 0.017 mmol) was added dropwise, and the reaction mixture was slowly warmed to room temperature. After 1 h, the reaction was quenched with triethylamine, and filtered through a pad of celite. Purification via silica column chromatography (7:1 \rightarrow 5:1 \rightarrow 3:1 hexanes/ethyl acetate) afforded the desired compound **63** in 85 % yield.

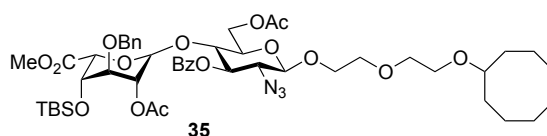
¹H NMR (300 MHz, CDCl₃): δ 8.06 (d, J = 8.4, 1H), 7.59 (t, , 2H), 7.47 (t, , 1H), 5.62 (m, 2H), 5.18 (t, J = 9, 8.7, 1H), 4.62 (d, J = 8.1, 1H), 4.28 (dd, J = 4.8, 4.5, 2H), 3.99 (m, 1H), 3.91 (m, 1H), 3.25-3.90 (m, 9H), 2.38 (m, 1H), 2.11 (s, 3H), 1.2-2.0 (m, 10H), 0.743 (s, 9H), -0.004 (s, 3H), -0.201 (s, 3H); ESI MS: *m/z* calcd for [C₃₃H₅₂SiN₃O₉]: 662.3441, obsd 662.3472.



2-(2-(Cyclooct-4-enyloxy)ethoxy)ethyl 6-O-acetyl-2-azido-3-benzoyl-4-deoxy- β -D-glucopyranoside (64). In a plastic container, compound **63** (18.5 mg, 0.0279 mmol) was dissolved in a mixture of 1:1 pyridine:THF (0.9 mL) and cooled to 0 °C. This mixture was stirred for 30 min, and HF•pyr (143 μ L) was added slowly. The reaction was slowly

warmed to room temperature and left to stir overnight. After confirmation of the reaction completion via TLC, the reaction mixture was diluted with ethyl acetate, quenched with aqueous NaHCO₃, then extracted with ethyl acetate (3 x 50 mL). Purification via silica gel column chromatography (3:1 hexanes/ethyl acetate) afforded compound **64** in 80% yield.

¹H NMR (300 MHz, CDCl₃): δ 8.10 (d, J = 8.4, 2H), 7.61 (t, J = 7.2, 1H), 7.51 (t, J = 7.8, 2H), 5.62 (m, 2H), 5.03 (t, J = 9.6, 1H), 4.58 (d, J = 8.1, 1H), 4.40 (dd, J = 4.2, 2H), 4.02 (m, 1H), 3.85 (m, 1H), 3.25-3.8 (m, 9H), 3.21 (d, J = 4.2, 1H), 2.33 (m, 1H), 2.12 (s, 3H), 1.25-2.0 (m, 10H); ESI MS: *m/z* calcd for [C₂₇H₃₇N₃O₉ + H] 548.25, obsvd 548.26.



2-(2-(Cyclooct-4-enyloxy) ethoxy) ethyl (methyl 2-O-acetyl-3-O-benzyl-4-O-tertbutylsilyl- α -L-idopyranosid)uronate)-(1 \rightarrow 4)-6-O-acetyl-2-azido-3-benzoyl-4-deoxy- β -D-glucopyranoside (35**). Compound **64** (25 mg, 0.046 mmol) and **19** (38.2 mg, 0.059 mmol) were combined in a reaction flask and azeotroped with toluene (3 x 2 mL). This anhydrous material was dissolved in CH₂Cl₂ (0.5 mL), and freshly activated 4Å molecular sieves (46 mg, 1g/mmol) were added. The reaction mixture was cooled to -30 °C, and TBSOTf (15.7 μ L, 0.069 mmol) was added dropwise. This was allowed to warm to 0 °C for 2 h. After completion, the reaction mixture was quenched with triethylamine and concentrated under reduced pressure. Silica column chromatography (4:1 hexanes/ethyl acetate) afforded compound **35** in 86% yield.**

¹H NMR (500MHz, CDCl₃): δ 8.06 (d, J = 7.2, 2H), 7.55 (t, J = 7.2, 1H), 7.43 (t, J = 7.8, 2H), 7.26 (m, 5H), 5.66 (m, 2H), 5.26 (t, J = 9.3, 1H), 5.12 (d, J = 4.8, 1H), 4.73 (t, J

= 4.2, 1H), 4.61 (dd, J = 19.8, 12, 2H), 4.49 (s, 1H), 4.47 (d, J = 10.5, 1H), 4.16 (dd, J = 4.2, 4.5, 2H), 4.08 (m, 2H), 3.3-3.90 (m, 9H), 3.42 (s, 3H), 2.12 (s, 3H), 1.93 (s, 3H), 1.0-1.83 (m, 10H), 1.32 (m, 1H), -0.75 (s, 9H), -0.21 (d, J = 5.4, 6H); ESI MS: *m/z* calcd for [C₅₀H₆₁N₃O₁₆ + Na⁺] 982.41, obsvd 982.37.

BIBLIOGRAPHY

Chapter 1

- 1 Varti, A. *et al.* *Essentials of Glycobiology*. (Cold Spring Harbor Laboratory Press, 1999).
- 2 Esko, J. D., Kimata, K. & Lindahl, U. in *Essentials of Glycobiology* (eds A. Varki, R. D. Cummings, & J.D. Esko) Ch. 16, (Cold Spring Harbor Laboratory Press, 2009).
- 3 Esko, J. D. & Lindahl, U. Molecular diversity of heparan sulfate. *J Clin Invest* **108**, 169-173, doi:10.1172/JCI13530 (2001).
- 4 Trowbridge, J. M. & Gallo, R. L. Dermatan sulfate: new functions from an old glycosaminoglycan. *Glycobiology* **12**, 117R-125R (2002).
- 5 Laine, R. A. in *Glycosciences* 1-14 (Wiley-VCH Verlag GmbH, 2008).
- 6 Reuter, G. & Gabius, H. J. Eukaryotic glycosylation: whim of nature or multipurpose tool? *Cellular and molecular life sciences : CMLS* **55**, 368-422 (1999).
- 7 Gabius, H. J. Cell surface glycans: the why and how of their functionality as biochemical signals in lectin-mediated information transfer. *Critical reviews in immunology* **26**, 43-79 (2006).
- 8 Sasisekharan R Fau - Raman, R., Raman R Fau - Prabhakar, V. & V, P. - Glycomics approach to structure-function relationships of glycosaminoglycans. *Annu Rev Biomed Eng* **8**, 181-231 (2006).
- 9 Sugahara, K. *et al.* Recent advances in the structural biology of chondroitin sulfate and dermatan sulfate. *Current opinion in structural biology* **13**, 612-620 (2003).
- 10 Monzavi-Karbassi B Fau - Stanley, J. S. *et al.* - Chondroitin sulfate glycosaminoglycans as major P-selectin ligands on metastatic breast cancer cell lines. *Int J Cancer* **120**, 1179-1191 (2007).
- 11 Sasisekharan, R., Shriver, Z., Venkataraman, G. & Narayanasami, U. Roles of heparan-sulphate glycosaminoglycans in cancer. *Nature Reviews Cancer* **2**, 521-528, doi:10.1038/nrc842 (2002).
- 12 Lin, X., Buff, E. M., Perrimon, N. & Michelson, A. M. Heparan sulfate proteoglycans are essential for FGF receptor signaling during *Drosophila* embryonic development. *Development* **126**, 3715-3723 (1999).

- 13 Shukla, D. & Spear, P. G. Herpesviruses and heparan sulfate: an intimate relationship in aid of viral entry. *The Journal of Clinical Investigation* **108**, 503-510, doi:10.1172/jci13799 (2001).
- 14 Carter, G. C., Law, M., Hollinshead, M. & Smith, G. L. Entry of the vaccinia virus intracellular mature virion and its interactions with glycosaminoglycans. *Journal of General Virology* **86**, 1279-1290, doi:10.1099/vir.0.80831-0 (2005).
- 15 Bandtlow, C. E. & Zimmermann, D. R. Proteoglycans in the developing brain: new conceptual insights for old proteins. *Physiological reviews* **80**, 1267-1290 (2000).
- 16 Kitagawa, H., Tsutsumi, K., Tone, Y. & Sugahara, K. Developmental regulation of the sulfation profile of chondroitin sulfate chains in the chicken embryo brain. *The Journal of biological chemistry* **272**, 31377-31381 (1997).
- 17 Gallagher, J. T. & Hampson, I. N. Proteoglycans in cellular differentiation and neoplasia. *Biochemical Society transactions* **12**, 541-543 (1984).
- 18 Hook, M., Kjellen, L., Johansson, S. & Robinson, J. Cell-surface Glycosaminoglycans. *Annual Review of Biochemistry* **53**, 847-869 (1984).
- 19 Bissell, M. J., Hall, H. G. & Parry, G. How does the extracellular matrix direct gene expression? *Journal of theoretical biology* **99**, 31-68 (1982).
- 20 Hay, E. D. Extracellular matrix. *The Journal of cell biology* **91**, 205s-223s (1981).
- 21 Kanwar, Y. S., Linker, A. & Farquhar, M. G. Increased permeability of the glomerular basement membrane to ferritin after removal of glycosaminoglycans (heparan sulfate) by enzyme digestion. *The Journal of cell biology* **86**, 688-693 (1980).
- 22 Obrind, B., Pertoft, H., Iverius, P. H. & Laurent. The effect of calcium on the macromolecular properties of heparan sulfate. *Connective tissue research* **3**, 187-193 (1975).
- 23 Linhardt, R. J. 2003 Claude S. Hudson Award address in carbohydrate chemistry. Heparin: structure and activity. *J Med Chem* **46**, 2551-2564, doi:10.1021/jm030176m (2003).
- 24 Lindahl, U., Kusche-Gullberg, M. & Kjelle, N. Regulated diversity of heparan sulfate. *Journal of Biological Chemistry* **273**, 24979-24982 (1998).
- 25 Kjellen, L. & Lindahl, U. Proteoglycans: structures and interactions. *Annu Rev Biochem* **60**, 443-475, doi:10.1146/annurev.bi.60.070191.002303 (1991).
- 26 Rong, J., Habuchi, H., Kimata, K., Lindahl, U. & Kusche-Gullberg, M. Substrate specificity of the heparan sulfate hexuronic acid 2-O-sulfotransferase. *Biochemistry* **40**, 5548-5555 (2001).

- 27 Merry, C. L. & Wilson, V. A. Role of heparan sulfate-2-O-sulfotransferase in the mouse. *Biochimica et biophysica acta* **1573**, 319-327 (2002).
- 28 Habuchi, H. *et al.* The occurrence of three isoforms of heparan sulfate 6-O-sulfotransferase having different specificities for hexuronic acid adjacent to the targeted N-sulfoglucosamine. *The Journal of biological chemistry* **275**, 2859-2868 (2000).
- 29 Smeds, E. *et al.* Substrate specificities of mouse heparan sulphate glucosaminyl 6-O-sulphotransferases. *Biochemical Journal* **372**, 371-380, doi:10.1042/BJ20021666 (2003).
- 30 Shworak, N. W. *et al.* Multiple isoforms of heparan sulfate D-glucosaminyl 3-O-sulfotransferase. Isolation, characterization, and expression of human cdnas and identification of distinct genomic loci. *The Journal of biological chemistry* **274**, 5170-5184 (1999).
- 31 Xia, G. *et al.* Heparan sulfate 3-O-sulfotransferase isoform 5 generates both an antithrombin-binding site and an entry receptor for herpes simplex virus, type 1. *The Journal of biological chemistry* **277**, 37912-37919, doi:10.1074/jbc.M204209200 (2002).
- 32 Mochizuki, H. *et al.* Characterization of a heparan sulfate 3-O-sulfotransferase-5, an enzyme synthesizing a tetrasulfated disaccharide. *The Journal of biological chemistry* **278**, 26780-26787, doi:10.1074/jbc.M301861200 (2003).
- 33 Gabius, H. J., Andre, S., Kaltner, H. & Siebert, H. C. The sugar code: functional lectinomics. *Biochimica et biophysica acta* **1572**, 165-177 (2002).
- 34 Carlsson P Fau - Kjellen, L. & L, K. - Heparin biosynthesis. *Handbook of Experimental Pharmacology* **207**, 23-41 (2012).
- 35 Casu, B., Petitou, M., Provasoli, M. & Sinay, P. Conformational flexibility: a new concept for explaining binding and biological properties of iduronic acid-containing glycosaminoglycans. *Trends in biochemical sciences* **13**, 221-225 (1988).
- 36 Mikhailov, D., Mayo, K. H., Pervin, A. & Linhardt, R. J. 13C-NMR relation study of heparin-disaccharide interactions with tripeptides GRG and GKG. *Biochemical Journal* **315 (Pt 2)**, 447-454 (1996).
- 37 Mulloy, B. & Forster, M. J. Conformation and dynamics of heparin and heparan sulfate. *Glycobiology* **10**, 1147-1156 (2000).
- 38 Mizumoto, S., Kitagawa, H. & Sugahara, K. in *Chemistry and Biology of Heparin and Heparan Sulfate* (eds H. G. Garg, R. J. Linhardt, & C. A. Hales) (Elsevier Ltd, 2005).

- 39 Lindahl, U., Kusche-Gullberg, M. & Kjellen, L. Regulated diversity of heparan sulfate. *The Journal of biological chemistry* **273**, 24979-24982 (1998).
- 40 Jackson, R. L., Busch, S. J. & Cardin, A. D. Glycosaminoglycans: molecular properties, protein interactions, and role in physiological processes. *Physiological reviews* **71**, 481-539 (1991).
- 41 Spillmann, D. & Lindahl, U. Glycosaminoglycan-protein interactions: a question of specificity. *Current Opinions in Structural Biology* **4**, 677-682 (1994).
- 42 Liu J Fau - Shriver, Z. *et al.* - Characterization of a heparan sulfate octasaccharide that binds to herpes simplex virus type 1 glycoprotein D. *The Journal of biological chemistry* **277**, 33456-33467 (2002).
- 43 Ye, S. *et al.* Structural basis for interaction of FGF-1, FGF-2, and FGF-7 with different heparan sulfate motifs. *Biochemistry* **40**, 14429-14439 (2001).
- 44 Guimond, S., Maccarana, M., Olwin, B. B., Lindahl, U. & Rapraeger, A. C. Activating and inhibitory heparin sequences for FGF-2 (basic FGF). Distinct requirements for FGF-1, FGF-2, and FGF-4. *The Journal of biological chemistry* **268**, 23906-23914 (1993).
- 45 Abramsson, A. *et al.* Defective N-sulfation of heparan sulfate proteoglycans limits PDGF-BB binding and pericyte recruitment in vascular development. *Genes & development* **21**, 316-331 (2007).
- 46 Lyon, M., Deakin, J. A., Mizuno, K., Nakamura, T. & Gallagher, J. T. Interaction of hepatocyte growth factor with heparan sulfate. Elucidation of the major heparan sulfate structural determinants. *Journal of Biological Chemistry* **269**, 11216-11223 (1994).
- 47 Chen, Y. *et al.* Dengue virus infectivity depends on envelope protein binding to target cell heparan sulfate. *Nature medicine* **3**, 866-871 (1997).
- 48 Sasaki, T. *et al.* Structural basis and potential role of heparin/heparan sulfate binding to the angiogenesis inhibitor endostatin. *The EMBO journal* **18**, 6240-6248, doi:10.1093/emboj/18.22.6240 (1999).
- 49 Lortat-Jacob, H., Grosdidier, A. & Imberty, A. Structural diversity of heparan sulfate binding domains in chemokines. *Proceedings of the National Academy of Sciences* **99**, 1229-1234 (2002).
- 50 Bourin, M. C. & Lindahl, U. Glycosaminoglycans and the regulation of blood coagulation. *Biochemical Journal* **289** (Pt 2), 313-330 (1993).
- 51 Howell, W. H. The factors concerned in the process of the clotting of blood. *Therapeutic Gazette* **36**, 95-98 (1912).

- 52 Levine, M. *et al.* A comparison of low-molecular-weight heparin administered primarily at home with unfractionated heparin administered in the hospital for proximal deep-vein thrombosis. *New England Journal of Medicine* **334**, 677-681 (1996).
- 53 Contejean, C. Recherches sur les injections intraveineuses de peptone et leur influence sur la coagulabilite du sang chez le chieu. *Arch. Physiol. Norm. Pathol* **7**, 45-53 (1895).
- 54 Brinkhous, K. M., Smith, H. P., Warner, E. D. & Seegers, W. H. The inhibition of blood clotting: an unidentified substance which acts in conjunction with heparin to prevent the conversion of prothrombin into thrombin. *American Journal of Physiology* **125**, 683-687 (1939).
- 55 Waugh, D. F. & Fitzgerald, M. A. Quantitative aspects of antithrombin and heparin in plasma. *The American journal of physiology* **184**, 627-639 (1956).
- 56 Monkhouse, F. C., France, E. S. & Seegers, W. H. Studies on the antithrombin and heparin cofactor activities of a fraction adsorbed from plasma by aluminum hydroxide. *Circulation research* **3**, 397-402 (1955).
- 57 Abildgaard, U. Highly purified antithrombin 3 with heparin cofactor activity prepared by disc electrophoresis. *Scandinavian Journal of Clinical & Laboratory Investigation* **21**, 89-91 (1968).
- 58 Rosenberg, R. D. & Damus, P. S. The purification and mechanism of action of human antithrombin-heparin cofactor. *The Journal of biological chemistry* **248**, 6490-6505 (1973).
- 59 Damus, P. S., Hicks, M. & Rosenberg, R. D. Anticoagulant action of heparin. *Nature* **246**, 355-357 (1973).
- 60 R.J., L. Heparin: An important drug enters its seventh decade. *Chemistry and industry* **2**, 45-50 (1991).
- 61 Lam, L. H., Silbert, J. E. & Rosenberg, R. D. The separation of active and inactive forms of heparin. *Biochemical and biophysical research communications* **69**, 570-577 (1976).
- 62 Hook, M., Bjork, I., Hopwood, J. & Lindahl, U. Anticoagulant activity of heparin: separation of high-activity and low-activity heparin species by affinity chromatography on immobilized antithrombin. *FEBS letters* **66**, 90-93 (1976).
- 63 Hopwood, J., Hook, M., Linker, A. & Lindahl, U. Anticoagulant activity of heparin: isolation of antithrombin-binding sites. *FEBS letters* **69**, 51-54 (1976).
- 64 Andersson, L. O., Barrowcliffe, T. W., Holmer, E., Johnson, E. A. & Sims, G. E. Anticoagulant properties of heparin fractionated by affinity chromatography on

- matrix-bound antithrombin iii and by gel filtration. *Thrombosis research* **9**, 575-583 (1976).
- 65 Petitou, M. & van Boeckel, C. A. A synthetic antithrombin III binding pentasaccharide is now a drug! What comes next? *Angewandte Chemie International Edition* **43**, 3118-3133, doi:10.1002/anie.200300640 (2004).
- 66 Atha, D. H., Lormeau, J. C., Petitou, M., Rosenberg, R. D. & Choay, J. Contribution of monosaccharide residues in heparin binding to antithrombin III. *Biochemistry* **24**, 6723-6729 (1985).
- 67 Hirsh, J., O'Donnell, M. & Eikelboom, J. W. Beyond Unfractionated Heparin and Warfarin: Current and Future Advances. *Circulation* **116**, 552-560 (2007).
- 68 Gray, E., Mulloy, B. & Barrowcliffe, T. W. Heparin and low-molecular-weight heparin. *Journal of Thrombosis and Haemostasis* **99**, 807-818, doi:10.1160/TH08-01-0032 (2008).
- 69 Petitou, M. *et al.* Synthesis of thrombin-inhibiting heparin mimetics without side effects. *Nature* **398**, 417-422, doi:10.1038/18877 (1999).
- 70 Choay, J. *et al.* Process for the organic synthesis of oligosaccharides and derivatives thereof. (1987).
- 71 Seifert, J., Singh, L., Ramsdale, T. E., West, M. L. & Drinnan, N. B. (2009).
- 72 Howard, P. A. Dalteparin: a low-molecular-weight heparin. *The Annals of pharmacotherapy* **31**, 192-203 (1997).
- 73 Barradell, L. & Buckley, M. Nadroparin Calcium. *Drugs* **44**, 858-888, doi:10.2165/00003495-199244050-00010 (1992).
- 74 Lindahl, U. *et al.* Generation of "neoheparin" from E. coli K5 capsular polysaccharide. *J Med Chem* **48**, 349-352, doi:10.1021/jm049812m (2005).
- 75 Zhang, Z. *et al.* Solution structures of chemoenzymatically synthesized heparin and its precursors. *Journal of the American Chemical Society* **130**, 12998-13007, doi:10.1021/ja8026345 (2008).
- 76 Chen, J., Jones, C. L. & Liu, J. Using an enzymatic combinatorial approach to identify anticoagulant heparan sulfate structures. *Chemistry & biology* **14**, 986-993, doi:10.1016/j.chembiol.2007.07.015 (2007).
- 77 Liu, R. *et al.* Chemoenzymatic design of heparan sulfate oligosaccharides. *The Journal of biological chemistry* **285**, 34240-34249, doi:10.1074/jbc.M110.159152 (2010).

- 78 Kuberan, B., Lech, M. Z., Beeler, D. L., Wu, Z. L. & Rosenberg, R. D. Enzymatic synthesis of antithrombin III-binding heparan sulfate pentasaccharide. *Nature Biotechnology* **21**, 1343-1346, doi:10.1038/nbt885 (2003).
- 79 Xu, Y., Pempe, E. H. & Liu, J. Chemoenzymatic synthesis of heparin oligosaccharides with both anti-factor Xa and anti-factor IIa activities. *The Journal of biological chemistry* **287**, 29054-29061, doi:10.1074/jbc.M112.358523 (2012).
- 80 Loganathan, D., Wang, H. M., Mallis, L. M. & Linhardt, R. J. Structural variation in the antithrombin III binding site region and its occurrence in heparin from different sources. *Biochemistry* **29**, 4362-4368 (1990).
- 81 Wang, Z. *et al.* E. coli K5 fermentation and the preparation of heparosan, a bioengineered heparin precursor. *Biotechnology and Bioengineering* **107**, 964-973, doi:10.1002/bit.22898 (2010).
- 82 Cronin, R. E. & Reilly, R. F. Unfractionated heparin for hemodialysis: still the best option. *Seminars in dialysis* **23**, 510-515, doi:10.1111/j.1525-139X.2010.00770.x (2010).
- 83 J., L. R. & Toida, T. in *Carbohydrates in Drug Design* (eds Z. J. Witczak & K. A. Nieforth) Ch. Chapter 7, 277-341 (Marcel Dekker, 1997).
- 84 *Contaminant detected in heparin material of specified origin in the USA and in Germany; serious adverse events reported; recall measures initiated.*, <http://www.who.int/medicines/publications/drugalerts/Alert_118_Heparin.pdf> (2008).
- 85 *Heparin Recall Information. Baxter Investigation Updates*, <<http://www.baxter.com/products/biopharmaceuticals/heparin.html>> (2008).
- 86 Liu, H., Zhang, Z. & Linhardt, R. J. Lessons learned from the contamination of heparin. *Natural product reports* **26**, 313-321, doi:10.1039/b819896a (2009).
- 87 Zhang, Z. *et al.* Oversulfated Chondroitin Sulfate: Impact of a Heparin Impurity, Associated with Adverse Clinical Events, on Low-Molecular-Weight Heparin Preparation. *Journal of Medicinal Chemistry* **51**, 5498-5501, doi:10.1021/jm800785t (2008).
- 88 Guerrini M, B. D., Shriver Z, Naggi A, Viswanathan K, Bisio A, Capila I, Lansing JC, Guglieri S, Fraser B, Al-Hakim A, Gunay NS, Zhang Z, Robinson L, Buhse L, Nasr M, Woodcock J, Langer R, Venkataraman G, Linhardt RJ, Casu B, Torri G, Sasisekharan R. Oversulfated chondroitin sulfate is a contaminant in heparin associated with adverse clinical events. *Nature Biotechnology* **26**, 669-675 (2008).
- 89 Naggi, A. *et al.* Sulfamino-galactosaminoglycans, a new class of semi-synthetic polysaccharides. Preparation, characterization, and lipase-releasing properties.

Biomedical and Biotechnological Advances in Industrial Polysaccharides, 101-108 (1989).

- 90 Siegmeth W Fau - Radi, I. & I, R. - [Comparison of glycosaminoglycan polysulfate (Arteparon) and physiological saline solution in arthrosis of the large joints. Results of a multicenter double-blind study]. *Z Rheumatol* **42**, 223-228 (1983).

Chapter 2

- 1 Corey, E. J., Cho, H., Rücker, C. & Hua, D. H. Studies with trialkylsilyltriflates: new syntheses and applications. *Tetrahedron Letters* **22**, 3455-3458, doi:[http://dx.doi.org/10.1016/S0040-4039\(01\)81930-4](http://dx.doi.org/10.1016/S0040-4039(01)81930-4) (1981).
- 2 Abe, H., Shuto, S., Tamura, S. & Matsuda, A. An efficient method for preparing fully O-silylated pyranoses conformationally restricted in the unusual 1C4-form. *Tetrahedron Letters* **42**, 6159-6161, doi:[http://dx.doi.org/10.1016/S0040-4039\(01\)01233-3](http://dx.doi.org/10.1016/S0040-4039(01)01233-3) (2001).
- 3 Johnson, D. J., Li, W., Adams, T. E. & Huntington, J. A. Antithrombin-S195A factor Xa-heparin structure reveals the allosteric mechanism of antithrombin activation. *The EMBO journal* **25**, 2029-2037, doi:10.1038/sj.emboj.7601089 (2006).
- 4 Petitou, M. *et al.* Synthesis of thrombin-inhibiting heparin mimetics without side effects. *Nature* **398**, 417-422, doi:10.1038/18877 (1999).
- 5 Arndt, S. & Hsieh-Wilson, L. C. Use of cerny epoxides for the accelerated synthesis of glycosaminoglycans. *Organic letters* **5**, 4179-4182, doi:10.1021/ol035606h (2003).
- 6 Becker, R. C. Optimizing heparin compounds: a working construct for future antithrombotic drug development. *Journal of thrombosis and thrombolysis* **18**, 55-58, doi:10.1007/s11239-004-0176-x (2004).
- 7 Van Hijfte, L. & Little, R. D. Intramolecular 1,3-diyl trapping reactions. A formal total synthesis of (+,-)-coriolin. *The Journal of Organic Chemistry* **50**, 3940-3942, doi:10.1021/jo00220a058 (1985).
- 8 Hirsh, J., O'Donnell, M. & Weitz, J. I. New anticoagulants. *Blood* **105**, 453-463, doi:10.1182/blood-2003-12-4195 (2005).
- 9 Brummond, K. M. & Hong, S.-p. A Formal Total Synthesis of (-)-FR901483, Using a Tandem Cationic Aza-Cope Rearrangement/Mannich Cyclization Approach. *The Journal of Organic Chemistry* **70**, 907-916, doi:10.1021/jo0483567 (2004).

- 10 Kelton, J. G. Heparin-induced thrombocytopenia: an overview. *Blood reviews* **16**, 77-80, doi:10.1054/blre.2001.0189 (2002).
- 11 Tobu, M. *et al.* Erythropoietin-induced thrombosis as a result of increased inflammation and thrombin activatable fibrinolytic inhibitor. *Clinical and applied thrombosis/hemostasis : official journal of the International Academy of Clinical and Applied Thrombosis/Hemostasis* **10**, 225-232 (2004).
- 12 Weitz, J. I. Potential of new anticoagulants in patients with cancer. *Thrombosis research* **125 (suppl. 2)**, S30-S35 (2010).
- 13 Weitz, J. I. & Linkins, L.-A. Beyond heparin and warfarin: the new generation of anticoagulants. *Expert opinion on investigational drugs* **16**, 271-282, doi:doi:10.1517/13543784.16.3.271 (2007).
- 14 Schenone, M., Furie, B. C. & Furie, B. The blood coagulation cascade. *Current opinion in hematology* **11**, 272-277 (2004).
- 15 Casu, B. & Lindahl, U. Structure and biological interactions of heparin and heparan sulfate. *Advances in carbohydrate chemistry and biochemistry* **57**, 159-206 (2001).
- 16 Huntington, J. A. & Carrell, R. W. The serpins: nature's molecular mousetraps. *Science progress* **84**, 125-136 (2001).
- 17 Sie, P. *et al.* Respective role of antithrombin III and heparin cofactor II in the in vitro anticoagulant effect of heparin and of various sulphated polysaccharides. *British journal of haematology* **64**, 707-714 (1986).
- 18 Desai, U. R. New antithrombin-based anticoagulants. *Medicinal research reviews* **24**, 151-181, doi:10.1002/med.10058 (2004).
- 19 Huntington, J. A. in *Chemistry and Biology of Heparin and Heparan Sulfate* (eds H. G. Garg, R. J. Linhardt, & C. A. Hales) 367-398 (Elsevier, 2005).
- 20 Olson, S. T. & Shore, J. D. Binding of high affinity heparin to antithrombin III. Characterization of the protein fluorescence enhancement. *The Journal of biological chemistry* **256**, 11065-11072 (1981).
- 21 Olson, S. T., Srinivasan, K. R., Bjork, I. & Shore, J. D. Binding of high affinity heparin to antithrombin III. Stopped flow kinetic studies of the binding interaction. *The Journal of biological chemistry* **256**, 11073-11079 (1981).
- 22 Nordenman, B. & Bjork, I. Binding of low-affinity and high-affinity heparin to antithrombin. Ultraviolet difference spectroscopy and circular dichroism studies. *Biochemistry* **17**, 3339-3344 (1978).

- 23 Nordenman, B., Danielsson, A. & Bjork, I. The binding of low-affinity and high-affinity heparin to antithrombin. Fluorescence studies. *European journal of biochemistry / FEBS* **90**, 1-6 (1978).
- 24 Olson, S. T. & Bjork, I. Role of protein conformational changes, surface approximation and protein cofactors in heparin-accelerated antithrombin-proteinase reactions. *Advances in experimental medicine and biology* **313**, 155-165 (1992).
- 25 Bray, B., Lane, D. A., Freyssinet, J. M., Pejler, G. & Lindahl, U. Anti-thrombin activities of heparin. Effect of saccharide chain length on thrombin inhibition by heparin cofactor II and by antithrombin. *Biochemical Journal* **262**, 225-232 (1989).
- 26 Casu, B. Structure and biological activity of heparin. *Advances in carbohydrate chemistry and biochemistry* **43**, 51-134 (1985).
- 27 Petitou, M., Casu, B. & Lindahl, U. 1976-1983, a critical period in the history of heparin: the discovery of the antithrombin binding site. *Biochimie* **85**, 83-89 (2003).
- 28 Oosta, G. M., Gardner, W. T., Beeler, D. L. & Rosenberg, R. D. Multiple functional domains of the heparin molecule. *Proceedings of the National Academy of Sciences* **78**, 829-833 (1981).
- 29 Herbert, J. M. *et al.* SR 123781A, a synthetic heparin mimetic. *Journal of Thrombosis and Haemostasis* **85**, 852-860 (2001).
- 30 Petitou, M. & van Boeckel, C. A. A synthetic antithrombin III binding pentasaccharide is now a drug! What comes next? *Angewandte Chemie International Edition* **43**, 3118-3133, doi:10.1002/anie.200300640 (2004).
- 31 Atha, D. H., Lormeau, J. C., Petitou, M., Rosenberg, R. D. & Choay, J. Contribution of monosaccharide residues in heparin binding to antithrombin III. *Biochemistry* **24**, 6723-6729 (1985).
- 32 van Boeckel, C. A. A. & Petitou, M. The Unique Antithrombin III Binding Domain of Heparin: A Lead to New Synthetic Antithrombotics. *Angewandte Chemie International Edition in English* **32**, 1671-1690, doi:10.1002/anie.199316713 (1993).
- 33 Garg, H. G., Linhardt, R. J. & Hales, C. A. *Chemistry and Biology of Heparin and Heparan Sulfate*. (Elsevier, 2005).
- 34 Kiessling, L. L., Gestwicki, J. E. & Strong, L. E. Synthetic multivalent ligands in the exploration of cell-surface interactions. *Current opinion in chemical biology* **4**, 696-703 (2000).

- 35 Lee, S.-G. *et al.* End-functionalized glycopolymers as mimetics of chondroitin sulfate proteoglycans. *Chemical Science* **1**, 322-325 (2010).
- 36 Rawat, M., Gama, C. I., Matson, J. B. & Hsieh-Wilson, L. C. Neuroactive Chondroitin Sulfate Glycomimetics. *Journal of the American Chemical Society* **130**, 2959-2961, doi:10.1021/ja709993p (2008).
- 37 Li, W., Johnson, D. J., Esmon, C. T. & Huntington, J. A. Structure of the antithrombin-thrombin-heparin ternary complex reveals the antithrombotic mechanism of heparin. *Nature structural & molecular biology* **11**, 857-862, doi:10.1038/nsmb811 (2004).
- 38 Das, S. K. *et al.* Synthesis of conformationally locked L-iduronic acid derivatives: direct evidence for a critical role of the skew-boat 2S0 conformer in the activation of antithrombin by heparin. *Chemistry* **7**, 4821-4834 (2001).
- 39 van Boeckel, C. A. A., Beetz, T. & van Aelst, S. F. Synthesis of a potent antithrombin activating pentasaccharide: A new heparin-like fragment containing two 3-O-sulphated glucosamines. *Tetrahedron Letters* **29**, 803-806, doi:[http://dx.doi.org/10.1016/S0040-4039\(00\)80214-2](http://dx.doi.org/10.1016/S0040-4039(00)80214-2) (1988).
- 40 Grootenhuis, P. D., Westerduin, P., Meuleman, D., Petitou, M. & van Boeckel, C. A. Rational design of synthetic heparin analogues with tailor-made coagulation factor inhibitory activity. *Nature structural biology* **2**, 736-739 (1995).
- 41 Danielsson, A., Raub, E., Lindahl, U. & Bjork, I. Role of ternary complexes, in which heparin binds both antithrombin and proteinase, in the acceleration of the reactions between antithrombin and thrombin or factor Xa. *The Journal of biological chemistry* **261**, 15467-15473 (1986).
- 42 Laurent, T. C., Tengblad, A., Thunberg, L., Hook, M. & Lindahl, U. The molecular-weight-dependence of the anti-coagulant activity of heparin. *Biochemical Journal* **175**, 691-701 (1978).
- 43 Lane, D. A., Denton, J., Flynn, A. M., Thunberg, L. & Lindahl, U. Anticoagulant activities of heparin oligosaccharides and their neutralization by platelet factor 4. *Biochemical Journal* **218**, 725-732 (1984).
- 44 Wittmann, V. The Organic Chemistry of Sugars. Edited by Daniel E. Levy and Péter Fügedi. *Angewandte Chemie International Edition* **45**, 3399-3400, doi:10.1002/anie.200685377 (2006).
- 45 Sheng, G. J., Oh, Y. I., Chang, S. K. & Hsieh-Wilson, L. C. Tunable Heparan Sulfate Mimetics for Modulating Chemokine Activity. *Journal of the American Chemical Society* **In Preparation** (2013).

- 46 Paz, J.-Luis d., Ojeda, R., Reichardt, N. & Martín-Lomas, M. Some Key Experimental Features of a Modular Synthesis of Heparin-Like Oligosaccharides. *European Journal of Organic Chemistry* **2003**, 3308-3324, doi:10.1002/ejoc.200300210 (2003).
- 47 Vasella, A., Witzig, C., Chiara, J.-L. & Martin-Lomas, M. Convenient Synthesis of 2-Azido-2-deoxy-aldoses by Diazo Transfer. *Helvetica Chimica Acta* **74**, 2073-2077, doi:10.1002/hlca.19910740842 (1991).
- 48 Alper, P. B., Hung, S.-C. & Wong, C.-H. Metal catalyzed diazo transfer for the synthesis of azides from amines. *Tetrahedron Letters* **37**, 6029-6032, doi:[http://dx.doi.org/10.1016/0040-4039\(96\)01307-X](http://dx.doi.org/10.1016/0040-4039(96)01307-X) (1996).
- 49 Nyffeler, P. T., Liang, C.-H., Koeller, K. M. & Wong, C.-H. The Chemistry of Amine–Azide Interconversion: Catalytic Diazotransfer and Regioselective Azide Reduction. *Journal of the American Chemical Society* **124**, 10773-10778, doi:10.1021/ja0264605 (2002).
- 50 Palme, M. & Vasella, A. O-(1-Phenyl-1H-tetrazol-5-yl) Glycosides: Alternative synthesis and transformation into glycosyl fluorides. *Helvetica Chimica Acta* **78**, 959-969, doi:10.1002/hlca.19950780418 (1995).
- 51 Luo, S.-Y., Thopate, S. R., Hsu, C.-Y. & Hung, S.-C. Synthesis of d-ribo-C18-phytosphingosine from d-glucosamine via the d-allosamine derivatives as key intermediates. *Tetrahedron Letters* **43**, 4889-4892, doi:[http://dx.doi.org/10.1016/S0040-4039\(02\)00919-X](http://dx.doi.org/10.1016/S0040-4039(02)00919-X) (2002).
- 52 Toepfer, A. & Schmidt, R. R. A convenient synthesis of N-acetyllactosamine derivatives from lactal. *Carbohydrate research* **247**, 159-164 (1993).
- 53 Murakata, C. & Ogawa, T. Stereoselective synthesis of glycobiosyl phosphatidylinositol, a part structure of the glycosyl-phosphatidylinositol (GPI) anchor of *Trypanosoma brucei*. *Carbohydrate research* **234**, 75-91 (1992).
- 54 Orgueira, H. A. *et al.* Modular synthesis of heparin oligosaccharides. *Chemistry* **9**, 140-169, doi:10.1002/chem.200390009 (2003).
- 55 Angibeaud, P., Defaye, J., Gabelle, A. & Utille, J. Mild deprotection of benzyl ether protective groups with ozone. *Synthesis*, 1123-1125 (1985).
- 56 Carlsen, P. H. J., Katsuki, T., Martin, V. S. & Sharpless, K. B. A greatly improved procedure for ruthenium tetroxide catalyzed oxidations of organic compounds. *The Journal of Organic Chemistry* **46**, 3936-3938, doi:10.1021/jo00332a045 (1981).
- 57 Maehr, H., Perrotta, A. & Smallheer, J. Synthetic (S)-5-(benzoyloxy)-6-oxohexanoic acid ethyl ester and [S,S-(E)-3-(hydroxymethyl)oxiranebutanoic acid

- methyl ester, important synthons for leukotrienes B4 and A4, from D-arabinose. *The Journal of Organic Chemistry* **53**, 832-836, doi:10.1021/jo00239a028 (1988).
- 58 Schuda, P. F., Cichowicz, M. B. & Heimann, M. R. A facile method for the oxidative removal of benzyl ethers: the oxidation of benzyl ethers to benzoates by ruthenium tetroxide. *Tetrahedron Letters* **24**, 3829-3830, doi:[http://dx.doi.org/10.1016/S0040-4039\(00\)94286-2](http://dx.doi.org/10.1016/S0040-4039(00)94286-2) (1983).
- 59 Cao, H. & Yu, B. Synthesis of a S-linked heparan sulfate trisaccharide as the substrate mimic of heparanase. *Tetrahedron Letters* **46**, 4337-4340 (2005).
- 60 Stepowska, H. & Zamojski, A. Elongation of the pentose chain at the terminal carbon atom with Grignard C1 reagents. A study of the homologation reaction. *Tetrahedron* **55**, 5519-5538, doi:[http://dx.doi.org/10.1016/S0040-4020\(99\)00197-0](http://dx.doi.org/10.1016/S0040-4020(99)00197-0) (1999).
- 61 Krajewski, J. W. *et al.* Synthesis, crystal structure, and conformation of methyl 6-deoxy-2,3-O-isopropylidene- α -D-manno-heptofuranoside. *Carbohydrate research* **252**, 97-105, doi:[http://dx.doi.org/10.1016/0008-6215\(94\)90008-6](http://dx.doi.org/10.1016/0008-6215(94)90008-6) (1994).
- 62 Orgueira, H. A., Bartolozzi, A., Schell, P. & Seeberger, P. H. Conformational locking of the glycosyl acceptor for stereocontrol in the key step in the synthesis of heparin. *Angew Chem Int Edit* **41**, 2128-2131, doi:Doi 10.1002/1521-3773(20020617)41:12<2128::Aid-Anie2128>3.0.Co;2-V (2002).
- 63 Lubineau, A., Gavard, O., Alais, J. & Bonnaffe, D. New accesses to L-iduronyl synthons. *Tetrahedron Letters* **41**, 307-311, doi:Doi 10.1016/S0040-4039(99)02080-8 (2000).
- 64 Lohman, G. J., Hunt, D. K., Hogermeier, J. A. & Seeberger, P. H. Synthesis of iduronic acid building blocks for the modular assembly of glycosaminoglycans. *J Org Chem* **68**, 7559-7561, doi:10.1021/jo0340760 (2003).
- 65 Seebach, D. Metalated Orthothioformates. *Angewandte Chemie International Edition in English* **6**, 442-443, doi:10.1002/anie.196704421 (1967).
- 66 Silveira, C. C., Bernardi, C. R., Braga, A. L. & Kaufman, T. S. Thioorthoesters in the activated Pictet-Spengler cyclization. Synthesis of 1-thiosubstituted tetrahydroisoquinolines and carbon-carbon bond formation via sulfonyl iminium ions generated from N,S-sulfonyl acetals. *Tetrahedron Letters* **44**, 6137-6140, doi:[http://dx.doi.org/10.1016/S0040-4039\(03\)01452-7](http://dx.doi.org/10.1016/S0040-4039(03)01452-7) (2003).
- 67 Mukaiyama, T., Narasaka, K. & Furusato, M. Convenient synthesis of 1,4-diketones. Application to the synthesis of dihydrojasnone. *Journal of the American Chemical Society* **94**, 8641-8642, doi:10.1021/ja00779a091 (1972).

- 68 Dondoni, A., Marra, A. & Perrone, D. Efficacious modification of the procedure for the aldehyde release from 2-substituted thiazoles. *The Journal of Organic Chemistry* **58**, 275-277, doi:10.1021/jo00053a055 (1993).
- 69 Jacquinet, J.-C. *et al.* Synthesis of heparin fragments. A chemical synthesis of the trisaccharide O-(2-deoxy-2-sulfamido-3,6-di-O-sulfo- α -D-glucopyranosyl)-(1 \rightarrow 4)-O-(2-O-sulfo- α -L-idopyranosyluronic acid)-(1 \rightarrow 4)-2-deoxy-2-sulfamido-6-O-sulfo-D-glucopyranose heptasodium salt. *Carbohydrate research* **130**, 221-241, doi:[http://dx.doi.org/10.1016/0008-6215\(84\)85281-7](http://dx.doi.org/10.1016/0008-6215(84)85281-7) (1984).
- 70 Gavard, O. *et al.* Efficient preparation of three building blocks for the synthesis of heparan sulfate fragments: towards the combinatorial synthesis of oligosaccharides from hypervariable regions. *European Journal of Organic Chemistry*, 3603-3620 (2003).
- 71 La Ferla, B. *et al.* Synthesis of disaccharide sub-units of a new series of heparin related oligosaccharides. *Tetrahedron* **55**, 9867-9880 (1999).
- 72 Magaud, D. *et al.* Synthesis of the two monomethyl esters of the disaccharide 4-O- α -D-galacturonosyl-D-galacturonic acid and of precursors for the preparation of higher oligomers methyl uronated in definite sequences. *Carbohydrate research* **314**, 189-199 (1998).
- 73 Magaud, D. *et al.* Differential reactivity of α - and β -anomers of glycosyl acceptors in glycosylations. A remote consequence of the endo-anomeric effect? *Organic letters* **2**, 2275-2277 (2000).
- 74 Kochetkov, N. K., Khorlin, A. J. & Bochkov, A. F. A new method of glycosylation. *Tetrahedron* **23**, 693-707, doi:[http://dx.doi.org/10.1016/0040-4020\(67\)85014-2](http://dx.doi.org/10.1016/0040-4020(67)85014-2) (1967).
- 75 Ravidà, A., Liu, X., Kovacs, L. & Seeberger, P. H. Synthesis of Glycosyl Phosphates from 1,2-Orthoesters and Application to in Situ Glycosylation Reactions. *Organic letters* **8**, 1815-1818, doi:10.1021/ol0603155 (2006).
- 76 Collins, P. & Ferrier, R. *Monosaccharides: their chemistry and their roles in natural products*. (John Wiley & Sons Ltd, 1995).
- 77 Toshima, K. & Tatsuta, K. Recent progress in O-glycosylation methods and its application to natural products synthesis. *Chemical reviews* **93**, 1503-1531, doi:10.1021/cr00020a006 (1993).
- 78 Hashimoto, S.-i., Honda, T. & Ikegami, S. A rapid and efficient synthesis of 1,2-trans-[small β]-linked glycosides via benzyl- or benzoyl-protected glycopyranosyl phosphates. *Journal of the Chemical Society, Chemical Communications* **0**, 685-687, doi:10.1039/C39890000685 (1989).

- 79 Nakajima, N., Horita, K., Abe, R. & Yonemitsu, O. MPM (4-methoxybenzyl) protection of hydroxy functions under mild acidic conditions. *Tetrahedron Letters* **29**, 4139-4142, doi:[http://dx.doi.org/10.1016/S0040-4039\(00\)80438-4](http://dx.doi.org/10.1016/S0040-4039(00)80438-4) (1988).
- 80 Rai, A. N. & Basu, A. An efficient method for para-methoxybenzyl ether formation with lanthanum triflate. *Tetrahedron Letters* **44**, 2267-2269 (2003).
- 81 Tummatorn, J., Albiniak, P. A. & Dudley, G. B. Synthesis of Benzyl Esters Using 2-Benzyloxy-1-methylpyridinium Triflate. *The Journal of Organic Chemistry* **72**, 8962-8964, doi:10.1021/jo7018625 (2007).
- 82 Poon, K. W. C., Albiniak, P. A. & Dudley, G. B. Protection of alcohols using 2-benzyloxy-1-methylpyridinium trifluoromethanesulfonate: methyl®-(-)-3-benzyloxy-2-methyl propanoate. *Organic Syntheses* **84**, 295-305 (2007).
- 83 Okada, Y., Ohtsu, M., Bando, M. & Yamada, H. Benzyl N-Phenyl-2,2,2-trifluoroacetimidate: A new and stable reagent for O-benylation. *Chemistry Letters* **36**, 992-993 (2007).
- 84 Wessel, H., Iversen, T. & Bundle, D. Acid-catalyzed benzylation and allylation by alkyl trichloroacetimidates. *J. Chem. Soc. Perkin Trans. I*, 2247-2250 (1985).
- 85 Lee, S. G. *et al.* End-functionalized glycopolymers as mimetics of chondroitin sulfate proteoglycans. *Chemical Science* **1**, 322-325, doi:10.1039/C0SC00271B (2010).
- 86 Odian, G. *Principles of Polymerization*. (Wiley, 2004).
- 87 Ogawa, N., Mizuno, S., Tsukamoto, S. & Mori, A. Relationships of structure to binding of gamma-aminobutyric acid (GABA) and related compounds with the GABA and benzodiazepine receptors. *Research communications in chemical pathology and pharmacology* **43**, 355-368 (1984).
- 88 Wuts, P. G. M. & Greene, T. W. *Greene's Protective Groups in Organic Synthesis*. 4th ed edn, (Wiley-Interscience, 2006).
- 89 Tully, S. E. *Synthesis and biological activity of chondroitin sulfate biopolymers* Ph. D. thesis, California Institute of Technology, (2007).
- 90 Plante, O. J., Palmacci, E. R., Andrade, R. B. & Seeberger, P. H. Oligosaccharide synthesis with glycosyl phosphate and dithiophosphate triesters as glycosylating agents. *Journal of the American Chemical Society* **123**, 9545-9554 (2001).
- 91 Dayal, B. *et al.* Lithium hydroxide/aqueous methanol: mild reagent for the hydrolysis of bile acid methyl esters. *Steroids* **55**, 233-237 (1990).

- 92 Noti, C., de Paz, J. L., Polito, L. & Seeberger, P. H. Preparation and use of microarrays containing synthetic heparin oligosaccharides for the rapid analysis of heparin-protein interactions. *Chemistry* **12**, 8664-8686, doi:10.1002/chem.200601103 (2006).
- 93 Jaurand, G., Tabeur, C. & Petitou, M. Synthesis of the basic disaccharide unit of heparin. *Carbohydrate research* **255**, 295-301 (1994).
- 94 Lucas, H. *et al.* Synthesis of heparin-like pentamers containing "opened" uronic acid moieties. *Tetrahedron* **46**, 8207-8228 (1990).
- 95 Raghuraman, A., Riaz, M., Hindle, M. & Desai, U. R. Rapid and efficient microwave-assisted synthesis of highly sulfated organic scaffolds. *Tetrahedron Letters* **48**, 6754-6758, doi:10.1016/j.tetlet.2007.07.100 (2007).
- 96 Maza, S., Paz, J. L. & Nieto, P. Microwave-assisted sulfonation of heparin oligosaccharides. *Tetrahedron letters* **52**, 441-443 (2011).
- 97 Krylov, V., Ustyuzhanina, N., Grachev, A. & Nifantiev, N. Efficient acid-promoted per-O-sulfation of organic polyols. *Tetrahedron Letters* **49**, 5877-5879 (2008).
- 98 Hashimoto, K., Ohfuné, Y. & Shirahama, H. Synthesis of conformationally restricted analogs of kainic acid. Is the conformation of the C4-substituent of kainoid important to its neuroexcitatory activity? *Tetrahedron Letters* **36**, 6235-6238, doi:[http://dx.doi.org/10.1016/0040-4039\(95\)01094-X](http://dx.doi.org/10.1016/0040-4039(95)01094-X) (1995).

Chapter 3

- 1 Camm, K. D. & Fogg, D. E. in *Metathesis Chemistry: From Nanostructure Design to Synthesis of Advanced Materials* NATO Science Series (eds Y. Imamoglu & V. Dragutan) 285-303 (Springer, 2007).
- 2 Cunliffe, D., Pennadam, S. & Alexander, C. Synthetic and biological polymers—merging the interface. *European Polymer Journal* **40**, 5-25, doi:<http://dx.doi.org/10.1016/j.eurpolymj.2003.10.020> (2004).
- 3 Jean-Louis Hérisson, P. & Chauvin, Y. Catalyse de transformation des oléfines par les complexes du tungstène. II. Télomérisation des oléfines cycliques en présence d'oléfines acycliques. *Die Makromolekulare Chemie* **141**, 161-176, doi:10.1002/macp.1971.021410112 (1971).
- 4 Ramakrishna, S., Mayer, J., Wintermantel, E. & Leong, K. W. Biomedical applications of polymer-composite materials: a review. *Composites Science and Technology* **61**, 1189-1224, doi:[http://dx.doi.org/10.1016/S0266-3538\(00\)00241-4](http://dx.doi.org/10.1016/S0266-3538(00)00241-4) (2001).

- 5 Trnka, T. M. & Grubbs, R. H. The development of L₂X₂Ru=CHR olefin metathesis catalysts: an organometallic success story. *Acc Chem Res* **34**, 18-29 (2001).
- 6 Gestwicki, J. E., Cairo, C. W., Strong, L. E., Oetjen, K. A. & Kiessling, L. L. Influencing receptor-ligand binding mechanisms with multivalent ligand architecture. *Journal of the American Chemical Society* **124**, 14922-14933 (2002).
- 7 Lee, K. Y. & Mooney, D. J. Hydrogels for tissue engineering. *Chemical reviews* **101**, 1869-1879 (2001).
- 8 Haag, R. & Kratz, F. Polymer Therapeutics: Concepts and Applications. *Angewandte Chemie International Edition* **45**, 1198-1215, doi:10.1002/anie.200502113 (2006).
- 9 Grubbs, R. H. *Handbook of Metathesis*. (Wiley-VCH, 2003).
- 10 Ivin, K. J. & Mol, J. C. *Olefin Metathesis and Metathesis Polymerization*. (Academic Press, 1997).
- 11 Grubbs, R. H. Olefin Metathesis. *Tetrahedron* **60**, 7117-7140 (2004).
- 12 Connon, S. J. & Blechert, S. Recent developments in olefin cross-metathesis. *Angewandte Chemie International Edition* **42**, 1900-1923, doi:10.1002/anie.200200556 (2003).
- 13 Deiters, A. & Martin, S. F. Synthesis of oxygen- and nitrogen-containing heterocycles by ring-closing metathesis. *Chemical reviews* **104**, 2199-2238, doi:10.1021/cr0200872 (2004).
- 14 McReynolds, M. D., Dougherty, J. M. & Hanson, P. R. Synthesis of phosphorus and sulfur heterocycles via ring-closing olefin metathesis. *Chemical reviews* **104**, 2239-2258, doi:10.1021/cr020109k (2004).
- 15 Baughman, T. & Wagener, K. in *Metathesis Polymerization Vol. 176 Advances in Polymer Science* (ed Michael R Buchmeiser) Ch. 1, 1-42 (Springer Berlin Heidelberg, 2005).
- 16 Lehman, S. E. & Wagener, K. B. in *Handbook of Metathesis* 283-353 (Wiley-VCH Verlag GmbH, 2008).
- 17 Lehman, S. E. & Wagener, K. B. in *Late Transition Metal Polymerization Catalysis* 193-229 (Wiley-VCH Verlag GmbH & Co. KGaA, 2005).
- 18 Morgan, J. P., Morrill, C. & Grubbs, R. H. Selective ring opening cross metathesis of cyclooctadiene and trisubstituted cycloolefins. *Organic letters* **4**, 67-70 (2002).

- 19 Mayo, P. & Tam, W. Ring-opening metathesis-cross-metathesis reactions (ROM-CM) of substituted norbornadienes and norbornenes. *Tetrahedron* **58**, 9513-9525, doi:10.1016/s0040-4020(02)01276-0 (2002).
- 20 Frenzel, U. & Nuyken, O. Ruthenium-based metathesis initiators: Development and use in ring-opening metathesis polymerization. *Journal of Polymer Science Part A: Polymer Chemistry* **40**, 2895-2916, doi:10.1002/pola.10324 (2002).
- 21 Schrock, R. R. Living ring-opening metathesis polymerization catalyzed by well-characterized transition-metal alkylidene complexes. *Acc Chem Res* **23**, 158-165, doi:10.1021/ar00173a007 (1990).
- 22 Buchmeiser, M. R. Homogeneous Metathesis Polymerization by Well-Defined Group VI and Group VIII Transition-Metal Alkylidenes: Fundamentals and Applications in the Preparation of Advanced Materials. *Chemical reviews* **100**, 1565-1604 (2000).
- 23 Schrock, R. R. & Hoveyda, A. H. Molybdenum and tungsten imido alkylidene complexes as efficient olefin-metathesis catalysts. *Angewandte Chemie International Edition* **42**, 4592-4633, doi:10.1002/anie.200300576 (2003).
- 24 Matson, J. B. & Grubbs, R. H. Synthesis of fluorine-18 functionalized nanoparticles for use as in vivo molecular imaging agents. *Journal of the American Chemical Society* **130**, 6731-6733, doi:10.1021/ja802010d (2008).
- 25 Guidry, E. N., Li, J., Stoddart, J. F. & Grubbs, R. H. Bifunctional [c2]daisy-chains and their incorporation into mechanically interlocked polymers. *Journal of the American Chemical Society* **129**, 8944-8945, doi:10.1021/ja0725100 (2007).
- 26 Gorodetskaya, I. A., Choi, T. L. & Grubbs, R. H. Hyperbranched macromolecules via olefin metathesis. *Journal of the American Chemical Society* **129**, 12672-12673, doi:10.1021/ja0759040 (2007).
- 27 Gilliom, L. R. & Grubbs, R. H. Titanacyclobutanes derived from strained, cyclic olefins: the living polymerization of norbornene. *Journal of the American Chemical Society* **108**, 733-742, doi:10.1021/ja00264a027 (1986).
- 28 Schrock, R. R. *et al.* Further studies of imido alkylidene complexes of tungsten, well-characterized olefin metathesis catalysts with controllable activity. *Organometallics* **9**, 2262-2275, doi:10.1021/om00158a025 (1990).
- 29 Schrock, R. R. *et al.* Preparation and reactivity of several alkylidene complexes of the type W(CHR')(N-2,6-C6H3-iso-Pr2)(OR)2 and related tungstacyclobutane complexes. Controlling metathesis activity through the choice of alkoxide ligand. *Journal of the American Chemical Society* **110**, 1423-1435, doi:10.1021/ja00213a014 (1988).

- 30 Agüero, A., Kress, J. & Osborn, J. A. Tungsten Wittig reagents: an efficient synthesis of [small alpha]-functionalised tri- and tetrasubstituted alkenes. *Journal of the Chemical Society, Chemical Communications* **0**, 531-533 (1986).
- 31 Schrock, R. R. *et al.* Synthesis of molybdenum imido alkylidene complexes and some reactions involving acyclic olefins. *Journal of the American Chemical Society* **112**, 3875-3886, doi:10.1021/ja00166a023 (1990).
- 32 Schrock, R. R., Weinstock, I. A., Horton, A. D., Liu, A. H. & Schofield, M. H. Preparation of rhenium(VII) monoimido alkylidyne complexes and metathesis of acetylenes via rhenacyclobutadiene intermediates. *Journal of the American Chemical Society* **110**, 2686-2687, doi:10.1021/ja00216a071 (1988).
- 33 Toreki, R. & Schrock, R. R. A well-defined rhenium(VII) olefin metathesis catalyst. *Journal of the American Chemical Society* **112**, 2448-2449, doi:10.1021/ja00162a071 (1990).
- 34 Castarlenas, R., Esteruelas, M. A. & Oñate, E. N-Heterocyclic Carbene–Osmium Complexes for Olefin Metathesis Reactions. *Organometallics* **24**, 4343-4346, doi:10.1021/om050569e (2005).
- 35 Castarlenas, R., Esteruelas, M. A. & Oñate, E. Preparation of [C,N,O]-Pincer Osmium Complexes by Alkylidene Metathesis with a Methyl Group of 2,6-Diacetylpyridine. *Organometallics* **26**, 3082-3084, doi:10.1021/om700326f (2007).
- 36 Nguyen, S. T., Grubbs, R. H. & Ziller, J. W. Syntheses and activities of new single-component, ruthenium-based olefin metathesis catalysts. *Journal of the American Chemical Society* **115**, 9858-9859, doi:10.1021/ja00074a086 (1993).
- 37 Sanford, M. S., Love, J. A. & Grubbs, R. H. Mechanism and Activity of Ruthenium Olefin Metathesis Catalysts. *Journal of the American Chemical Society* **123**, 6543-6554, doi:10.1021/ja010624k (2001).
- 38 Novak, B. M. & Grubbs, R. H. The ring opening metathesis polymerization of 7-oxabicyclo[2.2.1]hept-5-ene derivatives: a new acyclic polymeric ionophore. *Journal of the American Chemical Society* **110**, 960-961, doi:10.1021/ja00211a043 (1988).
- 39 Schwab, P., France, M. B., Ziller, J. W. & Grubbs, R. H. A Series of Well-Defined Metathesis Catalysts—Synthesis of [RuCl₂(JCHR')(PR₃)₂] and Its Reactions. *Angewandte Chemie International Edition in English* **34**, 2039-2041, doi:10.1002/anie.199520391 (1995).
- 40 Scholl, M., Trnka, T. M., Morgan, J. P. & Grubbs, R. H. Increased ring closing metathesis activity of ruthenium-based olefin metathesis catalysts coordinated with

- imidazolin-2-ylidene ligands. *Tetrahedron Letters* **40**, 2247-2250, doi:[http://dx.doi.org/10.1016/S0040-4039\(99\)00217-8](http://dx.doi.org/10.1016/S0040-4039(99)00217-8) (1999).
- 41 Garber, S. B., Kingsbury, J. S., Gray, B. L. & Hoveyda, A. H. Efficient and Recyclable Monomeric and Dendritic Ru-Based Metathesis Catalysts. *Journal of the American Chemical Society* **122**, 8168-8179, doi:10.1021/ja001179g (2000).
- 42 Sanford, M. S., Love, J. A. & Grubbs, R. H. A Versatile Precursor for the Synthesis of New Ruthenium Olefin Metathesis Catalysts. *Organometallics* **20**, 5314-5318 (2001).
- 43 Lee, S.G. *et al.* End-functionalized glycopolymers as mimetics of chondroitin sulfate proteoglycans. *Chemical Science* **1**, 322-325 (2010).
- 44 Funk, T. W., Berlin, J. M. & Grubbs, R. H. Highly Active Chiral Ruthenium Catalysts for Asymmetric Ring-Closing Olefin Metathesis. *Journal of the American Chemical Society* **128**, 1840-1846, doi:10.1021/ja055994d (2006).
- 45 Stewart, I. C. *et al.* Highly Efficient Ruthenium Catalysts for the Formation of Tetrasubstituted Olefins via Ring-Closing Metathesis. *Organic letters* **9**, 1589-1592, doi:10.1021/ol0705144 (2007).
- 46 Hong, S. H. & Grubbs, R. H. Highly Active Water-Soluble Olefin Metathesis Catalyst. *Journal of the American Chemical Society* **128**, 3508-3509, doi:10.1021/ja058451c (2006).
- 47 Mammen, M., Choi, S.-K. & Whitesides, G. M. Polyvalent Interactions in Biological Systems: Implications for Design and Use of Multivalent Ligands and Inhibitors. *Angewandte Chemie International Edition* **37**, 2754-2794, doi:10.1002/(sici)1521-3773(19981102)37:20<2754::aid-anie2754>3.0.co;2-3 (1998).
- 48 Kiessling, L. L. & Pohl, N. L. Strength in numbers: non-natural polyvalent carbohydrate derivatives. *Chemistry & biology* **3**, 71-77 (1996).
- 49 Kiessling, L. L., Strong, L. E. & Gestwicki, J. E. Principles for multivalent ligand design. *Annu Rep Med Chem* **35**, 321-330, doi:Doi 10.1016/S0065-7743(00)35030-8 (2000).
- 50 Bovin, N. V. & Gabius, H. J. Polymer-immobilized carbohydrate ligands: versatile chemical tools for biochemistry and medical sciences. *Chemical Society Reviews* **24**, 413-421 (1995).
- 51 Spain, S. G., Gibson, M. I. & Cameron, N. R. Recent advances in the synthesis of well-defined glycopolymers. *Journal of Polymer Science Part A: Polymer Chemistry* **45**, 2059-2072, doi:10.1002/pola.22106 (2007).

- 52 Roy, R. Blue-prints, syntheses and applications of glycopolymers. *Trends in Glycoscience and Glycotechnology* **8**, 79-99 (1996).
- 53 Roy, R. in *Modern Methods in Carbohydrate Synthesis* (eds S.H. Khan & R.A. O'Neill) (Harwood Academic, 1996).
- 54 Kobayashi, K. e. a. in *Neoglycoconjugates: Preparation and Applications* (eds Y. C. Lee & R. T. Lee) 261-284 (Academic Press, 1994).
- 55 Yamada, K., Minoda, M. & Miyamoto, T. Controlled Synthesis of Amphiphilic Block Copolymers with Pendant N-Acetyl-d-glucosamine Residues by Living Cationic Polymerization and Their Interaction with WGA Lectin. *Macromolecules* **32**, 3553-3558, doi:10.1021/ma9816315 (1999).
- 56 Kolonko, E. M., Pontrello, J. K., Mangold, S. L. & Kiessling, L. L. General Synthetic Route to Cell-Permeable Block Copolymers via ROMP. *Journal of the American Chemical Society* **131**, 7327-7333, doi:10.1021/ja809284s (2009).
- 57 Ouchi, T. & Ohya, Y. in *Neoglycoconjugates: Preparation and Applications* (eds Y. C. Lee & R. T. Lee) 465-498 (Academic Press, 1994).
- 58 Lee, S.-G. Unpublished results.
- 59 Mortell, K. H., Gingras, M. & Kiessling, L. L. Synthesis of Cell Agglutination Inhibitors by Aqueous Ring-Opening Metathesis Polymerization. *Journal of the American Chemical Society* **116**, 12053-12054, doi:10.1021/ja00105a056 (1994).
- 60 Kiessling, L. L. & Owen, R. M. in *Handbook of Metathesis* Vol. 3 (ed R. H. Grubbs) 180-225 (Wiley-VCH, 2003).
- 61 Kiessling, L. L., Gestwicki, J. E. & Strong, L. E. Synthetic multivalent ligands as probes of signal transduction. *Angewandte Chemie International Edition* **45**, 2348-2368, doi:10.1002/anie.200502794 (2006).
- 62 Fogg, D. E. & Foucault, H. M. in *Comprehensive Organometallic Chemistry III* (eds H. Crabtree Editors-in-Chief: Robert & D. Michael P. Mingos) 623-652 (Elsevier, 2007).
- 63 Black, G., Maher, D. & Risse, W. in *Handbook of Metathesis* 2-71 (Wiley-VCH Verlag GmbH, 2008).
- 64 Odian, G. *Principles of Polymerization*. (Wiley, 2004).
- 65 Noshay, A. & McGrath, J. E. *Block Copolymers*. (Academic, 1977).

- 66 Meier, S. *et al.* Carbohydrate analogue polymers by ring opening metathesis polymerisation (ROMP) and subsequent catalytic dihydroxylation. *Chemical Communications* **0**, 855-856 (2001).
- 67 Rule, J. D. & Moore, J. S. ROMP Reactivity of endo- and exo-Dicyclopentadiene. *Macromolecules* **35**, 7878-7882 (2002).
- 68 Mohr, B., Lynn, D. M. & Grubbs, R. H. Synthesis of Water-Soluble, Aliphatic Phosphines and Their Application to Well-Defined Ruthenium Olefin Metathesis Catalysts. *Organometallics* **15**, 4317-4325, doi:10.1021/om9603373 (1996).
- 69 Lynn, D. M., Mohr, B., Grubbs, R. H., Henling, L. M. & Day, M. W. Water-Soluble Ruthenium Alkylidenes: Synthesis, Characterization, and Application to Olefin Metathesis in Protic Solvents. *Journal of the American Chemical Society* **122**, 6601-6609, doi:10.1021/ja0003167 (2000).
- 70 Strong, L. E. & Kiessling, L. L. A general synthetic route to defined, biologically active multivalent arrays. *J. Am. Chem. Soc.* **121**, 6193-6196 (1999).
- 71 Kanai, M., Mortell, K. H. & Kiessling, L. L. Varying the Size of Multivalent Ligands: The Dependence of Concanavalin A Binding on Neoglycopolymer Length. *Journal of the American Chemical Society* **119**, 9931-9932, doi:10.1021/ja972089n (1997).
- 72 Claverie, J. P. & Soula, R. Catalytic polymerizations in aqueous medium. *Progress in polymer science* **28**, 619-662 (2003).
- 73 Fraser, C. & Grubbs, R. H. Synthesis of Glycopolymers of Controlled Molecular Weight by Ring-Opening Metathesis Polymerization Using Well-Defined Functional Group Tolerant Ruthenium Carbene Catalysts. *Macromolecules* **28**, 7248-7255, doi:10.1021/ma00125a030 (1995).
- 74 Manning, D. D., Strong, L. E., Hu, X., Beck, P. J. & Kiessling, L. L. Neoglycopolymer inhibitors of the selectins. *Tetrahedron* **53**, 11937-11952, doi:[http://dx.doi.org/10.1016/S0040-4020\(97\)00707-2](http://dx.doi.org/10.1016/S0040-4020(97)00707-2) (1997).
- 75 Rawat, M., Gama, C. I., Matson, J. B. & Hsieh-Wilson, L. C. Neuroactive Chondroitin Sulfate Glycomimetics. *Journal of the American Chemical Society* **130**, 2959-2961, doi:10.1021/ja709993p (2008).
- 76 Binder, J. B. & Raines, R. T. Olefin metathesis for chemical biology. *Current opinion in chemical biology* **12**, 767-773, doi:<http://dx.doi.org/10.1016/j.cbpa.2008.09.022> (2008).
- 77 Lynn, D. M., Kanaoka, S. & Grubbs, R. H. Living Ring-Opening Metathesis Polymerization in Aqueous Media Catalyzed by Well-Defined Ruthenium Carbene

Complexes. *Journal of the American Chemical Society* **118**, 784-790, doi:10.1021/ja950327d (1996).

- 78 Lipshutz, B. H., Aguinaldo, G. T., Ghorai, S. & Voigtritter, K. Olefin Cross-Metathesis Reactions at Room Temperature Using the Nonionic Amphiphile “PTS”: Just Add Water†. *Organic letters* **10**, 1325-1328, doi:10.1021/ol800028x (2008).

Chapter 4

- 1 Pallister, C. J. & Watson, M. S. *Haematology*. 334-336 (Scion Publishing, 2010).
- 2 Avci, F. Y., Karst, N. A. & Linhardt, R. J. Synthetic oligosaccharides as heparin-mimetics displaying anticoagulant properties. *Current pharmaceutical design* **9**, 2323-2335 (2003).
- 3 Lever, R. & Page, C. P. Novel drug development opportunities for heparin. *Nature Reviews Drug Discovery* **1**, 140-148 (2002).
- 4 Xie, J., Murugesan, S. & Linhardt, R. J. in *Carbohydrate Chemistry, Biology, and Medical Applications* (eds H. G. Garg, M. K. Cowman, & C. A. Hales) Ch. 10, (Elsevier Ltd, 2008).
- 5 Lindahl, U. in *Heparin-chemical and biological properties, clinical applications* (eds D. A. Lane & U. Lindahl) 159-189 (Edward Arnold, 1989).
- 6 Marieb, E. N. & Hoehn, K. in *Human Anatomy & Physiology* 649-650 (Benjamin Cummings, 2010).
- 7 Furie, B. & Furie, B. C. Thrombus formation in vivo. *J Clin Invest* **115**, 3355-3362, doi:10.1172/jci26987 (2005).
- 8 Boon, G. D. An Overview of Hemostasis. *Toxicologic Pathology* **21**, 170-179 (1993).
- 9 Norris, L. A. Blood coagulation. *Best practice & research. Clinical obstetrics & gynaecology* **17**, 369-383 (2003).
- 10 Coleman, R. W. Biological activities of the contact factors in vivo: potentiation of hypotension, inflammation and fibrinolysis and inhibition of cell adhesion, angiogenesis, and thrombosis. *Thrombosis and haemostasis* **82**, 1568-1577 (1999).
- 11 Jaques, L. B. Heparins--anionic polyelectrolyte drugs. *Pharmacological reviews* **31**, 99-166 (1979).
- 12 Greinacher, A., Alban, S., Dummel, V., Franz, G. & Mueller-Eckhardt, C. Characterization of the structural requirements for a carbohydrate based

- anticoagulant with a reduced risk of inducing the immunological type of heparin-associated thrombocytopenia. *Journal of Thrombosis and Haemostasis* **74**, 886-892 (1995).
- 13 McCrae, K. R., Bussel, J. B., Mannucci, P. M., Remuzzi, G. & Cines, D. B. Platelets: an update on diagnosis and management of thrombocytopenic disorders. *Hematology / the Education Program of the American Society of Hematology. American Society of Hematology. Education Program*, 282-305 (2001).
 - 14 Francis, J. L., Palmer, G. J., 3rd, Moroosse, R. & Drexler, A. Comparison of bovine and porcine heparin in heparin antibody formation after cardiac surgery. *The Annals of thoracic surgery* **75**, 17-22 (2003).
 - 15 Bauer, T. L. *et al.* Prevalence of heparin-associated antibodies without thrombosis in patients undergoing cardiopulmonary bypass surgery. *Circulation* **95**, 1242-1246 (1997).
 - 16 Warkentin, T. E. & Kelton, J. G. A 14-year study of heparin-induced thrombocytopenia. *The American journal of medicine* **101**, 502-507 (1996).
 - 17 Amiral, J. *et al.* Generation of antibodies to heparin-PF4 complexes without thrombocytopenia in patients treated with unfractionated or low-molecular-weight heparin. *American journal of hematology* **52**, 90-95, doi:10.1002/(SICI)1096-8652(199606)52:2<90::AID-AJH4>3.0.CO;2-0 (1996).
 - 18 Picker, S. M. & Gathof, B. S. [Heparin induced thrombocytopenia. A frequently unrecognised complication after major orthopedic surgery]. *Der Orthopade* **33**, 1300-1308, doi:10.1007/s00132-004-0695-3 (2004).
 - 19 Amiral, J. *et al.* Absence of cross-reactivity of SR90107A/ORG31540 pentasaccharide with antibodies to heparin-PF4 complexes developed in heparin-induced thrombocytopenia. *Blood coagulation & fibrinolysis : an international journal in haemostasis and thrombosis* **8**, 114-117 (1997).
 - 20 Smythe, M. A., Koerber, J. M. & Mattson, J. C. The incidence of recognized heparin-induced thrombocytopenia in a large, tertiary care teaching hospital. *Chest* **131**, 1644-1649, doi:10.1378/chest.06-2109 (2007).
 - 21 Sheng, G. J., Oh, Y. I., Chang, S. K. & Hsieh-Wilson, L. C. Tunable Heparan Sulfate Mimetics for Modulating Chemokine Activity. *Journal of the American Chemical Society* **In Preparation** (2013).
 - 22 Desai, U. R., Petitou, M., Bjork, I. & Olson, S. T. Mechanism of heparin activation of antithrombin: evidence for an induced-fit model of allosteric activation involving two interaction subsites. *Biochemistry* **37**, 13033-13041, doi:10.1021/bi981426h (1998).

- 23 Johnson, D. J., Li, W., Adams, T. E. & Huntington, J. A. Antithrombin-S195A factor Xa-heparin structure reveals the allosteric mechanism of antithrombin activation. *The EMBO journal* **25**, 2029-2037, doi:10.1038/sj.emboj.7601089 (2006).
- 24 Oosta, G. M., Gardner, W. T., Beeler, D. L. & Rosenberg, R. D. Multiple functional domains of the heparin molecule. *Proceedings of the National Academy of Sciences* **78**, 829-833 (1981).
- 25 Danielsson, A., Raub, E., Lindahl, U. & Bjork, I. Role of ternary complexes, in which heparin binds both antithrombin and proteinase, in the acceleration of the reactions between antithrombin and thrombin or factor Xa. *The Journal of biological chemistry* **261**, 15467-15473 (1986).
- 26 Laurent, T. C., Tengblad, A., Thunberg, L., Hook, M. & Lindahl, U. The molecular-weight-dependence of the anti-coagulant activity of heparin. *Biochemical Journal* **175**, 691-701 (1978).
- 27 Lane, D. A., Denton, J., Flynn, A. M., Thunberg, L. & Lindahl, U. Anticoagulant activities of heparin oligosaccharides and their neutralization by platelet factor 4. *Biochemical Journal* **218**, 725-732 (1984).
- 28 Suchman, A. L. & Griner, P. F. Diagnostic uses of the activated partial thromboplastin time and prothrombin time. *Annals of internal medicine* **104**, 810-816 (1986).
- 29 Van Cott, E. M. & Laposata, M. in *The Laboratory Test Handbook* (eds D. S. Jacobs, D. K. Oxley, & W. R. DeMott) 327-358 (Lexi-Comp, 2001).
- 30 White, G. C., Marder, V. J., Coleman, R. W., Hirsh, J. & Salzman, E. W. in *Hemostasis and Thrombosis: Basic Principles and Clinical Practice* (eds R. W. Coleman, J. Hirsh, V. J. Marder, & E. W. Salzman) 1134-1147 (JP Lippincott, Co., 1994).
- 31 Bates, S. M. & Weitz, J. I. Coagulation assays. *Circulation* **112**, e53-60, doi:10.1161/CIRCULATIONAHA.104.478222 (2005).
- 32 <http://www.meditec.com/resourcestools/medical-reference-links/normal-lab-values/>.
- 33 Schenone, M., Furie, B. C. & Furie, B. The blood coagulation cascade. *Current opinion in hematology* **11**, 272-277 (2004).
- 34 Andersson, L. O., Barrowcliffe, T. W., Holmer, E., Johnson, E. A. & Sims, G. E. Anticoagulant properties of heparin fractionated by affinity chromatography on matrix-bound antithrombin iii and by gel filtration. *Thrombosis research* **9**, 575-583 (1976).

- 35 Proctor, R. R. & Rapaport, S. I. The partial thromboplastin time with kaolin. A simple screening test for first stage plasma clotting factor deficiencies. *American journal of clinical pathology* **36**, 212-219 (1961).
- 36 Rawat, M., Gama, C. I., Matson, J. B. & Hsieh-Wilson, L. C. Neuroactive Chondroitin Sulfate Glycomimetics. *Journal of the American Chemical Society* **130**, 2959-2961, doi:10.1021/ja709993p (2008).
- 37 Orgueira, H. A. *et al.* Modular synthesis of heparin oligosaccharides. *Chemistry* **9**, 140-169, doi:10.1002/chem.200390009 (2003).